

University of Groningen

Novel approaches for the redesign of flavoprotein Oxidases

Winter, Remko Tsjibbe

IMPORTANT NOTE: You are advised to consult the publisher's version (publisher's PDF) if you wish to cite from it. Please check the document version below.

Document Version

Publisher's PDF, also known as Version of record

Publication date:

2012

[Link to publication in University of Groningen/UMCG research database](#)

Citation for published version (APA):

Winter, R. T. (2012). *Novel approaches for the redesign of flavoprotein Oxidases*. s.n.

Copyright

Other than for strictly personal use, it is not permitted to download or to forward/distribute the text or part of it without the consent of the author(s) and/or copyright holder(s), unless the work is under an open content license (like Creative Commons).

The publication may also be distributed here under the terms of Article 25fa of the Dutch Copyright Act, indicated by the "Taverne" license. More information can be found on the University of Groningen website: <https://www.rug.nl/library/open-access/self-archiving-pure/taverne-amendment>.

Take-down policy

If you believe that this document breaches copyright please contact us providing details, and we will remove access to the work immediately and investigate your claim.

Downloaded from the University of Groningen/UMCG research database (Pure): <http://www.rug.nl/research/portal>. For technical reasons the number of authors shown on this cover page is limited to 10 maximum.

Novel approaches for the redesign of flavoprotein oxidases

© Remko Tsjibbe Winter, Groningen (The Netherlands), 2011

ISBN (printed version): 978-90-367-5248-0

ISBN (electronic version): 978-90-367-5249-7

Printed by: Ipskamp Drukkers, Enschede (The Netherlands)



The research described in this thesis was carried out in the Groningen Biomolecular Sciences and Biotechnology Institute (Biochemical laboratory of the University of Groningen) according to the requirements of the Graduate School of Science (Faculty of Mathematics and Natural Sciences, University of Groningen) and was supported by the Dutch Technology Foundation STW, which is the applied science division of NWO, and the Technology Programme of the Ministry of Economic Affairs. (Project number GBC.07726)



rijksuniversiteit
groningen

Novel approaches for the redesign of flavoprotein oxidases

Proefschrift

ter verkrijging van het doctoraat in de
Wiskunde en Natuurwetenschappen
aan de Rijksuniversiteit Groningen
op gezag van de
Rector Magnificus, dr. E. Sterken,
in het openbaar te verdedigen op
vrijdag 13 januari 2012
om 16:15 uur

door

Remko Tsjibbe Winter

geboren op 7 januari 1982
te Libreville, Gabon

Promotor:

Prof. dr. ir. M. W. Fraaije

Beoordelingscommissie:

Prof. dr. W. J. H. van Berkel

Prof. dr. D. B. Janssen

Prof. dr. J. G. Roelfes

Voor Noortje

Table of Contents

Chapter 1	General introduction: redesign of flavoprotein oxidases	9
Chapter 2	Multiple pathways guide oxygen diffusion in flavoenzymes	25
Chapter 3	Export of <i>S. coelicolor</i> alditol oxidase to the periplasm and surface of <i>E. coli</i>	43
Chapter 4	Functionalizing oxidases with peroxidase activity creates oxiperoxidases	63
Chapter 5	Hot or not? A thermostable alditol oxidase from <i>A. cellulolyticus</i> 11B	83
Chapter 6	Oxidase redesign by active site randomization	115
Chapter 7	The nose knows: biotechnological production of vanillin	145
Chapter 8	Oxidase engineering: summary and future prospects	157
	English summary	171
	Nederlandse samenvatting	183
	Curriculum vitae	196
	List of publications	197
	Dankwoord	199

Chapter 1

General introduction: redesign of flavoprotein oxidases

Remko T. Winter and Marco W. Fraaije

Laboratory of Biochemistry, Groningen Biomolecular Sciences and Biotechnology Institute,
University of Groningen, Nijenborgh 4, 9747 AG Groningen, The Netherlands

1.1 The power of enzymes

Enzymes are a diverse and extremely powerful class of protein based catalysts. They are highly specific and able to perform almost any type of chemical reaction, generally under mild conditions. The catalytic potential of enzymes is being increasingly appreciated by the chemical industry in their search for greener alternatives to currently used industrial processes (1-3). Nowadays, there are many examples of enzymes being employed as biocatalysts in industrial processes (4-6). The sublime specificity of enzymes makes them desirable biocatalysts. At the same time it is their Achilles heel as the number of reactions an enzyme can catalyse is generally restricted, each enzyme having evolved to fulfil a distinct physiological role. Furthermore, enzymes are adapted to the environment in which they have to function, which creates such limitations as being active only at ambient temperatures or having a catalytic turnover rate that is not optimized for speed but for compatibility with metabolic enzyme partners. These paradigms exclude the existence of enzymes that do not fit within the boundaries set by nature. The challenge is thus to go beyond these natural boundaries and to develop methodologies to create 'unnatural' enzymes (7). Ideally it would be possible to (re)design or engineer enzymes to convert pre-defined substrates for which no natural enzyme exists. It goes without saying that such engineered enzymes would be of significant interest for a wide range of industrial applications.

1.2 Enzyme engineering: rewards and pitfalls

Research in the last two decades has produced a significant increase in the number of enzyme engineering methodologies. Up until the late 1980's enzymes could only be modified through the replacement of single amino acid residues, in a form of rational design called 'site directed mutagenesis'. Such approaches often met with limited success, generally due to an incomplete understanding of how protein structure influences function and because more than one mutation is often required to obtain the desired effect. It is also contrary to how enzyme 'engineering' occurs in nature, where natural selection (e.g. survival of the fittest) drives the alteration of enzymes towards optimal characteristics. Since the 1990's, however, enzyme engineering in the laboratory became possible in a fashion modelled on Darwinian evolution. This approach, named 'directed evolution', involves the generation of genetic diversity through (random) mutagenesis followed by screening libraries of created variants for mutants that exhibit improved characteristics (8). By applying multiple rounds of mutagenesis and screening, evolutionary processes can be mimicked under laboratory

conditions (9, 10) (Figure 1.1). Using directed evolution, existing enzymes have been altered to exhibit impressively improved catalytic performance, different specificities or novel mechanistic features. These engineered enzymes not only yield fundamental information concerning enzyme functioning but are also often employed as valuable synthetic biocatalysts (11).

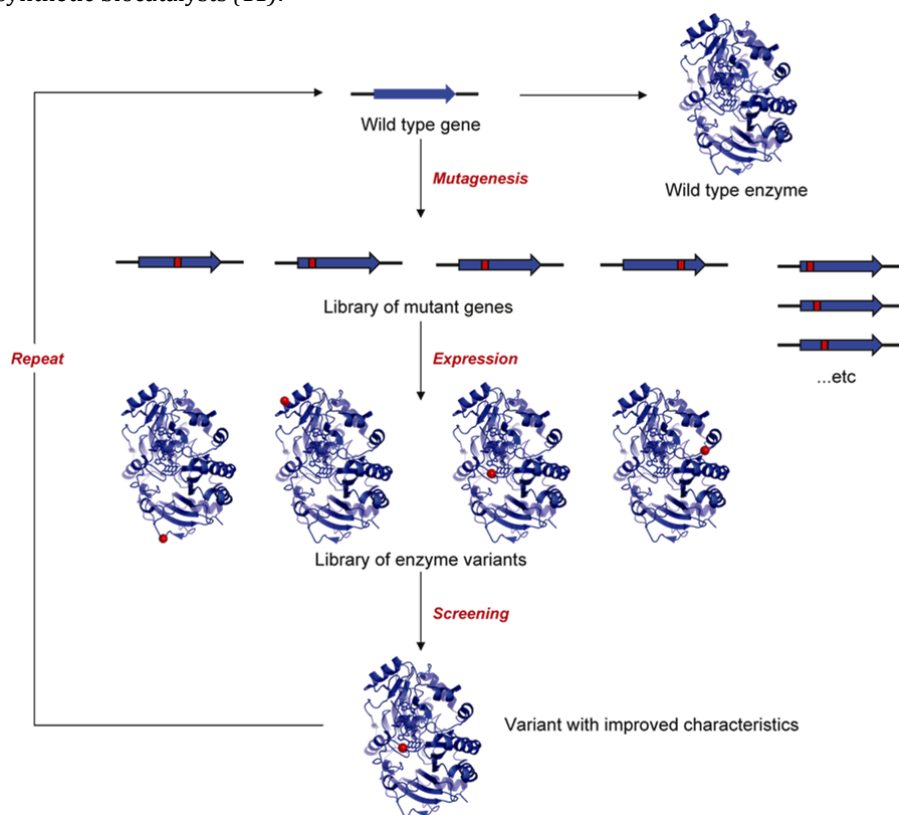


Figure 1.1 Directed evolution of enzymes. This involves multiple rounds of mutagenesis and screening for desired characteristics (7).

Anno 2011, there are two opposing approaches that can be followed when using directed evolution to perform enzyme engineering: screening large, diversity based libraries (the random approach) (12) or the knowledge-based design and screening of a few variants (the rational approach) (13). With the random approach, one compensates for an incomplete understanding of sequence-structure-function relationships by attempting to access large numbers of variants. The bottleneck for such an approach, however, is generally the absence of a screening method that can

push beyond the low- to medium-throughput barrier (Table 1.1). As a result, the extent to which the sequence space of a particular enzyme (class) can be explored remains limited. On the other hand, the rational approach is no panacea; even structure-based rational design cannot yet reliably yield improved variants. Here the limitation is not computational power, but the deficiencies in scoring and search functions applied when modelling active sites and the catalysis reactions they perform, although significant advances have been made in this field (14, 15). The direct consequence of the limitations of rational design is that large collections of variants still need to be screened to find sufficient improvements, resulting in the screening method being the bottleneck.

Table 1.1 Different screening strategies have differing capacities (12).

Throughput capacity	Screening strategy	Maximum library size	Advantage	Disadvantage
Low-medium	Microtiter plate	$\sim 10^4$	All analytical techniques possible; excellent dynamic range	Labour-intensive; limited screening capacity
High	Agar plate	$\sim 10^5$	Facile operation	Limited dynamic range
Ultra-high	FACS	$\sim 10^9$	Extremely fast; very large libraries possible	Detection needs to be based on fluorescence

Recently, a third approach to enzyme engineering has been emerging that takes advantage of both methods; designing a library based on rational or computational predictions (16). Thus the shortcomings of modelling are offset by screening a larger number of variants. The idea is to significantly reduce the size of the library that needs to be screened, without compromising the chance of finding that one variant with significantly improved characteristics. For example, for many enzymes it may be sufficient to target only those residues lining the active site; the so-called first-shell (17). A typical enzyme will contain in the order of 10-20 residues in this first-shell that are all involved directly with either substrate recognition or binding, catalysis or determining the active site environment. Extensive analysis performed by Morley *et al* revealed that mutations in this first shell generally have more potential to create a desired variant, particularly when one is searching for enhanced or altered substrate specificity or enantioselectivity (18). While this rational-random based approach to enzyme engineering is very attractive, the screening capacity that is required should not be underestimated; if one was to target all the residues in a 10 amino acid first

shell for complete randomization this would still result in 20^{10} ($=1 \times 10^{13}$) unique variants! Screening all these variants would require an enormous effort and is not necessarily required, as recent work van Leeuwen and co-workers shows. They screen multiple libraries of haloalkane dehalogenase first shell residues in parallel to obtain two impressive enantiocomplementary variants, after having screened only 5500 clones (19). As this also study illustrates, it is very interesting to develop enzyme engineering methodologies that are biased towards creating variants by mutating predominantly the first shell residues. Alterations in this subset of residues are expected to have a relatively high chance of translating into new reactivities and specificities; after all, they form the heart of every biocatalyst.

Whatever approach to enzyme engineering is chosen, the challenge is a reliable and robust screening method that allows one to select for the desired characteristic. As the above three approaches highlight, the bottleneck for any enzyme engineering effort is nearly always the screening method used, and invariably this is because of a capacity issue. It is therefore very attractive to develop novel screening methods that can handle libraries in an ultra-high throughput manner. Recently, fluorescence activated cell sorters (FACS) have been emerging as highly effective tools in the screening of extremely large enzyme libraries (20, 21). FACS sorters are specialized instruments that can detect several fluorescent parameters belonging to individual particles (cells, microbeads, emulsions) at rates up to 10^7 per hour, and isolate those particles with the desired properties (Figure 1.2) (22, 23). The screening of large libraries for novel enzyme activities with FACS can be classified according to the method used to couple genotype and phenotype: 1.) cell surface display of active enzymes; 2.) reporting of enzyme activity with GFP or its variants; 3.) entrapment of the product within the cells or 4.) *in vitro* compartmentalization (24). A robust FACS based assay could enable the complete screening of a first-shell library, heightening the chance of finding a variant with novel specificity and/or activity and maximizing the potential of both the rational and random approaches to enzyme engineering.

This PhD thesis focuses on enzyme engineering and the development of cell sorting based, ultra-high throughput, screening assays.

1.3 Flavoprotein oxidases as target

Oxidases (EC 1.x.3.x) catalyse the two or four-electron oxidation of substrates using molecular oxygen (O_2) as electron acceptor. In the course of this reaction dioxygen is reduced to either hydrogen peroxide or water (Figure 1.3). Energetically, the direct reduction of oxygen is a very unfavourable course of action for any organism; all the

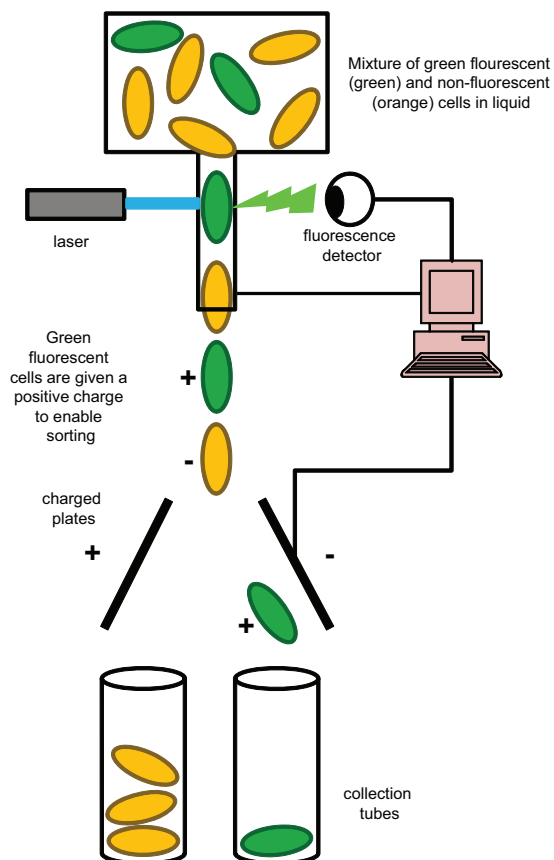


Figure 1.2 Schematic overview of screening by fluorescence activated cell sorting (FACS). The acronym FACS is trademarked and owned by Becton Dickinson and Company (BD), but is common in the scientific literature. FACS is a specialized type of flow cytometry; in the above diagram the flow cytometer unit is responsible for the analysis of the fluorescent properties of each cell. Cell sorters are equipped with an added unit that can furnish analysed cells with a charge to enable sorting. In this diagram, a population of green fluorescent cells is sorted from a mixture of fluorescent and non-fluorescent cells.

energy rich electrons are transferred directly to oxygen resulting in the formation of H_2O_2 or H_2O . This instead of being transferred to an alternative electron acceptor like $NAD(P)^+$ (dehydrogenases), where they can be used to generate ATP in the electron transport chain. It is no surprise then to discover that oxidases are relatively rare enzymes, typically involved in catabolic routes. While rare, oxidases are highly valuable enzymes for industrial applications precisely because of the fact that they transfer electrons directly to molecular oxygen and do not require an expensive

cofactor. Furthermore, oxidation chemistry by chemical means is notoriously dirty, often using stoichiometric amounts of potentially toxic metals like chromium and manganese. Using an oxidase that can function under mild, aqueous conditions and requires only oxygen is thus very attractive to an industry trying to become “greener” (25).



Figure 1.3 Typical reaction catalysed by oxidases. S, substrate; P, product.

The vanillyl-alcohol oxidase (VAO) family is a sub-class of oxidases that is particularly catalytically diverse (26). Research has shown that members of this family, that are all flavoproteins, can catalyse an incredibly wide range of oxidation reactions while typically exhibiting exquisite chemo-, regio-, and enantioselectivity (27). Besides the relatively simple oxidations of aliphatic alcohols (28) and sugar molecules (29, 30), VAO family members can also hydroxylate aromatic compounds (31), perform decarboxylations (32), oxidize steroids (33) and perform oxidative cyclization reactions with alkaloid-like compounds (34) (Figure 1.4). These examples, which by no means presume to be all-inclusive of the complete catalytic scope of VAO-type oxidases, indicate that it is a protein fold capable of harbouring a plethora of oxidation chemistries. This makes enzymes in this class attractive targets for enzyme engineering.

The research presented in this thesis focuses on two recently discovered flavoprotein oxidases, eugenol oxidase (EUGO) from *Rhodococcus jostii* RHA1 and alditol oxidase (AldO) from *Streptomyces coelicolor* A3(2). EUGO accepts a number of different phenolic compounds and is a close homologue of VAO (36), while AldO prefers polyols (29) and has recently been explored for its biocatalytic potential (37). Both enzymes contain a covalent 8 α -N¹-histidyl-FAD linkage that anchors the flavin to the protein backbone (38), giving the enzymes their characteristic bright yellow colour (Figure 1.5). The soluble, heterologous expression levels of both proteins in *E. coli* are impressive; from 1 litre of bacterial culture 160 mg of EUGO and 350 mg of AldO can be purified (29, 36). Combined, these features made both enzymes attractive candidates for oxidase engineering. At the same time they can also serve as model oxidases in efforts to pioneer such approaches into generic ones, suitable for any oxidase.

This thesis details the enzyme engineering carried out on the flavoprotein oxidases eugenol oxidase and alditol oxidase.

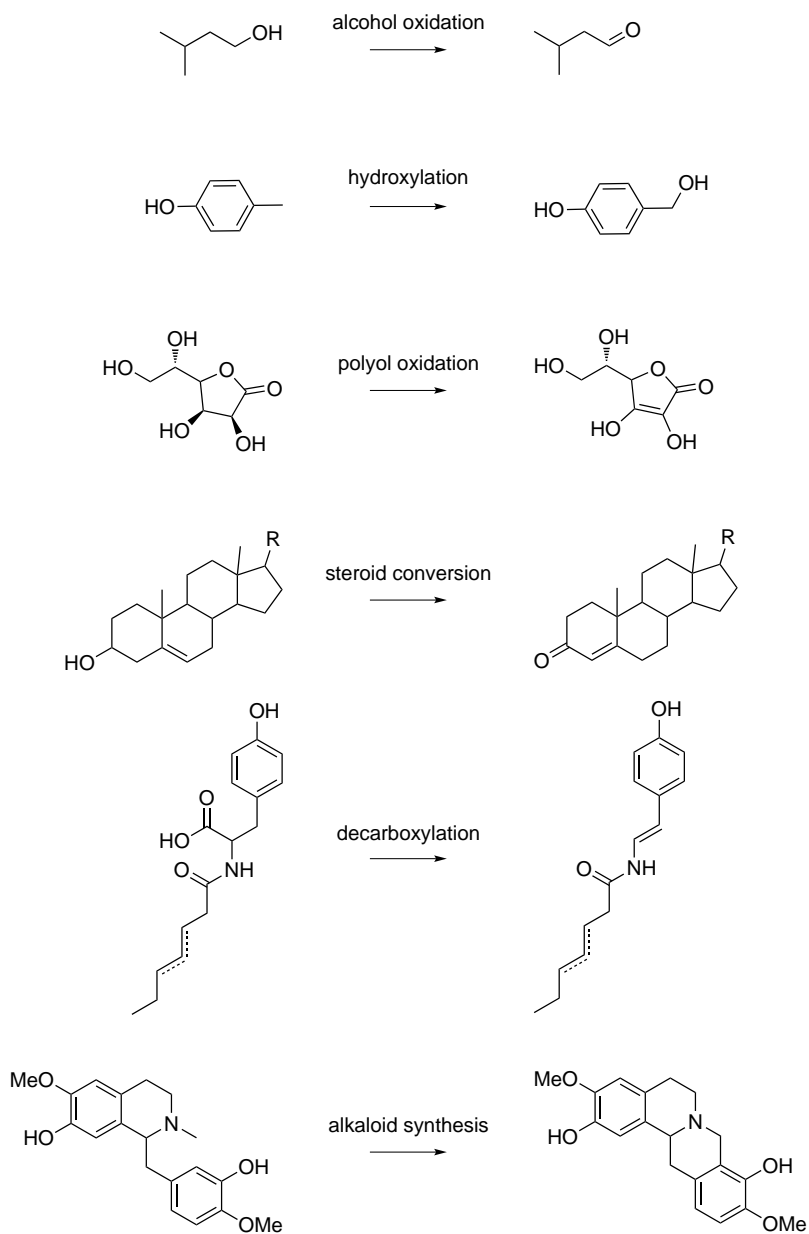


Figure 1.4 Examples of reactions catalysed by VAO-type oxidases (28, 31-35).

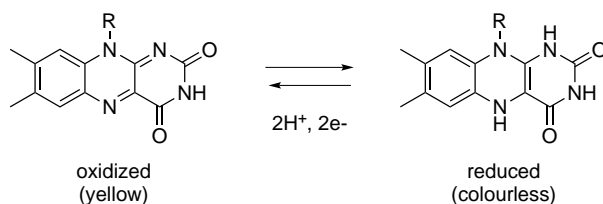


Figure 1.5 Oxidation chemistry of VAO type oxidases is possible due to their flavin cofactor. The isoalloxazine ring system (shown here) is the redox active portion of the flavin cofactor, and can undergo one or two electron reductions. In its oxidized form flavin is bright yellow, giving flavoenzymes their characteristic yellow colour (*flavus* = yellow; *Latin*). **R** can be a ribityl side chain (riboflavin), ribityl + phosphate (FMN) or ribityl + phosphate + AMP (FAD).

1.4 Oxidase engineering: how to get what you screen for

The engineering of oxidase activity is a relatively unexplored field; only a handful of examples exist where oxidases have successfully been engineered to display enhanced reactivity or altered substrate specificity. Recently, a rationally designed library of *Fusarium* NRRL 2903 galactose oxidase mutants was successfully screened for variants exhibiting improved activity towards D-glucose (39). The directed evolution of monoamine oxidase from *Aspergillus niger* by Turner and co-workers is an enzyme engineering success story; after several rounds of directed evolution a variant was discovered (MAO-N-D5) that exhibited broader substrate specificity and improved enantioselectivity (40). In these two examples the capacity of the screening methods employed (microtiterplate and agar plate, respectively) was relatively limited. A recent example where a large (10^7) library of glucose oxidase variants was screened with FACS technology (41) shows that oxidase engineering is also compatible with ultra-high throughput screening technology. The research described in this thesis aims to create new oxidative enzymes active on unnatural substrates.

Structural analysis has shown that oxidases belonging to the VAO enzyme family harbour the oxidative flavin cofactor, FAD, in a structurally conserved cofactor binding domain (26). The second variable domain forms the major part of the substrate binding pocket (Figure 1.6). The substrate binding domain ensures proper positioning of the substrate with respect to the oxidative flavin cofactor, explaining the high selectivity of these biocatalysts. Analysis of the available structures of VAO-homologs has revealed that only a limited number of residues in the substrate binding domain are directly involved in substrate binding, and that it is these residues that tune the specificity of these redox enzymes (38, 42-46). By randomly mutating these first shell residues, while retaining the rest of the protein as a scaffold, a collection of oxidase variants can be created exhibiting novel substrate specificities (Figure 1.6).

Novel ultra-high throughput screening methods will then have to be developed in order to recover these new enzymes from the library of proteins with randomized active site architectures. By designing a robust and reliable ultra-high throughput screening method based on the detection of H_2O_2 —the by-product of a successful oxidase conversion—means that it can be generically applied to similar engineering strategies for all oxidases.

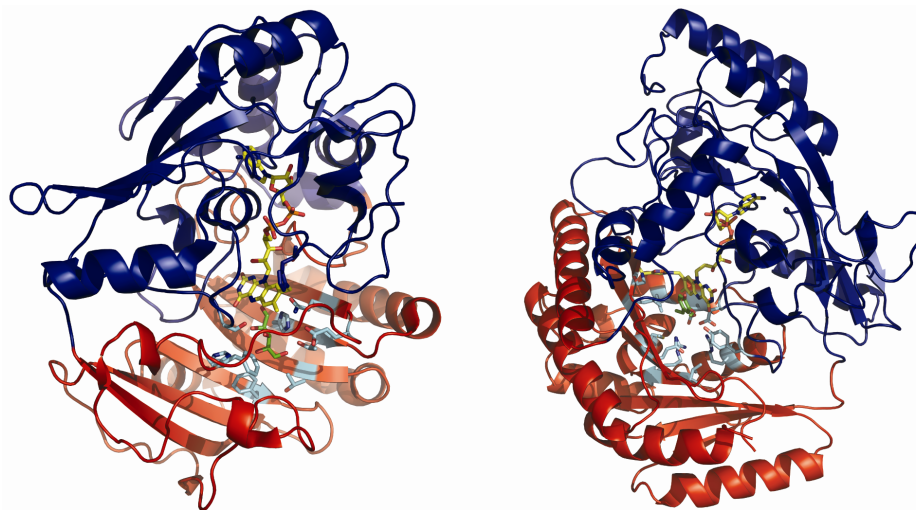


Figure 1.6 Two model flavoprotein oxidases. Depicted are the structures of *Streptomyces coelicolor* A3(2) alditol oxidase (AldO, left) and *Rhodococcus jostii* RHA1 eugenol oxidase (EUGO, right). Shown are the FAD binding domain (blue), the variable substrate binding domain (red) and the covalently bound FAD cofactor (yellow sticks). The first shell residues, involved in substrate recognition and binding, are shown as light blue sticks. Bound substrates (xylylitol for AldO, isoeugenol for EUGO) are shown as green sticks.

1.5 Aim and scope of this thesis

The aim of this thesis was the redesign and engineering of flavoprotein oxidases through active site reconstruction, thus creating novel substrate specificities. Parallel to this, we aimed to develop new methodologies to enable the ultra-high throughput screening of oxidase libraries.

The research in this PhD thesis was financed by STW (Stichting Technologische Wetenschappen; Dutch Technology Foundation) under the auspices of grant number GBC.7726. The utilization commission included representatives from DSM, Friesland

Foods and Organon/MSD. Under the headings below we summarize the work done as part of this thesis and attempt to place it in the context of the overall aim stated above.

1.5.1 Engineering the O in oxidase

The ability to react with molecular oxygen (O_2) is a feature inherent to all oxidases. In **chapter 2** we for the first time map the pathways dioxygen takes on its way to the active site, and use this knowledge in an attempt to engineer the oxygen reactivity of alditol oxidase.

1.5.2 Surface display & periplasmic secretion of oxidases can be engineered

E. coli is an ideal host for the expression of large protein libraries due to its amenability to genetic manipulation and capability of expressing recombinant proteins in high yields. In the interest of developing generic screening methods, intracellular expression is often not acceptable, due to the inability of target substrate to cross the cell wall. To circumvent this issue, in **chapter 3** we describe the engineering of a stable platform for the expression of flavoprotein oxidases in the periplasm or on the cell surface of *E. coli*. We also review bacterial cell surface display in **van Bloois, Winter et al. Trends Biotechnol (2011)**.

1.5.3 Oxidases can be engineered to contain peroxidase functionality

When designing a screening method suitable for the identification of novel oxidase activities, hydrogen peroxide (H_2O_2) is an attractive hand-hold: it is formed as a by-product in nearly all oxidase conversions. Peroxidases can easily be used to detect H_2O_2 , but unfortunately these enzymes cannot be expressed in *E. coli*. To overcome these problems, **chapter 4** describes the engineering of an oxidase to contain peroxidase functionality. In a related effort, we describe a novel peroxidase that is able to be expressed in *E. coli* in **van Bloois, Winter et al. Appl Microbiol Biotechnol (2010)**.

1.5.4 A useful diversion: engineering oxidase thermostability

Mutations in the active sites of enzymes can sometimes have an advantageous effect on activity, while reducing the overall (thermo)stability of the protein. This often results in such variants being missed in high throughput screens. To overcome this one can first engineer a protein for enhanced (thermo)stability, before screening it against improved activity. Alternatively, one can search for a thermostable homologue by genome mining and use this as an alternative platform for enzyme engineering. This is what we have done in **chapter 5**, where we describe the identification and characterization of a thermostable alditol oxidase.

1.5.5 Oxidase redesign and ultra-high throughput screening

Using a fluorescent probe specific for hydrogen peroxide we pioneer a screening assay with the potential to screen oxidase libraries in an ultra-high throughput manner with cell sorting technology. In **chapter 6** we detail the development of this assay along with our attempts to screen a randomized first shell library of eugenol oxidase.

1.5.6 EUGO: an oxidase fit for the classroom

A lot of research is still possible in the field of oxidase engineering, making it very important to interest future generations of scientists in this exciting class of enzymes. Thus, in **chapter 7** we describe a practical course suitable for undergraduate university students which highlights the biotechnological potential of oxidases by using EUGO to synthesize of the common flavouring agent vanillin.

1.5.7 And finally...

In **chapter 8** we present a summary of the work described in this thesis, and ponder on the future perspectives of oxidase engineering.

1.6 References

1. Sheldon RA (2008) E factors, green chemistry and catalysis: An odyssey. *Chem Commun* **29**: 3352-3365.
2. Wohlgemuth R (2009) The locks and keys to industrial biotechnology. *N Biotechnology* **25**: 204-213.
3. Schoemaker HE, Mink D & Wubbolts MG (2003) Dispelling the myths - biocatalysis in industrial synthesis. *Science* **299**: 1694-1697.
4. Patel RN (2008) Chemo-enzymatic synthesis of pharmaceutical intermediates. *Expert Opin Drug Dis* **3**: 187-245.
5. Pollard DJ & Woodley JM (2007) Biocatalysis for pharmaceutical intermediates: The future is now. *Trends Biotechnol* **25**: 66-73.
6. Panke S, Held M & Wubbolts M (2004) Trends and innovations in industrial biocatalysis for the production of fine chemicals. *Curr Opin Biotechnol* **15**: 272-279.
7. Turner NJ (2009) Directed evolution drives the next generation of biocatalysts. *Nat Chem Biol* **5**: 568-574.
8. Arnold FH (1996) Directed evolution: creating biocatalysts for the future. *Chem Eng Sci* **51**: 5091-5102.
9. Alexeeva M, Carr R & Turner NJ (2003) Directed evolution of enzymes: new biocatalysts for asymmetric synthesis. *Org Biomol Chem* **1**: 4133-4137.
10. Bershtein S & Tawfik DS (2008) Advances in laboratory evolution of enzymes. *Curr Opin Chem Biol* **12**: 151-158.
11. Fox RJ, Davis SC, Mundorff EC, Newman LM, Gavrilovic V, Ma SK, Chung LM, Ching C, Tam S, Muley S, Grate J, Gruber J, Whitman JC, Sheldon RA & Huisman GW (2007) Improving catalytic function by ProSAR-driven enzyme evolution. *Nat Biotechnol* **25**: 338-344.

12. **Leemhuis H, Kelly RM & Dijkhuizen L** (2009) Directed evolution of enzymes: library screening strategies. *IUBMB Life* **61**: 222-228.
13. **Damborsky J & Brezovsky J** (2009) Computational tools for designing and engineering biocatalysts. *Curr Opin Chem Biol* **13**: 26-34.
14. **Röthlisberger D, Khersonsky O, Wollacott AM, Jiang L, DeChancie J, Betker J, Gallaher JL, Althoff EA, Zanghellini A, Dym O, Albeck S, Houk KN, Tawfik DS & Baker D** (2008) Kemp elimination catalysts by computational enzyme design. *Nature* **453**: 190-195.
15. **Jiang L, Althoff EA, Clemente FR, Doyle L, Röthlisberger D, Zanghellini A, Gallaher JL, Betker JL, Tanaka F, Barbas CF 3rd, Hilvert D, Houk KN, Stoddard BL & Baker D** (2008) *De novo* computational design of retro-aldol enzymes. *Science* **319**: 1387-1391.
16. **Shivange AV, Marienhagen J, Mundhada H, Schenk A & Schwaneberg U** (2009) Advances in generating functional diversity for directed protein evolution. *Curr Opin Chem Biol* **13**: 19-25.
17. **Park S, Morley KL, Horsman GP, Holmquist M, Hult K & Kazlauskas RJ**. (2005) Focusing mutations into the *P. fluorescens* esterase binding site increases enantioselectivity more effectively than distant mutations. *Chem Biol* **12**: 45-54.
18. **Morley KL & Kazlauskas RJ** (2005) Improving enzyme properties: when are closer mutations better? *Trends Biotechnol* **23**: 231-237.
19. **van Leeuwen JGE, Wijma HJ, Floor RJ, van der Laan J & Janssen DB** (2011) Directed evolution strategies for enantiocomplementary haloalkane dehalogenases: from chemical waste to enantiopure building blocks. *Chembiochem* doi: 10.1002/cbic.201100579.
20. **Becker S, Schmoltdt HU, Adams TM, Wilhelm S & Kolmar H** (2004) Ultra-high throughput screening based on cell-surface display and fluorescence-activated cell sorting for the identification of novel biocatalysts. *Curr Opin Biotechnol* **15**: 323-329.
21. **Farinas ET** (2006) Fluorescence activated cell sorting for enzymatic activity. *Comb Chem High T Scr* **9**: 321-328.
22. **Givan AL** (1992) Flow cytometry: first principles (Wiley-Liss, New York)
23. **Shapiro HM** (2004) Practical flow cytometry (Wiley-Liss, New York)
24. **Yang G & Withers SG** (2009) Ultra-high throughput FACS-based screening for directed enzyme evolution. *Chembiochem* **10**: 2704-2715.
25. **Hollmann F, Arends IWCE, Buehler K, Schallmey A & Buhler B** (2011) Enzyme-mediated oxidations for the chemist. *Green Chem* **13**: 226-265.
26. **Fraaije MW, Van Berkel WJ, Benen JA, Visser J & Mattevi A** (1998) A novel oxidoreductase family sharing a conserved FAD-binding domain. *Trends Biochem Sci* **23**: 206-207.
27. **Turner NJ** (2011) Enantioselective oxidation of C-O and C-N bonds using oxidases. *Chem Rev* **111**: 4073-87.
28. **Yamashita N, Motoyoshi T & Nishimura A** (2000) Molecular cloning of the isoamyl alcohol oxidase-encoding gene (*mreA*) from *Aspergillus oryzae*. *J Biosci Bioeng* **89**: 522-527.
29. **Heuts DP, van Hellemond EW, Janssen DB & Fraaije MW** (2007) Discovery, characterization, and kinetic analysis of an alditol oxidase from *Streptomyces coelicolor*. *J Biol Chem* **282**: 20283-20291.
30. **Heuts DP, Janssen DB & Fraaije MW** (2007) Changing the substrate specificity of a chitooligosaccharide oxidase from *Fusarium graminearum* by model-inspired site-directed mutagenesis. *FEBS Lett* **581**: 4905-4909.
31. **Fraaije MW, van den Heuvel RH, Roelofs JC & Van Berkel WJ** (1998) Kinetic mechanism of vanillyl-alcohol oxidase with short-chain 4-alkylphenols. *Eur Jour Biochem* **253**: 712-719.

32. **Brady SF, Chao CJ & Clardy J** (2002) New natural product families from an environmental DNA (eDNA) gene cluster. *J Am Chem Soc* **124**: 9968-9969.
33. **Croteau N & Vrielink A** (1996) Crystallization and preliminary X-ray analysis of cholesterol oxidase from *Brevibacterium sterolicum* containing covalently bound FAD. *J Struct Biol* **116**: 317-319.
34. **Winkler A, Lyskowski A, Riedl S, Puhl M, Kutchan TM, Macheroux P & Gruber K** (2008) A concerted mechanism for berberine bridge enzyme. *Nat Chem Biol* **4**: 739-741.
35. **Nishikimi M & Yagi K** (1991) Molecular-basis for the deficiency in humans of gulonolactone oxidase, a key enzyme for ascorbic-acid biosynthesis. *Am J Clin Nutr* **54**: 1203-1208.
36. **Jin J, Mazon H, van den Heuvel RH, Janssen DB & Fraaije MW** (2007) Discovery of a eugenol oxidase from *Rhodococcus* sp. strain RHA1. *FEBS J* **274**: 2311-2321.
37. **van Hellemond EW, Vermote L, Koolen W, Sonke T, Zandvoort E, Heuts DP, Janssen DB & Fraaije MW** (2009) Exploring the biocatalytic scope of alditol oxidase from *Streptomyces coelicolor*. *Adv Synth Catal* **351**: 1523-1530.
38. **Forneris F, Heuts DP, Delvecchio M, Rovida S, Fraaije MW & Mattevi A** (2008) Structural analysis of the catalytic mechanism and stereoselectivity in *Streptomyces coelicolor* alditol oxidase. *Biochemistry* **47**: 978-985.
39. **Lippow SM, Moon TS, Basu S, Yoon SH, Li X, Chapman BA, Robison K, Lipovšek D & Prather KL** (2010) Engineering enzyme specificity using computational design of a defined-sequence library. *Chem Biol* **17**: 1306-1315.
40. **Carr R, Alexeeva M, Enright A, Eve TS, Dawson MJ & Turner NJ** (2003) Directed evolution of an amine oxidase possessing both broad substrate specificity and high enantioselectivity. *Angew Chem Int Ed* **42**: 4807-4810.
41. **Prodanovic R, Ostafe R, Scacioc A & Schwaneberg U** (2011) Ultra-high throughput screening system for directed glucose oxidase evolution in yeast cells. *Comb Chem High T Scr* **14**: 55-60.
42. **Mattevi A, Fraaije MW, Mozzarelli A, Olivi L, Coda A & van Berkel WJ** (1997) Crystal structures and inhibitor binding in the octameric flavoenzyme vanillyl-alcohol oxidase: the shape of the active-site cavity controls substrate specificity. *Structure* **5**: 907-920.
43. **Cunane LM, Chen ZW, Shamala N, Mathews FS, Cronin CN & McIntire WS** (2000) Structures of the flavocytochrome *p*-cresol methylhydroxylase and its enzyme-substrate complex: gated substrate entry and proton relays support the proposed catalytic mechanism. *J Mol Biol* **295**: 357-374.
44. **Dym O, Pratt EA, Ho C & Eisenberg D** (2000) The crystal structure of D-lactate dehydrogenase, a peripheral membrane respiratory enzyme. *Proc Natl Acad Sci U S A* **97**: 9413-9418.
45. **Coulombe R, Yue KQ, Ghisla S & Vrielink A** (2001) Oxygen access to the active site of cholesterol oxidase through a narrow channel is gated by an arg-glu pair. *J Biol Chem* **276**: 30435-30441.
46. **Malito E, Coda A, Bilyeu KD, Fraaije MW & Mattevi A** (2004) Structures of michaelis and product complexes of plant cytokinin dehydrogenase: implications for flavoenzyme catalysis. *J Mol Biol* **341**: 1237-1249.

Chapter 2

Multiple pathways guide oxygen diffusion in flavoenzymes

Remko T. Winter, Petra Popken, Dominic P. H. M. Heuts, Marco W. Fraaije

Laboratory of Biochemistry, Groningen Biomolecular Sciences and Biotechnology Institute,
University of Groningen, Nijenborgh 4, 9747 AG Groningen, The Netherlands

Riccardo Baron, J. Andrew McCammon

Department of Chemistry & Biochemistry and Center for Theoretical Biological Physics,
Howard Hughes Medical Institute, University of California at San Diego, La Jolla, CA 92093-0365

Willem J. H. van Berkel

Laboratory of Biochemistry, Wageningen University, Dreijenlaan 3, 6703 HA Wageningen, The Netherlands

Andrea Mattevi

Department of Genetics and Microbiology, University of Pavia, Via Ferrata 1, 27100 Pavia, Italy

This chapter is based on:

Proceedings of the National Academy of Sciences of the United States of America
(2009) **106**: 10603-10608

&

Flavins and Flavoproteins (Frago, S., ed.) (2008) 237-242

Abstract

Dioxygen (O₂) and other gas molecules have a fundamental role in a variety of enzymatic reactions. However, it is only poorly understood which O₂ uptake mechanism enzymes employ to promote efficient catalysis and how general this is. We investigated O₂ diffusion pathways into the flavoenzyme alditol oxidase (AldO) using an integrated computational and experimental approach. Enhanced-statistics molecular dynamics simulations reveal spontaneous protein-guided O₂ diffusion from the bulk solvent to preorganized protein cavities. The predicted protein-guided diffusion paths and the importance of key cavity residues for oxygen diffusion were verified by combining site-directed mutagenesis, rapid kinetics experiments, and high-resolution X-ray structures. This study indicates that the oxidase AldO employs multiple funnel-shaped diffusion pathways to absorb O₂ from the solvent and direct it to the reacting C4a atom of the flavin cofactor. The difference in O₂ reactivity among dehydrogenases and oxidases ultimately resides in the fine modulation of the local environment embedding the reactive locus of the flavin.

2.1 Introduction

Dioxygen (O_2) and other gas molecules have a fundamental role in a variety of enzymatic reactions carried out in living organisms. Oxygen-using enzymes usually have kinetic rates many folds higher than those attained by artificial catalysts (1–4). One crucial unsolved question concerns how these small gas molecules reach their active sites in an effective manner. Past studies supported the general model of passive diffusion through proteins (5, 6). However, it was more recently proposed that O_2 preferentially follows highly specific tunnels to reach the core of protein matrices (7–13). Is it possible to generalize these features for different classes of enzymes? Do proteins preferentially employ single specific pathways or a multitude of routes to optimize the O_2 uptake process?

Pioneering studies on gas-diffusion in biomolecular systems focused on single diffusion pathways in proteins of the globin family (2, 14). For example, myoglobin served as an ideal test system for the first computational studies on gaseous reactants (14). Fluorescence-quenching experiments were used to correlate the diffusion behaviour with solvent properties, e.g., viscosity (15, 16). Reaction intermediates of small gas molecules can be trapped in X-ray enzyme structures in limited favourable cases (17, 18) whereas time-resolved X-ray crystallography provides single-molecule-averaged insight (19). A general observation emerging from recent engineering studies of an O_2 transport protein is that design efforts based on static-structure models fail to address the molecular complexity critical for function (20). Thus, complementing experimental and computational approaches can improve our understanding of these dynamic processes at the atomic-level scale (7, 8, 21–25). However, no molecular dynamics (MD) study to date reported on the spontaneous, nonbiased diffusion of O_2 molecules from the bulk solvent to the active site of a flavoenzyme.

Flavoenzymes catalyse a wide range of reactions essential for maintaining cellular processes. Their striking chemical versatility is largely based on their ability to control the reaction of a flavin cofactor with O_2 . Three major groups of flavoenzymes can be distinguished (3, 26, 27). First, the dehydrogenases, that are characterized by poor or no reactivity with oxygen. Second, the monooxygenases, that react very fast with O_2 , forming a flavin adduct intermediate (C4a-hydroperoxyflavin; Figure 2.1), which subsequently inserts an oxygen atom into the substrate molecule. Third, the oxidases, that catalyse a rapid 2-electron transfer to O_2 to produce H_2O_2 , typically—but not always (28)—with no detectable catalytic intermediates. The reaction of reduced flavins with O_2 proceeds through an electron-transfer step that generates a caged radical pair, which is generally thought to be rate limiting. Reduced flavoprotein

monooxygenases and oxidases typically react very rapidly with O_2 , exhibiting bimolecular rate constants (up to $10^6 \text{ M}^{-1}\cdot\text{s}^{-1}$) that are close to a diffusion-controlled rate.

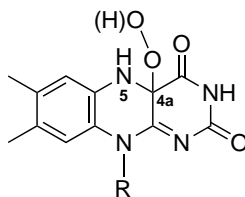


Figure 2.1 Chemical formula of the C4a-hydroperoxyflavin molecule. The N5 and C4a atoms are labelled. The flavin is facing the viewer with its *re*-side (the *si*-side is on the opposite side).

The biochemical and structural basis of the ability of flavoenzymes to react with O_2 remains to a large extent poorly understood, representing a most fascinating issue in flavoenzymology (3, 26). A key requirement for monooxygenases is that O_2 reaches the flavin to promote the catalysed reaction through a C4a covalent adduct (3, 26, 27) (Figure 2.1). However, only little is known about how oxidases react with O_2 . A direct contact between the oxidase flavin and O_2 may not be necessary, leaving open the possibility that the enzymes of this class may react by tunnelling pathways (24, 29) or electron transfer processes similar to what was reported for heme-containing enzymes (30).

Here, we investigate O_2 diffusion in alditol oxidase (AldO) from *Streptomyces coelicolor* A3(2) (31) using an integrated computational and experimental procedure. Enhanced-statistics MD simulations capture the spontaneous (unbiased) diffusion of O_2 , filling the gap between current sampling times in protein simulations with explicit solvent ($\approx 10^1$ ns scale) (32, 33) and measured diffusion times (>10 ns scale). Our theoretical predictions were followed by experimental verification through site-directed mutagenesis, rapid kinetics measurements, and structural analysis of the enzyme. The same experimental approach described here was used by collaborators Pimchai *et al* (39) to study the O_2 diffusion in the flavin-containing monooxygenase component (C2) of *p*-hydroxyphenylacetate hydroxylase from *Acinetobacter baumannii* (34), yielding similar results. This integrated approach indicates that the O_2 diffusion into oxidase and monooxygenase flavoenzymes is effectively guided by multiple funnel-like pathways that lead to defined O_2 entry points in the active sites. Our data provides structural insight into the mechanism of O_2 uptake by flavoenzymes, emphasizing the importance of the protein microenvironment that surrounds the flavin cofactor in modulating oxygen reactivity.

2.2 Materials & Methods

2.2.1 Molecular Model and Enhanced-Statistics MD Simulations

Ten MD trajectories of the AldO monomer (418 residues; FADH⁻ cofactor; initial model PDB entry 2VFR; 1.1 Å resolution) (31) at 300 and 350 K were generated using the GROMOS05 software for biomolecular simulation (35), the GROMOS 53A6 parameter set (36), and compatible ion parameters (37) and SPC water model (38). A summary is reported in Table 2.1 (39, SI Text). A procedure for enhanced-statistics MD simulation was used for O₂ spontaneous diffusion. It involves (i) reduced masses (1.6 u) for the oxygen atoms in the O₂ molecules (21); (ii) enhanced statistics from 100 (independent and non-interacting) O₂ molecules in the system, kept beyond a minimum pair distance by a network of repulsive half-harmonic distance-restraining potentials during the equilibration phase (to avoid biasing their initial location before

Table 2.1 Parameter overview of the simulated AldO system. A procedure for enhanced-statistics MD simulation was used to model spontaneous O₂ diffusion. The MD simulation was carried out at 300 and 350K with identical parameter values.

Parameter	Value
PDB ID initial coordinates	2vfr
T [K]	300 or 350
nr. O ₂ molecules	100
cofactor	FADH ⁻
nr. solute atoms	4009
nr. solvent molecules	15342
nr. atoms in the system	50245
nr. of ions	1 Cl ⁻ , 3 Mg ²⁺ , 6 K ⁺
total system charge	0
equilibration period [ns]	2.7
nr. MD replicas	5
equilibrium period [ns]	5.0

diffusion); (iii) a fast grid-based pair list-construction algorithm (40) as implemented in the GROMOS05 MD++ module (35); (iv) enhanced statistics from 10 independent MD runs at 300 and 350 K. O₂ diffusion statistics were collected over a total of 10 independent trajectories of systems with 100 O₂ molecules each, monitored for a total enhanced-MD time of 50 ns. The rather high O₂ apparent concentrations (AldO \approx 0.3 M; an O₂ saturated buffer, by comparison, is \approx 1.2 mM) allow for the capture of sufficient statistics of O₂-protein encounter events without perturbing overall protein structure at both 300 and 350 K. RMSD time series of AldO backbone C α -atoms are reported in Figure 2.2. Computer simulations were used to predict the location of oxygen diffusion pathways along AldO configurational distributions; kinetic properties were measured by experiments. The term “enhanced-statistics” emphasizes that an improved statistics is achieved compared with standard MD simulation. No biasing force or potential is used to bring O₂ molecules inside the enzyme active sites. Instead, O₂ freely diffuses on the free-energy landscape starting from a non-arbitrary configuration and spontaneously reaches the preorganized cavities described in the text. The Pymol (41) and VMD (42) software packages were used for graphical representations.

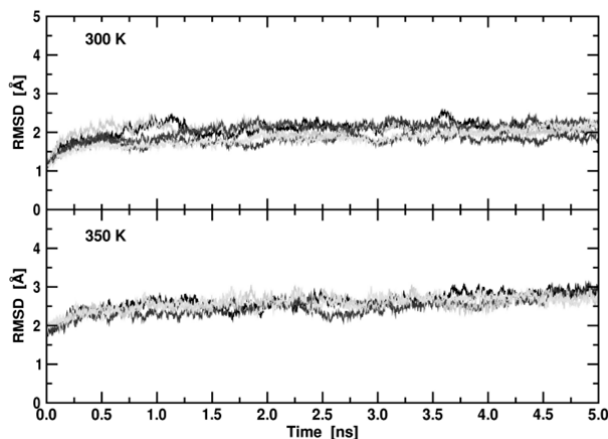


Figure 2.2 Root mean square deviation, RMSD, of AldO backbone C α -atoms. Taken from the x-ray structure during the MD runs. Different traces represent independent MD runs.

2.2.2 Rapid Kinetics and Oxygen Reactivity

2.2.2.1 Site-directed Mutagenesis & Enzyme Production

To increase protein yield AldO was expressed as a fusion with maltose binding protein (MBP), denoted m-AldO (42). m-AldO A105G, A105S, A105T and A105I mutants were prepared with the QuikChange mutagenesis kit (Stratagene) using pBAD-MBP-*aldo* as

template. Protein was expressed and purified from TB cultures as described by Heuts *et al* (42). Due to poor expression and subsequent difficulty in obtaining pure protein, the A105T mutant was cloned into a pBAD expression vector modified to contain an N-terminal His-tag. The protein was subsequently purified from cell free extracts using Ni-NTA Agarose (Qiagen) using the purification protocol described by van Bloois *et al* (44).

2.2.2.2 Analytical Methods

All measurements were performed at 300 K in 50 mM KP_i buffer (pH 7.5). Steady-state kinetic parameters of the purified mutants were determined by an indirect spectrophotometric assay coupling the production of H₂O₂ by m-AldO mutants to the horseradish peroxidase mediated oxidation of 4-aminoantipyrine and 3,5-dichloro-2-hydroxybenzenesulfonic acid. The formation of the resulting pink-purple product can be measured at 515 nm ($\epsilon_{515} = 26 \text{ mM}^{-1} \text{ cm}^{-1}$) (45). By comparing the absorption spectra of purified mutants before and after incubation with 0.1 % SDS the extinction coefficient was determined. It was assumed that the flavin spectrum of denatured m-AldO mutants was equal to that of free FAD ($\epsilon_{450} = 11.3 \text{ mM}^{-1} \text{ cm}^{-1}$) (46).

2.2.2.3 Kinetic Measurements

Pre-steady-state studies were performed with an Applied Photophysics model SX17MV stopped-flow apparatus. Single wavelength traces were measured with a photomultiplier detector while a diode array detector was used to collect spectral data at time intervals of 4.5 ms. Diode array spectral data was deconvoluted with the program Pro-K (Applied Photophysics). In order to estimate the oxidized/reduced ratio of the mutants under steady-state conditions equal amounts of a solution containing 20 μM enzyme was mixed with 40 mM xylitol and the absorbance measured at 450 nm over time. Steady-state conditions were identified as when the slope of the absorbance trace was equal to zero. The reductive half-reaction was measured under anaerobic conditions after mixing the enzyme solution with 5 or 50 mM xylitol. The oxidative half-reaction was followed at 452 nm by mixing a solution containing reduced enzyme with a solution containing varying amounts of oxygen. Measurements that required anoxic conditions contained 1 mM 4-ethylphenol and were made anaerobic by flushing with nitrogen for 15 min. Vanillyl alcohol oxidase (VAO) was added to a final concentration of 100 nM to remove any residual oxygen. Traces obtained by photomultiplier measurements were fitted to the exponential function Equation 2.1:

$$A(t) = A + C \times e^{(-kt)} \quad \text{Equation 2.1}$$

2.3 Results

2.3.1 Oxygen Diffusion into AldO

O₂ diffusion into an oxidase was addressed for AldO, a soluble monomeric flavoprotein belonging to the vanillyl-alcohol oxidase family (47), which contains a covalently bound FAD cofactor (31, 43). AldO catalyses the typical 2-electron flavin-mediated oxidation of a terminal C-OH moiety of a polyol substrate to the corresponding aldehyde, with the concomitant reduction of the flavin cofactor. The reduced flavin (FADH⁻) then reacts with O₂ to form H₂O₂, which completes the catalytic cycle. Because its crystal structure has been solved at high resolution (1.1 Å) (31) and the kinetic mechanism has been established by pre-steady-state kinetic analyses (43), AldO serves as an excellent oxidase prototype.

Enhanced-statistics MD simulations were initialized based on the 3-dimensional structure of FADH⁻-complexed AldO and extended for 50 ns of overall enhanced-time (Table 2.1). These simulations were set-up to capture O₂ diffusion before FADH⁻ oxidation. Out of a total of 500 O₂ trajectories at 300 K, we observe 5 complete spontaneous diffusion pathways (10 events) that bring O₂ molecules in front of the isoalloxazine ring of the FADH⁻ cofactor (Figure 2.1), starting from random configurations in the bulk solvent. Simulations at 350 K confirm the location of these successful paths (22 events; data not shown). Several O₂ molecules that initially reside in cavities on the protein surface subsequently diffuse into the AldO interior (e.g., Figure 2.3B, steps A, B, D, F, and H). These surface cavities typically display at least one hydrophobic residue, such as Ala and/or Ile, something that was also observed in the C₂ monooxygenase system (39). A remarkable example is the AldO all-Ala pocket of Ala-88, Ala-91, and Ala-277 used to capture O₂ molecules from the bulk solvent (Figure 2.4).

The spontaneous O₂ diffusion into AldO matches a model consisting of multiple diffusion paths converging toward a few key residues neighbouring the reactive moiety of the flavin cofactor, something that was also observed in the O₂ diffusion study of C₂ monooxygenase (39). In AldO all protein-guided diffusion pathways converge into a site defined by Ala-105, Tyr-87, and Thr-120 at ≈6 Å from the *re*-side of FADH⁻ (Figure 2.3 and Figure 2.4). Once O₂ molecules reach Tyr-87 or Thr-120, they (3 paths out of 5) eventually proceed to a preorganized cavity defined by flavin C4a and Ala-105, which coincides with the cavity previously proposed based on AldO X-ray structures (31). Thus, the side chain of Ala-105 creates a favourable hydrophobic environment to stabilize the presence of an O₂ molecule next to the reduced flavin (Figure 2.3A and B, steps C and G).

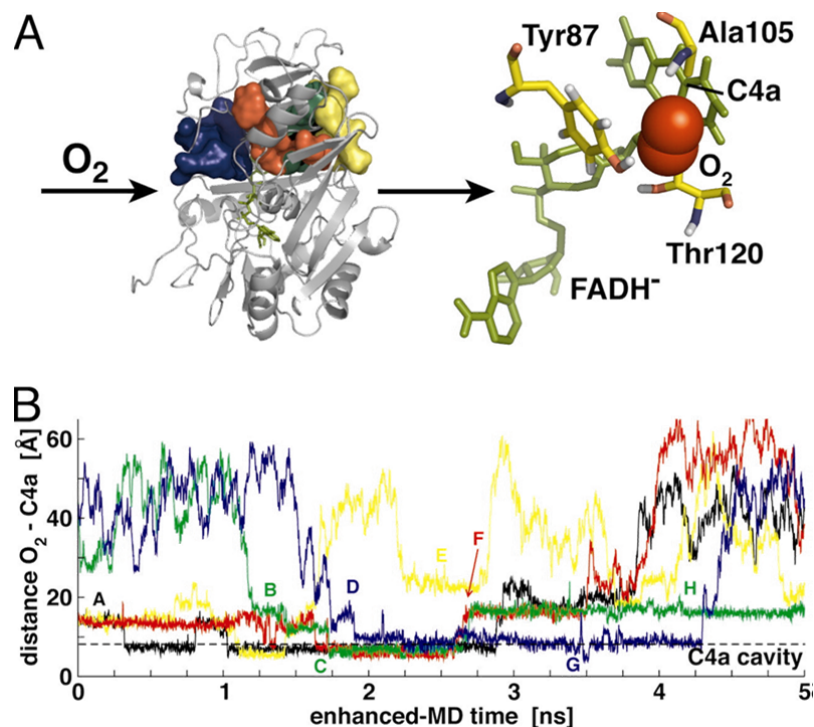


Figure 2.3 O_2 spontaneous diffusion into alditol oxidase. **A**, five paths are observed at 300 K (volume isosurfaces) (Left). All paths conduct O_2 molecules (red spheres) (Right) to the *re*-side of the $FADH^-$ reduced flavin cofactor (green sticks). **B**, Time series of the $O_2 - C4a$ distance for the successful diffusion paths and key steps (see *Oxygen Diffusion into AldO*). The dashed horizontal line defines the $C4a$ flavin cavity.

Clearly, protein dynamics is required for the successful diffusion of O_2 molecules to the active site. It is striking to observe that, similar to C_2 (39), all complete diffusion pathways (i.e. all pathways carrying oxygen from the bulk solvent to the flavin cofactor) converge to only one side of the reduced flavin (*re*-side) (Figure 2.1 and Figure 2.5). Moreover, they all cross only a limited part of the AldO protein structure, i.e., the substrate binding-domain.

Table 2.2 summarizes the pre-steady-state parameters of AldO and its Ala-105 mutants. The data show that the rate constant of AldO reoxidation ($13 \times 10^4 \text{ M}^{-1}\cdot\text{s}^{-1}$) is hardly affected by the Ala105Ser ($14 \times 10^4 \text{ M}^{-1}\cdot\text{s}^{-1}$) or Ala105Thr ($15 \times 10^4 \text{ M}^{-1}\cdot\text{s}^{-1}$) mutations whereas the Ala105Gly mutant is somewhat faster ($20 \times 10^4 \text{ M}^{-1}\cdot\text{s}^{-1}$) (Figure 2.6).

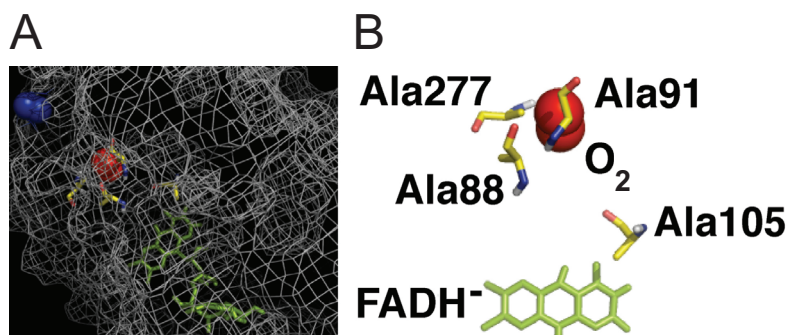


Figure 2.4 An alanine oxygen trap. The all-Ala cavity formed by AldO residues Ala-88, Ala-91 and Ala-277 is an example of an O_2 surface pocket used to capture O_2 molecules from the bulk solvent. O_2 molecules reside in this pocket before diffusion to the C4a flavin cavity defined by Ala-105. **A**, O_2 molecule when entering AldO surface (blue spheres) and trapped in the pocket (red spheres). **B**, positions of residues and FAD cofactor (sticks representation) when O_2 molecule is in the pocket (red spheres). The snapshot corresponds to stage A in Figure 2.2B. All 10 simulation events display O_2 molecules transiently occupying this cavity.

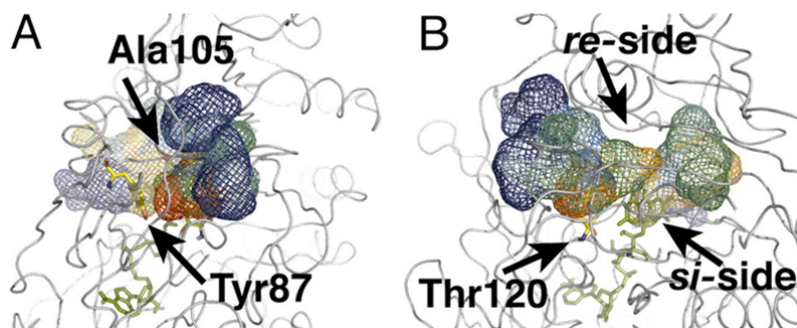


Figure 2.5 Oxygen pathways converge at Ala-105 and on the flavin re-side. **A**, time-dependent representation of 3 complete paths observed from simulations at 300 K converging in close contact with Ala-105 (volume surfaces, top view). **B**, all pathways conduct O_2 molecules to the flavin re-side (side view). For graphical purposes only 3 paths are displayed. Volume isosurfaces are coloured depending on simulation time from blue (entrance into the protein) to red (end of successful path).

Table 2.2 Kinetic parameters for reaction of AldO (mutant)-FADH⁻ with O₂. The steady state parameters were determined using xylitol as substrate. The k_{ox} reoxidation rate values denote the rate at which FADH⁻ in AldO is reacting with O₂ evidenced by flavin reoxidation.

Mutants	K_M (mM)	k_{cat} (s ⁻¹)	k_{cat}/K_M (mM ⁻¹ ·s ⁻¹)	k_{ox} (10 ⁴ M ⁻¹ ·s ⁻¹)
Wild-type	0.33	11.4	34.5	13
Ala105Gly	1.2	10.2	8.5	20
Ala105Ser	1.8	8.7	4.8	14
Ala105Thr	8.9	0.15	0.017	15

Apparently, small changes in the size of the side chain at position 105 have little effect on oxygen reactivity. In this regard, one would not expect a drastic increase in reactivity with oxygen in the Ala105Gly mutant, because the reaction rate of wild-type AldO is already high and is also limited by other funnel residues and the actual electron-transfer step from the flavin to O₂ (3, 31). Attempts to replace Ala-105 with an even larger side chain (isoleucine) failed because the mutant was extremely unstable and/or unable to bind FAD. The mutations can have a drastic effect on the overall reactivity, however, as evidenced by the A105T mutant which has a more than 1000-fold lower catalytic efficiency compared to WT. A major factor in this reduced efficiency is most likely a large drop in the flavin reduction (k_{red}); for the A105S mutant this was found to be 8 s⁻¹, compared to 99 s⁻¹ for the wild type enzyme (42, 48). Strong support for the role of Ala-105 as O₂ entry point to the active site is provided by recently reported mutagenesis data on plant L-galactono-1,4-lactone dehydrogenase (GALDH) (49), which shares 25% sequence identity with AldO. As a typical dehydrogenase, this enzyme reacts poorly with O₂. However, its oxygen reactivity could be substantially increased (400-fold) to a level comparable to that of typical oxidases by simply mutating Ala-113 (homologous to Ala-105 of AldO) to Gly (49). Apparently, Ala-105 in AldO already allows O₂ access to the reduced FAD whereas in GALDH—due to its specific active site—it needs to be replaced by a smaller residue to allow O₂ to pass through. This finding indicates that, consistent with our MD predictions for AldO, O₂ in GALDH also diffuses and approaches the flavin from the position corresponding to that of AldO Ala-105.

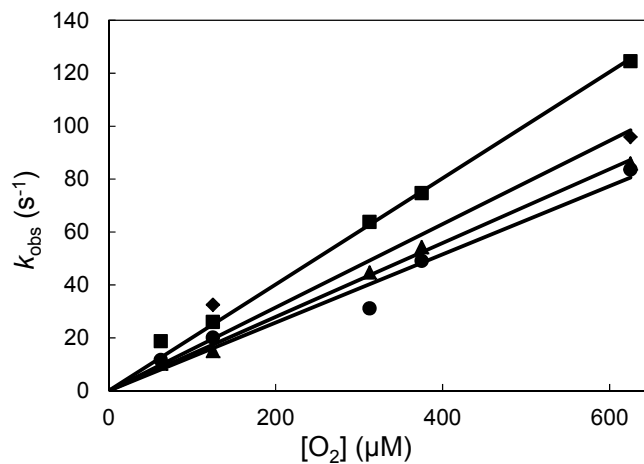


Figure 2.6 Measuring the reoxidation rate of AldO. Xylitol-reduced AldO variants (WT-AldO, ●; A105G-AldO, ■; A105S-AldO, ▲; A105T-AldO, ◆) were mixed with buffers containing various O₂ concentrations (62.5, 125, 312.5, 375 and 625 mM) in the stopped-flow spectrophotometer. The observed rates of flavin reoxidation are plotted against the O₂ concentrations. Second-order rate constants (k_{ox}) were calculated from the slope of the plots.

2.4 Discussion

We used an integrated computational and experimental procedure, combining X-ray crystallography, enhanced-statistics MD simulations, rapid kinetic experiments, and site-directed mutagenesis to shed light on how O₂ molecules diffuse into the active site of the flavoprotein oxidase AldO. In a parallel study, the same approach was used to examine the oxygen reactivity of C₂ monooxygenase, also a flavoprotein but one with a different catalytic activity and folding topology (39). In both simulated systems, distinct and multiple protein-guided O₂ diffusion pathways converge toward defined active site entry points, forming funnel architectures. The observation that a specific set of residues form entry sites for the access of oxygen to the flavin cofactor—Ala-105 in AldO and Phe-266 in C₂ monooxygenase—is consistent with what was recently reported for cholesterol oxidase (12) and sarcosine oxidase (50). However, this does not strictly imply the presence of individual diffusion pathways. Instead, our results suggest that multiple diffusion pathways, converging to a few key residues, are operative and represent a more effective structural model to combine high specificity and high kinetic efficiency in oxygen-using flavoenzymes. From a computational standpoint, we emphasize that in this work, O₂ diffusion was only solvent- or protein-guided—i.e., no biasing force was used to direct the reactants to the protein active sites. We stress, therefore, that a direct picture of the diffusion process at the atomic

scale was obtained *a priori* and only subsequently used as a prediction tool to design the experiments addressing oxygen reactivity.

The mutagenesis data confirms the notion that multiple diffusion pathways are active as single mutants did not have a significant effect on the O₂ reactivity of AldO. Only the A105G mutant displays a somewhat higher k_{ox} , which is in line with a role of this residue as gatekeeper. The original hypothesis that a single bulky mutation at position Ala-105 can (completely) block the access of oxygen to the reactive C4a locus was not shown here; in fact the oxygen reactivity of the mutant with the largest side chain at position 105, A105T-AldO, was still comparable to that of the WT-AldO. Another, more subtle effect could be at play, however; the oxygen reactivity that is required for the covalent flavinylation of the protein. It was observed that for progressively larger side chains at position 105 the yield of protein dropped substantially from 350 mg per litre of culture volume for WT-AldO to 25 mg for A105S-AldO to 3.5 mg for A105T-AldO; a 100-fold drop in yield. A105I-AldO, which contains an even larger side chain substitution, was expressed in such low amounts that it could not be purified and only activity in cell free extracts was detected (data not shown). From earlier work it is known (51, 52) that the maturation of covalent flavoenzymes is an autocatalytic process whereby the covalent linkage between the FAD cofactor and the protein backbone is formed after correct folding of the protein and concomitant incorporation of FAD. The mechanism for covalent flavinylation involves the reduction of the FAD cofactor, which subsequently requires molecular oxygen to be reoxidized. Our finding that successively larger side chain substitutions at position 105 drastically reduces the yield of soluble and correctly folded AldO supports the hypothesis that Ala105 is a crucial residue as a gatekeeper for oxygen reactivity, not only during catalysis but also for correct folding and maturation of the protein. Although larger substitutions at position 105 of AldO do not appear to have a huge effect the O₂ reactivity of the correctly folded, mature protein, they do, however, have a profound effect on the covalent incorporation of FAD, which is a post-translational modification that requires good oxygen reactivity. Variants with bulky side chains at position 105 are less efficient at incorporating covalent FAD, resulting in much reduced protein yields.

Our observations are also relevant to the understanding of the reaction mechanism of oxygen with reduced flavin (3, 26). MD simulations indicate that O₂ is specifically able to reach the flavin C4a atom both in AldO (Figure 2.3) and C₂ monooxygenase (39). This implies that—independent of the nature of the enzymatic reaction—O₂ would react with the flavin by direct contact with the C4a atom of the cofactor. In this scenario, the C4a atom appears to be the locus directly involved in the electron transfer from the reduced cofactor to O₂, which is consistent with isotope

effect studies performed on glucose oxidase (29). The combination of our data with the results obtained by site-directed mutagenesis on various other flavoenzymes (49, 50) indicates that the difference among dehydrogenases, monooxygenases, and oxidases ultimately resides in the fine modulation of the local environment embedding the C4a atom; its accessibility, the distribution of charged and polar groups to favour electron transfer between reduced flavin and O₂, and the extent to which the oxygen cavity is capable of stabilizing the C4a-hydroperoxyflavin.

2.5 Acknowledgments

We acknowledge A. Westerbeek for supplying the modified pBAD-NtermHis expression vector. This work was supported by the Dutch Technology Foundation Stichting Technische Wetenschappen Grant 7726, the Nederlandse Organisatie voor Wetenschappelijk Onderzoek applied science division, the Technology Program of the Ministry of Economic Affairs and the EU-FP7 “Oxygreen” project.

2.6 References

1. **Que L Jr & Tolman WB** (2008) Biologically inspired oxidation catalysis. *Nature* **455**: 333–340.
2. **Perutz MF** (1979) Regulation of oxygen affinity of hemoglobin: Influence of structure of the globin on the heme iron. *Annu Rev Biochem* **48**: 327–386.
3. **Massey V** (1994) Activation of molecular oxygen by flavins and flavoproteins. *J Biol Chem* **269**: 22459–22462.
4. **Zou S, Baskin JS & Zewail AH** (2002) Molecular recognition of oxygen by protein mimics: Dynamics on the femtosecond to microsecond time scale. *Proc Natl Acad Sci USA* **99**: 9625–9630.
5. **Calhoun DB, Vanderkooi JM, Woodrow GV III & Englander SW** (1983) Penetration of dioxygen into proteins studied by quenching of phosphorescence and fluorescence. *Biochemistry* **22**: 1526–1532.
6. **Calhoun DB, Vanderkooi JM & Englander SW** (1983) Penetration of small molecules into proteins studied by quenching of phosphorescence and fluorescence. *Biochemistry* **22**: 1533–1539.
7. **Johnson BJ, Cohen J, Welford RW, Pearson AR, Schulten K, Klinman JP & Wilmot CM** (2007) Exploring molecular oxygen pathways in *Hansenula polymorpha* copper-containing amine oxidase. *J Biol Chem* **282**: 17767–17776.
8. **Saam J, Ivanov I, Walther M, Holzhutter HG & Kuhn H** (2007) Molecular dioxygen enters the active site of 12/15-lipoxygenase via dynamic oxygen access channels. *Proc Natl Acad Sci USA* **104**: 13319–13324.
9. **Chen L, Lyubimov AY, Brammer L, Vrielink A & Sampson NS** (2008) The Binding and release of oxygen and hydrogen peroxide are directed by a hydrophobic tunnel in cholesterol oxidase. *Biochemistry* **47**: 5368–5377.
10. **Koutsoupakis K, Stavrakis S, Soulimane T & Varotsis C** (2003) Oxygen-linked equilibrium CuB-CO species in cytochrome ba₃ oxidase from *Thermus thermophilus*. Implications for an oxygen channel at the CuB site. *J Biol Chem* **278**: 14893–14896.

11. **Lario PI, Sampson N & Vrielink A** (2003) Sub-atomic resolution crystal structure of cholesterol oxidase: What atomic resolution crystallography reveals about enzyme mechanism and the role of the FAD cofactor in redox activity. *J Mol Biol* **326**: 1635–1650.
12. **Piubelli L, Pedotti M, Molla G, Feindler-Boeckh S, Ghisla S, Pilone MS & Pollegioni L.** (2008) On the oxygen reactivity of flavoprotein oxidases: An oxygen access tunnel and gate in *Brevibacterium sterolicum* cholesterol oxidase. *J Biol Chem* **283**: 24738–24747.
13. **Riistama S, Puustinen A, García-Horsman A, Iwata S, Michel H & Wikström M.** (1996) Channelling of dioxygen into the respiratory enzyme. *Biochim Biophys Acta* **1275(1-2)**: 1–4.
14. **Elber R & Karplus M** (1990) Enhanced sampling in molecular dynamics: Use of the time-dependent hartree approximation for a simulation of carbon monoxide diffusion through myoglobin. *J Am Chem Soc* **112**: 9161–9175.
15. **Lakowicz JR & Weber G** (1973) Quenching of fluorescence by oxygen. A probe for structural fluctuations in macromolecules. *Biochemistry* **12**: 4161–4170.
16. **Jameson DM, Gratton E, Weber G & Alpert B** (1984) Oxygen distribution and migration within Mbdes Fe and Hbdes Fe. Multifrequency phase and modulation fluorometry study. *Biophys J* **45**: 795–803.
17. **Chu K, Vojtchovský J, McMahon BH, Sweet RM, Berendzen J & Schlichting I.** (2000) Structure of a ligand-binding intermediate in wild-type carbonmonoxy myoglobin. *Nature* **403**: 921–923.
18. **Widboom PF, Fielding EN, Liu Y & Bruner SD** (2007) Structural basis for cofactor independent dioxygenation in vancomycin biosynthesis. *Nature* **447**: 342–345.
19. **Schotte F, Lim M, Jackson TA, Smirnov AV, Soman J, Olson JS, Phillips GN Jr, Wulff M & Anfinrud PA** (2003) Watching a protein as it functions with 150-ps time-resolved X-ray crystallography. *Science* **300**: 1944–1947.
20. **Koder RL, Anderson JL, Solomon LA, Reddy KS, Moser CC & Dutton PL** (2009) Design and engineering of an O₂ transport protein. *Nature* **458**: 305–309.
21. **Hofacker I & Schulten K** (1998) Oxygen and proton pathways in cytochrome *c* oxidase. *Proteins* **30**: 100–107.
22. **Cohen J, Kim K, Posewitz M, Ghirardi ML, Schulten K, Seibert M & King P** (2005) Molecular dynamics and experimental investigation of H₂ and O₂ diffusion in [Fe]-hydrogenase. *Biochem Soc Trans* **33(Pt 1)**: 80–82.
23. **Cohen J, Kim K, King P, Seibert M & Schulten K** (2005) Finding gas diffusion pathways in proteins: Application to O₂ and H₂ transport in CpI [FeFe]-hydrogenase and the role of packing defects. *Structure* **13**: 1321–1329.
24. **Masgrau L, Roujeinikova A, Johannissen LO, Hothi P, Basran J, Ranaghan KE, Mulholland AJ, Sutcliffe MJ, Scrutton NS & Leys D** (2006) Atomic description of an enzyme reaction dominated by proton tunneling. *Science* **312**: 237–241.
25. **Hummer G, Schotte F & Anfinrud PA** (2004) Unveiling functional protein motions with picosecond X-ray crystallography and molecular dynamics simulations. *Proc Natl Acad Sci USA* **101**: 15330–15334.
26. **Mattevi A** (2006) To be or not to be an oxidase: Challenging the oxygen reactivity of flavoenzymes. *Trends Biochem Sci* **31**: 276–283.
27. **Massey V** (1995) Introduction: Flavoprotein structure and mechanism. *FASEB J* **9**: 473–475.
28. **Sucharitakul J, Prongjit M, Haltrich D & Chaiyen P** (2008) Detection of a C4a hydroperoxyflavin intermediate in the reaction of a flavoprotein oxidase. *Biochemistry* **47**: 8485–8490.

29. Roth JP, Wincek R, Nodet G, Edmondson DE, McIntire WS & Klinman JP (2004) Oxygen isotope effects on electron transfer to O₂ probed using chemically modified flavins bound to glucose oxidase. *J Am Chem Soc* **126**: 15120–15131.
30. Pau MY, Lipscomb JD & Solomon EI (2007) Substrate activation for O₂ reactions by oxidized metal centers in biology. *Proc Natl Acad Sci USA* **104**: 18355–18362.
31. Forneris F, Heuts DP, Delvecchio M, Rovida S, Fraaije MW & Mattevi A (2008) Structural analysis of the catalytic mechanism and stereoselectivity in *Streptomyces coelicolor* alditol oxidase. *Biochemistry* **47**: 978–985.
32. Adcock SA & McCammon JA (2006) Molecular dynamics: Survey of methods for simulating the activity of proteins. *Chem Rev* **106**: 1589–1615.
33. van Gunsteren WF, Bakowies D, Baron R, Chandrasekhar I, Christen M, Daura X, Gee P, Geerke DP, Glättli A, Hünenberger PH, Kastenholz MA, Oostenbrink C, Schenk M, Trzesniak D, van der Vegt NF & Yu HB (2006) Biomolecular modeling: goals, problems, perspectives. *Angew Chem Int Ed Engl* **45**: 4064–4092.
34. Alfieri A, Fersini F, Ruangchan N, Prongjit M, Chaiyen P & Mattevi A (2007) Structure of the monooxygenase component of a two component flavoprotein monooxygenase. *Proc Natl Acad Sci USA* **104**: 1177–1182.
35. Christen M, Hünenberger PH, Bakowies D, Baron R, Bürgi R, Geerke DP, Heinz TN, Kastenholz MA, Kräutler V, Oostenbrink C, Peter C, Trzesniak D & van Gunsteren WF (2005) The GROMOS software for biomolecular simulation: GROMOS05. *J Comput Chem* **26**: 1719–1751.
36. Oostenbrink C, Villa A, Mark AE & van Gunsteren WF (2004) A biomolecular force field based on the free enthalpy of hydration and solvation: The GROMOS force-field parameter sets 53A5 and 53A6. *J Comput Chem* **25**: 1656–1676.
37. Åqvist J (1990) Ion Water Interaction Potentials Derived from Free-Energy Perturbation Simulations. *J Phys Chem* **94**: 8021–8024.
38. Berendsen HJC (1981) Interaction Models for Water in Relation to Protein Hydration (Pullman, Dordrecht, The Netherlands).
39. Baron R, Riley C, Chenprakhon P, Thotsaporn K, Winter RT, Alfieri A, Forneris F, van Berkel WJ, Chaiyen P, Fraaije MW, Mattevi A & McCammon JA (2009) Multiple pathways guide oxygen diffusion into flavoenzyme active sites. *Proc Natl Acad Sci U S A*. **106**:10603-10608.
40. Heinz TN & Hunenberger PH (2004) A fast pairlist-construction algorithm for molecular simulations under periodic boundary conditions. *J Comput Chem* **25**: 1474–1486.
41. De Lano WL (2002) Pymol (DeLano Scientific, Palo Alto, CA).
42. Humphrey W, Dalke A & Schulten K (1996) VMD: Visual molecular dynamics. *J Mol Graphics* **14**: 33–38, 27–38.
43. Heuts DP, van Hellemond EW, Janssen DB & Fraaije MW (2007) Discovery, characterization, and kinetic analysis of an alditol oxidase from *Streptomyces coelicolor*. *J Biol Chem* **282**: 20283–20291.
44. van Bloois E, Torres Pazmiño DE, Winter RT & Fraaije MW (2010) A robust and extracellular heme-containing peroxidase from *Thermobifida fusca* as prototype of a bacterial peroxidase superfamily. *Appl Microbiol Biotechnol* **86**: 1419–1430.
45. Frederico R, Angelini R, Ercolini L, Venturini G, Mattevi A & Ascenzi P (1997) Competitive inhibition of swine kidney copper amine oxidase by drugs: amiloride, clonidine, and gabexate mesylate. *Biochem Bioph Res Co* **240**: 150–152.
46. de Jong E, van Berkel WJ, van der Zwan RP & de Bont JA (1992) Purification and characterization of vanillyl-alcohol oxidase from *Penicillium simplicissimum*. A novel aromatic alcohol oxidase containing covalently bound FAD. *Eur J Biochem* **208**: 651–657.

47. **Leferink NG, Heuts DP, Fraaije MW & van Berkel WJ** (2008) The growing VAO flavoprotein family. *Arch Biochem Biophys* **474**: 292–301.
48. **Winter RT, Heuts DP, Popken P, van Bloois E & Fraaije MW** (2008) Exploring the oxygen reactivity of alditol oxidase from *Streptomyces coelicolor*. In: *Flavins and Flavoproteins* (Frago, S., ed.) 237-242.
49. **Leferink NG, Fraaije MW, Joosten HJ, Schaap PJ, Mattevi A & van Berkel WJ** (2009) Identification of a gatekeeper residue that prevents dehydrogenases from acting as oxidases. *J Biol Chem* **284**: 4392–4397.
50. **Zhao G, Bruckner RC & Jorns MS** (2008) Identification of the oxygen activation site in monomeric sarcosine oxidase: role of Lys265 in catalysis. *Biochemistry* **47**: 9124–9135.
51. **Heuts DP, Scrutton NS, McIntire WS & Fraaije MW** (2009) What's in a covalent bond? On the role and formation of covalently bound flavin cofactors. *FEBS J* **276**: 3405-3427.
52. **Jin J, Mazon H, van den Heuvel RH, Heck AJ, Janssen DB & Fraaije MW** (2008) Covalent flavinylation of vanillyl-alcohol oxidase is an autocatalytic process. *FEBS J* **275**(20): 5191-5200.

Chapter 3

Export of *S. coelicolor* alditol oxidase to the periplasm and surface of *E. coli*

Remko T. Winter, Edwin van Bloois, Dick B. Janssen and Marco W. Fraaije

Laboratory of Biochemistry, Groningen Biomolecular Sciences and Biotechnology Institute,
University of Groningen, Nijenborgh 4, 9747 AG Groningen, The Netherlands

This chapter is based on:
Applied Microbiology and Biotechnology (2009) **83**: 679-687

Abstract

Streptomyces coelicolor A3(2) alditol oxidase (AldO) is a soluble monomeric flavoprotein in which the flavin cofactor is covalently linked to the polypeptide chain. AldO displays high reactivity towards different polyols such as xylitol and sorbitol. These characteristics make AldO industrially relevant, but full biotechnological exploitation of this enzyme is at present restricted by laborious and costly purification steps. To eliminate the need for enzyme purification, this study describes a whole-cell AldO biocatalyst system. To this end, we have directed AldO to the periplasm or cell surface of *Escherichia coli*. For periplasmic export, AldO was fused to endogenous *E. coli* signal sequences known to direct their passenger proteins into the SecB, signal recognition particle (SRP), or Twin-arginine translocation (Tat) pathway. In addition, AldO was fused to an ice nucleation protein (INP)-based anchoring motif for surface display. The results show that Tat-exported AldO and INP-surface-displayed AldO are active. The Tat-based system was successfully employed in converting xylitol by whole cells, whereas the use of the INP-based system was most likely restricted by lipopolysaccharides (LPS) in wild-type cells. It is anticipated that these whole-cell systems will be a valuable tool for further biological and industrial exploitation of AldO and other cofactor-containing enzymes.

3.1 Introduction

Carbohydrate oxidases oxidize their substrates with excellent regio- and/or enantioselectivity, which makes these enzymes of considerable industrial value. This is nicely illustrated by their use in diagnostics (biosensors for blood sugar) and in the food and drink industry (sweeteners and flavours) (1). Most carbohydrate oxidases belong to a distinct subgroup of sequence-related flavoproteins, namely the vanillyl-alcohol oxidase (VAO) family. Members of this family are characterized by a similar overall structure comprising a FAD binding domain and a substrate binding domain (2, 3). Recently, we identified a novel member of the VAO family in the proteome of *Streptomyces coelicolor* A3(2), called AldO (alditol oxidase). AldO is a soluble monomeric flavoprotein of 45.1 kDa in which the flavin cofactor is covalently linked to the polypeptide chain (4). The covalent anchoring of the FAD cofactor is an autocatalytic process that takes place in the cytoplasm and will only occur upon correct folding of the polypeptide chain. Therefore, the covalently incorporated FAD can be used as a folding reporter. AldO catalyses the C1 oxidation of several polyols, such as xylitol and sorbitol (4). The recent determination of its atomic structure at a resolution of 1.1 Å has revealed the structural features that determine the catalytic mechanism and substrate specificity of AldO (5).

AldO is industrially relevant and can be used in various applications. At present, biotechnological exploitation of this enzyme is restricted by costly and laborious purification steps. It is therefore desirable to eliminate the need for enzyme purification by using a whole-cell biocatalyst system. The use of AldO in such a system, however, is limited by the accessibility of substrates. Several strategies have been presented for *Escherichia coli*-based whole-cell biocatalyst systems to increase the accessibility of substrates. These include transport of foreign proteins to the periplasm and/or display at the cell surface (6–8).

Proteins that function outside the cytoplasm (secretory proteins) can be exported to the periplasm of *E. coli* by different pathways. The vast majority of secretory proteins are exported across the inner membrane in an unfolded state via the Sec-translocon, which works as a protein conducting channel (9). Most secretory proteins are targeted to the Sec-translocon in a posttranslational fashion by the chaperone SecB in concert with the ATPase SecA, which drives protein translocation (10, 11). A subset of secretory proteins is targeted to the Sec-translocon in a co-translational fashion that involves the signal recognition particle (SRP) and its receptor FtsY (12). In contrast to the Sec-translocon, the Twin-arginine translocation (Tat) system is able

to export folded and often cofactor-containing secretory proteins to the periplasm posttranslationally (13).

Various systems have been described for display of foreign proteins on the surface of *E. coli*, including phage display and systems based on anchoring motifs derived from outer membrane proteins, lipoproteins, or auto-transporters (6, 8, 14). One such recently explored anchoring motif is derived from the ice-nucleation protein (INP) InaK from *Pseudomonas syringae*. This protein is attached to the cell surface by a glycosyl-phosphatidylinositol (GPI) anchor and comprises three structurally different domains: the non-repetitive N- and C-terminal domains and a repetitive central domain (15, 16). Both full-length INP and a truncated variant lacking the central repeating domain are able to facilitate the surface display of foreign proteins, indicating that the non-repetitive domains are required for targeting and anchoring to the cell surface. As several studies have demonstrated, an INP derivative constituting the N- and C-terminal domains can be used to display foreign proteins on the surface of *E. coli* (17–24; for review see 8).

In the present study, we have developed a whole-cell AldO biocatalyst system by directing AldO to the periplasm or cell surface of *E. coli*. For the transport across the inner membrane, we have explored several export systems. For periplasmic transport, AldO was fused to endogenous *E. coli* Sec and Tat signal sequences. A truncated INP derivative was used for surface display of AldO. The export of these constructs was analysed by cellular fractionation and immunoblotting. Additionally, cellular fractions were assayed for oxidase activity. The results show that Tat-exported AldO and INP-surface-displayed AldO are active. The Tat-based system was successfully employed in converting xylitol by whole cells, whereas the use of the INP-based system was most likely restricted by LPS in wild-type cells. It is anticipated that these whole-cell systems, cells decorated with the biocatalyst of interest, will be a valuable tool for further biological and industrial exploitation of AldO and other cofactor-containing enzymes.

3.2 Materials and methods

3.2.1 Reagents, enzymes and sera

Restriction enzymes were from Roche Applied Science and New England Biolabs. Expand long template polymerase chain reaction (PCR) system and *Pfu* DNA polymerase was from Roche Applied Science and Invitrogen. Enhanced chemiluminescence (ECL) Western blotting detection reagent was from Amersham Biosciences. Horseradish peroxidase was from Fluka. All other chemicals were supplied by Sigma and of analytical grade. Antiserum against AldO was raised in a

rabbit against the purified native protein and was prepared by Innovagen (Lund, Sweden). OmpA and DsbA antisera were kind gifts of H.D. Bernstein and J. Beckwith, respectively. DnaK antiserum was kindly provided by A. Mogk. Antiserum against riboflavin was from Abcam.

3.2.2 Strains, plasmids, and growth conditions

E. coli strains MC1061 (25) and TOP10 (Invitrogen) were used as routine hosts for all plasmid constructs. Strains MC1061 and MC4100 (26) were used for subcellular localization experiments and whole cell-based conversions of xylitol. The *waaC* null mutant JW3596-1 (GGSC no. 11805) has been described previously (27) and was obtained from the *E. coli* genetic stock centre. JW3596-1 was used for the whole cell-based conversion of xylitol.

The plasmids pBAD-AldO and pBAD-MBP-AldO have been described earlier (4). The different signal sequence chimeras were constructed as follows. For transport via the Tat pathway, the signal sequence of TorA and the first four amino acid residues of the mature protein were PCR-amplified from *E. coli* K-12 genomic DNA. The PCR product was cloned *NdeI/EcoRI* into pBAD-MBP-AldO, thereby replacing the N-terminal MBP tag and yielding pBAD-Tat-AldO. The plasmid pBAD-Sec-AldO, encoding a *malE* signal sequence-AldO hybrid, was obtained in a similar fashion after PCR amplification of the *malE* signal sequence using pMal-p2X (New England Biolabs) as template. SRP-AldO was obtained by PCR from pBAD-MBP-AldO as template and using a forward primer that included the codons for the DsbA signal sequence and the first two residues of the mature protein. The PCR product was cloned into pBAD (Invitrogen), yielding pBAD-SRP-AldO. For cell surface display of AldO, a truncated variant of the *inaK* gene comprising the N- and C-terminal domains was synthesized by Sloning BioTechnology (München, Germany) and subsequently cloned *NdeI/EcoRI* into vector pBAD-MBP-AldO, thereby replacing the N-terminal MBP tag and yielding pBAD-INP-AldO. Nucleotide sequences were verified by DNA sequencing (GATC-Biotech, Constance, Germany). Primer sequences are available upon request.

Cultures were grown to saturation at 37°C overnight. The following day, overnight cultures were back-diluted 1:100 into fresh media containing 0.02% l-arabinose to induce the expression of AldO or its derivatives and grown for 48 h at 17°C. All strains were routinely grown in Luria-Bertani medium (per litre, 10 g tryptone, 5 g yeast extract, 5 g NaCl) under aerobic conditions unless indicated otherwise. Where appropriate, ampicillin (100 µg/ml) or kanamycin (5 µg/ml) were added to the culture medium.

3.2.3 Cell fractionations

Cells expressing AldO or its signal sequence derivatives were grown as described above. 15 to 20 OD₆₆₀ units of cells were harvested and fractionated into a spheroplast and periplasmic fraction as described (28). The cytoplasmic fraction was obtained as follows. After disruption of the spheroplasts by sonication and a brief clarifying spin, the clarified lysate was ultracentrifuged (100,000×*g* for 40 min at 4°C) and the supernatant was taken as the cytoplasmic fraction. Cells expressing INP-AldO were grown as described above. 75 OD₆₆₀ units of cells were harvested and disrupted by sonication. The soluble, total membrane, inner membrane, and outer membrane fractions were obtained as described (29). In both fractionation procedures, proteins were precipitated by trichloroacetic acid and analysed by sodium dodecyl sulphate-polyacrylamide gel electrophoresis (SDS-PAGE) and immunoblotting.

3.2.4 SDS-PAGE and immunoblotting

Cellular fractions were normalized on the basis of the OD₆₆₀, and samples of these fractions containing equal OD₆₆₀ units were analysed on standard 12% SDS-PAGE gels. Proteins were transferred to nitrocellulose membrane (Amersham Biosciences) using a semidry apparatus from Bio-Rad. Immunodetection was performed using the primary antisera described above, a secondary horseradish-peroxidase-coupled antiserum (Rockland), and the ECL system from Amersham Biosciences (according to the instructions of the manufacturer). Proteins were visualized using the Fujifilm LAS-3000 imaging system.

3.2.5 Analytical methods

The oxidase activity of cellular fractions and whole cells expressing Tat-AldO or INP-AldO was determined by coupling the production of H₂O₂ by AldO or its derivatives to a horseradish-peroxidase-mediated oxidation of 4-aminoantipyrine and 3,5-di-chloro-2-hydroxybenzenesulfonic acid. The resulting pink adduct can be detected spectrophotometrically at 515 nm ($\epsilon_{515} = 26 \text{ mM}^{-1} \text{ cm}^{-1}$, 30). For the detection of oxidase activity phosphate-buffered saline (pH 7.4) was used as assay buffer containing 0.1 mM 4-aminoantipyrine, 1 mM 3,5-di-chloro-2-hydroxybenzenesulfonic acid, 3 U horseradish peroxidase, 5 mM xylitol, 0.01 OD₆₆₀ units of cells (expressing Tat-AldO or INP-AldO) or samples of cellular fractions. Prior to the analysis of oxidase activity, total membrane fractions were detergent-solubilized (2% n-dodecyl- β -D-maltoside). Alkaline phosphatase activity was measured spectrophotometrically at 405 nm (31) using Tris-buffered saline (pH 7.4) as assay buffer containing 1.2 $\mu\text{g } \mu\text{l}^{-1}$ phosphatase substrate (Sigma; $\epsilon_{405} = 12.5 \text{ mM}^{-1} \text{ cm}^{-1}$) and 0.02 OD₆₆₀ units of cells

(expressing INP-AldO). All activity measurements were performed at ambient temperature, and where appropriate 5 mM MgCl₂ was included in the assay buffer to stabilize the outer membrane.

3.3 Results

3.3.1 Design of fusion constructs and experimental strategy

Here, we have developed a whole-cell AldO biocatalyst system by directing *S. coelicolor* AldO to the periplasm or cell surface of *E. coli*. For periplasmic transport, we have fused AldO N-terminally to the signal sequences of the endogenous *E. coli* proteins MalE, DsbA, or TorA, known to direct their substrates into the SecB, SRP, or Tat pathway, respectively (32–34). Additionally, we have used a truncated INP variant comprising the InaK N- and C-terminal domain and lacking the central repeating domain for surface display. This INP derivative was fused N-terminally to AldO (Table 3.1). All fusions are based on a cassette system (Figure 3.1) in which the coding region of *aldo* is cloned *EcoRI/HindIII* downstream of the indicated export signal, giving rise to Sec-AldO, SRP-AldO, Tat-AldO and INP-AldO. Wild-type AldO, lacking a signal sequence, is included in the present study as a negative control. Expression of all constructs is under control of the arabinose-inducible P_{BAD} promoter, allowing moderate overexpression to prevent saturation of export pathways and accompanying cell toxicity.

Table 3.1 Sequences of export signals used in this study.

Signal peptide	Sequence
MalE	MKIKTGARILALSALTTMMFSASALA
DsbA	MKKIWLALAGLVLAFSASAAQ
TorA	MNNNDLFQASRRRFLAQLGGLTVAGMLGPSLLTPRRATAAQAA
INP (InaK _{NC})	MTLDKALVLRTCANNMADHCGLIWPASGTVESRYWQSTRRHENGLVGLLWGAGTSA FLSVHADARWIVCEVAVADIISLEEPGMVKFPRAEVVHVGDRISASHFISARQADPAST STSTSTSTLTPMPTAIPTPMPAVASVTLPVAEQARHEVFDVASVSAAAAPVNTLPVTTP QNLQTATYGSTLSGDNHSRLIAGYGSNETAGNHSDLIGGHDCTLMAGDQSRLTAGKN SVLTAGARSKLIGSEGSTLSAGEDSTLIFRLWDGKRYRQLVARTGENGV EADIPYYVN EDDDIVDKPDEDDDWIEVK

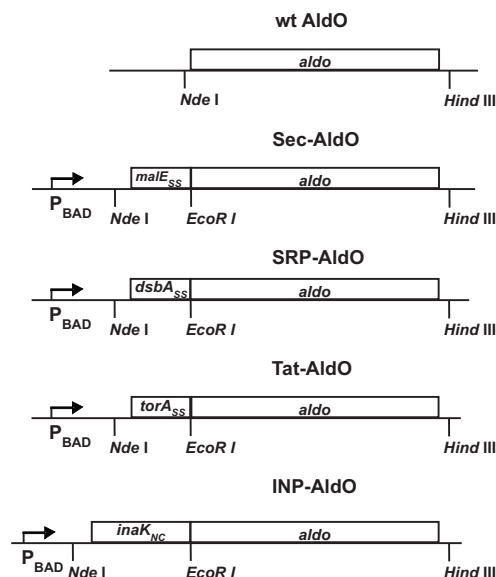


Figure 3.1 Schematic representation of the hybrid constructs used in this study. All fusions were constructed as described in *Materials and methods*. For Sec-dependent export, AldO was fused to the signal sequences (ss) of MalE or DsbA, resulting in Sec-AldO or SRP-AldO, respectively. For export by the Tat-system, AldO was fused to the signal sequence of TorA, yielding Tat-AldO. AldO was fused to a truncated variant of INP comprising the N- and C-terminal domains for surface display. This construct was termed INP-AldO. Expression of all constructs is driven from an arabinose-inducible P_{BAD} promoter and relevant restriction sites are indicated.

Previous work indicated that AldO expressed in *E. coli* is a soluble protein in agreement with a cytoplasmic localization as predicted by PSORT (4, 35). To unambiguously assess its cellular localization, we first studied the localization of wild-type AldO in *E. coli*. Therefore, cells expressing wild-type AldO were grown to saturation at 17°C, harvested, converted to spheroplasts by EDTA/lysozyme treatment, after which the periplasmic fraction was obtained by osmotic shock. Subsequently, the spheroplasts were disrupted by sonication and subjected to ultracentrifugation to obtain the cytoplasmic fraction. The different subcellular fractions were analysed by immunoblotting using antisera directed against AldO or riboflavin to study (i) the AldO content of the samples and (ii) whether AldO contained covalently bound FAD. Figure 3.2a shows that wild-type AldO is cytoplasmically localized and contains covalently bound FAD as previously reported (4). This indicates that AldO is properly folded, as evidenced by the presence of covalent FAD, and functional, as confirmed by the detection of oxidase activity in the cytoplasmic fraction. As controls to monitor the efficiency of the fractionation procedure, the levels

of DnaK and DsbA, which serve as cytoplasmic or periplasmic marker, were analysed in the same samples by immunoblotting. The data show that DnaK is restricted to the cytoplasmic fraction and DsbA is mainly detected in the periplasmic fraction, demonstrating the efficiency of the fractionation procedure and thereby validating our assay conditions.

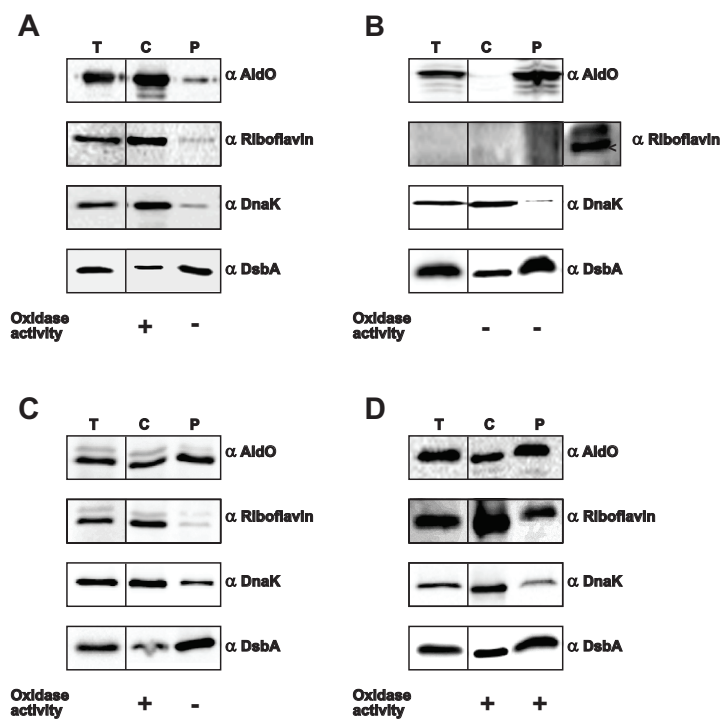


Figure 3.2 Subcellular localization of wild-type and signal sequence equipped AldO. Wild type AldO, (A); Sec-AldO, (B); SRP-AldO, (C); Tat-AldO, (D). *E. coli* cells expressing the indicated constructs were fractionated into total cells (T), cytoplasm (C), and periplasm (P). Samples were normalized on the basis of OD₆₆₀ and analysed by immunoblotting with the indicated antisera. Black lines indicate that intervening lanes have been spliced out. Oxidase activity in the cytoplasmic and periplasmic fraction was determined using xylitol as substrate. Plus sign (+), oxidase activity; minus sign (-), no oxidase activity.

3.3.2 Sec-dependent export of AldO to the periplasm

To examine whether AldO could be functionally transported to the periplasm via the Sec-translocon, AldO was fused to the MalE (Sec-AldO) or DsbA (SRP-AldO) signal sequence. First, we studied the export of Sec-AldO by cell fractionation and immunoblotting (Figure 3.2b). The results show that Sec-AldO is exported to the periplasm. However, Sec-AldO does not contain covalently bound FAD, unlike purified

wild-type AldO, which was included as a positive control (indicated by an arrowhead) in this immunoblot experiment. The absence of FAD indicates that Sec-exported AldO is not folded into its biologically active conformation which was verified by the lack of oxidase activity in the cytoplasmic and periplasmic fraction. Notably, the inability to covalently incorporate FAD destabilizes AldO, resulting in degradation and cytoplasmic aggregation of AldO as indicated by its co-fractionation with other insoluble proteins (data not shown). The efficiency of the fractionation procedure was confirmed by analysing the DnaK and DsbA levels in the same samples by immunoblotting.

Next, we investigated the periplasmic export of SRP-AldO using the same experimental setup as described above. Figure 3.2c shows that SRP-AldO is transported to the periplasm similar to Sec-AldO. Remarkably, a considerable amount of mature-sized AldO is present in the cytoplasmic fraction, which may result from degradation of the DsbA signal sequence by cytoplasmic proteases. This cytoplasmic population of mature-sized AldO contains covalently bound FAD, indicating that it is folded into its active conformation and displays oxidase activity as expected. In contrast, periplasmic AldO does not contain FAD and is not active. Control blots were performed using antisera against DnaK and DsbA, showing that the fractionation protocol is effective.

These results show that Sec-exported AldO is not active because FAD is not assembled properly into the protein. Apparently, cofactor incorporation is blocked due the inherent requirement of the protein to be unfolded for Sec-dependent export (9).

3.3.3 Tat-dependent export of AldO to the periplasm

In contrast to the Sec-translocon, the Tat-system is able to transport folded and often cofactor containing proteins to the periplasm (13). To test whether this pathway can be used for transport of active AldO to the periplasm, we fused AldO to the Tat signal sequence of TorA (Tat-AldO). The export of Tat-AldO was assayed by cell fractionation and immunoblotting. As shown in Figure 3.2d, a substantial proportion of AldO is clearly exported to the periplasm, whereas a considerable amount of mature-sized AldO is also present in the cytoplasmic fraction, which may result from cytoplasmic degradation of the TorA signal sequence as observed previously with a GFP-TorA signal sequence chimera and similar to SRP-AldO (Figure 3.2c; 36). Interestingly, the cytoplasmic and periplasmic populations of mature-sized AldO contain covalently linked FAD, indicating that AldO is folded into its active conformation as confirmed by the detection of oxidase activity in both fractions. The efficiency of the fractionation procedure was verified by analysing the DnaK and DsbA content in the same samples

by immunoblotting. In conclusion, these data show that AldO can be transported to the periplasm in an active form by the Tat pathway.

3.3.4 Surface display of AldO

AldO was displayed on the surface of *E. coli* using a truncated INP variant. To examine outer membrane localization of INP-AldO, cells expressing this construct were fractionated into a soluble (cytoplasm and periplasm) and total membrane fraction. The total membrane fraction was further separated into an inner membrane and outer membrane fraction by sarcosyl extraction (29). Samples were analysed by immunoblotting using the indicated antisera. Figure 3.3a shows that INP-AldO is detected in the cell extract, soluble fraction, and total membrane fraction. After sarcosyl extraction, INP-AldO is exclusively observed in the outer membrane fraction, suggesting that INP-AldO is indeed localized to the outer membrane. This is in agreement with other recent studies using INP for the surface display of foreign proteins in *E. coli* (18, 22, 23). Moreover, INP-AldO present in these fractions clearly contains covalently bound FAD. This indicates that INP-AldO is properly folded and functional as confirmed by the detection of oxidase activity in the cell extract, soluble fraction, and total membrane fraction. Unfortunately, no oxidase activity could be detected in the inner membrane and outer membrane fractions after sarcosyl extraction, probably due to inactivation of AldO by the detergent used. As controls to verify the efficiency of the fractionation protocol, OmpA and DsbA levels in the same samples were analysed by immunoblotting. OmpA, which serves as an outer membrane marker, is, as expected, mainly detected in the outer membrane fraction together with INP-AldO. DsbA, which serves as a soluble marker, is exclusively detected in the soluble fraction. Thus far, the data show that a considerable fraction of FAD-containing INP-AldO is present in outer membrane. However, these data do not confirm whether this protein is indeed surface-localized. To verify surface localization, the accessibility of INP-AldO towards exogenously added proteinase K on whole cells was tested. Samples were analysed by immunoblotting using the indicated antisera (Figure 3.3b). Clearly, INP-AldO is almost completely degraded after proteinase K treatment when compared to mock-treated cells. To monitor the integrity of the cells, we analysed the levels of the periplasmic protein DsbA in the same samples which were unaltered by proteinase K treatment. These data confirm that INP-AldO is indeed surface-localized.

Combined, the results show that AldO is successfully displayed at the surface of *E. coli* using a truncated INP variant. Notably, AldO presented at the cell surface contains covalently bound FAD, suggesting that it has attained a correctly folded and active conformation.

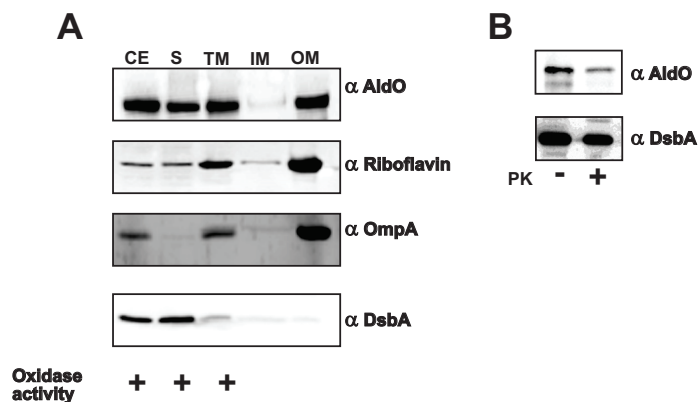


Figure 3.3 Subcellular localization of INP-AldO. (A) *E. coli* cells expressing INP-AldO were fractionated into a cell extract (CE), soluble (S), and total membrane (TM) fraction. The total membrane fraction was further separated into an inner membrane (IM) and outer membrane (OM) fraction by extraction with 0.5% sarcosyl. Samples were normalized on the basis of OD₆₆₀ and analysed by immunoblotting with the indicated antisera. Oxidase activity in the cell extract, soluble, and total membrane fraction was determined using xylitol as substrate. Plus sign (+), oxidase activity; minus sign (-), no oxidase activity. (B) Protease accessibility analysis of surface displayed INP-AldO. *E. coli* cells expressing INP-AldO were treated (plus sign, +) or mock-treated (minus sign, -) with proteinase K (PK) to degrade cell surface proteins. Samples were normalized on the basis of OD₆₆₀ and analysed by immunoblotting with the indicated antisera.

3.3.5 Whole-cell biocatalysis with periplasmic or surface-displayed AldO

The export of active AldO to the periplasm or cell surface is of considerable value as it may facilitate the use of these systems in whole-cell biocatalysis. As proof of principle, we therefore assayed spectrophotometrically whether wild-type *E. coli* cells expressing AldO, Tat-AldO, or INP-AldO could be successfully employed in the conversion of xylitol. A representative data set is shown in Figure 3.4. As expected, control cells expressing wild-type AldO did not show significant conversion of xylitol. This suggests that no substantial lysis of the cells has occurred under these conditions. Only upon permeabilization of the cells with toluene was significant conversion of xylitol observed, indicating that cytoplasmically localized, wild-type AldO is unable to react with xylitol, most likely because xylitol is unable to pass the inner membrane. In the absence of arabinose, no conversion is observed. Interestingly, xylitol is readily converted by cells expressing Tat-AldO. Permeabilization of these cells did not further improve oxidase activity. In contrast, cells expressing INP-AldO only displayed oxidase activity upon permeabilization by toluene, suggesting that the activity and/or substrate accessibility of INP-AldO is compromised in wild-type cells. From these data, we conclude that export of AldO to the periplasm by the Tat-system is a successful strategy for applying this protein in whole-cell biocatalysis.

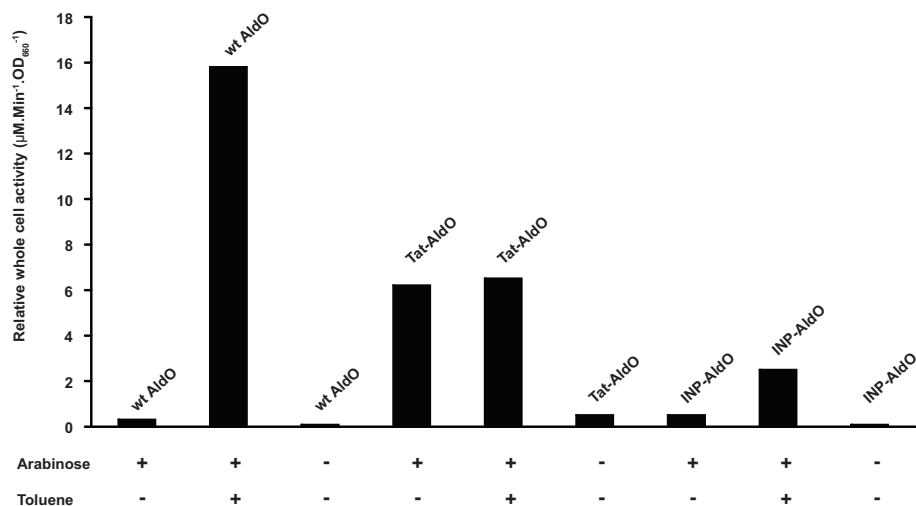


Figure 3.4 Conversion of xylitol by *E. coli* cells expressing Tat-AldO or INP-AldO. *E. coli* cells were grown in the absence or presence of arabinose to induce the expression of the indicated constructs; cells were harvested and resuspended in PBS. The conversion of xylitol, using equal amounts of cells, was monitored spectrophotometrically at room temperature. As a negative control, cells expressing wild-type (wt) AldO were included. Cells were permeabilized by the addition of 2% toluene, as indicated. The conversion of xylitol is given as the relative whole-cell activity normalized on the basis of OD₆₆₀

Cell-surface-displayed AldO, however, showed an unanticipated poor activity with xylitol. It is conceivable that prominent endogenous surface molecules, such as lipopolysaccharides (LPS), inhibit INP-AldO and/or restrict the accessibility of xylitol. To test whether AldO displayed on cells containing truncated LPS molecules is able to convert xylitol successfully, we used the *E. coli waaC* null strain JW3596-1 (27). The *waaC* gene product, a heptosyltransferase, plays a pivotal role in the early steps in the synthesis of the inner core region of LPS (37, 38). Consequently, *waaC*-deficient strains express truncated LPS molecules at the cell surface (37, 38). As before, wild-type cells expressing INP-AldO showed significant conversion of xylitol only upon permeabilization by toluene (Figure 3.5). In contrast, JW3596-1 cells expressing INP-AldO displayed significantly more oxidase activity without toluene treatment (Figure 3.5). Reassuringly, wild-type cells and JW3596-1 cells displayed comparable activities of the periplasmic enzyme alkaline phosphatase (Figure 3.6), indicating that the oxidase activity of JW3596-1 cells expressing INP-AldO is not due to leakage of periplasmic enzymes as has been reported for similar strains (37). Taken together, these data are in agreement with the notion that in wild-type cells, the use of cell-surface-displayed AldO in whole-cell biocatalysis is restricted by LPS.

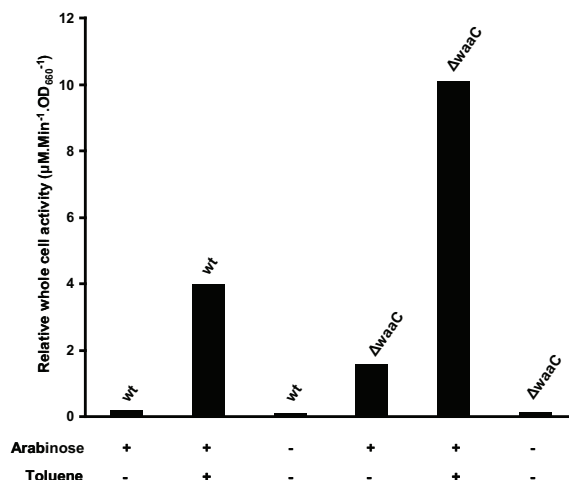


Figure 3.5 Conversion of xylitol by *E. coli* wt & $\Delta waaC$ cells expressing INP-AldO. *E. coli* wt and *waaC* null strain JW3596-1 cells were grown in the absence or presence of arabinose to induce the expression of INP-AldO. The *waaC* null strain expresses truncated LPS molecules on the cell surface, thus reducing the negative effect this prominent surface molecule has on the activity of INP-AldO and/or accessibility of xylitol. Cells were harvested and resuspended in PBS and the conversion of xylitol, using equal amounts of cells, was monitored spectrophotometrically at room temperature. Cells were permeabilized by the addition of 2% toluene, as indicated. The conversion of xylitol is given as the relative whole-cell activity normalized on the basis of OD₆₆₀.

3.4 Discussion

AldO is a recently discovered polyol flavoprotein oxidase that is primarily active with alditols. The enzyme displays exquisite stereoselectivity and is efficient in using molecular oxygen as oxidant (4). These characteristics render AldO a good candidate for further biotechnological exploitation, which is, at present, restricted by costly and laborious purification steps. In the present study, we have developed an *E. coli*-based whole-cell AldO biocatalyst system, eliminating the need for enzyme purification and enabling the full biotechnological exploitation of AldO. To increase substrate accessibility, which often constitutes a bottleneck in developing whole-cell biocatalyst systems, we directed AldO to the periplasm or cell surface of *E. coli*. For Sec-dependent export to the periplasm, we have fused AldO N-terminally to the endogenous *E. coli* signal sequences of MalE or DsbA. The MalE signal sequence, which directs its substrate into the posttranslational SecB pathway, is commonly used for the periplasmic transport of recombinant proteins (7, 32).

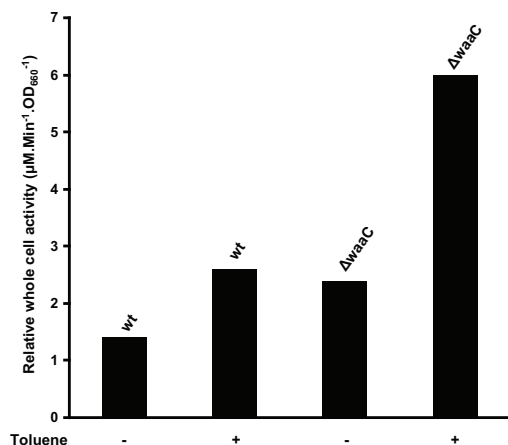


Figure 3.6 Periplasmic alkaline phosphatase activity of *E. coli* wt & $\Delta waaC$ cells. Both strains were expressing INP-AldO. *E. coli* wt and *waaC* null strain JW3596-1 cells were grown in the presence of arabinose to induce the expression of INP-AldO. Cells were harvested and resuspended in Tris-buffered saline (pH 7.4) and the conversion of phosphatase substrate (1.2 $\mu\text{g}/\mu\text{l}$, Sigma), using equal amounts of cells, was monitored spectrophotometrically at room temperature. Cells were permeabilized by the addition of 2% toluene, as indicated. The alkaline phosphatase activity is given as the relative whole-cell activity normalized on the basis of OD₆₆₀.

Although the DsbA signal sequence is less frequently used for this purpose, several studies have reported its successful application in directing passenger proteins to the periplasm via the co-translational SRP pathway (28, 33, 39). Additionally, we have fused AldO N-terminally to the signal sequence of TorA for Tat-dependent export to the periplasm. The TorA signal sequence is considered to be highly Tat-specific and is commonly employed for the transport of heterologous proteins to the periplasm (34, 40, 41). The export of these fusion constructs was examined by cellular fractionation and immunoblotting. The data show that all fusion constructs are directed to the periplasm. However, only Tat-exported AldO was fully active as shown by proper cofactor assembly and oxidase activity in the periplasmic fraction. Similarly, GFP, which is only able to fold in the cytoplasm, was transported to the *E. coli* periplasm when fused to a Sec or Tat signal sequence, but only Tat-exported GFP was active (36, 42). This result is explained by the export of proteins in a pre-folded, active conformation by the Tat system in contrast to Sec-dependent translocation (13). Therefore, our data reinforce the notion that the Tat system is dedicated to the export of pre-folded and often cofactor containing proteins to the periplasm.

Different systems have been described for display of foreign proteins on the cell surface of bacteria. For *E. coli*, these include phage display and systems based on surface anchoring motifs derived of outer membrane proteins, lipoproteins, and auto-transporters (6, 14, 16, 43). Most of these systems rely on the Sec-translocon for initial transport across the inner membrane. This requires the protein to be unfolded, which interferes with cofactor assembly and activity of AldO as indicated by our data, and therefore, these systems are ruled out for proper export. An alternative system based on an anchoring motif from the ice nucleation protein InaK from *P. syringae* is commonly used for surface display of foreign proteins in *E. coli*, such as viral antigens, single chain antibodies, and enzymes (17-24; for review see 8). The structural diversity of these surface-displayed proteins emphasizes the remarkable tolerance and flexibility of the INP system. INP is bound to the cell surface by a GPI anchor and comprises three structurally different domains: a non-repetitive N- and C-terminal domain and a central repetitive domain (15, 16). The molecular mechanism by which INP facilitates surface display is not clear as no signal sequence could be identified (44). In this respect, it is interesting to note that our data indicate that the export mechanism of INP most likely does not involve the Sec-translocon for translocation across the inner membrane, as surface-displayed INP-AldO contains covalently bound FAD and is functional in contrast to Sec-AldO and SRP-AldO. Different studies suggest that the non-repetitive domains are required for targeting and anchoring to the cell surface (18, 19, 23, 45). However, recent evidence indicates that the N-terminal domain alone is sufficient for cell surface display (22, 46). In the present work, we have used a truncated version of INP comprising the InaK N- and C-terminal domains for surface display of AldO in *E. coli*. The cellular localization of this construct was analysed by cellular fractionation and immunoblotting. The data show that INP-AldO is active as judged by the proper FAD incorporation and oxidase activity in the cell extract, soluble fraction, and total membrane fraction. As expected, INP-AldO is localized to the outer membrane and is surface-localized as demonstrated by its accessibility towards exogenously added proteinase K.

Compartmentalization of cells is employed by nature to create catalytically efficient environments as exemplified by the periplasmic or extracellular localization of enzymes in *E. coli*, which may be beneficial in cases where, for example, the substrate/product of interest cannot cross the membrane or where the substrate/product is also converted by another intracellular enzyme. Our data illustrate this by showing that wild-type *E. coli* cells expressing Tat-AldO are able to convert xylitol, whereas cells expressing wild-type AldO cannot. Surprisingly, cells expressing surface-displayed INP-AldO are unable to react with xylitol. Conceivably, INP-AldO may be inhibited and/or the accessibility of xylitol may be restricted in wild-

type cells by a prominent cell surface molecule, such as LPS. Indeed, surface-displayed AldO on cells of an *E. coli* mutant containing truncated LPS molecules was able to convert xylitol successfully, consistent with the idea that in wild-type cells, LPS restricts the availability of cell surface-displayed AldO for whole-cell biocatalysis.

These data nevertheless demonstrate proof of principle and will further the exploitation of AldO in broad biological and industrial applications. Furthermore, the strategies presented for periplasmic export and surface display are also applicable to other enzymes and, in particular, cofactor-containing enzymes.

3.5 Acknowledgments

This research is supported by the Dutch Technology Foundation STW, Applied Science Division of NWO, and the Technology Program of the Ministry of Economic Affairs.

3.6 References

1. **van Hellemond EW, Leferink NG, Heuts DP, Fraaije MW & van Berkel WJ** (2006) Occurrence and biocatalytic potential of carbohydrate oxidases. *Adv Appl Microbiol* **60**: 17–54.
2. **Fraaije MW, Van Berkel WJ, Benen JA, Visser J & Mattevi A** (1998) A novel oxidoreductase family sharing a conserved FAD-binding domain. *Trends Biochem Sci* **23**: 206–207.
3. **Leferink NG, Heuts DP, Fraaije MW & van Berkel WJ** (2008) The growing VAO flavoprotein family. *Arch Biochem Biophys* **474**: 292–301.
4. **Heuts DP, van Hellemond EW, Janssen DB & Fraaije MW** (2007) Discovery, characterization, and kinetic analysis of an alditol oxidase from *Streptomyces coelicolor*. *J Biol Chem* **282**: 20283–20291.
5. **Forneris F, Heuts DP, Delvecchio M, Rovida S, Fraaije MW & Mattevi A** (2008) Structural analysis of the catalytic mechanism and stereoselectivity in *Streptomyces coelicolor* alditol oxidase. *Biochemistry* **47**: 978–985.
6. **Samuelson P, Gunneriusson E, Nygren PA & Stahl S** (2002) Display of proteins on bacteria. *J Biotechnol* **96**:129–154.
7. **Mergulhao FJ, Summers DK & Monteiro GA** (2005) Recombinant protein secretion in *Escherichia coli*. *Biotechnol Adv* **23**:177–202.
8. **Van Bloois E, Winter RT, Kolmar H & Fraaije MW** (2011) Decorating microbes: surface display of proteins on *Escherichia coli*. *Trends Biotechnol* **29**: 79–86.
9. **Driessen AJ & Nouwen N** (2008) Protein translocation across the bacterial cytoplasmic membrane. *Annu Rev Biochem* **77**: 643–667.
10. **Vrontou E & Economou A** (2004) Structure and function of SecA, the preprotein translocase nanomotor. *Biochim Biophys Acta* **1694**: 67–80.
11. **Zhou J & Xu Z** (2005) The structural view of bacterial translocation-specific chaperone SecB: implications for function. *Mol Microbiol* **58**: 349–357.
12. **Luirink J & Sinning I** (2004) SRP-mediated protein targeting: structure and function revisited. *Biochim Biophys Acta* **1694**: 17–35.

13. **Lee PA, Tullman-Ercek D & Georgiou G** (2006) The bacterial twin-arginine translocation pathway. *Annu Rev Microbiol* **60**: 373–395.
14. **Lee SY, Choi JH & Xu Z** (2003) Microbial cell-surface display. *Trends Biotechnol* **21**: 45–52.
15. **Turner MA, Arellano F & Kozloff LM** (1991) Components of ice nucleation structures of bacteria. *J Bacteriol* **173**: 6515–6527.
16. **Graether SP & Jia Z** (2001) Modeling *Pseudomonas syringae* ice-nucleation protein as a beta-helical protein. *Biophys J* **80**: 1169–1173.
17. **Jung HC, Lebeault JM & Pan JG** (1998) Surface display of *Zymomonas mobilis* levansucrase by using the ice-nucleation protein of *Pseudomonas syringae*. *Nat Biotechnol* **16**: 576–580.
18. **Lee JS, Shin KS, Pan JG & Kim CJ** (2000) Surface-displayed viral antigens on Salmonella carrier vaccine. *Nat Biotechnol* **18**: 645–648.
19. **Shimazu M, Mulchandani A & Chen W** (2001) Cell surface display of organophosphorus hydrolase using ice nucleation protein. *Biotechnol Prog* **17**: 76–80.
20. **Cho CM, Mulchandani A & Chen W** (2002) Bacterial cell surface display of organophosphorus hydrolase for selective screening of improved hydrolysis of organophosphate nerve agents. *Appl Environ Microbiol* **68**: 2026–2030.
21. **Kang SM, Rhee JK, Kim EJ, Han KH & Oh JW** (2003) Bacterial cell surface display for epitope mapping of hepatitis C virus core antigen. *FEMS Microbiol Lett* **226**: 347–353.
22. **Li L, Kang DG & Cha HJ** (2004) Functional display of foreign protein on surface of *Escherichia coli* using N-terminal domain of ice nucleation protein. *Biotechnol Bioeng* **85**: 214–221.
23. **Wu PH, Giridhar R & Wu WT** (2006) Surface display of transglucosidase on *Escherichia coli* by using the ice nucleation protein of *Xanthomonas campestris* and its application in glucosylation of hydroquinone. *Biotechnol Bioeng* **95**: 1138–1147.
24. **Yim SK, Jung HC, Pan JG, Kang HS, Ahn T & Yun CH** (2006) Functional expression of mammalian NADPH-cytochrome P450 oxidoreductase on the cell surface of *Escherichia coli*. *Protein Expr Purif* **49**: 292–298.
25. **Casadaban MJ & Cohen SN** (1980) Analysis of gene control signals by DNA fusion and cloning in *Escherichia coli*. *J Mol Biol* **138**: 179–207.
26. **Casadaban MJ** (1976) Transposition and fusion of the *lac* genes to selected promoters in *Escherichia coli* using bacteriophage lambda and mu. *J Mol Biol* **104**: 541–555.
27. **Baba T, Ara T, Hasegawa M, Takai Y, Okumura Y, Baba M, Datsenko KA, Tomita M, Wanner BL & Mori H** (2006) Construction of *Escherichia coli* K-12 in-frame, single-gene knockout mutants: the Keio collection. *Mol Syst Biol* **2**: 2006.0008.
28. **Huber D, Boyd D, Xia Y, Olma MH, Gerstein M & Beckwith J** (2005) Use of thioredoxin as a reporter to identify a subset of *Escherichia coli* signal sequences that promote signal recognition particle-dependent translocation. *J Bacteriol* **187**: 2983–2991.
29. **Filip C, Fletcher G, Wulff JL & Earhart CF** (1973) Solubilization of the cytoplasmic membrane of *Escherichia coli* by the ionic detergent sodium-lauryl sarcosinate. *J Bacteriol* **115**: 717–722.
30. **Federico R, Angelini R, Ercolini L, Venturini G, Mattevi A & Ascenzi P** (1997) Competitive inhibition of swine kidney copper amine oxidase by drugs: amiloride, clonidine, and gabexate mesylate. *Biochem Biophys Res Commun* **240**: 150–152.
31. **Brickman E & Beckwith J** (1975) Analysis of the regulation of *Escherichia coli* alkaline phosphatase synthesis using deletions and phi80 transducing phages. *J Mol Biol* **96**: 307–316.
32. **Kumamoto CA & Beckwith J** (1985) Evidence for specificity at an early step in protein export in *Escherichia coli*. *J Bacteriol* **163**: 267–274.

33. **Schierle CF, Berkmen M, Huber D, Kumamoto C, Boyd D & Beckwith J** (2003) The DsbA signal sequence directs efficient, cotranslational export of passenger proteins to the *Escherichia coli* periplasm via the signal recognition particle pathway. *J Bacteriol* **185**: 5706–5713.
34. **Tullman-Ercek D, DeLisa MP, Kawarasaki Y, Iranpour P, Ribnicky B, Palmer T & Georgiou G** (2007) Export pathway selectivity of *Escherichia coli* twin arginine translocation signal peptides. *J Biol Chem* **282**: 8309–8316.
35. **Nakai K & Horton P** (1999) PSORT: a program for detecting sorting signals in proteins and predicting their subcellular localization. *Trends Biochem Sci* **24**: 34–36.
36. **Thomas JD, Daniel RA, Errington J & Robinson C** (2001) Export of active green fluorescent protein to the periplasm by the twin-arginine translocase (Tat) pathway in *Escherichia coli*. *Mol Microbiol* **39**: 47–53.
37. **Raetz CR & Whitfield C** (2002) Lipopolysaccharide endotoxins. *Annu Rev Biochem* **71**: 635–700.
38. **Firdich E & Whitfield C** (2005) Lipopolysaccharide inner core oligosaccharide structure and outer membrane stability in human pathogens belonging to the Enterobacteriaceae. *J Endotoxin Res* **11**: 133–144.
39. **Marrichi M, Camacho L, Russell DG & DeLisa MP** (2008) Genetic toggling of alkaline phosphatase folding reveals signal peptides for all major modes of transport across the inner membrane of bacteria. *J Biol Chem* **283**: 35223–35235.
40. **Cristobal S, de Gier JW, Nielsen H & von Heijne G** (1999) Competition between Sec- and TAT-dependent protein translocation in *Escherichia coli*. *EMBO J* **18**: 2982–2990.
41. **Bruser T** (2007) The twin-arginine translocation system and its capability for protein secretion in biotechnological protein production. *Appl Microbiol Biotechnol* **76**: 35–45.
42. **Feilmeier BJ, Iseminger G, Schroeder D, Webber H & Phillips GJ** (2000) Green fluorescent protein functions as a reporter for protein localization in *Escherichia coli*. *J Bacteriol* **182**: 4068–4076.
43. **Jose J & Meyer TF** (2007) The autodisplay story, from discovery to biotechnical and biomedical applications. *Microbiol Mol Biol Rev* **71**: 600–619.
44. **Schmid D, Pridmore D, Capitani G, Battistutta R, Neeser JR & Jann A** (1997) Molecular organisation of the ice nucleation protein InaV from *Pseudomonas syringae*. *FEBS Lett* **414**: 590–594.
45. **Shimazu M, Mulchandani A & Chen W** (2001) Simultaneous degradation of organophosphorus pesticides and *p*-nitrophenol by a genetically engineered *Moraxella* sp. with surface-expressed organophosphorus hydrolase. *Biotechnol Bioeng* **76**: 318–324.
46. **Wu ML, Tsai CY & Chen TH** (2006) Cell surface display of Chi92 on *Escherichia coli* using ice nucleation protein for improved catalytic and antifungal activity. *FEMS Microbiol Lett* **256**: 119–125.

Chapter 4

Functionalizing oxidases with peroxidase activity creates oxiperoxidases

**Remko T. Winter, Tomas E. van den Berg, Dana I. Colpa, Edwin van Bloois and
Marco W. Fraaije**

Laboratory of Biochemistry, Groningen Biomolecular Sciences and Biotechnology Institute, University of
Groningen, Nijenborgh 4, 9747 AG Groningen, The Netherlands

This chapter has been accepted for publication in:
ChemBioChem

Abstract

The covalent flavoprotein alditol oxidase (AldO) from *Streptomyces coelicolor* A3(2) was equipped with an extra catalytic functionality by fusing it to a microperoxidase. Purification of the construct resulted in the isolation of a synthetic bi-functional enzyme that was both fully flavinylated and heminylated: an oxiperoxidase. Characterization revealed that both oxidase and peroxidase functionalities were active, with the construct functioning as a single component xylitol biosensor. In an attempt to reduce the size of the oxidase-peroxidase fusion we replaced portions of the native AldO sequence with the bacterial cytochrome *c* CXXCH heme binding motif. By mutating only three residues of the AldO protein we were able to create a functional oxidase-peroxidase hybrid.

4.1 Introduction

Oxidases are a versatile class of enzymes capable of performing oxidation reactions with exquisite regio-, chemo- and/or enantioselectivity on a broad range of substrates (1). Most oxidases belong to the family of flavoproteins and often have their flavin cofactor covalently attached to the protein (2). One flavoprotein subfamily is relatively rich in oxidases containing a covalently bound flavin cofactor: the vanillyl alcohol oxidase (VAO) family (3). Recently, members of this specific class of enzymes have been attracting attention as potential industrially relevant biocatalysts in such diverse applications as biosensors (4, 5), dough optimizers (6), enantioselective catalysts (7) and most recently in the production of new antimicrobial scaffolds (8). Their specificity and ability to use molecular oxygen as electron acceptor, thereby circumventing the requirement of an expensive cofactor such as NAD(P)H, makes them ideally suited for a myriad of synthetic purposes and biosensing applications (9). While some oxidases reduce O_2 to H_2O , most produce H_2O_2 as only by-product.

Peroxidases (EC 1.11.x), like oxidases, belong to the class of oxidative enzymes and are typified by their use of the reduced form of dioxygen, hydrogen peroxide. Like oxidases, peroxidases are also of biotechnological interest (10). Examples of applications being developed include dye decolouration (11), enantioselective oxidation of phenols (12) and sulphides (13) and most recently in the degradation of lignin for biofuel generation (14). The peroxidase family is incredibly diverse and ubiquitous to all forms of life (15). A common feature, however, is a redox cofactor as part of the active site, generally in the form of an iron protoporphyrin IX. This heme cofactor is essential for peroxidase activity; heme itself, in fact, displays intrinsic peroxidase activity in the absence of any protein environment. In light of this fact, highly minimal peroxidases have been artificially created by the digestion of cytochrome *c*, so-called microperoxidases (16). These peptides retain their original peroxidase functionality and have found diverse applications as biosensors (17), electron carriers (18), photoreceptors (19), drugs (20), biocatalysts (21) and in biofuel cells (22).

Oxidases and peroxidases, whilst catalysing vastly different reactions, share hydrogen peroxide as a unifying feature. It is by-product for one, substrate for the other. Nature utilizes this complementarity in, for example, the lignin degradation pathway of white-rot fungi, where hydrogen peroxide produced by specific oxidases is used by lignin peroxidases to degrade lignin (23, 24). Inspired by this natural example in which peroxidase and oxidase activities are functionally coupled in a cascade reaction, we set out to design a synthetic biocatalyst that would merge both activities

in a single protein backbone. Such a construct would open possibilities for novel biosensor development and in the design of novel biochemical pathways while highlighting the power of synthetic biology as a tool to combine various cellular machineries to create an artificial enzyme system. At the same time, such a genetic fusion may possess certain catalytic advantages, such as faster peroxide transfer between the oxidase and peroxidase moiety in a fused variant compared to an unfused variant (38).

The model oxidase we chose to functionalize with peroxidase activity was the recently discovered (25) and extensively characterized (7, 26) polyol oxidase, alditol oxidase (AldO). This oxidase was chosen due to its amenability to enzyme engineering; it can be expressed at high yields in *E. coli*, its crystal structure has been elucidated at high resolution (27) and – most important for this study – it has been engineered for transport to the periplasm of *E. coli* via the Twin-arginine translocation (Tat) pathway (28). Choosing a suitable peroxidase system was confounded by the notoriously difficult expression of such enzymes in bacterial hosts. Most well-studied peroxidases, like horseradish peroxidase (HRP) (29), are eukaryotic in origin and cannot be expressed in *E. coli* (30, 31). While several examples of prokaryotic peroxidases belonging to the dye-decolorizing (DyP-type) superfamily (32) have recently appeared (13, 33), these enzymes are only active at low pH, which is incompatible with flavoprotein oxidases. Thus we turned to the recent work done on minimal bacterial peroxidases, where it has been shown that short peptide sequences containing the cytochrome *c* heme binding motif, CXXCH, are sufficient to express functional peroxidases in the periplasm of *E. coli* (34). Secretion is a prerequisite for these microperoxidases as covalent heme attachment takes place exclusively in the periplasm. In *E. coli* the eight proteins CcmA-H of the cytochrome *c* maturation (Ccm) apparatus are responsible for this process (35, 36). From a synthetic biology viewpoint, such microperoxidases are attractive building-blocks as they make it possible to create novel fusion enzymes by decorating the target protein (in this case AldO) with a small, defined hemopeptide exhibiting peroxidase activity.

Here, we fuse a microperoxidase to the flavoprotein oxidase AldO and express the entire bi-functional fusion protein in the periplasm of *E. coli* in an active form. The fusion was shown to exhibit oxidase, peroxidase and coupled oxidase-peroxidase activity both *in vivo* and *in vitro*. Characterization of the purified bi-functional enzyme revealed that it was both completely and covalently flavinylated and heminylated. This combination of cofactors, heme and FAD, where both are covalently bound to a single polypeptide chain has never been observed before in a natural protein. While naturally occurring protein complexes exist that contain both heme and FAD (e.g. cytochrome P450 BM3 and NO synthase), the redox cofactors in these proteins are

never found covalently bound to a single polypeptide chain. In order to create even smaller oxidase-peroxidases, we have also created AldO variants in which heme-binding segments were introduced in the AldO backbone. This revealed that it was possible to introduce peroxidase activity in AldO by replacing only three amino acid residues. Hence, we have shown that through the fusion of various protein encoding DNA fragments an artificial enzyme system can be designed and constructed resulting in an oxidase that has been functionalized with peroxidase activity to create a new enzyme: the oxiperoxidase.

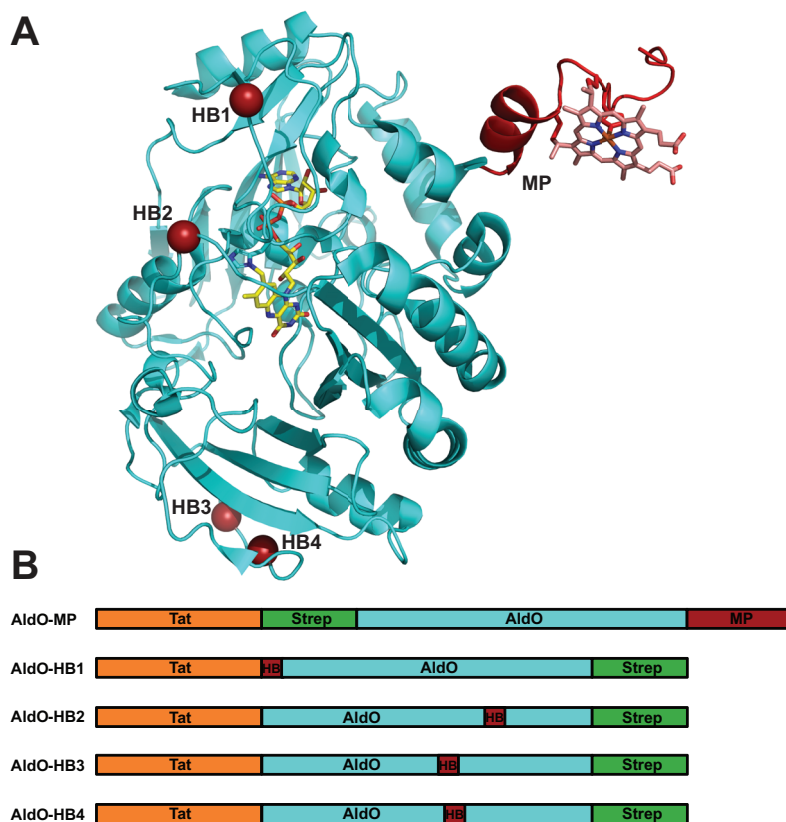


Figure 4.1 Designing oxidase-peroxidase hybrids. **A**, shown is the structure of *Streptomyces coelicolor* A3(2) alditol oxidase (AldO, PDB id: 2vfs) highlighting the locations that were mutated into the CXXCH heme binding motif (HB1-4, red spheres). Covalently bound FAD is shown as yellow sticks. A model of the microperoxidase (MP) peptide containing a covalently bound heme (pink sticks) that was fused to the C-terminus of AldO is shown in red. **B**, schematic overview of the prepared constructs; Tat, Twin arginine translocation signal sequence; Strep, Strep tag for purification of the constructs with Strep-tactin sepharose; AldO, alditol oxidase; HB, heme binding motif CXXCH; MP, microperoxidase MP292.

4.2 Materials and methods

4.2.1 Strains, plasmids and growth conditions

E. coli strain MC1061 was used for all routine cloning tasks. *E. coli* strain BL21(DE3) harbouring plasmid pEC86 (41) and the construct under study was used to express the oxidase-peroxidase fusions. pBAD-Tat-AldO was used to construct the various oxidase-peroxidase hybrids (28). Growth media contained antibiotics ampicillin (100 $\mu\text{g mL}^{-1}$) and chloramphenicol (34 $\mu\text{g mL}^{-1}$). For expression, Terrific Broth (1 L) was inoculated with the appropriate strain (1 mL) grown to saturation at 37°C, induced by the addition of L-arabinose (final concentration 0.2%, w/v) and incubated at 17°C under orbital shaking for 65 h.

4.2.2 Construction of hybrids

The sequence encoding microperoxidase MP292 (37) was obtained from Sigma-Aldrich as two complementary DNA strands with *Pst*I and *Sal*I overhangs. The strands were allowed to dimerize by mixing aliquots of DNA (5 μL , 100 μM) incubating at 72°C for 2 minutes and then cooling to 22°C in 45 minutes using a PCR thermocycler. Dimerized DNA was ligated into *Pst*I and *Sal*I digested pBAD-Tat-AldO, generating pBAD-Tat-AldO-MP. A Strep tag (WSHPQFEK) was introduced at the C-terminus of the *aldo* gene in pBAD-Tat-AldO and at the N-terminus of the *aldo* gene in pBAD-Tat-AldO-MP using PCR, generating pBAD-Tat-Strep-AldO and pBAD-Tat-Strep-AldO-MP (AldO-MP in Figure 4.1). Mutants of AldO that contain the heme binding CXXCH motif (AldOHB1-AldOHB4 in Figure 4.1) were generated by PCR (AldOHB1), and QuikChange PCR (AldOHB2-AldOHB4). For AldOHB1 residues 1-5 were mutated into the heme binding motif, for AldOHB2, AldOHB3 & AldOHB4 residues 280-284, 232-236 and 235-239, respectively, were mutated into the CXXCH motif by QuikChange PCR using plasmids pBAD-Tat-AldO-Strep as template. Primer sequences are available on request. All constructs were confirmed by DNA sequencing (GATC Biotech Ag, Konstanz, Germany).

4.2.3 Protein fractionation and purification

Cells expressing oxidase-peroxidase fusions were grown as described above. Periplasmic extracts were prepared via the osmotic shock method. Briefly, cells were harvested (20 OD₆₀₀ units) by centrifugation (5 000 x *g*, 10 min, 4°C) and washed with ice-cold Tris-HCl (10 mM, pH 7.4). Pelleted cells were resuspended in Tris-HCl (80 μL , 10 mM, pH 8.0) containing sucrose (25%, w/v), EDTA (10 μL 20 mM, pH 8.0) and lysozyme (10 μL , 5 mg mL⁻¹) and incubated on ice for 20 minutes. After centrifugation (12 000 x *g*, 30 min, 4°C) the supernatant was collected and designated as the

periplasmic extract. For large culture volumes the above periplasmic fractionation protocol was scaled according to the number of OD₆₀₀ units harvested. Strep-tag labelled proteins were purified from the periplasmic extract using Strep-Tactin Sepharose (IBA GmbH, Gottingen, Germany) according to the manufacturer's instructions. Eluted fractions were pooled, buffer exchanged to potassium phosphate buffer (50 mM, pH 7.5) and concentrated.

4.2.4 Analytical methods

Unless stated otherwise, all experiments were performed at 25°C and in potassium phosphate buffer (50 mM, pH 7.5). All measurements were carried out in triplo, and the standard deviation value in the experiments is 5%, unless stated otherwise. Heme binding constructs were detected in SDS-PAGE gels by using the intrinsic peroxidase activity of heme; gels were immersed in water (50 mL) containing 3-3'-dimethoxybenzidine dihydrochloride (DMB) (50 mg, 0.16 mmol) and H₂O₂ (0.7%, v/v). Total protein content was calculated using the Bradford method with BSA as standard. Absolute heme concentrations were determined with the pyridine ferro-hemochrome method, using the extinction coefficient of pyridine hemochrome c ($\epsilon_{550 \text{ nm}} = 30.27 \text{ mM}^{-1} \text{ cm}^{-1}$) (42). The oligomeric form of the fusion constructs was investigated by size-exclusion chromatography as described previously (13). Immunoblotting experiments to verify the fractionation procedure using antisera against AldO and DnaK were carried out according to van Bloois *et al* (28).

4.2.5 Determining FAD content

The FAD content was calculated by measuring the difference in extinction coefficients of the flavin in its oxidized and reduced forms. In an Applied Photophysics stopped-flow apparatus, model SX17MV, absorption spectra were collected at 2.5 ms intervals using a diode array detector. The reductive half-reaction of wild type AldO was followed as described previously (25) by reducing the flavin cofactor under anoxic conditions with an excess of xylitol. From the resulting absorption spectra the difference of the extinction coefficients of the FAD in the oxidized and reduced forms was calculated ($\Delta\epsilon_{\text{ox-red}}$) at 451 nm. Subsequently, the reductive half reaction of the relevant hybrids was followed in an identical fashion. The absorbance difference at 451 nm was extracted from the resulting spectra and using the $\Delta\epsilon_{\text{ox-red}}$ calculated for wild type AldO the FAD content of the hybrids was determined.

4.2.6 Activity assays

Oxidase activity was measured using a HRP coupled assay described previously (25). Peroxidase activity was measured using either DMB (1 mM) or DCHBS and AAP (1 mM

and 0.1 mM, respectively) as peroxidase substrate. Product formation was monitored spectrophotometrically at 460 nm ($\epsilon_{\text{DMB}} = 11.3 \text{ mM}^{-1} \text{ cm}^{-1}$) or 515 nm ($\epsilon_{\text{DCHBS/AAP}} = 26 \text{ mM}^{-1} \text{ cm}^{-1}$). Initial reaction rates were calculated and used to determine Michaelis-Menten kinetic parameters. *In vivo* oxidase activity of cells expressing AldO-MP was measured with a modification of the plate based assay developed by Alexeev *et al* (49): the lysis step and addition of HRP was omitted and xylitol and DMB (both 1 mM) were used as oxidase and peroxidase substrates, respectively.

4.3 Results

4.3.1 Hybrid design and experimental strategy

In *E. coli*, the covalent coupling of heme to microperoxidases occurs exclusively in the oxidizing periplasm (36). Hence the design of our chimeric oxidase-peroxidase required periplasmic transport of the oxidase. In previous studies the model oxidase AldO was successfully engineered for export to the *E. coli* periplasm via the Tat pathway (28), making it a logical candidate for peroxidase functionalization. Microperoxidases have been described that can be expressed in the periplasm of *E. coli* with varying yields (34). Due to its successful fusion to maltose binding protein (MBP) and export via the general type II secretion system (Sec), microperoxidase MP292 (37) was chosen to functionalize AldO. The hybrid was designed so that DNA encoding MP292 was cloned at the C-terminus of the Tat signal sequence equipped *aldo* gene. A Strep-tag was included at the N-terminus for purification purposes, creating Tat-Strep-AldO-MP (AldO-MP in Figure 4.1). A two plasmid system was used to express the hybrid proteins. A pBAD-derived expression plasmid contained the gene encoding the AldO hybrid and an N-terminal Tat signal sequence for periplasmic export. A second plasmid, pEC86 (41), contained the cytochrome *c* maturation apparatus *ccmA-H* under control of a constitutive promoter, required for the transport and covalent attachment of heme to the CXXCH motif under aerobic conditions (36). SDS-PAGE analysis and activity staining revealed that the construct was expressed in the periplasm of *E. coli* and contained both oxidase and peroxidase activity. Through affinity chromatography the oxiperoxidase AldO-MP (Figure 4.1) was successfully purified from periplasmic extracts (Figure 4.2).

4.3.2 Purification of an oxiperoxidase

The oxiperoxidase AldO-MP (Figure 4.1) was expressed in *E. coli* BL21(DE3) cells. As heme attachment to cytochromes occurs in the periplasm of gram-negative organisms (36), we anticipated obtaining only fully holo oxiperoxidase containing both FAD (incorporated in the cytoplasm) and heme (incorporated in the periplasm) by

purifying the fusion constructs from periplasmic extracts prepared via the osmotic shock method. Following incubation of Strep-tactin Sepharose resin with periplasmic extracts and subsequent washing of the resin, the column material displayed a dark red coloration, indicative of a protein bound containing a heme cofactor. Upon elution, a dark-red fraction was collected, which was revealed to run as one band on an SDS-PAGE gel stained for total protein (Figure 4.2), at approximately 50 kDa. This was in good agreement with the theoretical mass of the construct 50.6 kDa (- Tat signal sequence, + FAD and + heme) and in agreement with earlier work where the Tat signal sequence is cleaved off during transport of AldO to the periplasm (28). From 1 L of culture approximately 3 mg of protein was purified from the periplasmic extracts. A duplicate of the SDS-PAGE gel was stained for heme content (Figure 4.2), which revealed that the purified protein indeed contained heme. Immunoblotting was carried out using antiserum against AldO to verify periplasmic export; visualization revealed a band in the periplasmic fraction (Figure 4.3). The efficiency of the fractionation procedure was confirmed by analysing the levels DnaK which as serves as a cytoplasmic marker.

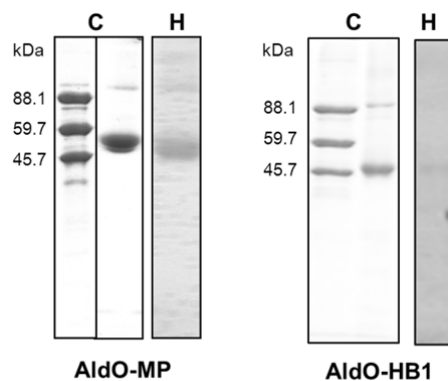


Figure 4.2 Purified oxidase-peroxidase fusions contain covalently bound heme. Both constructs were purified from periplasmic extracts with Strep-tactin sepharose, and subsequently analysed by SDS-PAGE. AldO-MP and AldO-HB1 refer to constructs shown in Figure 4.1. C, total protein stained with Coomassie Brilliant Blue; H, heme stain.

As it is known that microperoxidases adopt a variety of oligomeric states at physiological pH (21), we performed size-exclusion chromatography (SEC) to examine whether the monomeric state of native AldO (25) is altered by the addition of a microperoxidase tag. Analysis on a SEC column revealed that the purified fusion had the same retention time as wild type AldO. Comparison to a set of molecular weight standards allowed for the calculation of a protein mass that was in agreement with the

monomeric form. Thus, we have successfully cloned, expressed and purified a Strep-tag labeled fusion between a flavoprotein oxidase, AldO, and a microperoxidase in the periplasm of *E. coli*: an oxiperoxidase. Characterization of the oxiperoxidase by SDS-PAGE and SEC revealed it to be monomeric and to contain covalently bound heme.

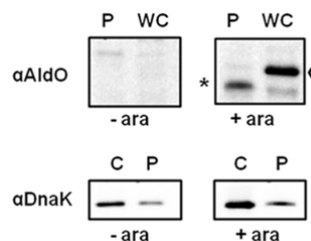


Figure 4.3 Analysis of periplasmic export of AldO-MP. Cells were fractionated and analysed by immunoblotting with antiserum against AldO. Control was carried out by immunoblotting same samples with antiserum against DnaK, a cytoplasmic protein. Ara, arabinose; P, periplasmic fraction; WC, whole cell fraction; C, cytoplasm. * denotes AldO-MP; < marks AldO-MP with Tat signal sequence.

4.3.3 An oxiperoxidase contains both covalent FAD and Heme

Upon establishing that the oxiperoxidase AldO-MP (Figure 4.1) contained both covalent heme and FAD, we set out to determine the ratio of heme and FAD incorporation. The pyridine hemochrome assay was used to determine the heme content of the fusion construct, which yielded an absorption peak at 557 nm. Absorbance at this wavelength is indicative of covalently bound heme *c* (42) and we determined a heme concentration of 20.3 μM . The concentration of flavoproteins is conventionally determined by examining the characteristic absorption spectrum caused by the flavin cofactor in the region between 350 and 500 nm (43). Due to the strong absorption of the heme cofactor in this region it was anticipated that this approach would not work. Indeed, as the absorption spectrum (Figure 4.4) of the fusion construct reveals, it predominantly exhibits the characteristics of a hemoprotein, with a characteristic Soret band at 410 nm and a peak at 280 nm. The shoulder between 420 and 260 nm (Figure 4.4) hints at the presence of a FAD cofactor. In order to measure the FAD concentration we specifically reduced the FAD cofactor under anaerobic conditions with xylitol and followed the absorption spectra in a stopped flow spectrophotometer fitted with a diode array detector. The difference spectrum revealed an absorbance maximum at 452 nm which confirms the presence of the covalently bound FAD (25). By calculating the difference in extinction coefficient between the oxidized and reduced forms and comparing this to the difference in extinction coefficients for wild type AldO, we were able to calculate the amount of covalent FAD contained within the oxiperoxidase AldO-MP. The concentration of FAD

was 18.5 μM , implying a 1:1 FAD:heme ratio (Table 4.1) which agrees with the fact that the Tat translocator exhibits quality-control mechanisms, meaning that only correctly flavinylated protein is transported into the periplasm via the Tat pathway (44). The total protein concentration was also determined via the Bradford method and was in good agreement ($20 \pm 2 \mu\text{M}$) with the FAD and heme determinations indicating that all of the AldO-MP transported to the periplasm is in a fully holo form, containing both covalently bound FAD and heme. Hence, we have produced a true oxiperoxidase; a hybrid enzyme that is fully covalently flavinylated and heminylated.

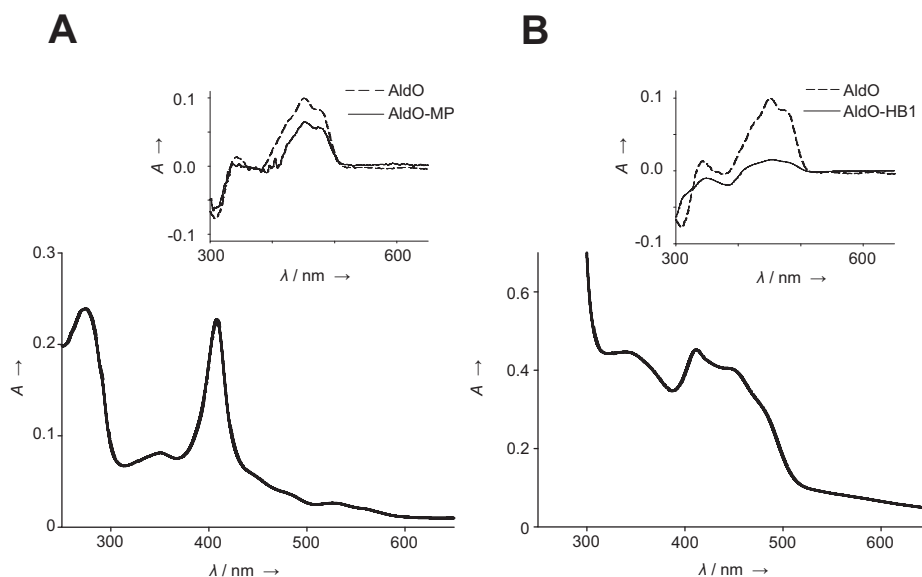


Figure 4.4 UV/Vis absorption spectra of the oxidase-peroxidase hybrids. **A**, AldO-MP, 4.6 μM . **B**, AldO-HB1, 30 μM . AldO-MP and AldO-HB1 refer to constructs shown in Figure 4.1. **Inset**: difference spectra of the oxidized and reduced forms of wild type AldO (10.5 μM) and the oxidase-peroxidase fusions (6.9 μM AldO-MP; 2.1 μM AldO-HB1) after reduction of FAD by xylitol.

4.3.4 Designed oxiperoxidase fusion hybrid can be used as a xylitol biosensor

An important aspect of the constructed AldO-MP hybrid (Figure 4.1) is their ability to act in concert; thus the peroxidase functionality can be used to detect and quantify the oxidase activity. Initial tests showed that coupled oxidase/peroxidase activity could be detected both in periplasmic extracts and with purified protein. A xylitol concentration of 2.3 mg L^{-1} (15 μM) was reliably detected with only 20 nM of AldO-MP in a colorimetric assay using dichloro-2-hydroxybenzenesulfonic acid (DCHBS) and 4-aminoantipyrine (AAP) as peroxidase substrate, indicating that a peroxidase fused to an oxidase can reliably be used to detect low levels of oxidase activity towards target

substrates. We were also interested if the oxiperoxidase could be used to detect *in vivo* oxidase activity. With a modification of the plate based oxidase screening assay developed by Alexeev *et al* (49), we showed that xylitol oxidase activity could be detected in whole cells expressing AldO-MP in the periplasm. This shows that the oxiperoxidase is fully functional in *E. coli* cells providing the bacterium with a new oxidative catalytic potential. The presence of a *PstI* cloning site between the *aldo* gene and the DNA encoding the microperoxidase also makes a directed evolution methodology possible, where, for example, the *aldo* gene is subjected to error prone PCR and then cloned into the MP vector to enable whole cell screening. In conclusion, we have successfully created an oxiperoxidase: a hybrid protein that is expressed in the periplasm of *E. coli* and exhibits both oxidase and peroxidase activities. Due to the complementary nature of these two activities our oxiperoxidase can also be employed to perform cascade chemistry, detecting oxidase activity directly with its peroxidase moiety both *in vitro* and *in vivo*.

4.3.5 An engineered CXXCH motif in AldO enables covalent heme attachment, merging peroxidase and oxidase activity on a single protein backbone

Bolstered by our success at creating a bi-functional oxidase-peroxidase hybrid by simply linking a short peptide encoding a microperoxidase to an oxidase, we wondered if we could go one step further and incorporate heme binding motifs within the oxidase sequence. Inspired by landmark studies on the maturation and heme binding of cytochrome *c* peptides wherefrom it is known that only the short CXXCH motif is required for covalent heme attachment (34) we hypothesized that it should be possible to mutate a portion of the AldO sequence to encode this motif, thus enabling it to covalently bind heme. Due to the possible mechanistic insights we could gain into the maturation of cytochromes and catalytic effects, like channelling H₂O₂ from the reduced flavin to a heme moiety anchored nearby (38), we decided to mutate a number of regions of the AldO protein into the CXXCH motif and examine the effects location has on heme anchoring and enzyme activity. The covalent incorporation of FAD in oxidases is an autocatalytic process that occurs in the *E. coli* cytoplasm (39, 40). Hence AldO is transported via the Tat pathway in a fully folded form and any heme incorporation at the chosen positions would give an indication of the degree of secondary structure that is tolerated by the Ccm apparatus.

From the crystal structure of AldO (27) three regions were identified as candidates for covalent heme attachment. Firstly, the N-terminus due to its lack of secondary structure; in the crystal structure the first four amino acids are not visible, indicating they have a highly random, undefined structure (Figure 4.1, AldO-HB1). Secondly, a loop near the entrance to the active site was chosen due to specific

catalytic effects that may be observed upon heme binding, such as H₂O₂ channelling (Figure 4.1, AldO-HB2). Finally, a loop on the surface of the protein was identified that displays by a high degree of flexibility, as evidenced by the high B-factors of these residues. This loop was mutated at two positions to generate heme-binding variants AldO-HB3 & 4 (Figure 4.1). All four heme binding mutants were expressed in the periplasm, contained covalently bound FAD and exhibited xylitol oxidase activity, as was observed by SDS-PAGE analysis, fluorescence staining for the flavin cofactor and oxidase activity measurements of periplasmic extracts (Data not shown). On the basis of heme staining and peroxidase assays only mutant AldOHB1 displayed peroxidase activity and contained covalently bound heme (Figure 4.2), thus acting as a true oxiperoxidase. AldOHB1 contained a C-terminal Strep tag to enable facile one-step purification with Strep-tactin Sepharose; approximately 100 µg of protein was purified from 1 L of culture. This was significantly less than the amount of AldO-MP that could be obtained from the same culture volume. As it was clear from heme stains and activity assays that AldOHB1 contained both covalently bound FAD and heme, we were interested if the degree of cofactor incorporation was as successful as for the oxidase-microperoxidase fusion AldO-MP. The absorption spectrum of AldOHB1 is very different to that of AldO-MP (Figure 4.4); the Soret band at 410 nm is much less pronounced and the underlying flavin spectrum is, as a result, much more visible. Pyridine hemochrome determination of the heme content revealed that only 15% of the hybrid contained heme when compared to the total protein content (Table 4.1). As expected because of the quality control carried out by the Tat translocator the protein was completely flavinylated; anaerobic reduction of FAD cofactor by xylitol and comparison of the oxidized and reduced spectra with those of wild type AldO revealed an FAD content that was equal to the total protein content. The other AldO-HB variants that encode the CXXCH motif within loop regions on the AldO surface, however, do not bind any heme. This is in line with the hypothesis that the Ccm apparatus requires the heme binding motif to contain no ordered secondary structure for proper heme incorporation (45).

4.3.6 Oxiperoxidases retain both oxidase and peroxidase activity

Once it was clear that the engineered oxidase-peroxidase hybrid contained both covalently bound FAD and heme and in the case of AldO-MP could be used as a xylitol biosensor, we wanted to establish the catalytic competence of their oxidase and peroxidase domains. Steady-state kinetic measurements were performed with the preferred AldO substrate, xylitol (25). Analysis of both purified oxiperoxidase hybrids, AldO-MP and AldO-HB1, revealed that the kinetic constants for xylitol were essentially unchanged when compared to wild type AldO (Table 4.1); $K_M = 0.29$ and 0.35 mM for

AldO-MP and AldO-HB1, respectively. The k_{cat} of AldO-MP (9.1 s^{-1}), was slightly lower than that of AldO-HB1 (12.2 s^{-1}), but both values compared favourably with the k_{cat} value of wild type AldO (13.0 s^{-1}) (25). The peroxidase activity of AldO-MP was analysed with dimethoxybenzidine (DMB) (Table 4.1). Peroxidase activity could be detected and both displayed saturating activity at high H_2O_2 concentrations. The K_M value for H_2O_2 with DMB is relatively high: $12 \pm 5 \text{ mM}$. The maximum rate is $9.1 \pm 2.2 \text{ s}^{-1}$. These values compare favourably with published values for other microperoxidases (34, 46), which are all in this range. Slow decay of the peroxidase activity of our oxiperoxidases hybrids was observed over time, a feature common to proteins containing such an exposed heme (20). The pH optimum of the peroxidase functionality of AldO-MP was also determined in Britton-Robinson buffer (47) and as expected from studies performed with microperoxidases (34, 46, 48) the optimum lies at pH 8.5. The experiments were carried out at the pH optimum of AldO (pH 7.5) (7), where the peroxidase functionality displayed roughly 60% of its optimal activity. Taken together, these results show that oxidase and peroxidase functionalities can successfully be combined on a single protein scaffold, without negatively influencing the activity of the other functionality, to create a novel and artificial hybrid enzyme which we have named an oxiperoxidase.

Table 4.1 Oxidase-peroxidase hybrids and their catalytic properties. Oxidase activity was determined with xylitol as substrate, peroxidase activity with dimethoxybenzidine as substrate. Numbering of hemebinding motif (HB) mutants and microperoxidase (MP) fusion refer to overview shown in Figure 4.1. *nd*, not determined.

Construct	Oxidase activity	Peroxidase activity	Kinetic parameters (Oxidase)		Kinetic parameters (Peroxidase)		FAD binding?	Heme binding?
			k_{cat} (s^{-1})	K_M (mM)	k_{cat} (s^{-1})	K_M (mM)		
AldO-MP	Yes	Yes	9.1	0.29	9.1	12	Yes (100%)	Yes (100%)
AldO-HB1	Yes	Yes	12.2	0.35	<i>nd</i>	<i>nd</i>	Yes (100%)	Yes (15%)

4.4 Discussion

We have engineered novel enzyme functionalities through the fusion of genes and protein encoding DNA fragments. By fusing the gene for an oxidase to a synthetic oligonucleotide encoding the heme binding CXXCH motif, we generated a novel breed of fusion protein with two complementary activities: an oxidase-peroxidase fusion,

which we call an oxiperoxidase. Both redox cofactors (heme and FAD) were covalently bound to the protein, and present in a 1:1 ratio to the protein backbone. Furthermore, we show that both the oxidase and peroxidase activities are maintained and that the oxiperoxidase functions as a cascade catalyst both *in vivo* and *in vitro*. In an attempt to reduce the size of the oxiperoxidase we created a truly chimeric enzyme by mutating only three residues of the flavoprotein oxidase AldO. By mutating three residues in the AldO N-terminus into the CXXCH heme binding motif, we created a functional oxiperoxidase. Following export to the *E. coli* periplasm and co-expression with the Ccm apparatus, heme was successfully incorporated into this construct, albeit with a much lower efficiency; only 15% of the secreted protein contained heme, compared to a 100% incorporation rate for the larger fusion variant. These data support current insights into the Ccm apparatus: the heme binding motif is the only prerequisite for covalent heme incorporation, but this motif cannot be contained in a (partially) folded holo structure. All known proteins that contain this heme-binding motif are transported via the Sec pathway (50). Therefore, this study is to the best of our knowledge the first instance where the Ccm apparatus has been used in conjunction with a protein exported via the Tat pathway. It has in fact been shown that the speed at which a protein folds after it has been transported to the periplasm is imperative for recognition and covalent coupling of heme. Studies performed with DsbD, a fast folding *E. coli* transmembrane oxidoreductase, mutated to contain the CXXCH motif, revealed that only a very small percentage (0.2%) contained covalently bound heme (45). The speed at which DsbD adopts its native conformation in the *E. coli* periplasm is rapid enough for it to avoid heme incorporation by the Ccm apparatus. This agrees with the findings presented here where only a small portion of the AldO-HB1 hybrid contains covalently bound heme. According to the crystal structure, the N-terminus is freely accessible, and its atoms have very high B-factors, indicating that they have a relatively large freedom of movement. The proximity to the folded structure seems to inhibit the incorporation of heme, providing an explanation for why only 15% of the exported protein contains covalently bound heme. Incorporating the heme binding motif in loop regions of the protein, while yielding stable AldO, did not lead to detectable levels of heme bound protein. It is clear that there are too many secondary structure elements in these regions, forcing the CXXCH motif to adopt a detrimental conformation and preventing covalent heme coupling by the Ccm apparatus. While it was known that heme could bind to very short peptides containing only the CXXCH motif (16), fusing one of these peptides to the AldO backbone to create an oxidase-peroxidase fusion was sufficient to enable complete heminylation; here the short peptide serves as a linker and the folded AldO protein does not inhibit the covalent coupling of heme. Earlier studies where a

microperoxidase was fused to the maltose binding protein MBP showed that the degree of heme incorporation was much lower than the 100% we observe for our oxidase-peroxidase fusion (37), but this is probably due to the maximum capacity of the Ccm apparatus being reached as the amount of MBP secreted via the Sec pathway is significantly higher than the amount of AldO secreted via the Tat pathway (28, 51).

Molecular biology supplies us with the technology to develop chimeric enzymes with novel and complementary functionalities. The merging of two complementary enzyme activities presented here to create a new breed of enzyme, the oxiperoxidase, is to our knowledge the first time that an oxidase and a peroxidase have been engineered onto a single protein backbone. The oxiperoxidase opens the door to a wide variety of biosensor-based applications that are based on such artificial enzyme hybrids.

4.5 Acknowledgements

This research is supported by the Dutch Technology Foundation STW, Applied Science Division of NWO, and the Technology Program of the Ministry of Economic Affairs grant no. 7726. M.W.F. received support from the EU-FP7 "OXYGREEN" project.

4.6 References

1. **Turner NJ** (2011) Enantioselective oxidation of C-O and C-N bonds using oxidases. *Chem Rev* **111**: 4073-4087.
2. **Heuts DP, Scrutton NS, McIntire WS & Fraaije MW** (2009) What's in a covalent bond? On the role and formation of covalently bound flavin cofactors. *Febs J.* **276**: 3405-3427.
3. **Leferink NG, Heuts DP, Fraaije MW & van Berkel WJ** (2008) The growing VAO flavoprotein family. *Arch Biochem Biophys* **474**: 292-301.
4. **Romero MR, Ahumada F, Garay F & Baruzzi AM** (2010) Amperometric biosensor for direct blood lactate detection. *Anal Chem* **82**: 5568-5572.
5. **Wilson GS & Gifford R** (2005) Biosensors for real-time *in vivo* measurements. *Biosens Bioelectron* **20**: 2388-2403.
6. **Cook MW & Thygesen HV** (2003) Safety evaluation of a hexose oxidase expressed in *Hansenula polymorpha*. *Food Chem Toxicol* **41**: 523-529.
7. **van Hellemond EW, Vermote L, Koolen W, Sonke T, Zandvoort E, Heuts DP, Janssen DB & Fraaije MW** (2009) Exploring the biocatalytic scope of alditol oxidase from *Streptomyces coelicolor*. *Adv Synth Catal* **351**: 1523-1530.
8. **Liu YC, Li YS, Lyu SY, Hsu LJ, Chen YH, Huang YT, Chan HC, Huang CJ, Chen GH, Chou CC, Tsai MD & Li TL** (2011) Interception of teicoplanin oxidation intermediates yields new antimicrobial scaffolds. *Nat Chem Biol* **7**: 304-309.
9. **Hollmann F, Arends IW, Buehler K, Schallmey A & Buhler B** (2011) Enzyme-mediated oxidations for the chemist. *Green Chem* **13**: 226-265.

10. **Regalado C, García-Almendárez BE & Duarte-Vázquez MA** (2004) Biotechnological applications of peroxidases. *Phytochem Rev* **3**: 243-256.
11. **An SY, Min SK, Cha IH, Choi YL, Cho YS, Kim CH & Lee YC** (2002) Decolorization of triphenylmethane and azo dyes by *Citrobacter* sp. *Biotechnol Lett* **24**: 1037-1040.
12. **Antipov E, Cho AE, Wittrup KD & Klibanov AM** (2008) Highly L and D enantioselective variants of horseradish peroxidase discovered by an ultrahigh-throughput selection method. *Proc Natl Acad Sci U S A* **105**: 17694-17699.
13. **van Bloois E, Pazmino DET, Winter RT & Fraaije MW** (2010) A robust and extracellular heme-containing peroxidase from *Thermobifida fusca* as prototype of a bacterial peroxidase superfamily. *Appl Microbiol Biotechnol* **86**: 1419-1430.
14. **Bugg TD, Ahmad M, Hardiman EM & Singh R** (2011) The emerging role for bacteria in lignin degradation and bio-product formation. *Curr Opin Biotechnol* **22**: 394-400.
15. **Hofrichter M, Ullrich R, Pecyna MJ, Liers C & Lundell T** (2010) New and classic families of secreted fungal heme peroxidases. *Appl Microbiol Biotechnol* **87**: 871-897.
16. **Braun M & Thony-Meyer L** (2004) Biosynthesis of artificial microperoxidases by exploiting the secretion and cytochrome *c* maturation apparatuses of *Escherichia coli*. *Proc Natl Acad Sci U S A* **101**: 12830-12835.
17. **Huang WM, Jia JB, Zhang ZL, Han XJ, Tang JL, Wang JG, Dong SJ & Wang EK** (2003) Hydrogen peroxide biosensor based on microperoxidase-11 entrapped in lipid membrane. *Biosens Bioelectron* **18**: 1225-1230.
18. **Sharp RE, Moser CC, Rabanal F & Dutton PL** (1998) Design, synthesis, and characterization of a photoactivatable flavocytochrome molecular maquette. *Proc Natl Acad Sci U S A* **95**: 10465-10470.
19. **Rau HK, DeJonge N & Haehnel W** (1998) Synthesis of *de novo* designed metalloproteins for light-induced electron transfer. *Proc Natl Acad Sci U S A* **95**: 11526-11531.
20. **Spector A, Zhou W, Ma WC, Chignell CF & Reszka KJ** (2000) Investigation of the mechanism of action of microperoxidase-11, (MP11), a potential anti-cataract agent, with hydrogen peroxide and ascorbate. *Exp Eye Res* **71**: 183-194.
21. **Kadnikova EN & Kostic NM** (2003) Effects of the environment on microperoxidase-11 and on its catalytic activity in oxidation of organic sulfides to sulfoxides. *J Org Chem* **68**: 2600-2608.
22. **Willner I, Katz E, Patolsky F & Buckmann AF** Biofuel cell based on glucose oxidase and microperoxidase-11 monolayer-functionalized electrodes. *J Chem Soc -Perkin Trans 2*: 1817-1822.
23. **Ander P & Marzullo L** (1997) Sugar oxidoreductases and veratryl alcohol oxidase as related to lignin degradation. *J Biotechnol* **53**: 115-131.
24. **Kirk TK & Farrell RL** (1987), Enzymatic combustion - the microbial-degradation of lignin. *Annu Rev Microbiol* **41**: 465-505.
25. **Heuts DP, van Hellemond EW, Janssen DB & Fraaije MW** (2007) Discovery, characterization, and kinetic analysis of an alditol oxidase from *Streptomyces coelicolor*. *J Biol Chem* **282**: 20283-20291.
26. **Baron R, Riley C, Chenprakhon P, Thotsaporn K, Winter RT, Alfieri A, Forneris F, van Berkel WJH, Chaiyen P, Fraaije MW, Mattevi A & McCammon JA** (2009) Multiple pathways guide oxygen diffusion into flavoenzyme active sites. *Proc Natl Acad Sci U S A* **106**: 10603-10608.
27. **Forneris F, Heuts DP, Delvecchio M, Rovida S, Fraaije MW, Mattevi A** (2008) Structural analysis of the catalytic mechanism and stereoselectivity in *Streptomyces coelicolor* alditol oxidase. *Biochemistry* **47**: 978-985.
28. **van Bloois E, Winter RT, Janssen DB & Fraaije MW** (2009) Export of functional *Streptomyces coelicolor* alditol oxidase to the periplasm or cell surface of *Escherichia coli* and its application in whole-cell biocatalysis. *Appl Microbiol Biotechnol* **83**: 679-687.

29. **Veitch NC** (2004) Horseradish peroxidase: a modern view of a classic enzyme. *Phytochemistry* **65**: 249-259.
30. **Lin ZL, Thorsen T & Arnold FH** (1999) Functional expression of horseradish peroxidase in *E. coli* by directed evolution. *Biotechnol Prog* **15**: 467-471.
31. **Smith AT, Santama N, Dacey S, Edwards M, Bray RC, Thorneley RNF & Burke JF** (1990) Expression of a synthetic gene for horseradish peroxidase-C in *Escherichia coli* and folding and activation of the recombinant enzyme with Ca²⁺ and heme. *J Biol Chem* **265**: 13335-13343.
32. **Sugano Y** (2009) DyP-type peroxidases comprise a novel heme peroxidase family. *Cell Mol Life Sci* **66**: 1387-1403.
33. **Roberts JN, Singh R, Grigg JC, Murphy MEP, Bugg TDH & Eltis LD** (2011) Characterization of dye-decolorizing peroxidases from *Rhodococcus jostii* RHA1. *Biochemistry* **50**: 5108-5119.
34. **Braun M & Thony-Meyer L** (2004) Biosynthesis of artificial microperoxidases by exploiting the secretion and cytochrome *c* maturation apparatuses of *Escherichia coli*. *Proc Natl Acad Sci U S A* **101**: 12830-12835.
35. **Grove J, Tanapongpipat S, Thomas G, Griffiths L, Croke H & Cole J** (1996) *Escherichia coli* K-12 genes essential for the synthesis of *c*-type cytochromes and a third nitrate reductase located in the periplasm. *Mol Microbiol* **19**: 467-481.
36. **Thonymeyer L, Fischer F, Kunzler P, Ritz D & Hennecke H** (1995) *Escherichia coli* genes required for cytochrome *c* maturation. *J Bacteriol* **177**: 4321-4326.
37. **Braun M, Rubio IG & Thony-Meyer L** (2005) A heme tag for *in vivo* synthesis of artificial cytochromes. *Appl Microbiol Biotechnol* **67**: 234-239.
38. **Percival, ZYH** (2011) Substrate channeling and enzyme complexes for biotechnological applications. *Biotechnol Adv* **29**: 715-725.
39. **Jin J, Mazon H, van den Heuvel RH, Heck AJ, Janssen DB & Fraaije MW** (2008) Covalent flavinylation of vanillyl-alcohol oxidase is an autocatalytic process. *FEBS Journal*, **275**: 5191-5200.
40. **Hassan-Abdallah A, Bruckner RC, Zhao GH, Jorns MS** (2005) Biosynthesis of covalently bound flavin: isolation and *in vitro* flavinylation of the monomeric sarcosine oxidase apoprotein. *Biochemistry*, **44**: 6452-6462.
41. **Arslan E, Schulz H, Zufferey R, Kunzler P & Thony-Meyer L** (1998) Overproduction of the *Bradyrhizobium japonicum* *c*-type cytochrome subunits of the *cbb(3)* oxidase in *Escherichia coli*. *Biochem. Biophys. Res. Commun.* **251**: 744-747.
42. **Berry EA & Trumpower BL** (1987) Simultaneous determination of hemes-A, hemes-B, and hemes-C from pyridine hemochrome spectra. *Anal Biochem* **161**: 1-15.
43. **Macheroux P** in *Flavoprotein Protocols* (Eds: Chapman SK & Reid GA), Humana Press, (1999), 1-7.
44. **DeLisa MP, Tullman D & Georgiou G** (2003) Folding quality control in the export of proteins by the bacterial twin-arginine translocation pathway. *Proc Natl Acad Sci U S A* **100**: 6115-6120.
45. **Mavridou DAL, Braun M, Thony-Meyer L, Stevens JM & Ferguson SJ** (2008) Avoidance of the cytochrome *c* biogenesis system by periplasmic CXXCH motifs. *Biochem Soc Trans* **36**: 1124-1128.
46. **Primus JL, Boersma MG, Mandon D, Boeren S, Veeger C, Weiss R & Rietjens IMCM** (1999) The effect of iron to manganese substitution on microperoxidase 8 catalysed peroxidase and cytochrome P450 type of catalysis. *J Bio Inorg Chem* **4**: 274-283.
47. **Britton HTS & Robinson RA** (1931) Universal buffer solutions and the dissociation constant of veronal. *J Chem Soc* 1456-1462.

48. **Wilson MT, Ranson RJ, Masiakowski P, Czarnecka E & Brunori M** (1977) Kinetic study of pH-dependent properties of ferric undecapeptide of cytochrome *c* (microperoxidase). *Eur J Biochem* **77**: 193-199.
49. **Alexeeva M, Enright A, Dawson M, Mahmoudian M & Turner N** (2002) Deracemization of alpha-methylbenzylamine using an enzyme obtained by *in vitro* evolution. *Angew Chem, Int Ed* **41**: 3177-3180.
50. **Thony-Meyer L & Kunzler P** (1997) Translocation to the periplasm and signal sequence cleavage of preapocytochrome *c* depend on *sec* and *lep*, but not on the *ccm* gene products. *Eur J Biochem* **246**: 794-799.
51. **Kapust RB & Waugh DS** (1999) *Escherichia coli* maltose-binding protein is uncommonly effective at promoting the solubility of polypeptides to which it is fused. *Protein Sci* **8**: 1668-1674.

Chapter 5

Hot or not? A thermostable alditol oxidase from *A. cellulolyticus* 11B

Remko T. Winter, Egon M. A. Rijpkema, Edwin van Bloois, Hein J. Wijma and Marco W. Fraaije

Laboratory of Biochemistry, Groningen Biomolecular Sciences and Biotechnology Institute,
University of Groningen, Nijenborgh 4, 9747 AG Groningen, The Netherlands

Dominic P. H. M. Heuts

Manchester Interdisciplinary Biocentre and Faculty of Life Sciences,
University of Manchester, 131 Princess Street, Manchester M1 7DN, United Kingdom

This chapter has been published in:
Applied Microbiology and Biotechnology
DOI: 10.1007/s00253-011-3750-0

Abstract

We describe the discovery, isolation and characterization of a highly thermostable alditol oxidase from *Acidothermus cellulolyticus* 11B. This protein was identified by searching the genomes of known thermophiles for enzymes homologous to *Streptomyces coelicolor* A3(2) alditol oxidase (AldO). A gene (sharing 48% protein sequence identity to AldO) was identified, cloned and expressed in *E. coli*. Following 6xHis tag purification, characterization revealed the protein to be a covalent flavoprotein of 47 kDa with a remarkably similar reactivity and substrate specificity to that of AldO. A steady-state kinetic analysis with a number of different polyol substrates revealed lower catalytic rates but slightly altered substrate specificity when compared to AldO. Thermostability measurements revealed that the novel AldO is a highly thermostable enzyme with an unfolding temperature of 84°C and an activity half-life at 75°C of 112 min, prompting the name HotAldO. Inspired by earlier studies, we attempted a straightforward, exploratory approach to improve the thermostability of AldO by replacing residues with high B-factors with corresponding residues from HotAldO. None of these mutations resulted in a more thermostable oxidase, a fact that was corroborated by *in silico* analysis.

5.1 Introduction

The importance of enzymes as industrial biocatalysts has been steadily increasing over the past decades (1-3). Their exquisite chemo-, regio- and enantioselectivity make them extremely powerful and recent trends forcing the chemical industry to become more sustainable are making the development of enzymatic processes more attractive as replacements for conventional, less sustainable procedures. A major drawback of enzymatic processes is that optimal physiological conditions often do not translate well into industrial processes, with the thermostability of the protein proving to be a major challenge for enzyme engineers.

One of the most important reactions in synthetic organic chemistry is the oxidation of primary and secondary alcohols; both the alcohol and its oxidation product being used as building blocks in numerous synthetic routes. Chemical alcohol oxidation on an industrial scale often proceeds via methods involving stoichiometric amounts of potentially toxic metals like chromium and manganese. While the recent advances in transition metal-catalysed (4) and organocatalytic (5) oxidations using O₂ and H₂O₂ as oxidants are impressive, biocatalytic alternatives – which are both environmentally benign and more selective – are obviously highly desirable. Several oxidizing enzymes can be utilized in processes requiring the selective oxidation of alcohols, with alcohol dehydrogenases (ADHs) which catalyse the oxidation of an alcohol into a ketone with the concomitant reduction of the electron acceptor NAD(P)⁺ being used most extensively (6). The obvious drawback of these enzymes is the fact that they require stoichiometric amounts of an expensive cofactor, and for this reason the alcohol/carbohydrate oxidases have been attracting recent interest (7). These enzymes utilize molecular oxygen as a cheap and clean electron acceptor, which is reduced to hydrogen peroxide yielding the only by-product of the reaction. Positive aspects notwithstanding, there are at present relatively few of these enzymes available. Most, like the well-studied glucose oxidase (8), are eukaryotic in origin and consequently issues like expression and post-translational modifications are problematic. In this regard, the flavoprotein oxidase alditol oxidase (AldO), recently identified from the proteome of *Streptomyces coelicolor* A3(2) (9), is unique insofar that it is bacterial in origin and heterologous expression is not an issue. AldO has been studied for its biocatalytic potential (10) and recent studies on the display of AldO on the cell surface and in the periplasm of *E. coli* heighten its possible application as a (whole-cell) biocatalyst (11, 12). Since its discovery, two patents have been issued involving the biocatalytic application of AldO (WO 2008/051491 A2, Danisco US; WO 2007/054203 A2, Henkel AG), highlighting its industrial potential. AldO is a 45 kDa monomeric flavoprotein, expressed at high yields in *E. coli* (up to 350 mg L⁻¹) and

capable of selectively oxidizing the primary hydroxyl group of alditols, with xylitol being the best substrate. Its substrate specificity is relatively relaxed, with a broad range of aliphatic alcohols being converted. Notably, AldO is highly regio- and enantioselective for the oxidation of 1,2-diols, forming enantiopure alpha-hydroxy carboxylic acids (10). Despite these attractive characteristics the utilization of AldO in biocatalytic processes is limited by the fact that it is only moderately thermophilic with an activity half-life at 30°C of only 30 hours (10) and an unfolding temperature (T_m) of 61°C. Hence, the aim of this study was to identify a thermostable oxidase with the desirable biocatalytic properties of AldO, by searching bacterial genome databases. The secondary aim was then to reverse engineer this thermostability into AldO, thus gaining valuable insight into the mechanisms responsible for the thermal stability of these redox enzymes.

By genome mining, a homologue of alditol oxidase (AldO) was discovered in the genome of the thermophilic bacterium *Acidotherrmus cellulolyticus* 11B, an organism isolated from the acidic hot springs of northern Yellowstone national Park, Wyoming, USA (13, 14). Heterologous expression in *E. coli*, purification and characterization revealed a thermostable flavoprotein with highly similar substrate specificity to AldO. The unfolding temperature (T_m) was determined to be more than 20°C higher than AldO, inspiring the name HotAldO for this protein. Inspired by earlier studies (17), we attempted to improve the thermostability of AldO by replacing residues with high B-factors with corresponding residues from HotAldO. None of these mutations resulted in a more thermostable oxidase, a fact that was corroborated by *in silico* analysis.

With an increasing need for robust biocatalysts and the emerging importance of green, enzymatic oxidations (18) we believe that the discovered thermostable HotAldO described here is a valuable addition to the industrial enzyme toolbox.

5.2 Materials and methods

5.2.1 Reagents & enzymes

Restriction enzymes were obtained from New England Biolabs. The polymerase chain reaction (PCR) was carried out with the Expand Long Range PCR kit from Roche. QuikChange mutants were constructed using *Pfu*Turbo DNA polymerase from Stratagene. Vanillyl alcohol oxidase (VAO; EC 1.1.3.38) was a kind gift from Prof. Dr. W. J. H. van Berkel (Wageningen University, The Netherlands). Horseradish peroxidase (EC 1.11.1.7) was from Fluka. Ni²⁺-NTA agarose was obtained from Qiagen. All other chemicals used were from Sigma-Aldrich and of analytical grade.

5.2.2 Cloning and expressing the *hotaldo* gene and generation of thermostability mutants

Acidotherrnus cellulolyticus 11b (ATCC® no: 43068) genomic DNA was obtained from LGC Standards (Teddington, United Kingdom). The gene encoding HotAldO (KEGG entry: Acel_0723) was amplified from *Acidotherrnus cellulolyticus* 11B genomic DNA by PCR (primers available upon request). A synthetic gene encoding the HotAldO protein (RefSeq code: YP_872482) and optimized for expression in *E. coli* was obtained from GENEART (Regensburg, Germany). The gene (KEGG entry: Tfu_1946) encoding the putative thermostable alditol oxidase from *Thermobifida fusca* YX (TfuAldO; RefSeq code: YP_290002) was amplified from genomic DNA by PCR (primers available upon request). All three genes were cloned into the pBAD*Nde*IHis and pBAD-MBP expression vectors between the restriction sites *Nde*I/*Pst*I and *Eco*RI/*Pst*I, respectively. pBAD*Nde*IHis is a pBAD/myc-HisA derived expression vector (Invitrogen) in which the *Nde*I site is removed and the *Nco*I site is replaced by *Nde*I (19). In this vector, the myc-HisA epitope has also been removed and replaced by a 6xHis tag immediately downstream of the C-terminal *Pst*I site. pBAD-MBP is identical to pBAD*Nde*IHis save for the *Nde*I/*Eco*RI insertion of the *malE* gene and a factor Xa protease cleavage site from pMALc2x (New England Biolabs). The resulting expression plasmids, pBAD(m)HAG (HotAldO cloned from genomic DNA; m, MBP fusion), pBAD(m)HAS (HotAldO cloned from synthetic DNA; m, MBP fusion) or pBAD(m)*Tfu*Ox (*Tfu*Ox, putative thermostable oxidase cloned from *T. fusca*; m, MBP fusion) were used to transform *E. coli* TOP10 (Invitrogen), MC1061 (20) and BL21(DE3) (21) cells. Transformed strains were cultured to saturation at 37°C in Luria Bertani medium (LB; 10 g tryptone, 5 g yeast extract and 10 g NaCl per liter). In all cases medium was supplemented with 50 µg mL⁻¹ ampicillin. Saturated cultures were back diluted 1:100 into fresh LB medium containing 0.02% (w/v) L-arabinose and cultured at 17, 25, 30 and 37°C for 72, 18, 16 and 12 hours, respectively, to determine the optimal expression conditions for HotAldO. Expression levels were analysed with sodium dodecyl sulphate-poly acrylamide gel electrophoresis (SDS-PAGE) by comparing to uninduced controls.

Streptomyces coelicolor A3(2) alditol oxidase (AldO) thermostability QuikChange mutants (Table 5.2) were generated by site-directed mutagenesis using *Pfu*Turbo polymerase (primer sequences available on request) and pBAD-*aldo* (9) as template. Due to the high GC content (73.4%) of the AldO gene the mutagenesis protocol (Stratagene) was slightly modified. Briefly, QuikChange mixes contained 0.4 µM forward and reverse primers, 0.2 mM dNTPs, 50 ng template, polymerase buffer, 2.5 U polymerase, 4% (v/v) DMSO and sterile double distilled H₂O to a final volume of 50 µl.

The following PCR program was run on a TECHNE thermocycler: 5 min initial denaturation at 94°C followed by 18 identical cycles consisting of a 1 min denaturation step at 94°C, a 0.5 min annealing step at 55°C and a 13 min extension step at 68°C. The program was ended with a final extension step of 5 min at 68°C. Nucleotide sequences were verified by DNA sequencing (GATC Biotech Ag, Konstanz, Germany). *E. coli* MC1061 cells were transformed with AldO mutants and expressed in 50 mL Terrific Broth medium (TB; 12 g Bacto Tryptone, 24 g Yeast Extract, 4 mL glycerol, 16.4 g K₂HPO₄·3H₂O and 2.3 g KH₂PO₄ per liter) supplemented with 50 µg mL⁻¹ ampicillin and 0.02% (w/v) L-arabinose for 72 hours at 17°C.

5.2.3 Purification of recombinant HotAldO

Optimal protein expression was obtained by culturing *E. coli* TOP10 cells harbouring pBADHAS in TB supplemented with 50 µg mL⁻¹ ampicillin and 0.02% (w/v) L-arabinose at 37°C for 12 hours. Cells from 1 L of culture were harvested by centrifugation (6 000 x *g* for 15 min at 4°C), resuspended in 30 mL potassium phosphate buffer (50 mM, pH 7.5) and disrupted by sonication (20 kHz for 15 min at 4°C). Following a clarifying centrifugation step (23 000 x *g* for 30 min at 4°C) to remove cell debris, 6xHis labelled HotAldO was purified from the supernatant using Ni²⁺-NTA agarose as described earlier (22). Briefly, NaCl and imidazole were added to a concentration of 500 mM and 15 mM, respectively, and incubated with Ni²⁺-NTA agarose (1.5 mL, Qiagen) for 120 min at 4°C. The slurry was loaded into a chromatography column (PolyPrep, Bio-Rad) and washed with potassium phosphate buffer (50 mM, pH 7.5) containing 500 mM NaCl and successively 15 and 30 mM imidazole. HotAldO was eluted with 60 mM imidazole. Imidazole and NaCl were removed by applying the enzyme to a desalting column (Econo-Pac 10DG, Bio-Rad). Desalted HotAldO was concentrated using a 0.5 mL centrifugal filter (Millipore, 12000 MWCO). The purification procedure was monitored by analysing samples for xylitol oxidase activity and by SDS-PAGE.

Streptomyces coelicolor A3(2) alditol oxidase (AldO) was heterologously expressed in *E. coli* MC1061 cells with the pBAD-*aldo* (9) expression vector. Cells were cultured in TB supplemented with 50 µg mL⁻¹ ampicillin and 0.02% (w/v) L-arabinose for 72 hours at 17°C. Purification of AldO was carried out on an Äkta purifier (GE Healthcare) with a Q-Sepharose column as described previously (9).

5.2.4 Analytical methods

Unless stated otherwise, all experiments were performed at 25°C and in potassium phosphate buffer (50 mM, pH 7.5). All measurements were carried out in triplicate, and the standard deviation value in the experiments is <5%, unless stated otherwise.

Absorption spectra of HotAldO were recorded on a Perkin-Elmer LambdaBio40 spectrophotometer. The extinction coefficient was calculated by comparing the absorption spectra before and after denaturing with 0.1% SDS. The oligomeric form of HotAldO was determined as described previously by van Bloois *et al* (22), using a WorkBeads SEC40 preppacked column (15 mL; Bio-Works, Hong Kong) and potassium phosphate buffer (50 mM, pH 7.5) containing 150 mM KCl.

5.2.4.1 Steady-state kinetic parameters

An indirect assay coupling the production of hydrogen peroxide by HotAldO or AldO to the horseradish peroxidase (HRP) mediated oxidation of 4-aminoantipyrine (AAP) and 3,5-dichloro-2-hydroxybenzenesulfonic acid (DCHBS) was used to measure oxidase activity and determine the kinetic parameters of HotAldO and AldO. In this assay the formation of a pink/purple coloured product can be measured spectrophotometrically at 515 nm ($\epsilon_{515 \text{ nm}} = 26 \text{ mM}^{-1} \text{ cm}^{-1}$) (23). A typical reaction mixture contained 0.1 mM AAP, 1 mM DCHBS, 3 units HRP and 20 nM (Hot)AldO, as described earlier (9). To determine the pH optimum of HotAldO and AldO the above assay was performed in three different buffer systems: 50 mM citrate (pH 4.6 – 6.0), 50 mM phosphate (pH 6.0 – 8.3) and 50 mM glycine (pH 8.6 – 10.2).

5.2.4.2 Pre-steady-state kinetic studies

An Applied Photophysics stopped-flow apparatus, model SX17MV, was used. Absorption spectra were collected at 2.5 ms intervals using a diode array detector while absorption at single wavelengths was followed in time with a photomultiplier detector. Spectral data obtained by diode array measurements was deconvoluted using Pro-K software (Applied Photophysics). The reductive half-reaction was monitored by collecting spectra with the diode array detector and by measuring the absorbance over time at 452 nm with the photomultiplier detector after anaerobically mixing 12 μM enzyme with varying concentrations of xylitol. The oxidative half-reaction was followed at 452 nm with the photomultiplier detector after mixing a solution containing reduced enzyme (12 μM) with a buffer solution containing 31.25, 62.5 or 125.0 μM dioxygen. Anaerobic conditions were created by the addition of 1 mM 4-ethylphenol to all solutions and flushing with nitrogen. Subsequently, VAO was added to a final concentration of 100 nM to remove all traces of residual oxygen. Traces obtained with the photomultiplier tube were fitted to an exponential function (Equation 5.1):

$$A(t) = A + C \times e^{(-kt)} \quad \text{Equation 5.1}$$

Where A is absorption, C is a constant and k is an observed rate constant. The observed rates for substrate concentration dependent reduction of HotAldO were fitted using the following equation (Equation 5.2):

$$k_{obs} = \frac{k_{red} \times S}{K_d + S} \quad \text{Equation 5.2}$$

Where k_{obs} is an observed rate constant, k_{red} the reduction rate constant, S the substrate concentration and K_d the dissociation constant.

5.2.4.3 Assessing Thermostability

Thermostability was assessed by determining residual activity after incubation of the enzyme at high temperatures. Freshly purified 2 μM aliquots of HotAldO or AldO were incubated in a water bath at the appropriate temperature. At set intervals, samples were removed and assayed for xylitol oxidase activity, as described above. A constant xylitol concentration of 10 mM was used. The percentage of residual activity was plotted against time and from this plot the half-life of the enzyme $t_{1/2}$ $^{\circ}\text{C}$ was determined: the time at which the initial activity has dropped to 50% of the original activity after incubation at a certain temperature. The residual activity after incubation for 1 hour at various temperatures was also plotted.

The temperature optimum of HotAldO and AldO was determined by measuring the initial xylitol oxidase activity at increasing temperatures. Reaction mixtures were prepared as described above (10 mM xylitol, without enzyme) and equilibrated to a defined temperature using the spectrophotometer's Peltier. Enzyme was added and the initial rate measured. Temperature optimum was determined by plotting the observed activity as percentage of the maximum observed activity versus the temperature. Controls were carried out to ensure there was sufficient HRP activity at elevated temperatures.

5.2.4.4 Determining the unfolding temperature, T_m , using ThermoFAD

The unfolding temperature, T_m , of HotAldO was determined using the *ThermoFAD* method, a *ThermoFluor*® derived approach for measuring the stability of flavoproteins based on the intrinsic fluorescence of their flavin cofactor and first described by Forneris *et al* (24). While this method does not assess the unfolding equilibrium, it is valuable for establishing the thermostability of a protein. 20 μl of 1 mg mL^{-1} protein in potassium phosphate buffer (50 mM, pH 7.5) were loaded in a Real Time PCR (RT-PCR) machine (Eppendorf) fitted with a 470 – 543 nm excitation filter and a SYBR Green emission filter (523 – 543 nm). A temperature gradient from 20 to 90 $^{\circ}\text{C}$ was

applied ($1^{\circ}\text{C min}^{-1}$), and fluorescence data was recorded every 0.5°C after a 10 s stabilization delay. A sigmoidal curve was obtained after plotting the fluorescence against the temperature. The unfolding temperature, T_m , is then determined as the maximum of the derivative of this sigmoidal curve (25).

Due to the high soluble overexpression levels of AldO in *E. coli* MC1061 we modified this protocol to obtain accurate unfolding temperatures of AldO QuikChange thermostability mutants using cleared cell extracts instead of purified protein. Cells were harvested from 50 mL cultures by centrifugation ($6\ 000 \times g$ for 15 min at 4°C), washed twice with potassium phosphate buffer (50 mM, pH 7.5) and disrupted by sonication (20 kHz for 15 min at 4°C). Following a clarifying centrifugation step ($23\ 000 \times g$ for 30 min at 4°C) to remove cell debris, the supernatant was desalted to remove free FAD by applying the enzyme to a desalting column (Econo-Pac 10DG, Bio-Rad). Desalted cell extracts were concentrated using a 0.5 mL centrifugal filter (Millipore, 12000 MWCO). 20 μL of concentrated, desalted cell extracts were loaded in a RT-PCR machine and the T_m was determined as described above.

5.2.4.5 FoldX and Rosetta analysis

FoldX and Rosetta were used to predict the change in folding energy of the protein due to the mutation ($\Delta\Delta G^{\text{FOLD}}$). FoldX was originally designed (26) to predict the $\Delta\Delta G^{\text{FOLD}}$ and was calibrated on a set of 1088 single mutants with average error of 3.4 kJ mol^{-1} (this error did not include 5 % outliers). Rosetta is a more general molecular modelling software package which was recently adopted for the prediction of $\Delta\Delta G^{\text{FOLD}}$ (27). While Rosetta was shown to exhibit better prediction trends ($r = 0.67$, versus 0.5 for FoldX), no error expressed in kJ mol^{-1} was reported for Rosetta, and therefore an error of 5 kJ mol^{-1} was assumed. For Rosetta the protocol described earlier was used which includes repacking of all residues in the protein with a soft-rep function (27). With the soft-rep ('soft repulsion') function the repulsive energy does not increase as dramatically when two atoms are brought together. As a result, clashes are penalized less throughout the initial stages of a discrete optimization. A model of the Asp deletion mutant was made with Yasara (28).

MD simulations were used to predict the Root Mean Square Fluctuations (RMSF), which is a measure of protein flexibility. MD simulation with the Yamber3 force field (59) were carried out under Yasara (60) The 1.1 \AA resolution X-ray structure of ligand free AldO (40) was used (PDB id: 2VFR) for the MD simulation. The rectangular simulation box extended at least 7.5 \AA from each side of the protein and contained 23 sodium and 12 chloride atoms to neutralize the net negative charge of AldO. The MD simulation was run with LINCS (61) and SETTLE (62), with a timestep of 2 fs, and with periodic boundary conditions. Snapshots taken every 10 ps between 2 and 7 ns (the

first 2 ns was used for equilibration) and were used to calculate the RMSF. For all other details regarding the MD simulation, see (63). For comparison to the thus predicted RMSF free in solution, the RMSF of the crystal structure was calculated from its B-factors via $\text{RMSF} = \sqrt{(3/8B\text{-factor}/\pi^2)}$.

5.2.4.6 Sequence analysis

HotAldO was identified by PSI-BLAST searches of the NCBI bacterial genome sequence database. Sequence alignment was performed with ClustalW version 2.0 (29) with subsequent manual refinements. The structural model of HotAldO was constructed using the CPHmodels 3.0 server (30) (<http://www.cbs.dtu.dk/services/CPHmodels/>) and the crystal structure of AldO complexed with xylitol (Protein Data Bank id 2VFS). Pictures were generated using PyMOL software (<http://www.pymol.org/>).

5.3 Results

5.3.1 Identification, expression, purification and spectral characterization of HotAldO

The protein sequence of *Streptomyces coelicolor* A3(2) alditol oxidase (UniProt: Q9ZBU1), a prototype flavoprotein oxidase belonging to the VAO-family, was used to perform PSI-BLAST searches to identify putative oxidases. Several sequences were identified that originated from thermophilic organisms (Figure 5.1) including two from the actinomycetes *Thermobifida fusca* YX and *Acidothermus cellulolyticus* 11B. Both were attractive sources for putative thermostable oxidases; we have shown before that *T. fusca* is a good source of robust biocatalysts (22, 31) and *A. cellulolyticus* is known to produce many thermostable cellulose degrading enzymes, including an endoglucanase, E1, which is thermostable to 81°C (32). The fact that both organisms are obligate thermophiles with an optimal growth temperature (OGT) of 55°C and no growth below 37°C (13, 33) improved the chances of finding a thermostable oxidase within their genomes. The putative thermostable oxidase from *T. fusca* (KEGG entry: Tfu_1946; RefSeq code: YP_290002) consists of 433 amino acids and a theoretical mass of 48.0 kDa (minus FAD); a homologous protein from *A. cellulolyticus* (KEGG entry: Acel_0723; RefSeq code: YP_872482) is only 417 amino acids in length and has a theoretical mass of 46.0 kDa (minus FAD). Both proteins share high homology to the previously studied flavoprotein oxidases AldO (9) (31% and 48% sequence identity, respectively) and *Streptomyces* sp. IKD472 xylitol oxidase (34) (XylOx, 27% and 48% sequence identity, respectively) and contain the conserved FAD-linking histidine (Figure 5.1).

Hot or not? A thermostable alditol oxidase from *A. cellulolyticus* 11B

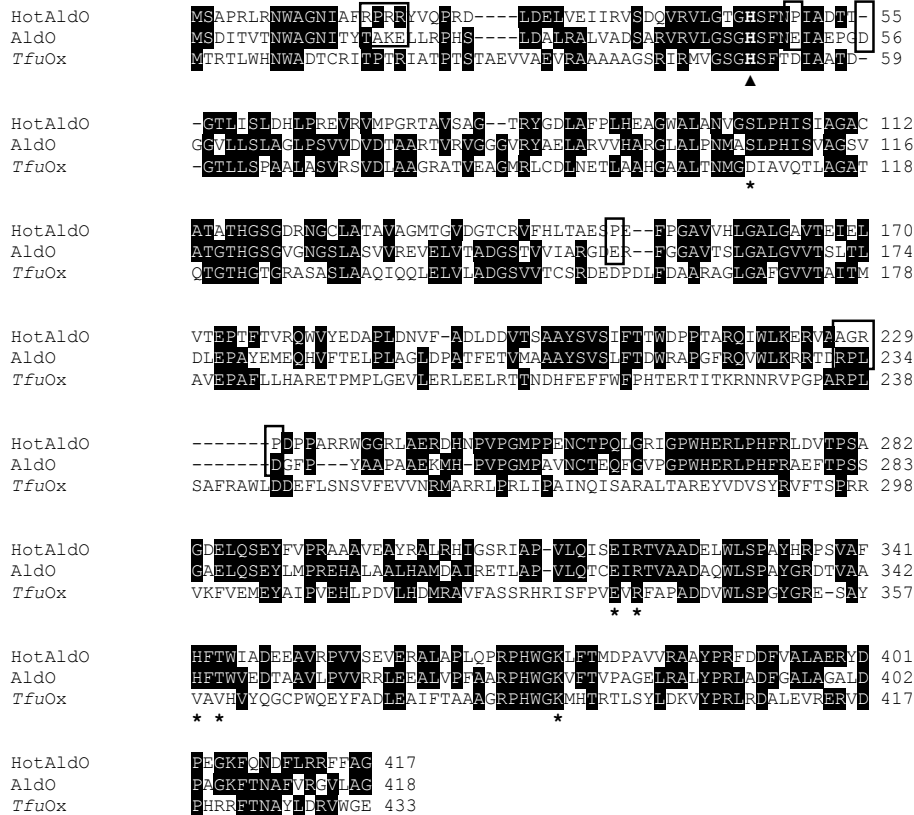


Figure 5.1 Multiple sequence alignment of AldO-type oxidases generated with ClustalW. Conserved residues are shaded, numbers refer to amino acid numbers and dashes correspond to gaps in the sequence alignment. The conserved FAD-binding histidine is in bold and marked with an arrowhead (▲). Residues involved in substrate binding and catalysis are marked with an asterisk (*). HotAldO, thermostable alditol oxidase from *Acidothermus cellulolyticus* 11B (RefSeq code: YP_872482); AldO, alditol oxidase from *Streptomyces coelicolor* A3(2) (UniProt: Q9ZBU1); TfuOx, putative thermostable oxidase from *Thermobifida fusca* YX (RefSeq code: YP_290002). Boxed are the AldO residues that have the highest B-factors and that were mutated into their HotAldO counterparts to explore their effect on thermostability.

High levels of soluble and covalently flavinylated expression of the putative thermostable oxidase from *T. fusca* was achieved in *E. coli* TOP10 cells cultured at 17°C, but a substrate screen of 86 potential oxidase substrates (9, 10), that included a wide variety of aliphatic and aromatic amines and alcohols, did not yield a positive result. As a result we decided to focus on the expression and characterization of the putative thermostable oxidase from *A. cellulolyticus*, HotAldO.

To enable heterologous expression the gene encoding HotAldO was PCR amplified from *A. cellulolyticus* genomic DNA and cloned into the arabinose inducible pBAD expression vector. With the resulting pBADHAG expression vector, recombinant expression in *E. coli* BL21(DE3), MC1061 and TOP10 cells was extremely low under all conditions tested. As it is known that soluble expression levels can be boosted by fusing a protein of interest to the C-terminus of maltose binding protein (MBP) (35), we constructed the expression vector pBADmHAG. Fusion of MBP to the N-terminus of the HotAldO gene did not have any visible effects on the expression level. Due to the fact that satisfactory recombinant protein expression in heterologous systems is often thwarted by divergent codon usage, a synthetic HotAldO gene was obtained that was codon optimized for expression in *E. coli* (36). Cloning of this gene into the pBAD and pBAD-MBP expression vectors yielded pBADHAS and pBADmHAS. Expression of the codon optimized HotAldO gene was only marginally better than the wild type gene, but by expressing the protein in TOP10 cells using the expression vector pBADHAS, in which the protein was fused to a C-terminal 6xHis tag, approximately 2.5 mg of pure protein could be obtained from 1 L of culture broth using a single Ni²⁺-NTA agarose chromatography step under native conditions. SDS-PAGE analysis revealed that purified HotAldO runs as a single band at about 47 kDa, which corresponds well with the calculated mass of 46.8 kDa (including FAD). After incubation in 5% (v/v) acetic acid and visualization under UV light, the respective protein band is clearly fluorescent (Figure 5.2), indicative of a covalently bound flavin cofactor (9, 37). Size exclusion chromatography was used to study the aggregation state of 6xHis-tag purified HotAldO under native conditions, and revealed that the protein is a monomer in solution, showing exactly the same elution volume as *S. coelicolor* AldO (Figure 5.3).

The absorption spectrum of HotAldO (Figure 5.2) is very similar to that of AldO (9); it has two absorption maxima at 350 and 450 nm, characteristic for an oxidized flavin cofactor, and shoulders at 370, 425 and 475 nm. The absorption maximum at 350 nm is at a relatively low wavelength, a typical feature of histidyl-bound flavin cofactors (38). Upon unfolding of the protein by SDS, the absorption maxima at 350 and 450 nm decrease slightly in intensity and shift slightly to lower wavelengths (Figure 5.2). Such a hypsochromic shift, compared to free FAD or FMN, is characteristic of 8 α -substituted flavin (39), like found in AldO. Assuming that the absorption spectrum of the unfolded protein can be compared to that of free FAD ($\epsilon_{450\text{ nm}} = 11.3\text{ mM}^{-1}\text{ cm}^{-1}$) (38), a molar extinction coefficient of $12.5\text{ mM}^{-1}\text{ cm}^{-1}$ (at 450 nm) can be calculated for the native enzyme.

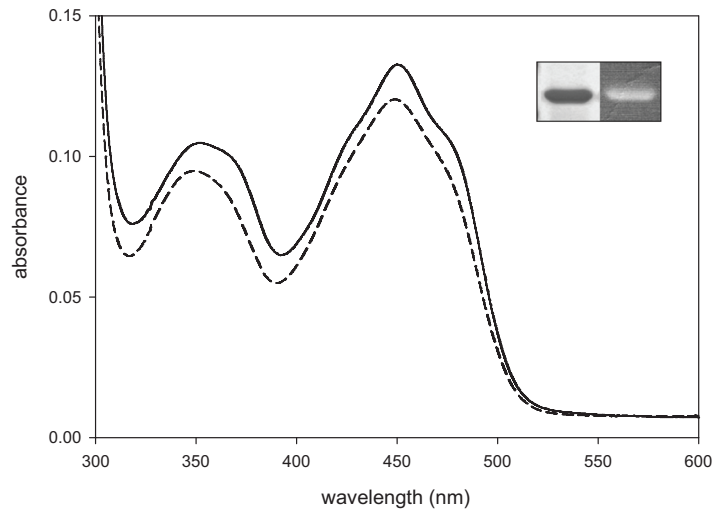


Figure 5.2 Visible absorption spectra of HotAldO. Spectra were recorded of native protein (*solid line*) and after unfolding by 0.1% SDS (*dashed line*). The inset shows SDS-PAGE analysis of HotAldO purified by Ni²⁺-NTA affinity chromatography. Shown are the protein band stained for flavin fluorescence (*right*) and total protein stained with Coomassie Brilliant Blue (*left*).

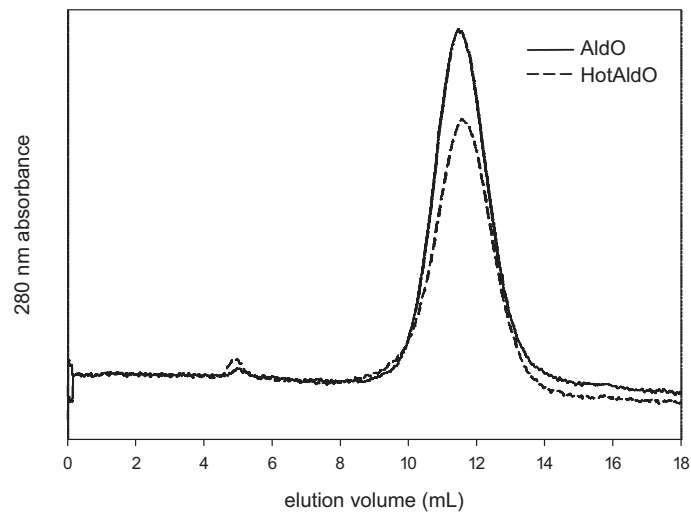


Figure 5.3 HotAldO is a monomer in solution, like AldO. Size exclusion chromatography elution profile of *S. coelicolor* AldO (*solid line*) and *A. cellulolyticus* HotAldO (*dotted line*). Equal volumes of AldO (13.5 mg mL⁻¹) and HotAldO (9.9 mg mL⁻¹) were analysed in separate runs on a WorkBeads SEC40 prepacked column (15 mL; Bio-Works) in potassium phosphate buffer (50 mM, pH 7.5) containing 150 mM KCl.

Comparing the spectral characteristics of AldO (9) and HotAldO reveals a large degree of similarity between the two proteins, and implies that the flavin cofactor in HotAldO is in a similar microenvironment and covalently bound to the protein backbone via an 8 α -*N*-histidyl linkage. The presence of a covalent histidyl linked FAD is supported by a model constructed of HotAldO; this revealed that His46 in HotAldO is in a similar position and orientation to the residue in AldO responsible for anchoring FAD, His46 (Figure 5.4) (40).

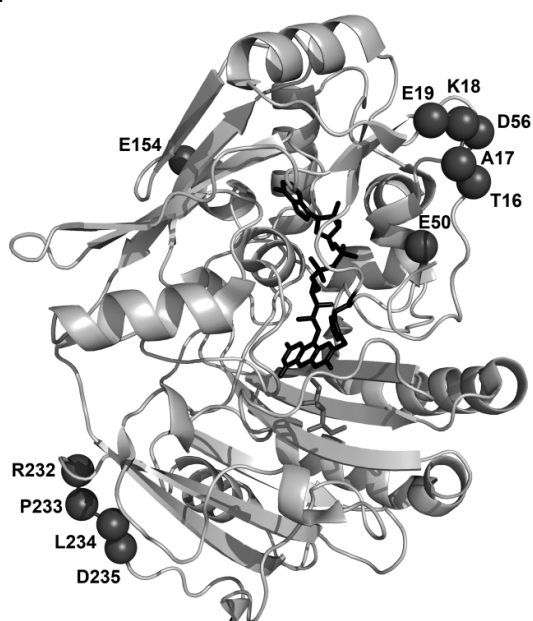


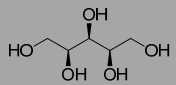
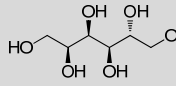
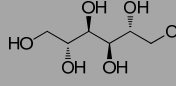
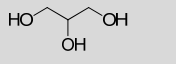
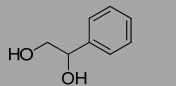
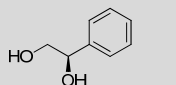
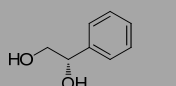
Figure 5.4 Mutating AldO into HotAldO. Crystal structure of AldO with xylitol bound (PDB id: 2VFS) showing the location of residues (dark spheres) that were mutated into their HotAldO counterparts in order to explore their effect on enzyme thermostability. The His46 bound FAD cofactor is shown as black sticks; xylitol as dark gray sticks. Mutants constructed are listed in Table 5.2.

5.3.2 Steady-state catalytic properties of HotAldO

Inspection of the ClustalW alignment of HotAldO and AldO (Figure 5.1) revealed a remarkably complete degree of conservation of the active site residues that are involved in substrate binding & catalysis (40). Closer analysis of the structural model shows that these residues in HotAldO all have a similar position and orientation as their AldO counterparts. As a result we anticipated that the substrate scope of HotAldO would be similar to that of AldO, acting on a broad range of aliphatic and aromatic diols and polyols, and preferring the C5 and C6 alditols xylitol and sorbitol (10). Table 5.1 details the steady-state kinetic parameters for a selection of HotAldO

substrates and reveals that the activity profile of this enzyme towards the substrates tested is remarkably similar to that of AldO. The 5-carbon alditol xylitol is the preferred substrate and increasing or reducing the alditol chain length only serves to reduce the substrate specificity as evidenced by a higher K_M value for the 3 carbon polyol glycerol and the 6 carbon alditol sorbitol. In agreement with the fact that the enzyme originates from a thermophilic organism and that the experiments were carried out at mesophilic temperatures, the measured k_{cat} values are nearly all significantly (between 70 and 90%) lower than those of AldO. The kinetic behaviour of HotAldO is the same as AldO for all of the substrates tested, with the exception of glycerol. Repeated experiments revealed significant substrate inhibition at high glycerol concentrations (>500 mM), something that was not observed for AldO. Using

Table 5.1 Steady-state kinetic parameters for recombinant HotAldO and AldO. The kinetic parameters of both enzymes were measured at 25°C in 50 mM potassium phosphate buffer (pH 7.5). The kinetic parameters of AldO have been described elsewhere (9, 10).

Substrate	HotAldO			AldO		
	K_M (mM)	k_{cat} (s ⁻¹)	k_{cat} / K_M (s ⁻¹ M ⁻¹)	K_M (mM)	k_{cat} (s ⁻¹)	k_{cat} / K_M (s ⁻¹ M ⁻¹)
xylitol 	0.07	1.9	27 000	0.32	13	41 000
D-sorbitol 	0.44	1.2	2700	1.4	17	12 000
D-mannitol 	5.5	2.5	450	36	9.2	260
glycerol 	270	1.3	4.8	350	1.6	4.6
1-phenyl-1,2-ethandiol 	68	0.1	1.5	83	0.36	4.3
(R)-1-phenyl-1,2-ethandiol 	18	0.1	5.6	101	0.74	7.3
(S)-1-phenyl-1,2-ethandiol 	27	0.0004	0.01	86	0.008	0.1

the modified Michaelis-Menten rate equation for substrate inhibition (41), an apparent inhibition constant (K_{si}) of 1500 mM was calculated. Apparent inhibition constant, as the inhibition was observed at such high glycerol concentrations (> 4%) that viscosity based effects cannot be ruled out (42). To offset this reduction in rate and supporting the fact that proteins from thermophilic organisms are often more rigid than their mesophilic counterparts (16) the substrate specificity of HotAldO for the substrates tested is slightly better than that of AldO, as evidenced by the fact that the Michaelis constants for HotAldO are mostly 65-85% lower than their AldO counterparts.

With 10 mM xylitol as substrate the pH optimum for enzyme activity was determined. Like AldO (10) purified HotAldO has a broad pH optimum; more than 80% of its maximum activity is found between pH 6 and 9. HotAldO is reasonably active at acidic pHs; at pH 4.5 it retains 20% of its maximum activity. This compares favourably to AldO, which is inactive at and below pH 5.

As it is known that AldO can selectively oxidize the (*R*)- enantiomer of several (aromatic) diols (10), we were intrigued if HotAldO exhibits the same enantioselectivity. For this reason we measured the steady state kinetic parameters of HotAldO with (*R*)-, (*S*)-, and racemic 1-phenyl-1,2-ethanediol. A similar trend was observed as for AldO (Table 5.1), but due to the improved selectivity of HotAldO for the *R* enantiomer an *E* value of 375 was calculated from the ratio between the specificity constants (k_{cat}/K_M) compared to an *E* value of only 74 for AldO (10), highlighting HotAldO's potential as an enantioselective biocatalyst. The notion that the mechanism of stereoselectivity is conserved between AldO and HotAldO is confirmed by the observation that the six carbon alditol D-mannitol is a worse substrate than the related compound D-sorbitol as evidenced by the 10-fold higher K_M value, a feature that the crystal structure of AldO revealed to be caused by the orientation of the secondary hydroxyl moiety of the substrate with respect to the imidazole ring of His343 (40).

The redox state of HotAldO during steady-state catalysis was determined by monitoring the flavin absorbance with stopped flow spectroscopy. After mixing 250 μ M O₂, 15 mM xylitol and 10 μ M HotAldO at 25°C a fast – within 100 ms – decrease in the absorbance at 450 nm was observed, before the steady-state phase was reached. The steady-state phase lasted for about 10 s, which agrees with the calculated k_{cat} value, and was followed by a rapid and complete reduction of the flavin due to the excess of xylitol. Under steady-state conditions 20% of the flavin is in the oxidized form, a much lower value than the 32% calculated for AldO (9) and in agreement with the finding that the re-oxidation rate of HotAldO is significantly lower than that of AldO (see: *pre-steady state kinetic analysis*).

5.3.3 HotAldO is a highly thermostable enzyme

As HotAldO originates from a thermophilic organism (*A. cellulolyticus* OGT = 55°C) we anticipated that it would function as a thermostable oxidase. Unfolding experiments performed using the *ThermoFAD* method, which measures the increase in flavin fluorescence as the protein denatures (24), revealed that the T_m of HotAldO is 84°C; significantly higher than the 61°C measured for AldO. Thermostability measurements were carried out on HotAldO and AldO to further characterize the thermal stability of these two oxidases. By incubating samples of the enzymes at various temperatures and measuring the activity at regular intervals the enzyme activity half-life was calculated at three different temperatures. These measurements revealed that HotAldO has an impressive thermostability; at 60°C its activity half-life, $t_{1/2}60^\circ\text{C}$, is a staggering 1700 min (28 hrs 20 min) compared to the 1.1 min of AldO. At 75 and 80°C the thermal inactivation of AldO was too rapid to enable determination of the activity half-life, while that of HotAldO was still a respectable 111.8 and 2.0 min, respectively. The thermostability data supports the unfolding temperatures calculated by *ThermoFAD*; at temperatures close to the T_m the activity half-life of both enzymes is mere minutes (T_m AldO = 61°C, $t_{1/2}60^\circ\text{C}$ = 1.1 min; T_m HotAldO = 84°C, $t_{1/2}80^\circ\text{C}$ = 2.0 min). The optimum temperature for initial activity was determined for both enzymes and also found to match the T_m values quite well; 55°C for AldO and 80°C for HotAldO. Figure 5.5 shows the residual activity of both AldO and HotAldO after incubation at different temperatures for 1 hr. From this graph it is immediately clear that HotAldO is an extremely thermostable oxidase when compared to its mesophilic counterpart AldO.

5.3.4 Pre-steady state kinetic analysis

To study the subtle mechanistic differences between AldO and HotAldO in more detail we decided to investigate the pre-steady-state kinetics of HotAldO with xylitol as substrate. Using a stopped-flow instrument equipped with diode-array detection for spectral scans and a photomultiplier tube for single wavelength measurements we could follow the spectral changes of the covalently linked flavin cofactor during the reductive and oxidative half reactions (measured separately). As the catalytic efficiency of HotAldO with xylitol is significantly lower than that of AldO with xylitol we set out to determine whether the reductive or oxidative half reaction is rate-limiting. The reductive half-reaction of HotAldO was monitored by anaerobically mixing the enzyme with different amounts of xylitol, as described previously (9). From the resulting spectral data a hyperbolic dependency of the reduction rate on the xylitol concentration was observed. Fitting of this data yielded a reduction rate

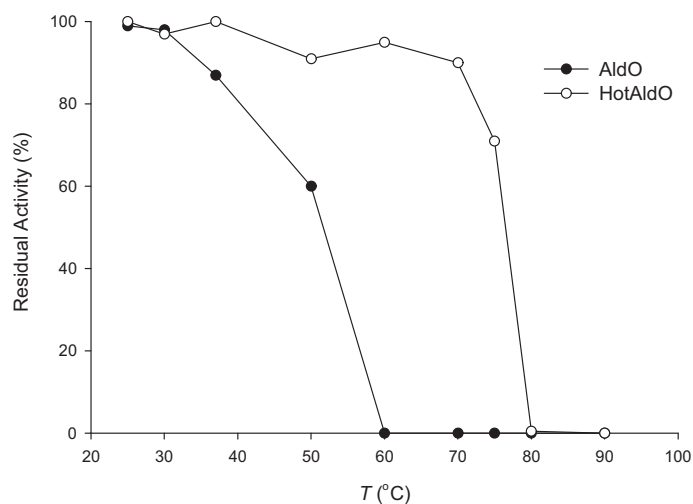


Figure 5.5 Thermostability of *S. coelicolor* AldO and *A. cellulolyticus* HotAldO. Shown are residual activity curves. Oxidase activity with xylitol as substrate was measured after enzyme solutions had been incubated at various temperatures (25-90°C) for 1 hour.

constant (k_{red}) of 53 s⁻¹ and a K_d of 2.0 mM. While significantly slower than the reduction rate of AldO (99 s⁻¹, 9), the reduction rate does not appear to be the rate limiting step in the catalytic cycle of HotAldO.

The oxidative half-reaction of HotAldO was measured by mixing reduced enzyme with different amounts of molecular oxygen and following the reoxidation of the flavin cofactor at 452 nm. After complete reduction of HotAldO by 3 equivalents of xylitol, mixing with molecular oxygen revealed relatively rapid reoxidation of the flavin cofactor. From the linear relation between k_{obs} and $[\text{O}_2]$ a bimolecular rate constant ($k_{\text{ox},1}$, 9) of $4.4 \times 10^4 \text{ M}^{-1} \text{ s}^{-1}$ was calculated. While this rate constant is lower than the $1.7 \times 10^5 \text{ M}^{-1} \text{ s}^{-1}$ found for AldO (9) it does not explain the lowered catalytic efficiency of HotAldO for xylitol. At ambient O_2 concentrations (250 μM) a k_{obs} for reoxidation of 11 s⁻¹ was observed, highlighting the fact that the oxidative half-reaction is, like the reductive half reaction, not the rate-limiting step in the catalytic cycle of HotAldO with xylitol. This finding is supported by the fact that the ‘oxygen gatekeeper’ residue (43) in HotAldO is a glycine (Gly101; Ala105 in AldO, Figure 5.1), indicative of optimal oxidase oxygen reactivity (44). Hence, more subtle effects such as substrate binding and product release are likely to determine the rate-limiting step.

5.3.5 Reverse engineering HotAldO thermostability into AldO

Due to the high degree of functional and sequence homology between AldO and HotAldO we wondered if it would be possible to engineer HotAldO's thermostability into its less stable counterpart, AldO. Due to the extremely high expression levels of AldO (up to 350 mg L⁻¹ culture, 9) and good catalytic efficiency this was a very attractive possibility, especially in lieu of AldO's potential for practical applications. Several high resolution crystal structures of AldO are available (40) and as it is known that residues with high B-factors contribute to protein instability (16) we decided to mutate those residues in AldO that have a very high B-factor, an approach that has been employed successfully in the past, most notably to improve the thermostability of a lipase from *Bacillus subtilis* (LipA) (17). By analysing the 1.6 Å crystal structure of AldO complexed with xylitol (PDB id: 2VFS) we identified three regions on the surface of the protein that possessed relatively high B-factors; residues 16-19, 56 and 232-235 (Figure 5.4). Looking to the highly thermostable oxidase HotAldO for inspiration, we inspected the sequence alignment of AldO and HotAldO (Figure 5.1) and identified the HotAldO residues that corresponded to the AldO residues with high B-factors. Consequently, AldO mutants were constructed by site directed mutagenesis (Table 5.2), whereby the AldO residue with a high B-factor was replaced by its HotAldO counterpart. As HotAldO is a much more thermostable enzyme we hypothesized that these residues would improve the thermal stability of AldO.

Inspection of the sequence alignment of AldO and HotAldO also revealed that HotAldO contains a high number of prolines compared to AldO (36 and 28, respectively). As it is known that prolines confer rigidity to a protein backbone and can bring a region into α -helix configuration, thereby having a positive effect on thermostability (45), two residues in AldO (Glu50 and Glu154, Table 2) were mutated into the corresponding HotAldO prolines (Figures 5.1 & 5.4).

Due to the large number of mutants that needed to be tested we designed a medium-throughput thermostability screen, based on measuring the unfolding temperature, T_m , of the AldO mutants in desalted cell extracts using the *ThermoFAD* method. The comparison between two homologous enzymes carried out in this study supports other studies (46, 47) that the T_m of a protein is a good measure of its thermostability. As the soluble expression of AldO is high in *E. coli* MC1061 (roughly 20% of total soluble protein, 9) it is not necessary to purify the protein to get accurate T_m data; *ThermoFAD* measurements are possible on cleared cell extracts. This approach was validated by measuring the T_m of wild-type AldO using purified protein and cell extracts. Cell extracts were desalted before measuring the T_m to reduce the background fluorescence present in the form of free FAD. Table 5.2 details the T_m

determined for wild type AldO in soluble extracts; the value is identical to the value when analysing purified protein: 61°C (see: *HotAldO is a highly thermostable enzyme*, above). While the temperature versus raw fluorescence traces for the two samples (pure protein and soluble cell extracts) are not identical, the maximum of the derivative of these sigmoidal curves is found at the same temperature and is highly reproducible over multiple samples (data not shown). Before assaying the AldO mutants for their unfolding temperature we determined if the soluble expression level and degree of covalent cofactor incorporation was unchanged compared to wild type. SDS-PAGE analysis and staining for cofactor fluorescence revealed that all nine mutants were expressed in *E. coli* MC1061 and contained covalently bound FAD, both at levels comparable to wild type AldO. Activity with 10 mM xylitol as substrate was also similar to wild-type AldO (data not shown). *ThermoFAD* measurements to calculate the unfolding temperature of the AldO mutants in cell free extracts did not reveal any significant increase in the T_m , and hence thermostability, for any of the mutants tested. For all mutants tested the T_m was the same or slightly lower than the wild type variant. The largest negative effect was the 3°C decrease in T_m caused by the D56 deletion and R232A/P233G/L234R/D235P mutations. On the whole it is interesting to note that AldO is a relatively robust enzyme, being able to withstand a large number of mutations with apparently no or marginal effects on its expression, activity and stability. In this case, however, we must conclude that replacing residues in AldO that have a high B-factor with corresponding residues from its thermostable counterpart HotAldO did not yield a more thermostable AldO mutant.

5.3.6 FoldX & Rosetta analysis of thermostability mutants

To explain why the mutations had a slightly negative or negligible effect on the melting temperature, the change in folding energy by the mutations was calculated via both FoldX and Rosetta software (Table 5.2). For most of the variants the predicted change in folding energy is within error identical to zero, and all these variants also have a melting temperature that differs maximally 1°C from the WT. For the E154P, a small but significant improvement in folding energy is predicted, which is not reflected in its melting temperature, which is within 0.5°C of the wild-type protein. For the R232A/P233G and R232A/P233G/L234R/D234P variants, both Rosetta and FoldX predict that the ΔG^{FOLD} is significantly worse than for WT, which is in line with the 2–3°C lower melting temperatures of these variants. Thus, the experimentally determined melting temperatures and the calculated changes in folding energy agree reasonably. For the Asp56 deletion mutant the loop in which it is located is predicted to change conformation due to the mutation, which can have resulted in strain, explaining the 3°C lower melting temperature. For the R232A/P233G and

R232A/P233G/L234R/D234P variants less damaging problems were found, most notably a loss of hydrophobic interactions by the L234R mutation that could (partially) explain the loss of folding free energy and corresponding reduction in melting temperature.

The original reason to mutate at the chosen positions was their high B-factor, which suggests it is a critical spot in the protein. Since the experimental results indicated that the T_m was only moderately affected, MD simulations were carried out to exclude that the relatively high B-factors in these regions were due to crystal packing interactions. The RMSF from an MD simulation was similar for the protein in solution and the X-ray structure (Figure 5.6), which indicates that the protein flexibility of free protein in solution is similar to that of the X-ray structure, which was earlier used to choose positions to mutate. Specifically, in both the X-ray structure and in the simulations, the N-terminus is the most mobile part of the enzyme while the region around residue 230, which was targeted by the mutations, is the second most mobile part. Also the region around residue 30 is one of the most mobile in the protein structure during the MD simulations.

Table 5.2 Measured T_m and predicted $\Delta\Delta G^{\text{FOLD}}$ of AldO thermostability mutants. Unfolding temperatures (T_m) were determined using a modification of the *ThermoFAD* method, as described in materials and methods. **In bold** are the $\Delta\Delta G^{\text{FOLD}}$ energies that are, taking the error into account, significant (error margin was taken as linearly dependent on the number of mutations).

Variant	T_m (°C)	$\Delta\Delta G^{\text{FOLD}}$ (kJ mol ⁻¹) predicted by:	
		FoldX	Rosetta
Wild-type	61.0	0	0
T16R/A17P	60.8	1.5	0.9
K18R/E19R	61.0	1.2	1.2
T16R/A17P/K18R/G19R	60.0	-3.4	2.3
E50P	59.9	2.3	-2.8
Asp56 deletion mutant	58.0	<i>nd</i> ^a	<i>nd</i> ^a
E154P	60.7	-5.5	-5.3
R232A/P233G	58.8	12.6	13.4
L234R/D235P	60.5	6.4	24.8
R232A/P233G/L234R/D235P	58.0	19.1	38.0

nd: not determined; ^a For deletion mutants the change in folding energy cannot be predicted reliably

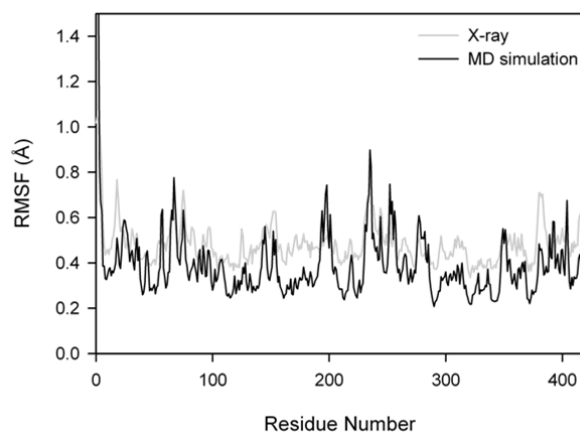


Figure 5.6 Comparison of AldO flexibility from MD simulation with that of the X-ray structure. AldO crystallographic B-factors were converted to RMSF as described in the experimental section. The agreement confirms that the most flexible parts of AldO were indeed targeted for mutagenesis.

5.4 Discussion

Flavoprotein oxidases represent a versatile class of oxidative biocatalysts, but their availability is limited; at present only a handful have been fully characterized (7) and most are of fungal origin and mesophilic in character. In this paper, we detail the search for a thermophilic oxidase by searching the bacterial genome database for homologues of the well-studied *Streptomyces coelicolor* AldO, a member of the VAO family of flavoprotein oxidases. We identified two putative thermophilic oxidases in the genomes of the thermophiles *T. fusca* and *A. cellulolyticus*. Subsequent cloning and heterologous expression in *E. coli* revealed that both proteins were covalent flavoproteins, as was expected from sequence analysis: both contained the distinguishing VAO family covalent-FAD motif (Figure 5.1, 15). As no oxidase substrate could be identified for the putative *T. fusca* oxidase, perhaps due to its rather low (31%) sequence identity with AldO, we continued with the characterization of the putative *A. cellulolyticus* oxidase, which we named HotAldO due to its thermophilic origin and its high homology (48%) and overlap in substrate specificity to *S. coelicolor* AldO. The physiological function of HotAldO, as with most other oxidases, is unknown. Besides *S. coelicolor* AldO, several other homologues with high sequence identities (%) have been identified in actinomycete genomes including *Streptomyces* sp. (55%), *Catenulispora acidiphila* (54%), *Frankia* sp. Eu1c (54%), *Verrucosispora maris* (54%), *Streptomyces flavogriseus* (53%) and *Kribbella flavida* (50%). The fact that AldO, HotAldO and the homologue XylOx (48%) from *Streptomyces* sp. IKD472 (34) all act as

oxidases, preferentially converting alditols, seems to indicate that the above organisms all harbor an alditol oxidase orthologue for some as yet unknown catabolic or anabolic route. Modification of some secondary metabolite is a realistic possibility; actinomycetes are well-known for their ability to produce such compounds, which often contain polyol moieties (48). It is also possible that HotAldO is used by the organism in a catabolic route for alditol degradation. Inspection of the genome of *A. cellulolyticus* shows that the HotAldO gene is flanked by several genes involved in carbohydrate modifications and transport, including a major facilitator transporter, a glycosyl transferase protein, a carbohydrate kinase, a fructose-biphosphate aldolase and a DeoR family transcriptional regulator.

Obtaining sufficient yield of heterologously expressed HotAldO proved to be problematic. Fusing the protein to MBP, which helped to boost the expression of AldO significantly (9) did not have any visible effects on HotAldO expression levels. The protein was finally isolated by expressing a synthetic gene, codon-optimized for *E. coli*. While codon optimization often has beneficial effect on the yields of heterologously expressed protein (36) in this case the improvement was marginal; only 2.5 mg of pure protein was obtained per liter of culture. It should be noted that the success of codon-optimization in improving the expression is extremely dependent on the optimization strategy employed; recent developments in this field seem to suggest that paradigms that have long been dogmatically adhered to have little empirical basis (49).

The most unique feature of HotAldO is its thermostability. Its high T_m (84°C) and long activity half-life at elevated temperatures ($t_{1/2}60^\circ\text{C} > 24$ hours) make it the most thermostable carbohydrate oxidase of bacterial origin described to date. It should be noted that relatively few thermostable flavoprotein oxidases are known; the most striking examples include pyranose oxidase (P2Ox), a carbohydrate oxidase recently isolated from the model white rot fungi *Phanerochaete chrysosporium* (50) with a T_m of 75.4°C and a $t_{1/2}50^\circ\text{C} > 24$ hours (51), and cholesterol oxidase (CHOLOX) from *Chromobacterium* sp. DS-1, which holds the oxidase thermostability record, retaining 90% of its original activity after incubation for 60 min at 80°C. (52). Due to the high homology to its mesophilic counterpart AldO, the thermostability of HotAldO is even more striking. As no crystal structure of HotAldO is available yet, we should be careful about drawing any conclusions about the structural & physical basis for this increased thermostability. Having a crystal structure is no panacea, however, as both in the case of CHOLOX and more thermostable mutants of *Trametes multicolor* P2Ox, high quality crystal structures did not reveal the structural basis for the high thermostability (53, 54). The relatively larger number of charged residues of HotAldO (Figure 5.7) is in agreement with the observation that salt-bridge networks are often responsible for

thermostabilization of proteins (55, 56). The relative amino acid content of the proteins is unlikely to be solely responsible for thermostability, however, as the trends observed here for the AldO-HotAldO pair are only in partial agreement with the trends observed elsewhere for a >100 protein set of mesophilic and thermophilic protein pairs (57). For the residues Pro, Arg, Ala, Ile, Gly and Asp, the trend observed here agrees with the trends observed for a much larger set, while the relative changes observed for Val, Leu and Glu (which should increase, not stay constant) do not agree. It is impossible to currently identify the mutations responsible for the higher thermostability of HotAldO since the sequence identity is only 48 % while far fewer mutations can potentially bridge the 23°C gap in melting temperature, as shown by protein engineering carried out on other enzymes (17, 58).

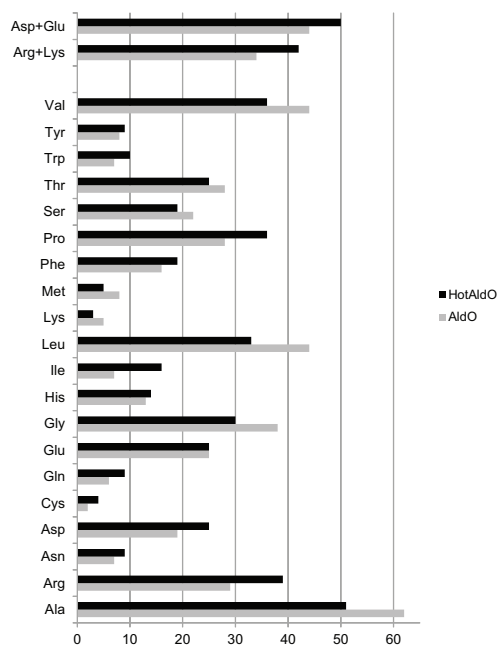


Figure 5.7 Occurrence overview of each amino acid occurring in two alditol oxidases. *S. coelicolor* AldO (grey) and *A. cellulolyticus* HotAldO (black). While the number of charged residues in HotAldO (92) is higher than in AldO (78), in agreement with the observation that salt-bridge networks are often responsible for thermostabilization of proteins (55, 56), it is unlikely that the relative amino acid content of the two proteins is solely responsible for the increased thermostability of HotAldO.

The substrate specificity of HotAldO is remarkably similar to that of AldO. The same range of polyols is converted, with alditols xylitol and sorbitol being preferred. This lends support to the notion that both enzymes have a similar functional role in their parent organisms. The high degree of conservation between the active-site residues of AldO and HotAldO that are involved in substrate recognition and binding (Figure 5.1) and the intricate network of hydrogen bonds that are involved in the binding of xylitol (40) also seem to suggest that an alditol highly similar to xylitol is probably the physiological substrate of these enzymes *in vivo*; other substrates simply do not fit as well in the alditol oxidase active site. Across the board, the catalytic rates of the substrates tested for HotAldO are lower than the corresponding rates for AldO, whereas the substrate recognition, as evidenced by the lower K_M values, is slightly better for HotAldO than for AldO. This is in line with the finding that thermophilic enzymes are more rigid than their mesophilic counterparts, and consequently have slower catalytic rates at ambient temperatures. A more rigid structure, however, improves substrate recognition, allowing for tighter substrate binding and lower K_m values. The enantioselectivity of HotAldO towards (*R*)-(aromatic) diols is also conserved compared to AldO, as evidenced by the selective oxidation of (*R*)-1-phenyl-1,2-ethanediol. Again, probably due to its thermophilic nature and more rigid structure, it displays an enhanced selectivity towards the (*R*)-enantiomer compared to AldO, which results in a higher *E*-value for this substrate.

We performed pre-steady-state kinetic analysis of the reductive and oxidative half-reactions separately in order to see if we could identify a rate-limiting step that would explain the lowered catalytic efficiency of HotAldO compared to AldO. While both half-reactions of HotAldO had lower rates than AldO, neither could explain the lower overall catalytic rate of HotAldO. Probably more subtle effects involving substrate binding and product release are at play. It is interesting to note that the reduced oxygen reactivity is in line with molecular dynamics simulations performed on the oxygen diffusion through the protein matrix of AldO (44). According to this study, diffusion of molecular oxygen through the protein matrix to the reduced flavin in the active site occurs through discrete, funnel-like pathways, which are conserved at higher temperatures. Thus, the overall rate of oxygen reactivity is governed by the overall flexibility of the protein and the movement of local side chains (partially) blocking the oxygen funnels.

Inspired by earlier studies (17) we attempted to reverse engineer the thermostability of HotAldO into its mesophilic counterpart AldO by replacing those residues with high B-factors in AldO with their HotAldO counterparts, generating seven AldO variants by site directed mutagenesis. Two further mutants were made; replacing AldO residues with corresponding HotAldO prolines (Figure 5.1, Table 5.2)

as such mutants can have beneficial effects on the thermostability (45). Although all nine mutants were overexpressed, soluble, contained covalently bound flavin and were active with xylitol, unfolding experiments revealed that none of the AldO mutants was more thermostable than the wild type variant. Due to the large number of mutant enzymes that had to be assayed for unfolding temperatures, we successfully pioneered a variation of the *ThermoFAD* method for determining the T_m of flavoproteins where we could obtain accurate T_m values from direct measurement of cell extracts.

Calculations carried out with FoldX and Rosetta confirmed that the variants that displayed the largest thermostability loss as evidenced by reduction in T_m were less stable than wild-type AldO. Inspection of the predicted 3D-structures indicated that this was due to local strain or packing problems such as loss of hydrophobic interactions. The relatively small (3°C) decreases in melting temperature by the quite drastic Asp56 deletion mutation and the R232A/P233G/L234R/D235P four-fold mutation may indicate that these residues are not in a so-called “weak spot” of the protein that is more sensitive for unfolding (58), although the higher B-factors had suggested it to be. It should be noted that the approach followed here was relatively simplistic, and that it is very possible that the mutations made were simply not the correct ones required to improve thermostability. It could be envisaged that performing saturation mutagenesis at these positions would yield a more thermostable variant, an approach successfully employed by Reetz *et al* (17). It is clear from our study, however, that care should be exercised when using B-factors alone to design more thermostable protein variants.

Taken together our data reveals that we have successfully identified a highly thermostable alditol oxidase from a thermophilic actinomycete, once again highlighting the biocatalytic potential of such heat-loving organisms. The biotechnological relevance of AldO has been studied and highlighted previously (10) but with the discovery of its thermophilic counterpart HotAldO, we have a new “prodigal son” alditol oxidase; one that has a highly similar substrate specificity, enantioselectivity and catalytic efficiency but a vastly improved thermostability.

5.5 Acknowledgements

This research is supported by the Dutch Technology Foundation STW (Grant number: GBC.7726), applied science division of NWO and the Technology Program of the Ministry of Economic Affairs.

5.6 References

1. **Pollard DJ & Woodley JM** (2007) Biocatalysis for pharmaceutical intermediates: the future is now. *Trends Biotechnol* **25**: 66-73.
2. **Sheldon RA** (2008) E factors, green chemistry and catalysis: An odyssey. *Chem Commun* 3352-3365.
3. **Wohlgemuth R** (2009) The locks and keys to industrial biotechnology. *New Biotechnol* **25**: 204-213.
4. **Punniyamurthy T, Velusamy S & Iqbal J** (2005) Recent advances in transition metal catalyzed oxidation of organic substrates with molecular oxygen. *Chem Rev* **105**: 2329-2363.
5. **Wong OA & Shi Y** (2008) Organocatalytic oxidation. Asymmetric epoxidation of olefins catalyzed by chiral ketones and iminium salts. *Chem Rev* **108**: 3958-3987.
6. **Liese A & Seelbach K** (2006) *Industrial Biotransformations*. (Wiley-VCH, Weinheim).
7. **van Hellemond EW, Leferink NG, Heuts DP, Fraaije MW & van Berkel WJ** (2006) Occurrence and biocatalytic potential of carbohydrate oxidases. *Adv Appl Microbiol* **60**: 17-54.
8. **Bankar SB, Bule MV, Singhal RS & Ananthanarayan L** (2009) Glucose oxidase - an overview. *Biotechnol Adv* **27**: 489-501.
9. **Heuts DP, van Hellemond EW, Janssen DB & Fraaije MW** (2007) Discovery, characterization, and kinetic analysis of an alditol oxidase from *Streptomyces coelicolor*. *J Biol Chem* **282**: 20283-20291.
10. **van Hellemond EW, Vermote L, Koolen W, Sonke T, Zandvoort E, Heuts DP, Janssen DB & Fraaije MW** (2009) Exploring the biocatalytic scope of alditol oxidase from *Streptomyces coelicolor*. *Adv Synth Catal* **351**: 1523-1530.
11. **van Bloois E, Winter RT, Janssen DB & Fraaije MW** (2009) Export of functional *Streptomyces coelicolor* alditol oxidase to the periplasm or cell surface of *Escherichia coli* and its application in whole-cell biocatalysis. *Appl Microbiol Biotechnol* **83**: 679-687.
12. **van Bloois E, Winter RT, Kolmar H & Fraaije MW** (2011) Decorating microbes: surface display of proteins on *Escherichia coli*. *Trends Biotechnol* **29**: 79-86.
13. **Barabote RD, Xie G, Leu DH, Normand P, Necsulea A, Daubin V, Medigue C, Adney WS, Xu XC, Lapidus A, Parales RE, Detter C, Pujic P, Bruce D, Lavire C, Challacombe JF, Brettin TS & Berry AM** (2009) Complete genome of the cellulolytic thermophile *Acidothermus cellulolyticus* 11B provides insights into its ecophysiological and evolutionary adaptations. *Genome Res* **19**: 1033-1043.
14. **Mohagheghi A, Grohmann K, Himmel M, Leighton L & Updegraff DM** (1986) Isolation and characterization of *Acidothermus cellulolyticus* gen. nov., sp. nov., a new genus of thermophilic, acidophilic, cellulolytic bacteria. *Int J Syst Bacteriol* **36**: 435-443.
15. **Fraaije MW, Van Berkel WJ, Benen JA, Visser J & Mattevi A** (1998) A novel oxidoreductase family sharing a conserved FAD-binding domain. *Trends Biochem Sci* **23**: 206-207.
16. **Vihinen M** (1987) Relationship of protein flexibility to thermostability. *Protein Eng* **1**: 477-480.
17. **Reetz MT, Carballeira JD & Vogel A** (2006) Iterative saturation mutagenesis on the basis of B factors as a strategy for increasing protein thermostability. *Angew Chem Int Ed* **45**: 7745-7751.
18. **Hollmann F, Arends IWCE, Buehler K, Schallmeyer A & Buhler B** (2011) Enzyme-mediated oxidations for the chemist. *Green Chem* **13**: 226-265.
19. **Jin J, Mazon H, van den Heuvel RH, Janssen DB & Fraaije MW** (2007) Discovery of a eugenol oxidase from *Rhodococcus* sp. strain RHA1. *FEBS J* **274**: 2311-2321.
20. **Casadaban MJ & Cohen SN** (1980) Analysis of gene control signals by DNA fusion and cloning in *Escherichia coli*. *J Mol Biol* **138**: 179-207.

21. **Studier FW & Moffatt BA** (1986) Use of bacteriophage-T7 RNA polymerase to direct selective high-level expression of cloned genes. *J Mol Biol* **189**: 113-130.
22. **van Bloois E, Pazmino DET, Winter RT & Fraaije MW** (2010) A robust and extracellular heme-containing peroxidase from *Thermobifida fusca* as prototype of a bacterial peroxidase superfamily. *Appl Microbiol Biotechnol* **86**: 1419-1430.
23. **Federico R, Angelini R, Ercolini L, Venturini G, Mattevi A, Ascenzi P** (1997) Competitive inhibition of swine kidney copper amine oxidase by drugs: amiloride, clonidine, and gabexate mesylate. *Biochem Bioph Res Co* **240**: 150-152.
24. **Forneris F, Orru R, Bonivento D, Chiarelli LR & Mattevi A** (2009) ThermoFAD, a ThermoFluor® adapted flavin *ad hoc* detection system for protein folding and ligand binding. *Febs J* **276**: 2833-2840.
25. **Pantoliano MW, Petrella EC, Kwasnoski JD, Lobanov VS, Myslik J, Graf E, Carver T, Asel E, Springer BA, Lane P & Salemme FR** (2001) High-density miniaturized thermal shift assays as a general strategy for drug discovery. *J Biomol Screen* **6**: 429-440.
26. **Guerois R, Nielsen JE & Serrano L** (2002) Predicting changes in the stability of proteins and protein complexes: a study of more than 1000 mutations. *J Mol Biol* **320**: 369-387.
27. **Kellogg EH, Leaver-Fay A & Baker D** (2011) Role of conformational sampling in computing mutation-induced changes in protein structure and stability. *Proteins* **79**: 830-838.
28. **Krieger E, Joo K, Lee J, Lee J, Raman S, Thompson J, Tyka M, Baker D & Karplus K** (2009) Improving physical realism, stereochemistry, and side-chain accuracy in homology modeling: Four approaches that performed well in CASP8. *Proteins* **77**: 114-122.
29. **Larkin MA, Blackshields G, Brown NP, Chenna R, McGettigan PA, McWilliam H, Valentin F, Wallace IM, Wilm A, Lopez R, Thompson JD, Gibson TJ & Higgins DG** (2007) Clustal W and Clustal X version 2.0. *Bioinformatics* **23**: 2947-2948.
30. **Nielsen M, Lundegaard C, Lund O & Petersen TN** (2010) CPHmodels-3.0-remote homology modeling using structure-guided sequence profiles. *Nucleic Acids Res* **38**: W576-W581.
31. **Fraaije MW, Wu J, Heuts DP, van Hellemond EW, Spelberg JL & Janssen DB** (2005) Discovery of a thermostable Baeyer-Villiger monooxygenase by genome mining. *Appl Microbiol Biotechnol* **66**: 393-400.
32. **Sakon J, Adney WS, Himmel ME, Thomas SR & Karplus PA** (1996) Crystal structure of thermostable family 5 endocellulase E1 from *Acidothermus cellulolyticus* in complex with cellotetraose. *Biochemistry* **35**: 10648-10660.
33. **Lykidis A, Mavromatis K, Ivanova N, Anderson I, Land M, DiBartolo G, Martinez M, Lapidus A, Lucas S, Copeland A, Richardson P, Wilson DB & Kyrpides N** (2007) Genome sequence and analysis of the soil cellulolytic actinomycete *Thermobifida fusca* YX. *J Bacteriol* **189**: 2477-2486.
34. **Yamashita M, Omura H, Okamoto E, Furuya Y, Yabuuchi M, Fukahi K & Murooka Y** (2000) Isolation, characterization, and molecular cloning of a thermostable xylitol oxidase from *Streptomyces* sp. IKD472. *J Biosci Bioeng* **89**: 350-360.
35. **Stevens RC** (2000) Design of high-throughput methods of protein production for structural biology. *Structure* **8**: R177-R185.
36. **Maertens B, Spriestersbach A, von Groll U, Roth U, Kubicek J, Gerrits M, Graf M, Liss M, Daubert D, Wagner R & Schafer F** (2010) Gene optimization mechanisms: a multi-gene study reveals a high success rate of full-length human proteins expressed in *Escherichia coli*. *Protein Sci* **19**: 1312-1326.
37. **Fraaije MW, Pikkemaat M & van Berkel WJH** (1997) Enigmatic gratuitous induction of the covalent flavoprotein vanillyl-alcohol oxidase in *Penicillium simplicissimum*. *Appl Environ Microbiol* **63**: 435-439.

38. **de Jong E, van Berkel WJH, van der Zwan RP & de Bont JAM** (1992) Purification and characterization of vanillyl alcohol oxidase from *Penicillium simplicissimum* - a novel aromatic alcohol oxidase containing covalently bound FAD. *Eur J Biochem* **208**: 651-657.
39. **Singer TP & Edmondson DE** (1980) in *Methods in Enzymology*, ed. McCormick DB (Academic Press), pp 253-264.
40. **Fornieris F, Heuts DP, Delvecchio M, Rovida S, Fraaije MW & Mattevi A** (2008) Structural analysis of the catalytic mechanism and stereoselectivity in *Streptomyces coelicolor* alditol oxidase. *Biochemistry* **47**: 978-985.
41. **Cornish-Bowden A** (1995) *Fundamentals of Enzyme Kinetics*. (Portland Press, London).
42. **Pocker Y & Janjic N** (1987) Enzyme kinetics in solvents of increased viscosity - dynamic aspects of carbonic anhydrase catalysis. *Biochemistry* **26**: 2597-2606.
43. **Leferink NGH, Fraaije MW, Joosten HJ, Schaap PJ, Mattevi A & van Berkel WJH** (2009) Identification of a gatekeeper residue that prevents dehydrogenases from acting as oxidases. *J Biol Chem* **284**: 4392-4397.
44. **Baron R, Riley C, Chenprakhon P, Thotsaporn K, Winter RT, Alfieri A, Fornieris F, van Berkel WJH, Chaiyen P, Fraaije MW, Mattevi A & McCammon JA** (2009) Multiple pathways guide oxygen diffusion into flavoenzyme active sites. *Proc Natl Acad Sci U S A* **106**: 10603-10608.
45. **Watanabe K, Masuda T, Ohashi H, Mihara H & Suzuki Y** (1994) Multiple proline substitutions cumulatively thermostabilize *Bacillus cereus* ATCC:7064 oligo-1,6-glucosidase - irrefragable proof supporting the proline rule. *Eur J Biochem* **226**: 277-283.
46. **Ericsson UB, Hallberg BM, DeTitta GT, Dekker N & Nordlund P** (2006) ThermoFluor-based high-throughput stability optimization of proteins for structural studies. *Anal Biochem* **357**: 289-298.
47. **Matulis D, Kranz JK, Salemme FR & Todd MJ** (2005) Thermodynamic stability of carbonic anhydrase: measurements of binding affinity and stoichiometry using ThermoFluor. *Biochemistry* **44**: 5258-5266.
48. **Mao YQ, Varoglu M & Sherman DH** (1999) Molecular characterization and analysis of the biosynthetic gene cluster for the antitumor antibiotic mitomycin C from *Streptomyces lavendulae* NRRL 2564. *Chem Biol* **6**: 251-263.
49. **Welch M, Govindarajan S, Ness JE, Villalobos A, Gurney A, Minshull J & Gustafsson C** (2009) Design parameters to control synthetic gene expression in *Escherichia coli*. *Plos One* **4**: e7002.
50. **Pisanelli I, Kujawa M, Spadiut O, Kittl R, Halada P, Volc J, Mozuch MD, Kersten P, Haltrich D & Peterbauer C** (2009) Pyranose 2-oxidase from *Phanerochaete chrysosporium*-expression in *E. coli* and biochemical characterization. *J Biotechnol* **142**: 97-106.
51. **Salaheddin C, Takakura Y, Tsunashima M, Stranzinger B, Spadiut O, Yamabhai M, Peterbauer CK & Haltrich D** (2010) Characterisation of recombinant pyranose oxidase from the cultivated mycorrhizal basidiomycete *Lyophyllum shimeji* (hon-shimeji). *Microb Cell Fact* **9**: 57.
52. **Doukyu N, Shibata K, Ogino H & Sagermann M** (2008) Purification and characterization of *Chromobacterium* sp DS-1 cholesterol oxidase with thermal, organic solvent, and detergent tolerance. *Appl Microbiol Biotechnol* **80**: 59-70.
53. **Sagermann M, Ohtaki A, Newton K & Doukyu N** (2010) Structural characterization of the organic solvent-stable cholesterol oxidase from *Chromobacterium* sp DS-1. *J Struct Biol* **170**: 32-40.
54. **Spadiut O, Leitner C, Salaheddin C, Varga B, Vertessy BG, Tan TC, Divne C & Haltrich D** (2009) Improving thermostability and catalytic activity of pyranose 2-oxidase from *Trametes multicolor* by rational and semi-rational design. *Febs Journal* **276**: 776-792.
55. **Karshikoff A & Ladenstein R** (2001) Ion pairs and the thermotolerance of proteins from hyperthermophiles: a 'traffic rule' for hot roads. *Trends Biochem Sci* **26**: 550-556.

56. **Missimer JH, Steinmetz MO, Baron R, Winkler FK, Kammerer RA, Daura X & van Gunsteren WF** (2007) Configurational entropy elucidates the role of salt-bridge networks in protein thermostability. *Protein Sci* **16**: 1349-1359.
57. **Greaves RB & Warwicker J** (2007) Mechanisms for stabilisation and the maintenance of solubility in proteins from thermophiles. *Bmc Struct Biol* **7**: 18.
58. **Eijsink VGH, Bjork A, Gaseidnes S, Sirevag R, Synstad B, van den Burg B & Vriend G** (2004) Rational engineering of enzyme stability. *J Biotechnol* **113**: 105-120.
59. **Krieger E, Darden T, Nabuurs SB, Finkelstein A & Vriend G** (2004) Making optimal use of empirical energy functions: force-field parameterization in crystal space. *Proteins* **57**: 678-683.
60. **Krieger E, Koraimann G & Vriend G** (2002) Increasing the precision of comparative models with YASARA NOVA-a self-parameterizing force field. *Proteins* **47**: 393-402.
61. **Hess B, Bekker H, Berendsen HJC & Fraaije JGEM** (1997) LINCS: a linear constraint solver for molecular simulations. *J Comp Chem* **18**: 1463-1472.
62. **Miyamoto S & Kollman PA** (1992) SETTLE: an analytical version of the SHAKE and RATTLE algorithm for rigid water models. *J Comp Chem* **13**: 952-962.
63. **Westerbeek A, Szymański W, Wijma HJ, Marrink SJ, Feringa BL & Janssen DB** (2011) Kinetic resolution of α -Bromoamides: experimental and theoretical investigation of highly enantioselective reactions catalyzed by haloalkane dehalogenases. *Adv Synth Catal* **353**: 931-944.

Chapter 6

Oxidase redesign by active site randomization

Remko T. Winter, Andrew R. Millar, Edwin van Bloois and Marco W. Fraaije

Laboratory of Biochemistry, Groningen Biomolecular Sciences and Biotechnology Institute,
University of Groningen, Nijenborgh 4, 9747 AG Groningen, The Netherlands

Abstract

The vanillyl alcohol oxidase (VAO) protein fold encompasses a group of flavoproteins capable of an exceedingly rich collection of oxidation reactions. The chemo-, regio- and enantioselective finesse with which these oxidations are catalysed makes VAO flavoproteins biotechnologically relevant and attractive candidates for enzyme engineering. The success of any enzyme engineering approach, however, is often limited by the availability of a robust high throughput screening assay. Here, we detail the pioneering of a generic ultra-high throughput screening assay for oxidase activity. Based on the hydrogen peroxide specific deprotection of a boronated fluorophore, our screening assay has the advantage that it can be applied generically to all oxidase activities and that the fluorescent signal is trapped intracellularly, enabling ultra-high throughput (10^7 hour⁻¹) screening with FACS (Fluorescent Activated Cell Sorter) technology. Using the model VAO-flavoprotein eugenol oxidase we show that our screening assay can be used under mock conditions to sort *E. coli* cells expressing active eugenol oxidase from cells expressing inactive oxidase. Unfortunately, our attempts to isolate active variants using our novel screening assay from a large (10^7) library of eugenol oxidase mutants have so far been unsuccessful.

6.1 Introduction

Enzymes are powerful catalysts, capable of a myriad of chemical transformations to create an enormous array of simple and complex, often chiral, compounds. Their ability to perform reactions under mild conditions makes them eminently suitable for green chemical processes (1, 2). While the last few years have witnessed an increase in the discovery and development of enzymes for biocatalytic processes (3-5), the number of mature, full scale commercial processes that employ enzymes – while on the rise – has not yet realized its full potential (6). Too often this is because enzymes have evolved to function optimally at physiological conditions, something that does not translate easily to industrial conditions (7). Furthermore, evolution has often restricted enzymes to catalyse only the reaction that is physiological relevant to the organism that harbours them (8). As a result, much effort has gone into developing the underutilized potential of enzymes for biocatalysis, as the many publications on enzyme engineering attest to (*see references 9-12 for some examples*).

Enzyme engineers follow one of two approaches when carrying out their modifications: rational or random. Rational redesign of enzyme functionalities requires a detailed understanding of structure-function relationships, something that high resolution protein structures cannot always offer (13). Random redesign on the other hand requires little in-depth knowledge of protein structure or mechanism and is in fact modelled on natural evolution (14). Directed evolution, as it is called, links multiple rounds of genetic diversification (the genotype) to improvements in the desired catalytic activity (the phenotype), thus enabling development of the required biocatalyst.

Enzyme engineering methods often require the ability to generate large collections of protein variants. With the advent of cheap and fast DNA sequencing and synthesis technology, there are now numerous techniques available for the generation of large mutant libraries (15-19). As an added benefit the generation of such libraries is now possible according to highly specific design parameters, with one being able to specify at which positions in a gene mutations should be introduced and what the nature of these mutations should be (17, 74). Although library generation is no longer a problem the challenge for any successful enzyme engineering project remains the development of a reliable high-throughput screening method to enable identification of the protein variant with the desired properties. Traditionally, screening methods for novel or improved enzyme activities rely on assays performed in microtiter or agar plates. Even with extensive robotic automation, the amount of variants that can be screened via this method remains limited; screening extremely large libraries in an ultra-high throughput manner ($>10^6$) remains a challenge. A lot of work has gone into

filling this gap between large library size and limited screening capacity by developing smaller, “smarter libraries” that randomize a limited number of residues in parallel rounds of mutation and screening and combine these mutations in subsequent rounds (20, 21). Unfortunately, a lot of protein sequence space goes unexplored in such approaches (22), making ultra-high throughput screening methods very desirable. Recently, fluorescent activated cell sorting (FACS) has been emerging as a powerful tool for the activity-based screening of mutants from extremely large libraries. FACS sorters are specialized instruments that can interrogate individual particles (cells, microbeads, emulsion droplets) according to fluorescence properties at extremely high rates (up to 10^7 per hour) and isolate those particles that exhibit the desired fluorescent characteristics. Sample particles enter a FACS as single droplets in a hydrodynamically focused liquid stream, where they are illuminated by a laser beam. The emitted fluorescence of each particle is recorded and if so desired a charge can be applied to the cells of interest, which allows them to be collected in a sample tube or microtiter plate well by the application of an electrostatic field (23, 24). As discussed in a recent review by Withers *et al*, FACS screening can be classified according to the method that is employed to couple the genotype to the phenotype: 1.) cell surface display of active enzymes 2.) reporting of enzyme activity with GFP or its variants 3.) entrapment of a product within the cells and 4.) *in vitro* compartmentalization (25).

Oxidases are a highly valuable class of enzymes; the exquisite chemo-, regio- and enantioselectivity with which they perform oxidations and the fact that they require no expensive co-substrate, but only molecular oxygen, make them industrially relevant (26-28). Although oxidases are a relatively rare class of enzymes, those that have been described catalyse oxidations on an enormously diverse range of compounds (29, 30). For this reason, oxidases are an attractive target for enzyme engineering in order to create new activities against non-natural substrates. An additional feature makes the engineering of oxidases attractive: the production of hydrogen peroxide. In most oxidase reactions catalysed by flavoprotein oxidases the molecular oxygen utilized as oxidant is reduced to hydrogen peroxide to form the only by-product of the reaction. This offers a valuable hand-hold for the development of an ultra-high throughput screening assay for novel oxidase activities that can potentially be applied in a generic fashion to any oxidase engineering project. In fact, a robust plate-based screening assay already exists for the screening of oxidase activity that relies on this generic production of hydrogen peroxide (31). While having proven itself in the directed evolution of more enantioselective amine oxidase variants (32) and in the discovery of a novel putrescine oxidase from a gene library (33), it is a screening method that is unsuitable for the screening of extremely large mutant libraries, having a maximum capacity of $\sim 10^5$.

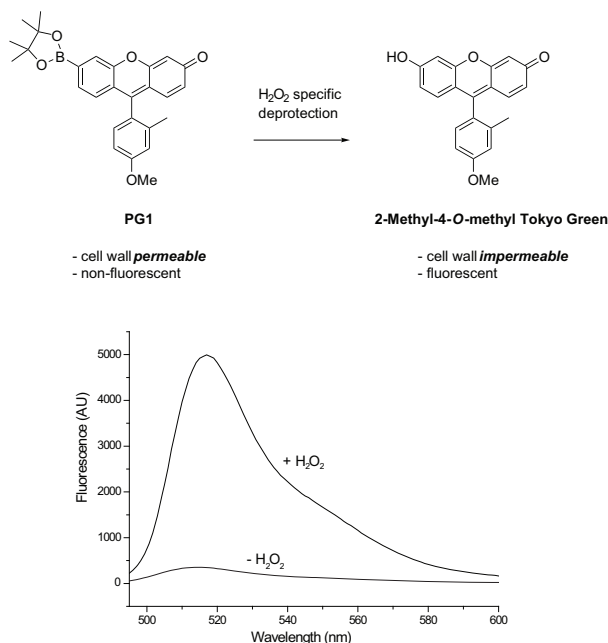


Figure 6.1 PG1 is a H₂O₂-specific fluorescent probe. H₂O₂ deprotection gives the highly fluorescent and cell-wall impermeable fluorophore Tokyo Green. Depicted is the fluorescence emission spectra after incubation of 50 μ M PG1 with 100 μ M H₂O₂. (λ_{ex} = 488 nm in 50 mM KPi buffer, pH 7.5)

Recent interest in the role of hydrogen peroxide as an important molecule in intracellular signalling pathways (34, 35) has spawned the development of a family of H₂O₂ specific fluorescent probes (36). The basis of these fluorescent probes is a boronate protected fluorophore, and all have the characteristic of being highly specific for hydrogen peroxide. In the protected, boronated form they display no fluorescence, but after hydrogen peroxide specific deprotection they become highly fluorescent. Peroxy Green 1, PG1 (Figure 6.1), is a member of this new class of hydrogen peroxide specific probes (37). Upon deprotection the strong fluorophore 2-methyl-4-O-methyl Tokyo Green is formed (38), which has an emission maximum at 518 nm following excitation at 488 nm (Figure 6.1). PG1 displays poor reactivity with other reactive oxygen species (ROS) like superoxide (O₂⁻), *t*-butoxy radical (\bullet O^tBu), *t*-butyl hydroperoxide (TBHP), hypochlorite anion (⁻OCl), hydroxyl radical (\bullet OH), ozone (O₃), singlet oxygen (¹O₂) and nitric oxide (NO). PG1 has the attractive feature of being cell wall permeable in its protected non-fluorescent form while being cell wall impermeable in its unprotected, fluorescent form (37). This makes it an ideal candidate for the development of a generic, ultrahigh throughput activity based screening assay with FACS technology via method 3.) described above: entrapment of

a product within cells (25). If a cell expresses active oxidase this can be coupled to the production of a fluorescent signal through the hydrogen peroxide mediated reaction with PG1, resulting in the entrapment within the cell of the cell-wall impermeable fluorescent dye 2-Methyl-4-O-methyl Tokyo Green and subsequent accumulation of a fluorescent signal, enabling detection and sorting by FACS technology (Figure 6.2).

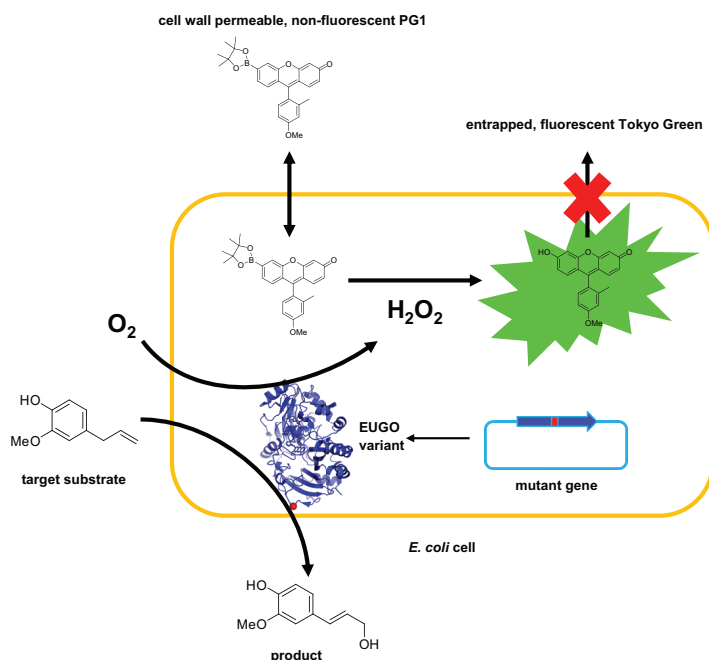


Figure 6.2 Ultrahigh-throughput activity-based screening of oxidase libraries. Each *E. coli* cell contains a mutated copy of the wild type eugenol oxidase (EUGO) gene on an expression plasmid. Expression of the EUGO variant can result in activity towards the target substrate (wild type substrate eugenol in this case; substrates must be cell wall permeable). The H₂O₂ formed reacts with the cell wall permeable, H₂O₂ specific dye Peroxy Green 1 (PG1). The resulting fluorescent product Tokyo Green is entrapped within the cells, causing the accumulation of a fluorescent signal and enabling detection by FACS technology.

Complementary to accumulation and entrapment of the fluorescent dye is a target substrate that will freely enter the cells expressing the target oxidase; this is of particular importance when choosing the oxidase that is to be engineered with the envisaged PG1 screening assay. For this reason we turned to the recently discovered and characterized member of the vanillyl alcohol oxidase (VAO) class of flavoprotein oxidases (39); *Rhodococcus jostii* RHA1 eugenol oxidase (EUGO). EUGO is a soluble flavoprotein of 59.5 kDa that is expressed at extremely high levels in *E. coli*; an impressive 160 mg ml⁻¹ of protein can be isolated from 1 litre of bacterial culture (40).

As a close homologue of VAO, the model protein for this family of flavoproteins, EUGO converts a wide range of phenolic compounds with vanillyl alcohol and eugenol being the preferred substrates, compounds that are known to pass across the *E. coli* cell membrane (41, 42). EUGO is an attractive target for enzyme engineering; although highly similar to VAO (45% sequence identity), there are marked differences in its substrate specificity. Alkylphenols, for example, are good VAO substrates (43) but are barely accepted by EUGO (40). Thus, an enzyme engineering approach where the active site residues governing substrate specificity are mutated should in theory be able to yield an enzyme with a more VAO-like activity. As the crystal structure for EUGO binding the substrate analogue isoeugenol was recently solved (44), we were able to design an extensive protein library targeting all the residues involved in substrate binding and recognition (the first shell), which could then be screened in an ultra-high throughput manner using the PG1-based FACS assay. Several target compounds were identified that are presently not or extremely poorly accepted by EUGO but that could be converted by variants from the EUGO first shell protein library (Figure 6.3). These target compounds were also chosen because of likelihood that they are able to diffuse across the *E. coli* cell membrane, a characteristic that is required for their compatibility with the envisaged screening assay.

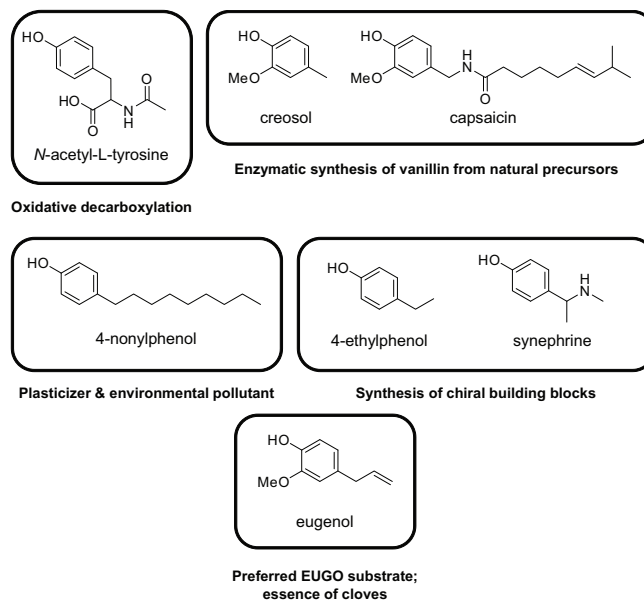


Figure 6.3 Engineering eugenol oxidase (EUGO) to accept novel substrates. A library of first shell mutants can be screened for the above target compounds. EUGO preferred wild type substrate eugenol is shown for comparison, along with the justification for choosing each target.

In this chapter we detail the development of an ultra-high throughput FACS based screening assay for the detection of novel oxidase activities. Using the recently developed H₂O₂ specific dye PG1 we design a whole-cell based screening assay where the successful intracellular conversion of an oxidase substrate results in the concomitant release of H₂O₂. This then reacts with PG1, trapping the resulting fluorescent product inside the cell and allowing for the detection of cells expressing active protein by flow cytometry. Using the model flavoprotein oxidase, EUGO, we designed and constructed an extremely large mutant library targeting all the first shell residues for (partial) randomization, coining the term *first shell library (FSL)* for such a protein library. This library of 6.4×10^7 unique variants was screened for activity towards creosol, 4-ethylphenol, synephrine and the wild-type substrate eugenol using a FACS sorter. While the screening method developed here was not successfully taken beyond the proof-of-principle stage, the potential it has shown for screening very large enzyme libraries in extremely short timeframes coupled with its generic nature (suitable for all oxidases), certainly warrants further development.

6.2 Materials and Methods

6.2.1 Reagents & enzymes

QuikChange mutants were constructed using *Pfu*Turbo DNA polymerase from Stratagene. Peroxy Green 1 (PG1) was a kind gift from Prof. Dr. C. J. Chang (University of California, Berkeley, U. S. A.) and from Dr. Peter Wiegerinck (Organon, Oss, The Netherlands). Bovine liver catalase (EC 1.11.1.6) was from Fluka. All other chemicals used were from Sigma-Aldrich and of analytical grade.

6.2.2 Strains, plasmids and growth conditions

E. coli strain TOP10 (Invitrogen) was used for all cloning and expression purposes. The final EUGO library was expressed using *E. coli* TOP10F' (Invitrogen). Plasmid pBADEUGOA has been described previously (40) and was used as template for *FSL* generation and for the generation of mutants EUGO Y471F and EUGO Y471K via the QuikChange mutagenesis protocol (Stratagene, primer sequences available upon request). Cultures were grown to saturation at 37°C overnight. The following day, overnight cultures were back-diluted 1:100 into fresh media containing 0.02% L-arabinose to induce the expression of EUGO variants and grown for 24h at 30°C. All cultures were routinely grown in Luria Bertani medium (LB; per litre, 10 g tryptone, 5 g yeast extract, 10 g NaCl) supplemented with ampicillin (100 µg ml⁻¹) under aerobic conditions.

6.2.3 Library design and construction

The EUGO first shell library (*FSL*) was designed as described in the results section and as per the specifications displayed in Table 6.1. Library construction and transformation was carried out by GeneArt AG (Regensburg, Germany) using their GeneArt® Combinatorial Library technology. pBADEUGOA was used as template, and the library was cloned *NdeI/HindIII* into this vector. The library was transformed into *E. coli* Top 10F' and the transformation rate was determined through the plating of a dilution series. The total number of transformants was 1.0×10^9 colony forming units (CFUs). 96 random colonies from the transformation plates were picked and sequence analysed to determine the quality of the delivered library. The library was supplied as a glycerol stock; 12 vials containing 0.5 ml at 0.6×10^{10} cells ml⁻¹.

Table 6.1 Design of the EUGO *FSL*. Wild type amino acid for each position is underlined. At each position the degeneracy is equally distributed.

First shell position	<i>FSL</i> degeneracy (equal distribution)
151	<u>Asp</u> , Asn, Ser, Gly
168	<u>Tyr</u> , Leu, Phe, His
276	<u>Val</u> , Ala, Gly, Thr, Asp
278	<u>Arg</u> , Ala
282	<u>Met</u> , Ala, Phe, Trp, Asn, Gln, Gly, Ser, Lys, Asp
366	<u>Arg</u> , Ser
378	<u>Glu</u> , Ala
381	<u>Leu</u> , Phe, Trp, Ser, Arg, Met, Cys, Ile, Gly, Asp
392	<u>Gly</u> , Asp, Leu, Phe, Trp, Ser, Arg, Met, Cys, Ile
425	<u>Gln</u> , Ala, Leu, Phe, Trp, Asn, Gly, Ser, Lys, Glu
438	<u>Leu</u> , Ala, Phe, Trp, Asn, Gln, Gly, Ser, Lys, Glu

6.2.4 Analytical methods

Cellular expression of EUGO variants was analysed with standard 12% SDS-PAGE gels. Upon harvesting cells were resuspended in KPi buffer (50 mM, pH 7.5), disrupted by sonification and centrifuged (14 000 $\times g$, 20 min). The supernatant was taken as the soluble fraction, the pellet as the insoluble fraction. Total protein was visualized by staining with SimplyBlue SafeStain (Invitrogen) and the presence of covalently bound flavin cofactor was visualized by incubating SDS-PAGE gels in 5% acetic acid for 5 min and examining the gels for flavin fluorescence under a UV-transilluminator. EUGO activity towards vanillyl alcohol or eugenol was determined by following the relevant changes in absorption. Activity with vanillyl alcohol was followed by measuring the formation of vanillin at 340 nm ($\epsilon = 14.0 \text{ mM}^{-1} \text{ cm}^{-1}$ at pH 7.5); activity with eugenol was followed by measuring the formation of coniferyl alcohol at 296 nm ($\epsilon = 6.8 \text{ mM}^{-1} \text{ cm}^{-1}$ at pH 7.5) (40). In both cases reaction mixtures contained 10 μl soluble cell extracts prepared by sonification and the reactions were carried out in potassium phosphate buffer (50 mM, pH 7.5). Catalase activity was evaluated by measuring the decrease in H_2O_2 concentration over time at 240 nm (45) ($\epsilon_{240 \text{ nm}} = 43.6 \text{ M}^{-1}$, 46). Assays were performed at room temperature in a quartz cuvette containing 1 ml 20 mM H_2O_2 in 50 mM KPi buffer (pH 7.5) and 10 μl soluble extracts. EUGO and catalase activity was normalized based on the protein concentration of CFE, as determined using the method of Bradford (47) with bovine albumin as standard. Fluorescence of cells due to H_2O_2 specific deprotection of PG1 was measured with a Bio-Tek FL600 Microplate Fluorescence Reader; $\lambda_{\text{ex}} = 460 \pm 20 \text{ nm}$, $\lambda_{\text{em}} = 530 \pm 10 \text{ nm}$ (bottom optics, sensitivity = 200) equipped with KC4 software package. Cells were incubated in the PG1 reaction mixture (described below) before washing and transferring to black-walled 96-wells microtiter plates suitable for fluorescence measurements.

6.2.5 Flow cytometry and FACS analysis

Cells were cultured and induced for EUGO expression as described above. Following induction cells were harvested by centrifugation (6 000 $\times g$ at 4°C) and washed with Phosphate Buffered Saline (PBS), which had been filtered with a sterile disposable 0.2 μm cellulose acetate filter unit (Whatman). Oxidase screening incubations contained 50 μM PG1 (5 mM stock solution prepared in DMSO), 1 mM oxidase substrate, 250 units ml^{-1} catalase and 1 mM NaCN in PBS. Washed cells expressing EUGO (variants) were added to a final OD_{600} of 1.0. Cells were incubated for 1-2 hours at room temperature while exposed to air, before washing three times with ice-cold, filtered PBS. Throughout flow cytometric analysis and sorting cells were stored on ice (4°C). Prior to analysis the cells were passed through a 0.4 mm diameter needle to break up

any aggregated cells. Before flow cytometric analysis, cells were diluted 10x in sterile filtered PBS. Flow cytometric analysis was performed on a Coulter Epics XL-MCL Flow Cytometer (Beckman-Coulter, Mijdrecht, NL) operating an argon laser (488 nm) essentially as described (48). For each sample, at least 20 000 cells were analysed. Data containing the green fluorescent signals were collected with a FITC filter ($\lambda_{em} = 505\text{-}545\text{ nm}$) and the photomultiplier voltage was set between 700 and 800 V. Data was captured using System II software (Beckman Coulter) and further analysed using WinMDI 2.8 software (<http://facs.scripps.edu/software.html>). FACS analysis was performed on a FACSAria cell sorter (BD biosciences), operating an argon laser (488 nm). Green fluorescent signals were collected in the FITC or GFP channel ($\lambda_{em} = 505\text{-}545\text{ nm}$). Event rate was set at about 3000 events s^{-1} . Gates were set on the basis of fluorescence and events falling into the gate were sorted into a 15 ml plastic tube. Sorted events were transferred to 5 ml fresh LB medium supplemented with ampicillin ($100\text{ }\mu\text{g ml}^{-1}$) and grown to saturation at 37°C. Plasmid DNA was isolated using the High Pure Plasmid Isolation Kit (Roche) and DNA sequencing was performed by GATC Biotech Ag (Konstanz, Germany).

6.3 Results

6.3.1 Fluorescent dye PG1 can be used to detect intracellular oxidase activity

As effective activity based screening of the EUGO *FSL* – due to its sheer size – is only possible using flow cytometric techniques we required an assay that would allow us to generically screen for novel oxidase activities in single cells. To be compatible with flow cytometric technology it would have to be rapid, sensitive and fluorescence based. Another important requirement is that it has to be intracellularly compatible: the signal (or lack of one) would need to remain temporally linked to the cell expressing the relevant protein variant. This enables the essential link between genotype and phenotype. To this end we chose the H_2O_2 specific fluorescent dye, peroxy green, PG1. Originally developed by Chang and co-workers as a tool to visualize the localization of intracellular H_2O_2 generation in eukaryotic cells (37), PG1 was an attractive candidate due to its sensitivity, specificity and cellular permeability. The reaction of PG1 with H_2O_2 is given in Figure 6.1. PG1 is non-fluorescent in its boronated form. Reaction with H_2O_2 is very specific and results in chemoselective deprotection of an arylboronate to a phenol, a reaction that was first described in the 1950's (49, 50) and which in the case of PG1 results in the highly fluorescent species 2-methyl-4-*O*-methyl Tokyo Green. In its protected, non-fluorescent form, PG1 is cell wall permeable while becoming cell wall impermeable after reacting with H_2O_2 . This means that if PG1 reacts with intracellular H_2O_2 , it will be trapped within the cell,

enabling detection by flow cytometric technology and offering a method to screen for cells expressing oxidase activity.

Initial tests revealed that although the *E. coli* cell membrane was permeable to PG1, due to the high alkyl hydroperoxide reductase (AhpCF) and catalase activity present in *E. coli* cells (51), the PG1 dye could not compete effectively for any hydrogen peroxide produced, substantially lowering the observed fluorescence. While very sensitive, the reaction of PG1 with H_2O_2 was known to be very slow, with a pseudo-first-order rate constant of $k_{obs} = 1.1 \times 10^{-3} s^{-1}$ (1 μM dye, 1 mM H_2O_2) (37). For comparison, we determined that the intracellular catalase activity of resting *E. coli* cells is between 10 and 40 units mg^{-1} protein, whereas the maximal EUGO wild type activity and concomitant H_2O_2 production is at most 1 unit mg^{-1} protein. Inhibiting the intracellular catalases with 1 mM sodium cyanide proved to be a simple and effective solution, as Figure 6.4 reveals (52).

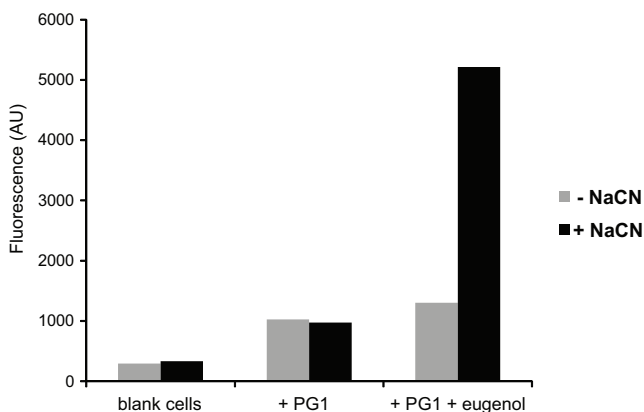


Figure 6.4 NaCN is essential to observe PG1 fluorescence in *E. coli*. Whole cell fluorescence of *E. coli* cells expressing eugenol oxidase and loaded with 5 μM H_2O_2 specific fluorescent dye PG1 and 1 mM eugenol. Cells were incubated for 2 h at room temperature with reaction components in phosphate buffered saline (PBS). Catalase activity was inhibited by the addition of 1 mM NaCN (+CN). Following incubation, cells were washed and fluorescence measured with a Microplate Fluorescence Reader; $\lambda_{ex} = 460 \pm 20$ nm, $\lambda_{em} = 530 \pm 10$ nm. Fluorescence is given in arbitrary units (AU).

As we expected the EUGO first shell library to contain a relatively small number of active clones it was important to be able to keep the number of false positives to a minimum. Thus it is essential that the fluorescent signal is generated only in those cells that contain active protein. The cell wall impermeability of PG1 after deprotection by H_2O_2 makes it very suited to this purpose. Hydrogen peroxide, however, is a small molecule that can freely diffuse across the *E. coli* membrane (53), potentially generating a false positive signal when it diffuses from a cell expressing

active enzyme to one expressing inactive enzyme. To prevent this H_2O_2 'cross-talk' between active and inactive cells an external hydrogen peroxide scavenger in the form of catalase was added (Figure 6.5). Due to the NaCN present, added to inhibit endogenous catalases, a substantial amount of external catalase had to be added: 250 Units ml^{-1} . Flow cytometric analysis revealed that the addition of catalase enabled better separation of cells expressing EUGO and cells expressing a flavoprotein oxidase that displays no reactivity towards the wild type substrate eugenol; alditol oxidase (AldO) (54) (Figure 6.6).

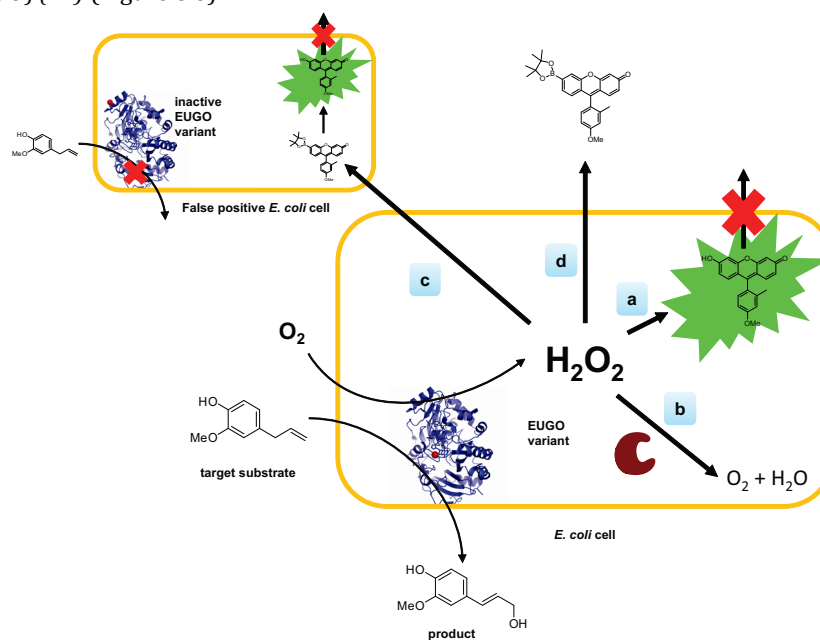


Figure 6.5 H_2O_2 produced by heterologously expressed oxidase has multiple fates. Path a is the desired fate of H_2O_2 ; reaction with PG1 yielding a fluorescent signal in the cell. Path b represents the scavenging of H_2O_2 by endogenous catalases. In path c H_2O_2 diffuses to a neighbouring cell expressing inactive protein, thereby generating a false positive signal. In path d, H_2O_2 diffuses out of the cell and reacts with extracellular PG1. Path b can be blocked by the addition of NaCN, path c by the addition of catalase and path d by wash steps.

As NaCN is a highly toxic compound that blocks bacterial respiration proteins, it was important to verify that the cells would survive treatment with NaCN. This is essential as we envisaged sorting cells expressing active protein from a large population and then culturing these active clones for further screening and protein isolation. *E. coli* cells expressing EUGO were incubated in 50 μM PG1, 1 mM eugenol and 250 Units ml^{-1} catalase for 1 hour. 1 mM NaCN was added to the incubation mixture to check its effect on the viability of the cells. Following incubation cells were

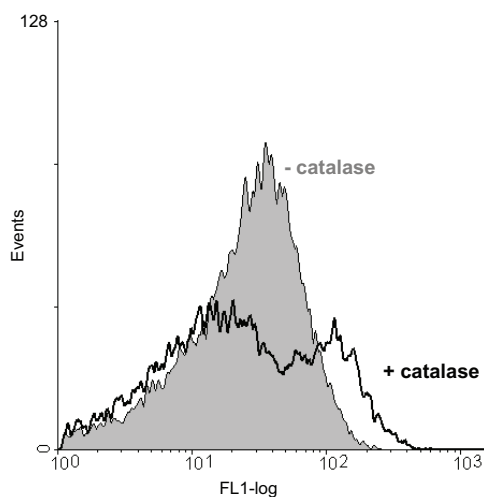


Figure 6.6 External catalase is essential to prevent hydrogen peroxide “cross-talk”. Depicted is a 1:1 mixture of *E. coli* cells expressing eugenol oxidase (EUGO) or alditol oxidase (AldO). Cells were incubated for 1 hour in PBS containing 1 mM eugenol, 50 μ M PG1 and 1 mM NaCN prior to washing and analysis by flow cytometry. Addition of catalase (250 units ml^{-1}) to the incubation mixture prevented H_2O_2 leaking from ‘active’ EUGO cells and reacting with PG1 dye in ‘inactive’ AldO cells (path c in Figure 6.5), enabling the visualization of two populations (fluorescent and non-fluorescent), as depicted in the + catalase histogram.

washed and equal amounts (as determined by OD_{600}) were plated on Lb^{Amp} agar. Negative control contained cells incubated only in PBS. We determined that incubation with 1 mM of NaCN for 1 hour does not appear to reduce the cellular viability, as determined from visual inspection of the amount of colony forming units (CFUs). Having optimized the conditions under which the screening would take place we were interested in the development of the fluorescent signal over time. Under mock screening conditions consisting of a 1:1 mixture of cells expressing wild-type EUGO and AldO we analysed the total cell mixture at multiple time points with a flow cytometer. After 45 minutes two populations displaying different fluorescent signals could clearly be seen to emerge, and remained defined as two distinct populations for 4 hours (Figure 6.7). The stability of the fluorescent signal means that the envisaged *FSL* can be screened by FACS technology, which allows for the screening of 10^7 variants per hour (25). The results show that a mixture of cells expressing either one of two different oxidases (EUGO or AldO) can be separated using flow cytometric technology based on their activity towards a target substrate, eugenol. At the same time the results imply that if cell sorting is combined with flow cytometry then it should be possible to sort cells expressing active enzyme from those expressing inactive variants.

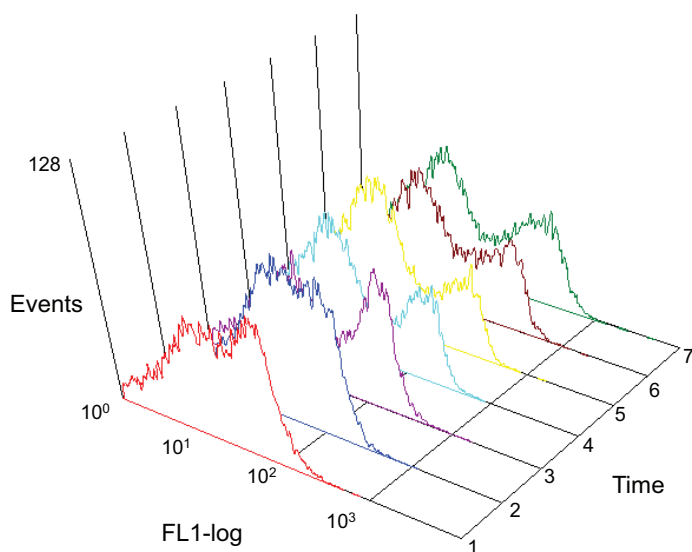


Figure 6.7 PG1-based whole-cell oxidase screen yields a stable fluorescent signal over time. Flow cytometric analysis of a 1:1 mixture of *E. coli* cells expressing eugenol oxidase (EUGO) or alditol oxidase (AldO) incubated with 50 μM PG1, 1 mM NaCN, 250 Units ml^{-1} catalase and 1 mM eugenol. Samples were taken at various time points, washed and analysed by flow cytometry. Histograms depict the emergence of two distinct populations (fluorescent and non-fluorescent) over the course of the experiment; 1, 10 min; 2, 30 min; 3, 45 min; 4, 60 min; 5, 75 min; 6, 100 min; 7, 240 min.

6.3.2 Designing the EUGO first shell library (FSL)

The substrate specificity of enzymes is determined predominantly by those amino acid residues that directly interact with the substrate during binding and catalysis; the so-called first-shell residues (55). As our aim was to achieve novel substrate specificities by targeting only these residues for mutagenesis (56) we had to identify the first shell in our model oxidase, EUGO. Using the recently solved crystal structure of EUGO with bound substrate (44) all residues having interactions with the substrate and/or lining the substrate binding cavity were identified and designated as first shell residues (Figure 6.8). To somewhat rationalize the choice of residues that are to be randomized in the EUGO first shell library, 73 EUGO homologues were identified by performing a BLAST search with EUGO as input, and aligned using the ClustalW algorithm. The resulting distribution and character of the first shell amino acids amongst the EUGO homologues was analysed and is plotted as a percentage in Figure 6.9. From this analysis three residues emerged that were highly conserved amongst all 73 homologues: Tyr91, Tyr471 and Arg472 (numbering refers to EUGO residue). Earlier work performed on vanillyl alcohol oxidase (VAO), a close homologue of EUGO

(45% sequence identity), had revealed that these residues were essential for catalysis due to their role in stabilizing the phenolate ion formed after deprotonation of the phenol moiety (57). To check if these residues in EUGO were equally important to catalytic function, two single mutants were generated by QuikChange mutagenesis: Tyr471Phe and Tyr471Lys. Analysis of the steady state kinetic parameters of these variants revealed that they indeed displayed a much lower catalytic efficiency. While the substrate specificity for eugenol remained constant, evidenced by an unchanged K_M value, the k_{cat} of the Tyr471Phe mutant was 10% of the wild type k_{cat} , while the Tyr471Arg mutant displayed only 0.1% of the wild type k_{cat} . Hence, we decided to leave this residue and the two other highly conserved residues, Tyr91 and Arg472, untouched when designing the EUGO first shell library.

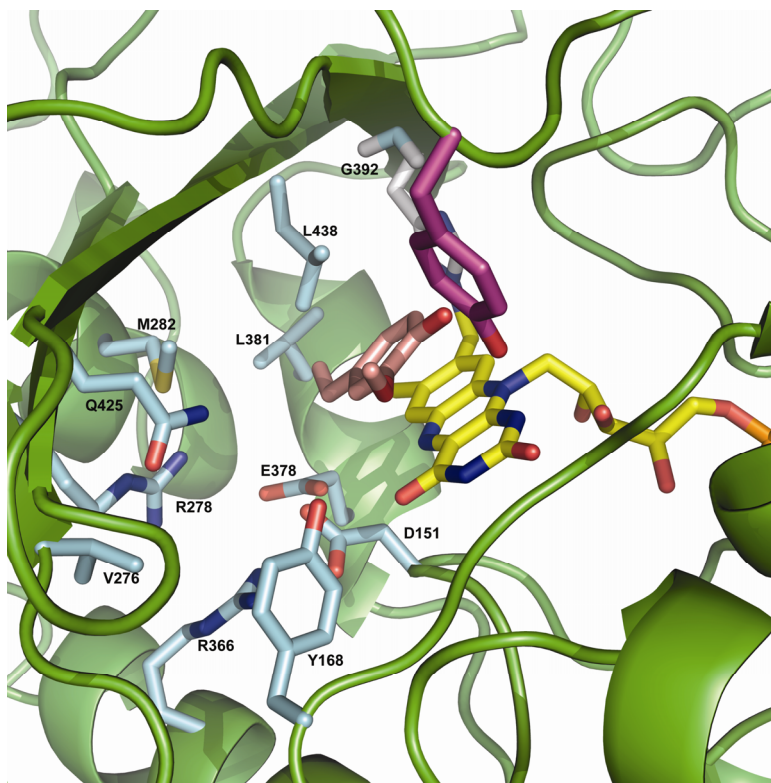


Figure 6.8 The Eugenol oxidase (EUGO) first shell was targeted for mutagenesis. Shown are the 11 EUGO first shell residues (light blue sticks) involved in substrate (eugenol, salmon sticks) recognition and binding. These residues were all targeted for mutagenesis in the EUGO *first shell library*. Conserved catalytic residue Tyr471 shown in magenta sticks (two other conserved catalytic residues Tyr91 and Arg472 are located next to Tyr471 and not shown for clarity). His390 that covalently links FAD (yellow sticks) to protein backbone is shown in grey sticks.

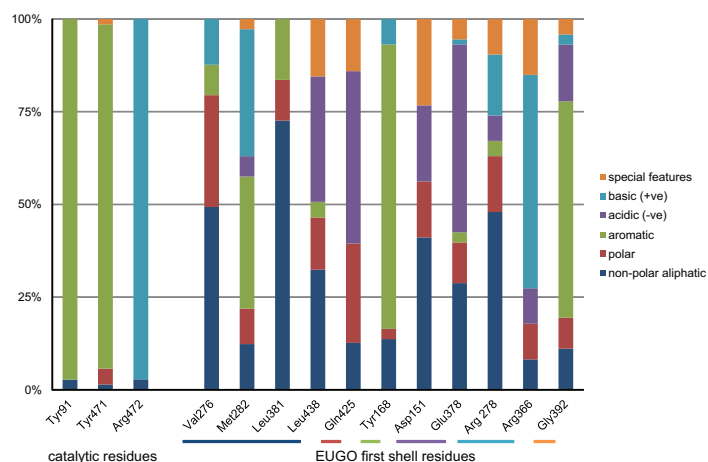


Figure 6.9 The EUGO-type first shell is extremely diverse. Analysis of the first shell residues of 73 aligned eugenol oxidase (EUGO) homologues revealed a high degree of diversity in the (type of) amino acids encoded at each position. Shown is the percentage distribution of the occurrence of each amino acid at each EUGO first shell-position, grouped according to amino acid characteristic: non-polar aliphatic (ala, val, leu, ile, met), polar (ser, thr, cys, asn, gln), aromatic (phe, tyr, trp), acidic (negatively charged; glu, asp), basic (positively charged; lys, arg, his) and special features (pro, gly). The three catalytic residues Tyr91, Tyr471 and Arg472 are almost completely conserved amongst the 73 homologues.

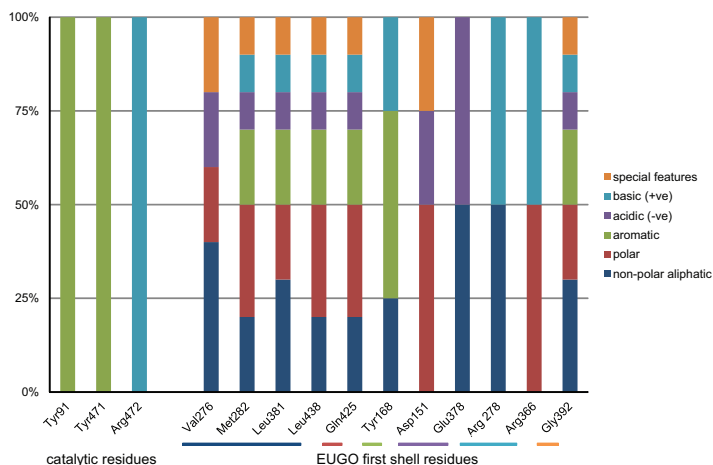


Figure 6.10 The EUGO FSL attempts to mimic natural diversity. Based on the diversity of amino acids observed amongst the first shell residues of eugenol oxidase (EUGO) homologues (Figure 6.9), the FSL was designed attempting to include as much of this diversity as possible. Shown is the percentage distribution of the occurrence of each amino acid in the EUGO *first shell library* (FSL) at each EUGO first shell-position, grouped according to amino acid characteristic: non-polar aliphatic (ala, val, leu, ile, met), polar (ser, thr, cys, asn, gln), aromatic (phe, tyr, trp), acidic (negatively charged; glu, asp), basic (positively charged; lys, arg, his) and special features (pro, gly). The three conserved catalytic residues Tyr91, Tyr471 and Arg472 were not mutated in the FSL.

As Figure 6.9 reveals, the distribution of amino acids amongst EUGO homologues at the other 11 EUGO first shell positions is very broad both in number and character. Hence the EUGO first shell library was designed by attempting to introduce as large as possible degree of randomization at these positions, while staying within the maximum total number of mutants that we envisage being able to screen with the current technology ($\sim 10^8$). The final design is depicted in Figure 6.10 and Table 6.1; due to its very large size and the level of rationality combined with randomness we decided to name such a collection of protein variants a *first shell library (FSL)*. Due to the technical hurdles involved in making such an extremely large (6.4×10^7 unique variants) yet highly specified library, the EUGO *FSL* was constructed, cloned into the pBAD expression vector, and used to transform *E. coli* TOP10 cells by GeneArt using their GeneArt® Combinatorial Library technology. GeneArt performed in-house quality control of the library which involved sequencing 96 randomly picked clones from the library. Analysis of this collection revealed that 31 clones had poor sequencing data and could not be analysed further; the remaining 65 were all unique. 22 of the 65 clones contained erroneous sequences with deletions (3x), insertions (3x) or unwanted non-silent substitutions (17x) within the reading frame. 43 of the 65 clones contained correct sequences; hence the library correctness was estimated as 66%. The distribution of amino acids at each of the mutated positions was close to or equal to the library design, leading us to conclude that despite the limited statistical analysis the library was of reasonable quality. In a further control we analysed an additional nine, randomly picked, clones from the library. Sequencing of these clones revealed a random collection of mutants at the designed positions (Figure 6.11). As expected from the quality control data obtained from GeneArt, two of these clones (clones 6 & 7, Figure 6.11) contained deleterious frameshifts resulting in prematurely truncated protein. Expression of the nine clones in *E. coli* did not yield FAD-containing protein; overexpression was only visible in the insoluble fraction (Figure 6.11). As expected from the lack of soluble expression, none of the nine clones displayed any activity towards the model substrate vanillyl alcohol. While disappointing that none of the sequenced and expressed sample clones from the library were expressed as soluble, FAD-binding protein with at least some residual activity, it was not entirely unexpected: all had five or more first shell mutations, some of which were deleteriously close to the FAD cofactor. This has the potential to disrupt proper FAD binding and subsequent folding of the protein, something which has been observed before for flavoprotein oxidases (58). Expression of the total EUGO *FSL* revealed a similar pattern when examined by SDS-PAGE; no visible soluble or FAD binding protein, but a large amount of protein expressed in the insoluble fraction (data not shown), identical to the expression pattern of the nine sequenced clones (Figure 6.11).

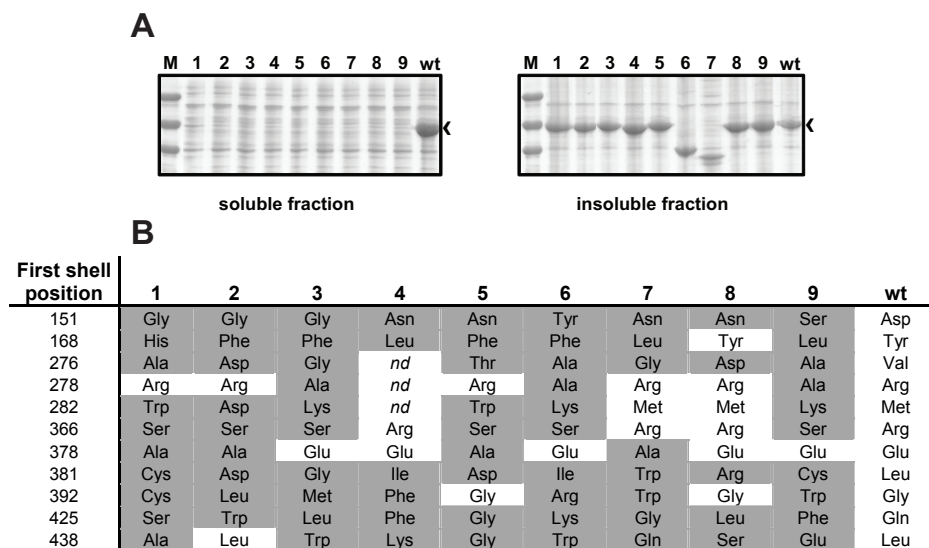


Figure 6.11 Clones from the EUGO FSL contain multiple mutations but do not express as soluble protein. **A**, 9 clones were randomly picked from the eugenol oxidase *first shell library* (EUGO FSL) and sequenced to determine the number and type of first shell mutations. Shown is the amino acid residue encoded at the first shell position of each sequenced clone; residues that differ from the wild type (wt) at that position are shaded grey. **B**, the same 9 clones were checked for expression of soluble EUGO. Depicted is an SDS-PAGE analysis after induction of expression (*E. coli* TOP10, 0.02% arabinose, 30°C, 12 hours). Wild type (wt) EUGO expression was checked as a control and is marked by an arrowhead (κ). All EUGO clones were expressed exclusively as insoluble protein. Clones 6 and 7 contained frameshifts resulting in prematurely truncated proteins, as visible from the SDS gel. *nd*, no data; M, molecular mass standards (from top to bottom): MBP-AldO, 88.1 kDa, EUGO, 59.4 kDa and AldO, 45.6 kDa.

6.3.3 Ultrahigh throughput screening of EUGO FSL

Before screening the entire EUGO FSL for novel substrate activities we performed several proof of principle measurement with a FACS sorter. By performing a simple mock-up of our sorting technique we tested if a cell sorter would be able to isolate cells expressing active protein from a mixture containing both active and inactive clones. Cells expressing a 1:1 mixture of AldO and wild type EUGO were mixed and incubated with eugenol and the PG1 reaction mixture. After washing they were analysed by FACS with a fixed sorting gate; all events falling into the defined sorting gate were collected (Figure 6.12). After collecting the positive fluorescent events these were plated on an LB agar plate containing ampicillin. Nine single colonies were transferred from this plate to LB medium, mini-prepped to obtain plasmid DNA and subjected to DNA sequencing to determine the efficiency of the sorting. From this analysis, 8 clones were shown to be EUGO wt, and 1 was AldO. While this yields a limited enrichment factor of 1.8, we found the results heartening enough to screen the

EUGO *FSL*. A second mock sort was performed with two different mixtures; cells expressing AldO and wild type EUGO in a 1:1 mixture and cells expressing wild type EUGO, EUGO Y471F and EUGO Y471K mutants in a 1:1:1 mixture. The results of this sort gave a similar result, and are summarized in Table 6.2.

The EUGO *FSL* was screened simultaneously for a mixture of three target substrates: synephrine, 4-ethyl phenol and creosol, all at 1 mM concentration. A positive control was carried out using 1 mM eugenol as substrate. Following incubation of cells expressing the *FSL* with the substrates and the PG1 reaction mixture 1.06×10^7 events were sorted at an approximate sorting speed of 3000 s^{-1} . A gate was defined on PG1 fluorescence and all events falling into this gate were collected. In total 1.12×10^5 events (cells) were collected. These cells were cultured and prepared for re-screening. It was hoped that these could be rescreened with the proven plate based assay of Turner et al (31). Unfortunately this screening assay was not compatible with the substrates used. This assay utilizes horseradish peroxidase (HRP) to detect hydrogen peroxide, which also accepts the aromatic phenols used to screen for novel EUGO activities.

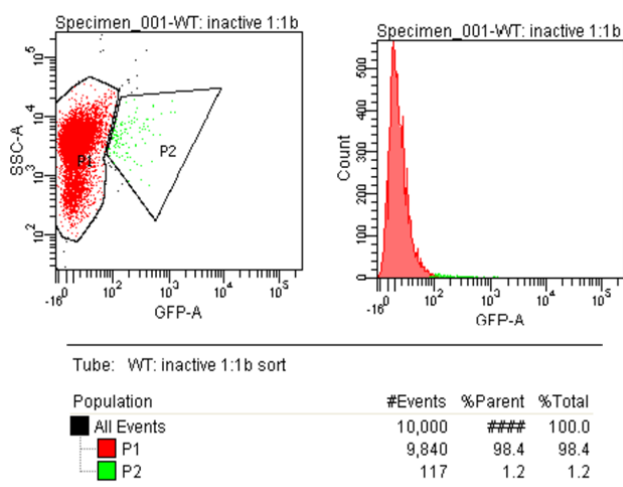


Figure 6.12 *E. coli* cells expressing EUGO activity can be sorted with a FACS. A 1:1 mixture of *E. coli* cells expressing eugenol oxidase (EUGO) or alditol oxidase (AldO) were incubated for 1 hour with $50 \mu\text{M}$ PG1, 1 mM NaCN, $250 \text{ units ml}^{-1}$ catalase and 1 mM eugenol before washing and sorting by FACS. Cells exhibiting fluorescence in the GFP channel (caused by H_2O_2 specific deprotection of PG1 yielding fluorescent Tokyo Green) were gated (dot plot; region P2) and sorted into a collection tube. Approximately 200K events were analysed before sorting was terminated. The histogram reveals that cells falling in region P2 indeed have increased fluorescence. 1.2% of analysed events were sorted into P2 as 'active' cells (~2400 cells). Data in the histogram and in the dot plot show only a representative sample of 10K events; SSC, side scatter; GFP, fluorescence emission 505-530 nm, $\lambda_{\text{ex}} = 488 \text{ nm}$. Sequencing of plasmid DNA isolated from 9 random 'active' cells revealed that 8 of the 9 were indeed cells expressing EUGO.

As the collection of supposed positive variants was still very large ($>10^5$) a re-screening was performed with FACS. Cells harbouring the selected variants were cultured, expression was induced and the cells were again incubated with the target substrates and PG1 reaction mixture before resorting by FACS. The result was highly disappointing; the sorted clones displayed less overall fluorescence than the original *FSL*, instead of the overall positive shift in fluorescence that was expected. Analysis of the expression revealed that these clones no longer appeared to produce EUGO; the distinctive EUGO band in the insoluble fraction was no longer visible. While the viability of the cells was not affected by the PG1 incubation mixture it is conceivable that the ability of the cells to overexpress EUGO was impaired by the PG1 incubation mix and/or subsequent sorting steps. In conclusion, our whole cell ultrahigh-throughput oxidase screening assay has to be optimized further before it can be applied to the ultra-high throughput screening of large mutant libraries.

Table 6.2 Summary of mock sorting experiments for cells expressing EUGO activity. Cells expressing either wild type eugenol oxidase (EUGO; wt), alditol oxidase (AldO), EUGO Y471F (10% of wt activity, YF) or EUGO Y471K (0.1% of wt activity, YK) were incubated with PG1 reaction mixture and 1 mM eugenol prior to sorting. (i) and (ii) represents two different sorting runs on different FACS sorters. Plasmid DNA from a portion of the 'active' clones was sequenced to determine if the sorted 'active' events actually represented EUGO.

Sorting mix (equal mixtures)	N° sorted 'active' clones sequenced	N° confirmed EUGO clones	Enrichment factor
wt, YK & YF	6	3	1.5 x
wt & AldO (i)	6	6	2.0 x
wt & AldO (ii)	9	8	1.8 x

6.4 Discussion

In this chapter we present the development of an ultra-high throughput FACS based screening assay for the identification of novel oxidase activities from extremely large collections of protein variants. In an effort to develop a generic assay for the screening of new oxidase activities we exploit the formation hydrogen peroxide, the by-product of most oxidase conversions. Screening for hydrogen peroxide production has been used successfully in the past to develop medium-throughput plate based screening assays (31) and has the advantage that it is a generic method suitable for nearly all oxidases, as hydrogen peroxide production indicates oxidase activity. In order to develop a screening assay that would be suitable for implementation with FACS technology we turned to the hydrogen peroxide specific fluorescent dye PG1 (37). PG1

is a member of a novel class of fluorescent probes (36) that can be used to detect hydrogen peroxide in highly specific manner and that have successfully been employed in flow cytometry applications (59). The power of this dye is not only its highly specific reaction with hydrogen peroxide, turning it into the highly fluorescent species 2-methyl-4-*O*-methyl Tokyo Green, but the fact that this reaction changes it from cell wall permeable to cell wall impermeable, enabling accumulation inside the cell and subsequent detection by FACS technology.

On the proof-of-principle scale we have shown that the PG1 based oxidase activity screening assay is able to distinguish between active and inactive oxidase populations, and that it has enormous potential for screening large libraries in an ultra-high throughput manner. Frustratingly, we were unsuccessful in applying the screening method to find novel oxidase activities in our EUGO *first shell library (FSL)*. Our efforts were confounded by several unanticipated results following the FACS based screening, including loss of (insoluble) expression after multiple rounds of screening and sorting. Although the EUGO *FSL* is a particularly complete library of first shell residues (all first shell residues are mutated) it is of course possible that the library design is lacking and that there is no activity present in the library for the target substrates screened. This does not agree with a wealth of enzyme engineering literature, however (56), and the fact that the library was also screened for wild type activity with eugenol. It was a highly rational decision to include the original wild type sequence in the design of the final *FSL*; this should make screening for eugenol oxidase activity as a positive control possible. It would be expected that a significant portion of the library would contain (some) eugenol oxidase activity, as not only is the wild type sequence present but also because a significant collection of variants have a mild mutation scope of only one or two mutations. Hence we expected our positive control screen with eugenol to yield some enrichment for variants expressing active protein. It was frustrating to discover that with a FACS sorter we could not even find clones with eugenol oxidase activity, all the more when it was discovered that inexplicable expression problems compounded our screening efforts.

While the PG1 screening method developed here worked on the proof of principle scale and allowed for the separation of a mixture of inactive and active oxidase populations, it is possible that in the subsequent actual screening of the *FSL* the number of positive cells was very low and that this fell under the detection limit of the screening method. No determination of the lower detection limit of the screening method was performed; a method for performing this could be spiking a collection of inactive EUGO clones with progressively lower amounts of wild type EUGO, running the FACS analysis and checking for the degree of enrichment. In this way it can be determined how sensitive the FACS analysis is, and what the minimum number of

positive variants is that can still be isolated from a collection of negative variants. Another problem with the screening method outlined here that we cannot fully control is the degree of leaking of the fluorescent dye from active cells. While the dye in its unprotected form is cell wall impermeable, it seems unlikely that a small amount will not escape the cells during the time course of the assay, which is quite long as it entails an incubation step of ~1 hour and a sorting step which due to the size of the library also takes around 1 hour. It is a possibility that such leaking reduces the fluorescence of positive cells, meaning that cells containing less active enzymes are not detected as positive clones.

The designed EUGO *FSL* is an extremely large library, encompassing almost complete randomization of the residues involved in substrate binding. There are, however, many indications that it could harbor a wide range of novel substrate activities. One of EUGO's closest homologues, VAO, shares 7 of its 14 first shell residues with EUGO. These seven different residues give it markedly different substrate specificity, with a marked selectivity for alkyl phenols being the most significant difference (40, 43). A recently described gene cluster, *feeA-M* (fatty acid enol ester), identified from eDNA libraries for its ability to produce long chain acyltyrosine antibiotics, contains a gene (*FeeG*) encoding a predicted decarboxylase. This protein exhibits significant similarity (23%) to EUGO, implying a novel tyrosine decarboxylation mechanism where the p-quinone methide intermediate, common to both VAO and EUGO, eliminates CO₂ to produce a decarboxylated long chain *N*-acyl tyrosine (Figure 3) (60). Tests with both VAO and EUGO with this compound indicate extremely limited reactivity (data not shown) but hint at the possibility of creating such radically different substrate specificity and reactivity in EUGO through the screening of the EUGO *FSL*.

The screening method described here has the potential to be generic for all oxidases as it detects the H₂O₂ produced as by-product in a successful oxidase conversion. In its current configuration the problem of substrate accessibility may prevent application to all oxidases, limiting its use to those with substrates and targets that can freely enter *E. coli* cells. With EUGO the phenolic substrates and targets will be accessible to the intracellularly expressed oxidase (41), but in the case of more hydrophilic substrates, as is the case for carbohydrate oxidases like AldO, the polyol substrates and targets, like glycerol, xylitol, sorbitol and mannitol, are actively taken up by the cell and phosphorylated upon entering the cytoplasm (61, 62), preventing utilization by the cytoplasmically expressed oxidase (63). To overcome these problems alternative screening methods will have to be developed, where the protein libraries are expressed on the cell surface or in the *E. coli* periplasm, so that substrate accessibility is not a problem. Numerous techniques exist for the surface display of

enzymes; for a recent review see van Bloois *et al* (64). Previous work has shown that AldO is amenable to periplasmic expression via the twin arginine translocation (Tat) pathway, and can be used for whole cell biocatalysis of xylitol (63). If the H₂O₂ specific dye PG1 is used in conjunction with periplasmic or surface displayed cells then an obvious hurdle that needs to be overcome is the linking of the fluorescent signal to those cells exhibiting oxidase activity. One possibility is to use the recently pioneered emulsion technology, where single cells are captured in small (oil) droplets that contain both the fluorescent dye and the target substrate (65). The emulsion droplets would have to capture the fluorescent signal to prevent it from escaping via diffusion. Another option for the screening of oxidases that are expressed in the *E. coli* periplasm or cell surface is the use of tyramide signal amplification technology. Here, tyramide derivatives react with hydrogen peroxide in a peroxidase mediated reaction to form an activated tyramide derivative which reacts in a random manner with the tyrosine side chains of membrane proteins. The tyramide derivatives can be functionalized with a fluorescent dye and the method has as an advantage that the production of H₂O₂ can be translated into a fluorescent signal that becomes covalently linked to the cell responsible for the production of hydrogen peroxide. The method has been used successfully to screen protein libraries with a FACS for improved HRP enantioselectivity and lipase activities (66-68). Recently the method was also used to screen a library of glucose oxidase variants expressed in yeast (69) for improved activity towards glucose. While the improvement in activity was only modest (1.2x decreased K_M and 2.7x increased k_{cat}) the results show that this screening method has the potential to screen large oxidase libraries for improved activity using FACS technology. As a peroxidase is required to convert the tyramide into its activated form, this method could benefit greatly from our recently developed system for labelling oxidases with peroxidases (see: Chapter 4); utilizing this technology a mutant library of oxidases could be equipped with peroxidase activity and be expressed in the periplasm of *E. coli*, bypassing the laborious step where cells are decorated with an externally added peroxidase (70).

Another possibility for the development of an oxidase assay that is compatible with ultra-high throughput screening is utilizing the regulatory domain of *E. coli*, OxyR-RD, which is sensitive to intracellular H₂O₂ production. Recently, Belousov and co-workers constructed a genetically encoded biosensor for H₂O₂ consisting of a circularly permuted GFP variant, cpYFP, that was inserted into the oxyR-RD (71, 72). This biosensor, called Hy-Per, displays sub-micromolar affinity for hydrogen peroxide, translating this affinity into a fluorescent signal through the interaction of hydrogen peroxide with OxyR, which causes a huge conformational change in the protein. HyPer was successfully used to image the hydrogen peroxide production of

HeLa cells upon stimulation with epidermal growth factor (73). Such a system may be suitable for the development of a generic ultrahigh-throughput oxidase screen, and has as additional benefit that it is genetically encoded, requiring the addition of very few external compounds; oxidase activity can directly be translated to a fluorescent signal on a genetic level.

The diversity encoded by the twenty natural amino acids in the form of proteins is enormous: the plethora of compounds and reactions that can be converted by naturally occurring enzymes is incredible. Tailoring these enzymes to exhibit all the desired characteristics for a particular application remains a daunting challenge, however. The variation possible is so immense and results in such enormous complexity, that choice is exactly what makes the work of enzyme engineers so challenging. Simply put: “what mutations will result in my desired activity?” is a question to which there is no straightforward answer. Too often screening capacity becomes the bottleneck in any enzyme engineering approach as one is limited by what can be screened. In this chapter we design and obtain a library of variants that randomizes a large portion of the first shell residues involved in substrate binding and recognition of the flavoprotein eugenol oxidase. While focusing on a limited area of the protein, the amount of randomization still resulted in an enormous library: 10^7 variants. We detail our efforts to develop an ultrahigh throughput FACS based screening assay that is suitable to screen this enormous oxidase library. Although we were not successful in optimizing our screening method beyond the proof-of-principle stage, we believe that it has enormous potential, especially as it will enable one to screen all the variants in such a highly focused yet extremely diverse library. While a lot of progress is being made in the screening of multiple, smaller (often computationally designed) libraries (see 74 for a very recent example), we feel that with such approaches you may miss out. After all, you are going to great lengths to reduce the size of your library. This while the available protein space is so diverse and seemingly limitless in its catalytic potential, that it seems a waste to not develop a screening method that will enable examination of (nearly) all variants.

6.5 Acknowledgements

We are indebted to Dr. Jort Gerritsma & Bianca Gielesen (DSM Biotechnology Centre, Delft), Geert Mesander (Flow Cytometrics Facility, UMCG, Groningen), Siger Holsappel (Molecular Genetics, University of Groningen, Groningen) and Dr. Loknath Gidijala (Molecular Cell Biology, University of Groningen, Groningen) for their time and valuable assistance with the various flow cytometry and cell sorting equipment.

6.6 References

1. **Wohlgemuth R** (2009) The locks and keys to industrial biotechnology. *N Biotechnol* **25**: 204-213.
2. **Soetaert W & Vandamme E** (2006) The impact of industrial biotechnology. *Biotechnol J* **1**: 756-769.
3. **Patel RN** (2008) Chemo-enzymatic synthesis of pharmaceutical intermediates. *Expert Opin Drug Dis* **3**: 187-245.
4. **Panke S, Held M & Wubbolts M** (2004) Trends and innovations in industrial biocatalysis for the production of fine chemicals. *Curr Opin Biotechnol* **15**: 272-279.
5. **Pollard DJ & Woodley JM** (2007) Biocatalysis for pharmaceutical intermediates: The future is now. *Trends Biotechnol* **25**: 66-73.
6. **Schoemaker HE, Mink D & Wubbolts MG** (2003) Dispelling the myths - biocatalysis in industrial synthesis. *Science* **299**: 1694-1697.
7. **Fox RJ & Clay MD** (2009) Catalytic effectiveness, a measure of enzyme proficiency for industrial applications *Trends Biotechnol* **27**: 137-140.
8. **Bornscheuer UT & Kazlauskas RJ** (2004) Catalytic promiscuity in biocatalysis: using old enzymes to form new bonds and follow new pathways. *Angew Chem Int Ed* **43**: 6032-6040.
9. **Fox RJ, Davis SC, Mundorff EC, Newman LM, Gavrilovic V, Ma SK, Chung LM, Ching C, Tam S, Muley S, Grate J, Gruber J, Whitman JC, Sheldon RA & Huisman GW** (2007) Improving catalytic function by ProSAR-driven enzyme evolution. *Nat Biotechnol* **25**: 338-344.
10. **Reetz MT, Carballeira JD, Peyralans J, Höbenreich H, Maichele A & Vogel A.** (2006) Expanding the substrate scope of enzymes: combining mutations obtained by CASTing. *Chem Eur J* **12**: 6031-6038.
11. **Prokop Z, Sato Y, Brezovsky J, Mozga T, Chaloupkova R, Koudelakova T, Jerabek P, Stepankova V, Natsume R, van Leeuwen JG, Janssen DB, Florian J, Nagata Y, Senda T & Damborsky J** (2010) Enantioselectivity of haloalkane dehalogenases and its modulation by surface loop engineering. *Angew Chem Int Ed* **49**: 6111-6115.
12. **van den Heuvel R, Fraaije M, Ferrer M, Mattevi A & van Berkel W** (2000) Inversion of stereospecificity of vanillyl-alcohol oxidase. *Proc Natl Acad Sci U S A* **97**: 9455-9460.
13. **Damborsky J & Brezovsky J** (2009) Computational tools for designing and engineering biocatalysts. *Curr Opin Chem Biol* **13**: 26-34.
14. **Arnold F** (1996) Directed evolution: Creating biocatalysts for the future. *Chem Eng Sci* **51**: 5091-5102.
15. **Stemmer W** (1994) Rapid evolution of a protein *in-vitro* by DNA shuffling. *Nature* **370**: 389-391.
16. **Cramer A, Raillard S, Bermudez E & Stemmer W** (1998) DNA shuffling of a family of genes from diverse species accelerates directed evolution. *Nature* **391**: 288-291.
17. **Reetz MT, Kahakeaw D & Lohmer R** (2008) Addressing the numbers problem in directed evolution. *Chembiochem* **9**: 1797-1804.
18. **Wong T, Tee K, Hauer B & Schwaneberg U** (2004) Sequence saturation mutagenesis (SeSaM): a novel method for directed evolution. *Nucleic Acids Res* **32**: e26.
19. **Xu H, Petersen E, Petersen S & El-Gewely M** (1999) Random mutagenesis libraries: optimization and simplification by PCR. *Biotechniques* **27**: 1102-1104.
20. **Chica R, Doucet N & Pelletier J** (2005) Semi-rational approaches to engineering enzyme activity: Combining the benefits of directed evolution and rational design. *Curr Opin Biotechnol* **16**: 378-384.

21. **Reetz M, Wang L & Bocola M** (2006) Directed evolution of enantioselective enzymes: iterative cycles of CASTing for probing protein-sequence space. *Angew Chem Int Ed* **45**: 1236-1241.
22. **Munoz E & Deem MW** (2008) Amino acid alphabet size in protein evolution experiments: Better to search a small library thoroughly or a large library sparsely? *Protein Eng Des Sel* **21**: 311-317.
23. **Givan AL** (1992) Flow cytometry: first principles. (Wiley-Liss, New York).
24. **Shapiro HM** (2004) Practical Flow Cytometry. (Wiley-Liss, New York).
25. **Yang G & Withers SG** (2009) Ultrahigh-throughput FACS-based screening for directed enzyme evolution. *Chembiochem* **10**: 2704-2715.
26. **Hollmann F, Arends IWCE, Buehler K, Schallmey A & Buhler B** (2011) Enzyme-mediated oxidations for the chemist. *Green Chem* **13**: 226-265.
27. **Dunsmore C, Carr R, Fleming T & Turner N** (2006) A chemo-enzymatic route to enantiomerically pure cyclic tertiary amines. *J Am Chem Soc* **128**: 2224-2225.
28. **Pilone M & Pollegioni L** (2002) D-amino acid oxidase as an industrial biocatalyst. *Biocatal Biotransfor* **20**: 145-159.
29. **Leferink NG, Heuts DP, Fraaije MW & van Berkel WJ** (2008) The growing VAO flavoprotein family. *Arch Biochem Biophys* **474**: 292-301.
30. **van Hellemond EW, Leferink NG, Heuts DP, Fraaije MW & van Berkel WJ** (2006) Occurrence and biocatalytic potential of carbohydrate oxidases. *Adv Appl Microbiol* **60**: 17-54.
31. **Alexeeva M, Enright A, Dawson M, Mahmoudian M & Turner N** (2002) Deracemization of alpha-methylbenzylamine using an enzyme obtained by *in vitro* evolution. *Angew Chem Int Ed* **41**: 3177-3180.
32. **Carr R, Alexeeva M, Enright A, Eve TS, Dawson MJ & Turner NJ** (2003) Directed evolution of an amine oxidase possessing both broad substrate specificity and high enantioselectivity. *Angew Chem Int Ed* **42**: 4807-4810.
33. **van Hellemond EW, van Dijk M, Heuts DP, Janssen DB & Fraaije MW** (2008) Discovery and characterization of a putrescine oxidase from *Rhodococcus erythropolis* NCIMB 11540. *Appl Microbiol Biotechnol* **78**: 455-463.
34. **Dickinson BC & Chang CJ** (2011) Chemistry and biology of reactive oxygen species in signaling or stress responses. *Nat Chem Bio* **7**: 504-511.
35. **Rhee S** (2006) H₂O₂, a necessary evil for cell signaling. *Science* **312**: 1882-1883.
36. **Lippart AR, Van de Bittner GC & Chang CJ** (2011) Boronate oxidation as a bioorthogonal reaction approach for studying the chemistry of hydrogen peroxide in living systems. *Acc Chem Res* **44**: 793-804.
37. **Miller EW, Tulyanthan O, Isacoff EY & Chang CJ** (2007) Molecular imaging of hydrogen peroxide produced for cell signaling. *Nat Chem Bio* **3**: 263-267.
38. **Urano Y, Kamiya M, Kanda K, Ueno T, Hirose K & Nagano T.** (2005) Evolution of fluorescein as a platform for finely tunable fluorescence probes. *J Am Chem Soc* **127**: 4888-4894.
39. **Fraaije MW, Van Berkel WJ, Benen JA, Visser J & Mattevi A** (1998) A novel oxidoreductase family sharing a conserved FAD-binding domain. *Trends Biochem Sci* **23**: 206-207.
40. **Jin J, Mazon H, van den Heuvel RH, Janssen DB & Fraaije MW** (2007) Discovery of a eugenol oxidase from *Rhodococcus* sp. strain RHA1. *FEBS J* **274**: 2311-2321.
41. **Overhage J, Steinbuchel A & Priefert H** (2003) Highly efficient biotransformation of eugenol to ferulic acid and further conversion to vanillin in recombinant strains of *Escherichia coli*. *Appl Environ Microbiol* **69**: 6569-6576.

42. **Yamada M, Okada Y, Yoshida T & Nagasawa T** (2008) Vanillin production using *Escherichia coli* cells over-expressing isoeugenol monooxygenase of *Pseudomonas putida*. *Biotechnol Lett* **30**: 665-670.
43. **Fraaije MW, van den Heuvel RH, Roelofs JC & Van Berkel WJ** (1998) Kinetic mechanism of vanillyl-alcohol oxidase with short-chain 4-alkylphenols. *Eur J Biochem* **253**: 712-719.
44. **Fraaije MW & Mattevi A** *Unpublished data*.
45. **Beers RF & Sizer IW** (1952) A spectrophotometric method for measuring the breakdown of hydrogen peroxide by catalase. *J Biol Chem* **195**: 133-140.
46. **Hildebrandt AG & Roots I** (1975) Reduced nicotinamide adenine-dinucleotide phosphate (NADPH)-dependent formation and breakdown of hydrogen-peroxide during mixed-function oxidation reactions in liver-microsomes. *Arch Biochem Biophys* **171**: 385-397.
47. **Bradford MM** (1976) A rapid and sensitive method for the quantitation of microgram quantities of protein utilizing the principle of protein-dye binding. *Anal Biochem* **72**: 248-254.
48. **Veening J, Hamoen L & Kuipers O** (2005) Phosphatases modulate the bistable sporulation gene expression pattern in *Bacillus subtilis*. *Mol Microbiol* **56**: 1481-1494.
49. **Kuivila H & Wiles R** (1955) Electrophilic displacement reactions. 7: catalysis by chelating agents in the reaction between hydrogen peroxide and benzenboronic acid. *J Am Chem Soc* **77**: 4830-4834.
50. **Kuivila H & Armour A** (1957) Electrophilic displacement reactions. 9: effects of substituents on rates of reactions between hydrogen peroxide and benzenboronic acid. *J Am Chem Soc* **79**: 5659-5662.
51. **Imlay JA** (2008) Cellular defenses against superoxide and hydrogen peroxide. *Annu Rev Biochem* **77**: 755-776.
52. **Chelikani P, Carpena X, Perez-Luque R, Donald LJ, Duckworth HW, Switala J, Fita I & Loewen PC** (2005) Characterization of a large subunit catalase truncated by proteolytic cleavage. *Biochemistry* **44**: 5597-5605.
53. **Seaver L & Imlay J** (2001) Hydrogen peroxide fluxes and compartmentalization inside growing *Escherichia coli*. *J Bacteriol* **183**: 7182-7189.
54. **Heuts DP, van Hellemond EW, Janssen DB & Fraaije MW** (2007) Discovery, characterization, and kinetic analysis of an alditol oxidase from *Streptomyces coelicolor*. *J Biol Chem* **282**: 20283-20291.
55. **Morley KL & Kazlauskas RJ** (2005) Improving enzyme properties: when are closer mutations better?. *Trends Biotechnol* **23**: 231-237.
56. **Toscano MD, Woycechowsky KJ & Hilvert D** (2007) Minimalist active-site redesign: teaching old enzymes new tricks. *Angew Chem Int Ed* **46**: 3212-3236.
57. **Mattevi A, Fraaije MW, Mozzarelli A, Olivi L, Coda A & van Berkel WJ**. (1997) Crystal structures and inhibitor binding in the octameric flavoenzyme vanillyl-alcohol oxidase: The shape of the active-site cavity controls substrate specificity. *Structure* **5**: 907-920.
58. **Baron R, Riley C, Chenprakhon P, Thotsaporn K, Winter RT, Alfieri A, Forneris F, van Berkel WJ, Chaiyen P, Fraaije MW, Mattevi A & McCammon JA** (2009) Multiple pathways guide oxygen diffusion into flavoenzyme active sites. *Proc Natl Acad Sci U S A* **106**: 10603-10608.
59. **Albers AE, Dickinson BC, Miller EW & Chang CJ** (2008) A red-emitting naphthofluorescein-based fluorescent probe for selective detection of hydrogen peroxide in living cells. *Bioorg Med Chem Lett* **18**: 5948-5950.
60. **Brady SF, Chao CJ & Clardy J** (2002) New natural product families from an environmental DNA (eDNA) gene cluster. *J Am Chem Soc* **124**: 9968-9969.
61. **Woodyer RD, Christ TN & Deweese KA** (2010) Single-step bioconversion for the preparation of L-gulose and L-galactose. *Carbohydr Res* **345**: 363-368.

62. **Reiner A** (1977) Xylitol and D-arabitol toxicities due to derepressed fructose, galactitol, and sorbitol phosphotransferases of *Escherichia coli*. *J Bacteriol* **132**: 166-173.
63. **van Bloois E, Winter RT, Janssen DB & Fraaije MW** (2009) Export of functional *Streptomyces coelicolor* alditol oxidase to the periplasm or cell surface of *Escherichia coli* and its application in whole-cell biocatalysis. *Appl Microbiol Biotechnol* **83**: 679-687.
64. **van Bloois E, Winter RT, Kolmar H & Fraaije MW** (2011) Decorating microbes: surface display of proteins on *Escherichia coli*. *Trends Biotechnol* **29**: 79-86.
65. **Aharoni A, Amitai G, Bernath K, Magdassi S & Tawfik D** (2005) High-throughput screening of enzyme libraries: thiolactonases evolved by fluorescence-activated sorting of single cells in emulsion compartments. *Chem Biol* **12**: 1281-1289.
66. **Becker S, Schmoltdt HU, Adams TM, Wilhelm S & Kolmar H** (2004) Ultra-high-throughput screening based on cell-surface display and fluorescence-activated cell sorting for the identification of novel biocatalysts. *Curr Opin Biotechnol* **15**: 323-329.
67. **Lipovsek D, Antipov E, Armstrong KA, Olsen MJ, Klivanov AM, Tidor B & Wittrup KD** (2007) Selection of horseradish peroxidase variants with enhanced enantioselectivity by yeast surface display. *Chem Biol* **14**: 1176-1185.
68. **Antipov E, Cho AE, Wittrup KD & Klivanov AM** (2008) Highly L and D enantioselective variants of horseradish peroxidase discovered by an ultrahigh-throughput selection method. *Proc Natl Acad Sci U S A* **105**: 17694-17699.
69. **Prodanovic R, Ostafe R, Scacioc A & Schwaneberg U** (2011) Ultrahigh throughput screening system for directed glucose oxidase evolution in yeast cells. *Comb Chem High T Scr* **14**: 55-60.
70. **Becker S, Michalczyk A, Wilhelm S, Jaeger K & Kolmar H** (2007) Ultrahigh-throughput screening to identify *E coli* cells expressing functionally active enzymes on their surface. *Chembiochem* **8**: 943-949.
71. **Markvicheva KN, Bilan DS, Mishina NM, Gorokhovatsky AY, Vinokurov LM, Lukyanov S & Belousov VV**. (2011) A genetically encoded sensor for H₂O₂ with expanded dynamic range. *Bioorg Med Chem* **19**: 1079-1084.
72. **Belousov VV, Fradkov AF, Lukyanov KA, Staroverov DB, Shakhbazov KS, Terskikh AV & Lukyanov S** (2006) Genetically encoded fluorescent indicator for intracellular hydrogen peroxide. *Nat Methods* **3**: 281-286.
73. **Markvicheva KN, Bogdanova EA, Staroverov DB, Lukyanov S & Belousov VV** (2009) Imaging of intracellular hydrogen peroxide production with HyPer upon stimulation of HeLa cells with epidermal growth factor. *Methods Mol Biol* **476**: 76-83.
74. **van Leeuwen JGE, Wijma HJ, Floor RJ, van der Laan J & Janssen DB** (2011) Directed evolution strategies for enantiocomplementary haloalkane dehalogenases: from chemical waste to enantiopure building blocks. *Chembiochem* doi: 10.1002/cbic.201100579.

Chapter 7

The nose knows: biotechnological production of vanillin

Remko T. Winter, Hugo L. van Beek and Marco W. Fraaije

Laboratory of Biochemistry, Groningen Biomolecular Sciences and Biotechnology Institute,
University of Groningen, Nijenborgh 4, 9747 AG Groningen, The Netherlands

This chapter has been published in:

The Journal of Chemical Education

DOI: 10.1021/ed200271u

Abstract

Vanillin, the compound responsible for the well-known vanilla aroma, is almost exclusively produced via a chemical process, with only a small fraction extracted from natural sources, namely the bean of the orchid *Vanilla planifolia*. Research is being done towards a green chemistry process to obtain natural vanillin. A model biotechnological process is described here that exposes students to the essentials of a greener, chemoenzymatic synthesis of vanillin in a multi-day laboratory experiment. Bacterial expression is utilized to produce the enzyme eugenol oxidase (EUGO), which is purified from cell extracts using inexpensive gravity-flow ion-exchange chromatography, and is highly visual due to the bright yellow colour of the enzyme caused by its covalently-bound flavin cofactor. Students evaluate its purity with SDS-PAGE and a purification table, and measure its kinetic parameters with UV-vis spectrophotometry. Vanillin is produced by EUGO through the enzymatic oxidation of vanillyl alcohol. Due to its highly visual and olfactory nature, this is an ideal experiment to expose undergraduate students to the basic principles of a biotechnological process, enzyme production and purification and elementary enzyme kinetics.

7.1 Introduction

Biotechnological processes are enjoying increasing interest in recent years due to their potential to produce a wide variety of industrially valuable compounds in processes that are cheaper, produce less unwanted side products and most importantly are “greener”, *i.e.*, can be performed under milder, less dangerous conditions and utilize less energy and produce less greenhouse gas emissions. Young people today are often environmentally engaged, and, as a result, a laboratory experiment for undergraduate chemistry/life sciences students that models a biotechnological process is attractive.

Vanillin (4-hydroxy-3-methoxybenzaldehyde) is the chemical compound responsible for the vanilla aroma and is widely used as a flavouring agent in food and personal products (1). Most vanillin is produced via synthetic chemical routes starting from lignin, coniferin, the glucoside of coniferyl alcohol, guaiacol or eugenol (1); approximately 12,000 tons of vanillin is produced in this fashion annually (2). The worldwide production of natural vanillin pales in comparison to this figure, with less than 1% of the total worldwide demand being isolated from the beans of the orchid *Vanilla planifolia*. Its ubiquitous use in many food products, and its characteristic smell and taste, make vanilla a perfect candidate to produce via a model biotechnological process employing the enzyme eugenol oxidase. The flavoenzyme eugenol oxidase was originally discovered in the bacterium *Rhodococcus jostii* strain RHA1 and catalyses the oxidation of eugenol to coniferyl alcohol (Figure 8.2, p. 160), thus, eugenol oxidase (EUGO) (3). The crystal structure (*unpublished data*) of the enzyme is shown in Figure 1.6 (p. 18). EUGO also catalyses the formation of vanillin (Figure 7.4).

The experiment is designed for three laboratory periods. In the first period students isolate EUGO from *E. coli* cells expressing the enzyme using the yellow colour of the covalently-attached flavin cofactor to follow the enzyme. The principles of protein expression and purification are highly relevant for an undergraduate biochemistry/biotechnology curriculum as is illustrated by the presence of numerous laboratory exercises in the literature (4-10). In the second period students analyse the purification process and determine activity of the purified enzyme spectrophotometrically at 340 nm. If a UV/vis spectrophotometer is not available, a less quantitative assay is possible: organoleptic detection of vanillin. Its distinctive smell makes vanillin a popular subject in numerous laboratory exercises described in the literature (11-14). In the third lab period students study the production of vanillin.

This experiment is routinely offered to large groups of students: up to 150 students spread over several laboratories (approximately 25 students per lab room). Students work as threesomes, although the workload is also suited to students working in pairs or individually. Working as threesomes has the added advantage that students can assist each other with calculations, thus reducing errors. This laboratory experiment has been designed to keep student errors to a minimum, although some common student mistakes include improper buffer preparation during purification and omission of dilution steps during the determination of kinetic parameters (see: Supporting Information, Instructor Notes).

7.2 Experimental Outline

This laboratory exercise takes three days. On the first day students are supplied with *E. coli* cells expressing eugenol oxidase (EUGO) (3) and are instructed on how to handle Genetically Modified Organisms (GMOs) and perform microbiology experiments. Students lyse the cells, prepare cell free extracts, and purify EUGO by a single anion-exchange chromatography step. EUGO has a pI of 4.9 and is negatively charged at neutral pH; it binds to the positively charged moieties of the Q-Sepharose resin. Elution takes place by increasing the salt concentration of the buffer, which displaces the protein from the column. The Bradford method (15) is used to determine the total protein content of the various fractions. The purified enzyme is stored at -20°C to guarantee optimal longevity.

On day two, students analyse their samples with sodium-dodecyl sulphate-polyacrylamide gel electrophoresis (SDS-PAGE), allowing them to visualize the various steps of the purification. Students determine the apparent molecular mass of the purified EUGO by comparing its migration to that of a set of standards of known molecular mass. By preparing a purification table, students are able to quantify the efficiency of their purification. The activity of the cell free extract and eluted fraction is determined by measuring the increase in absorbance at 340 nm caused by the conversion of vanillyl alcohol to vanillin. Using the activity and the protein concentration determined on day 1 the specific activity (unit mg⁻¹) can be calculated and a purification table is drawn up.

Day three is used for the synthesis of vanillin. By starting the reaction at the beginning of the day, students can take regular samples and determine the amount of vanillyl alcohol converted to vanillin over time. If time is limited, students may follow the conversion for 2-3 hours, taking samples every 30 minutes instead of every hour. To gain insight into the potency of the vanilla aroma and to put the amount of vanillin they produce into perspective, students determine the vanillin content of a packet of

vanilla sugar. Students also measure the steady-state kinetic parameters of their purified enzyme. By measuring the initial rate of vanillin production at several different substrate concentrations and analysing the data with the LucenzIII program for enzyme kinetics (16), students can determine the k_{cat} and K_M for EUGO, and compare their values to the published literature (3).

7.3 Equipment

The laboratory experiment requires several items of specialized equipment, most of which can commonly be found in a (molecular) biology laboratory. The gene encoding eugenol oxidase, *eugo*, is located on pBADEUGOA, a derivative of the pBADmychisA expression plasmid, which has been used to transform *E. coli* TOP10 cells (3), and is available from the authors upon request. An autoclave, a shaking incubator, and table top microcentrifuges are needed. The purification is carried out in Poly-Prep chromatography columns (2 mL bed volume [0.8 x 4 cm], 10 mL reservoir, Bio-Rad) using Q-Sepharose Fast Flow resin (GE Healthcare). Electrophoresis equipment (Mini-PROTEAN system, Bio-Rad) is needed for SDS-PAGE. To save time, pre-cast SDS-PAGE gels (12% Ready Gel Tris-HCl, Bio-Rad) can be purchased, although gel casting can easily be carried out by instructors beforehand or by the students. A UV-transilluminator is required to visualize the FAD fluorescence in the protein gel after electrophoresis. A standard UV/vis spectrophotometer that can measure absorption and change in absorption over time is suitable, and may be coupled to a PC. One or two spectrophotometers per lab room of 25 students are sufficient. To determine the Michaelis-Menten kinetic parameters the program LucenzIII (16) is used, freely available for download from:

http://www.vuw.ac.nz/staff/alan_clark/teaching/kinetics.htm.

7.4 Hazards

The *E. coli* strain should be handled with appropriate caution and according to any local regulations applying for the safe use of bacterial strains. All cultures should be sterilized by autoclaving before discarding. One of the components of the Bradford reagent contains concentrated phosphoric acid and should be handled with care. The SDS gels may contain unpolymerized acrylamide which is a neurotoxin and possible carcinogen, so should be handled with latex gloves at all times. The electrophoresis equipment may pose an electrical hazard if used incorrectly. The Coomassie Blue protein stain will cause stubborn stains on exposed skin and clothes if spilled; wear gloves and lab coats at all times. UV radiation is harmful to the eyes and care should be taken when using the UV-transilluminator not to look directly at the lamp without

protective goggles. The reaction components (buffer, possible quinoid side products) are potentially toxic. The NaOH solution is highly caustic and should be handled with care.

7.5 Results and Discussion

Due to the bright yellow colour of EUGO, students are able to follow all steps of the purification including binding, washing and elution, when a sharp yellow band (purified EUGO) migrates off the column (Figure 7.1) after washing the column with medium salt buffer (All figures and data in this paper represent actual typical student results). As the expression level of EUGO in *E. coli* is very high (approximately 40% of the intracellular, soluble proteins) students generally have no problem in purifying around 5 mg of protein, obtaining yields of 40-75%. A supply of purified EUGO is kept on hand for students who have problems obtaining sufficient amounts of pure protein.

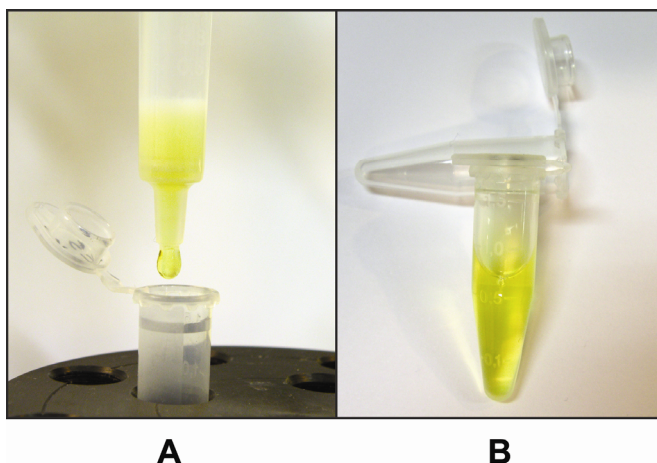


Figure 7.1 Bench-top purification of EUGO. Gravity flow anion-exchange ion chromatography is used. **A:** upon washing with medium salt buffer (50 mM Tris-HCl, 400 mM KCl, pH 7.5) EUGO elutes off the column as a sharp yellow band. **B:** around 1 mL of concentrated bright yellow protein is typically purified in this experiment. The distinctive colour is caused by the flavin cofactor which is covalently anchored to the protein.

Analysis by SDS-PAGE directly visualizes the expression of EUGO and the effect of the purification (Figure 7.2C). Gel visualization of the flavin fluorescence provides another highly visual method for the students to identify the protein (Figure 7.2F). The gel indicates that EUGO is about 80-90% homogeneous, which is sufficiently pure for the purposes of this experiment. Additional purification steps are discussed in the Instructors Notes, available online. The molecular mass of EUGO is calculated from the

SDS gel by plotting the log of the molecular mass versus the relative mobility of EUGO and that of a set of protein standards of known mass (Figure 7.3). In this case a molecular mass for EUGO of 61.4 kDa compares favourably to the literature value of 59.5 kDa (3). Typically, students obtain values that are ± 4 kDa from the published value. A purification table (Table 7.1) is prepared for the cell free extract (CFE) and purified protein. Typical values for specific activity are between 4-8 units mg^{-1} and purification factors of 1.5-4 are normal.

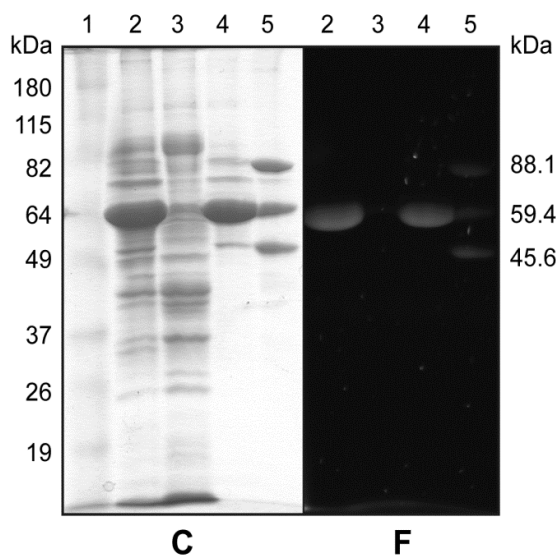


Figure 7.2 SDS-PAGE analysis of the purification of EUGO. Theoretical mass = 59.5 kDa. Gel is visualized for total protein with Coomassie Blue (C) and for flavin fluorescence (F). 1, molecular mass standards; 2, cell free extracts; 3, flowthrough; 4, yellow EUGO fraction eluted with medium salt buffer; 5, fluorescent molecular mass standards.

Table 7.1 Typical purification table. As the purification of EUGO only entails one step, the table contains a limited number of entries. 1 Unit is defined as 1 μmol vanillyl alcohol converted per minute. CFE = cell free extracts.

Fraction	Total protein (mg)	Total activity (Units)	Specific activity (Units mg^{-1})	Yield (%)	Purification factor
CFE	19.1	56.9	3.0	100	1
EUGO	8.1	39.4	4.9	70	1.6

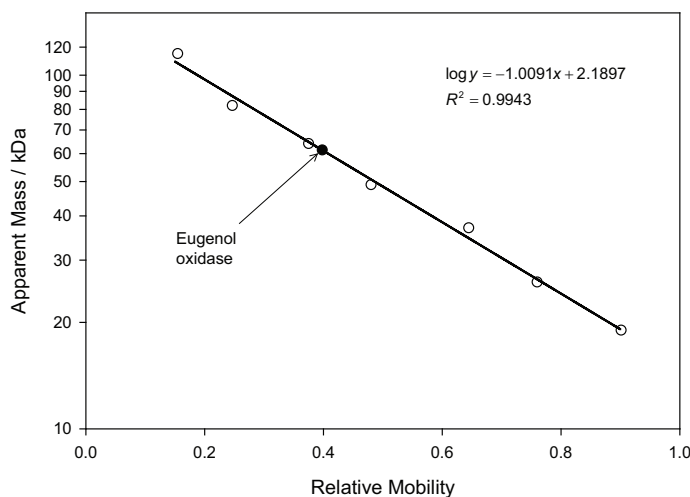


Figure 7.3 Calculating the mass of EUGO from an SDS-PAGE gel. The in-gel relative migration of EUGO and that of several known protein standards (Figure 7.2) is plotted versus their molecular mass on a logarithmic scale. Dotted lines indicate the measured relative mobility of EUGO and the corresponding calculated mass (61.4 kDa), which can also be calculated with the trend line equation.

The strong absorbance of vanillin at 340 nm allows for easy measuring of the initial rate of vanillyl alcohol to vanillin conversion. By measuring this rate at several substrate concentrations, the steady state kinetic parameters, k_{cat} and K_M , for their enzyme can be calculated. LucenzIII (16) is an intuitive and easy to use enzyme kinetics fitting program; a screenshot of the main screen of the program is shown in the Student Notes. A typical set of values is k_{cat} 9.6 s^{-1} and K_M $67 \text{ }\mu\text{M}$. The k_{cat} and K_M values are relative enzyme properties, and will depend on the conditions under which they are determined. The calculated parameters match the literature values quite well, although a deviation of 30% from published values is not uncommon. Here, the students can reflect on the accuracy of their work; if, for example, they have not accurately calculated the concentration of their protein, their k_{cat} value will be significantly influenced. This aspect of the lab brings to life the principles of enzymes kinetics, and allows students to assess the efficiency and specificity of the enzyme they have purified.

Students find the synthesis of vanillin one of the most rewarding aspects of the entire laboratory exercise. By starting the reaction at the beginning of the day, around 4 mM of vanillin (60 mg) is typically produced over six hours (Figure 7.4). This

amount clearly depends on the amount of EUGO added at the beginning of the conversion, and in the representative conversion curve in Figure 7.4 this corresponds to 20 mg vanillin per mg protein. Hydrogen peroxide formed in the reaction simply accumulates and creates no problems. Towards the end of the conversion the formation of a side product is sometimes observed as evidenced by the reaction mixture taking on a pink/red coloration, caused by the possible formation of quinone by-products.

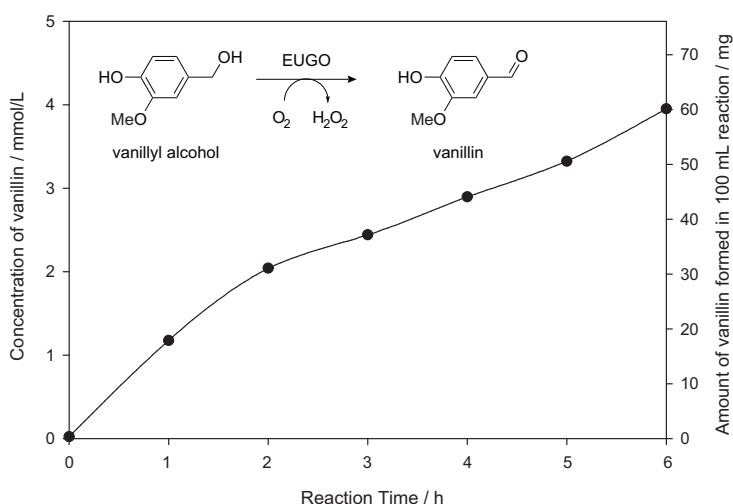


Figure 7.4 Conversion of vanillyl alcohol to vanillin by EUGO. 100 mL of 10 mM vanillyl alcohol in 50 mM Tris-HCl, pH 7.5 were incubated at room temperature under stirring with 2.94 mg EUGO. The concentration of vanillin was determined by measuring the absorption at 340 nm ($\epsilon = 27 \text{ mM}^{-1} \text{ cm}^{-1}$).

The purification of eugenol oxidase and chemoenzymatic production of vanillin has been a successful and well received laboratory exercise in our undergraduate biochemistry course for several years. The potential benefits of utilizing a cleaner and 'greener' chemoenzymatic process to produce vanillin are clear to students upon performing this experiment. Students enjoy performing this exercise as it has a clearly defined goal, namely the isolation and characterization of an enzyme followed by its use in the production of a compound of a very identifiable nature, namely vanillin. At the same time this is a powerful laboratory exercise from a didactic viewpoint as the principles of protein expression, protein purification, enzyme assays and Michaelis-Menten kinetics are seamlessly integrated in an exercise with a practical and clear goal, reinforcing the theory that is presented in the accompanying biochemistry lectures. The enzymatic synthesis of vanillin is a compelling example of biotechnology at work and unlike many other (bio)chemistry experiments it is an olfactory delight!

7.6 Supporting Information Available

Student instructions; notes for instructor; exercises and calculations for the students. The aforementioned material is available via the Internet at <http://pubs.acs.org> (DOI: 10.1021/ed200271u). The Instructor Notes contain additional comments on this experiment, including scaling up and expanding the experiment.

7.7 Acknowledgements

This work was supported by the Dutch Technology Foundation Stichting Technische Wetenschappen Grant 7726, the Nederlandse Organisatie voor Wetenschappelijk Onderzoek applied science division, and the Technology Program of the Ministry of Economic Affairs.

7.8 References

1. **Rao SR & Ravishankar GA** (2000) Vanilla flavour: production by conventional and biotechnological routes. *J Sc. Food Agric* **80**: 289-304.
2. **Dignum MJW, Kerler J & Verpoorte R** (2001) Vanilla production: technological, chemical, and biosynthetic aspects. *Food Rev Int* **17**: 199-219.
3. **Jin J, Mazon H, van den Heuvel RH, Janssen DB & Fraaije MW** (2007) Discovery of a eugenol oxidase from *Rhodococcus* sp. strain RHA1. *FEBS J* **274**: 2311-2321.
4. **Miller S, Indivero V & Burkhard C** (2010) Expression and Purification of Sperm Whale Myoglobin. *J Chem Educ* **87**: 303-305.
5. **Bering CL, Kuhns JJ & Rowlett R** (1998) Purification of Bovine Carbonic Anhydrase by Affinity Chromatography: An Undergraduate Biochemistry Laboratory Experiment. *J Chem Educ* **75**: 1021-1024.
6. **Timerman AP, Fenrick AM & Zamis TM** (2009) The Isolation of Invertase from Baker's Yeast: A Four-Part Exercise in Protein Purification and Characterization. *J Chem Educ* **86**: 379-381.
7. **Sommer C, Silva F & Novo M** (2004) Teaching molecular biology to undergraduate biology students: an illustration of protein expression and purification. *Biochem Mol Biol Educ* **32**: 7-10.
8. **Wu Y, Zhou Y, Song J, Hu X, Ding Y & Zhang Z** (2008) Using green and red fluorescent proteins to teach protein expression, purification, and crystallization. *Biochem Mol Biol Educ* **36**: 43-54.
9. **Bowen R, Hartung R & Gindt Y** (2000) A Simple Protein Purification and Folding Experiment for General Chemistry Laboratory. *J Chem Educ* **77**: 1456-1457.
10. **Vincent JB & Woski SA** (2005) Cytochrome c: a Biochemistry Laboratory Course. *J Chem Educ* **82**: 1211-1214.
11. **Taber DF, Patel S, Hambleton TM & Winkel EE** (2007) Vanillin Synthesis from 4-Hydroxybenzaldehyde. *J Chem Educ* **84**: 1158-1158.
12. **Fowler RG** (1992) Microscale reactions of vanillin. *J Chem Educ* **69**: A43.

13. **Lampman GM, Andrews J, Bratz W, Hanssen O, Kelley K, Perry D & Ridgeway A** (1977) Preparation of vanillin from eugenol and sawdust. *J Chem Educ* **54**: 776-778.
14. **Beckers JL** (2005) The Determination of Vanillin in a Vanilla Extract: An Analytical Undergraduate Experiment *J Chem Educ* **82**: 604-606.
15. **Bradford MM** (1976) A rapid and sensitive method for the quantitation of microgram quantities of protein utilizing the principle of protein-dye binding. *Anal Biochem* **72**: 248-254.
16. **Clark AG** (2004) Lucenz simulator: A tool for the teaching of enzyme kinetics. *Biochem Mol Biol Educ* **32**: 201-206.

Chapter 8

Oxidase engineering: summary and future prospects

Remko T. Winter

Laboratory of Biochemistry, Groningen Biomolecular Sciences and Biotechnology Institute,
University of Groningen, Nijenborgh 4, 9747 AG Groningen, The Netherlands

8.1 The power of enzymes

Enzymes are powerful natural catalysts, capable of performing a staggering array of chemical transformations. In a society that is becoming increasingly aware of its ecological footprint, the chemical industry is looking more and more to enzymes as a means to replace current processes with greener alternatives (1-3) and as tools to realize the Bio-based economy (4). In **chapter 1** we describe the potential of enzymes but at the same time highlight their Achilles heel. Due to their specificity and precise functional roles, enzymes can rarely be directly applied in industrial processes. One solution to this issue is enzyme engineering.

8.2 Enzyme engineering

In recent decades enzyme engineering has become a powerful technique to improve and optimize enzymes for a myriad of different purposes. Enzyme engineering is not only a tool to create 'unnatural' enzyme activities, or to make enzymes suitable for industrial application, but has also allowed us to gain a wealth of fundamental knowledge on how enzymes function. In **chapter 1** we describe the two opposing paradigms in enzyme engineering, rational and random, which are the two extremes used to define any enzyme engineering approach. Our most important conclusion in this chapter is that whatever approach one follows, a robust screening method is required in order to identify enzyme variants with the desired properties. The biggest challenge when designing a suitable screening method is achieving sufficient throughput; the more variants one can screen, the bigger the chance of finding a variant with the desired characteristics. This applies to both rational-based approaches, where one tries to limit the amount that needs to be screened, and to random-based approaches where very diverse libraries are screened.

When trying to obtain enzymes with novel substrate specificities, there is strong evidence to suggest that performing mutations close to the active site will have the greatest chance of success (5). But as we mention in **chapter 1**, a typical enzyme still has in the order of 10 residues lining the active site, meaning that a huge number of variants can potentially be screened when these 10 residues are subjected to complete randomization (20^{10}). Recently, a novel application of an established technique has been emerging that should make it possible to screen such libraries completely for novel substrate specificities: Fluorescent Activated Cell Sorting (FACS) (6). FACS sorters are devices capable of determining the fluorescence of individual particles (cells, microbeads, emulsions) at extremely high rates (10^7 hour⁻¹) and discretely isolating those particles from a heterogeneous mixture that exhibit the

desired characteristics (7, 8). Flavoprotein oxidases are a class of enzymes that nearly always produce H_2O_2 as a by-product; hence they are ideally suited for the development of a FACS based ultra-high throughput screening assay. After all, if such an assay can be designed to detect H_2O_2 as a marker for oxidase activity, then it can be generically applied to the screening of any oxidase mutant library.

8.3 Flavoprotein oxidases

As we describe in **chapter 1**, flavoprotein oxidases belonging to the vanillyl alcohol oxidase (VAO) class are a diverse group of enzymes that can perform a wide variety of oxidation chemistry (Figure 8.1) (9). Their ability to catalyse such oxidation reactions is what makes them relevant for biocatalytical applications.

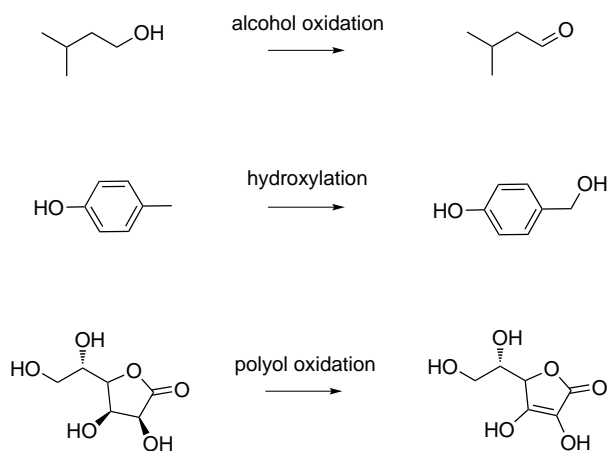


Figure 8.1 Examples of reactions catalysed by VAO-type oxidases. See Figure 1.4 (p.16) for more examples.

At the behest of the flavin cofactor – the common denominator of this enzyme class – VAO oxidases perform highly chemo-, regio-, and enantioselective oxidations. The wide variety of oxidation reactions this class carries out and the fact that they do not require expensive cofactors makes the VAO-class a very relevant enzyme scaffold to utilize in an engineering approach. As we describe in **chapter 1**, the enzyme engineering studies that are described in this thesis utilize two model VAO-type flavoproteins, namely, alditol oxidase (AldO) and eugenol oxidase (EUGO) (Figure 8.2). Both were selected due to their robustness, impressive levels of bacterial expression, availability of high resolution crystal structures, and the biocatalytic potential of the reactions they perform (10-12).

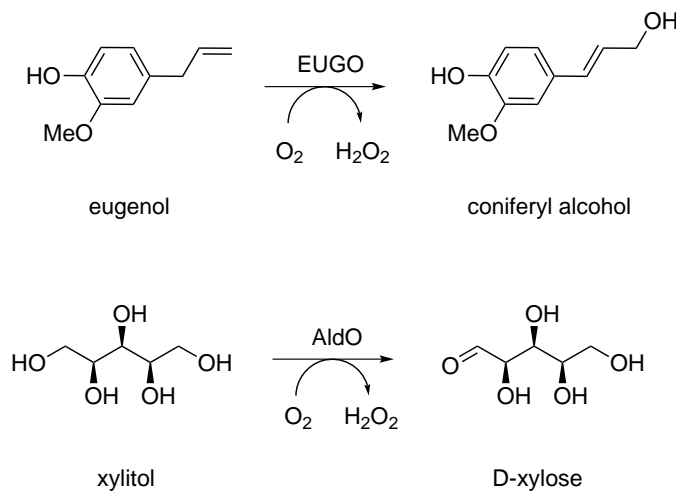


Figure 8.2 Preferred reaction performed by oxidases EUGO and AldO.

8.4 Redesigning oxidases by active site randomization

The aim of the work described in this thesis was redesigning flavoprotein oxidases through active site reconstruction. In this way we hoped to create novel substrate specificities in these reconstructed oxidases. To create novel substrate specificities we opted for the creation of entirely new active site architectures, by randomizing the first shell residues of the protein. The choice of which residues to mutate was a very rational one, based on the crystal structure of the protein in question. The choice of the type and frequency of mutations at each position was inspired by alignments with homologous proteins. So while having rational inspiration as a basis, the resulting new active site architectures are completely random. In our approach we relied on the creation of a very large number of different active site architectures, assuming that some would display novel substrate specificities, so that all we would have to do is screen the enzyme library for the desired variants. As detailed above and in [chapter 1](#), such a screening effort requires a very robust assay, capable of screening such a large collection of variants (10^7). No screening assay is available for the identification of novel oxidase activities on an ultra-high throughput ($>10^6$ hour) scale, so as described in [chapter 6](#) we had to design one. A lot of groundwork had to be covered before we were ready to develop and use our screening assay, which is summarized below and detailed in [chapter 2 – 5](#) of this thesis.

8.5 Engineering the O in oxidase

The ability to react with molecular oxygen is a fundamental feature of all oxidases. However, it is only poorly understood which O₂ uptake mechanism enzymes employ to promote efficient catalysis and how general this is. As this is essential knowledge when performing an oxidase engineering project we investigated O₂ diffusion pathways into our model flavoprotein oxidase AldO (**chapter 2**). Using an integrated computational and experimental approach we discovered spontaneous protein-guided O₂ diffusion from the bulk solvent to pre-organized protein cavities. This study indicated that the oxidase AldO employs multiple funnel-shaped diffusion pathways to absorb O₂ from the solvent and direct it to the reacting C4a atom of the flavin cofactor. We constructed a number of different AldO mutants that affect the oxidase activity, but did not hugely alter the reactivity of the protein towards oxygen. It appears that oxidases have evolved several diffusion pathways to cater to the wide variety of active site architectures that are possible amongst the VAO protein fold; while the substrate specificity is very diverse, the reactivity with oxygen remains close to optimal and never becomes rate limiting. This was an important finding as it indicated that our envisaged engineering approach –active site redesign – would only influence substrate specificity and not the fundamentally required oxygen reactivity.

8.6 Surface display & periplasmic secretion of oxidases can be engineered

It goes without saying that any enzyme engineering project requires stable, reproducible and robust (over)expression of the protein under study. *E. coli* is an imminently suitable expression host due to its amenability to genetic manipulation and high transformation efficiency, enabling it to express very large protein libraries. When developing a high throughput screening assay, however, heterologous expression of proteins in the cytoplasm of *E. coli* is not always desirable. Intracellular expression often confounds the development of many screening assays; in many cases the target compounds for enzymatic conversion are not able to cross the *E. coli* cell membrane, or issues like substrate or product toxicity may be problematic. To overcome this hurdle on the way to successful oxidase engineering, **chapter 3** details our efforts to develop a stable periplasmic and surface display platform in *E. coli* that is compatible with flavoprotein oxidases. Expression in the periplasm or on the cell surface has the benefit that the enzymes of interest are accessible to any target compound. Again we use AldO as a model flavoprotein oxidase. For periplasmic export, AldO was fused to endogenous *E. coli* signal sequences known to direct their

passenger proteins into the SecB, signal recognition particle (SRP), or Twin-arginine translocation (Tat) pathway. In addition, AldO was fused to an ice nucleation protein (INP)-based anchoring motif for surface display. The results show that both Tat-exported AldO and INP-surface-displayed AldO are active. We also reviewed the various forms of surface display that are possible for proteins heterologously expressed in *E. coli* in **van Bloois, Winter et al. Trends Biotechnol (2011)**. The results described in **chapter 3** are significant as AldO, like all VAO-type oxidases, contain a flavin cofactor that is bound to the protein upon folding in the cytoplasm. This means that the method of export to the periplasm or surface display has to be compatible with transporting a protein in its fully folded form, something that was achieved for flavoprotein oxidases for the first time in **chapter 3**.

8.7 Oxidases can be engineered to contain peroxidase functionality

When designing a screening method suitable for the identification of novel oxidase activities, hydrogen peroxide (H_2O_2) is an attractive hand-hold: it is formed as a by-product in nearly all oxidase conversions. This implies that measuring H_2O_2 formation can be used to generically screen for (novel) oxidase activity. Peroxidases are a class of enzymes that are commonly used to detect H_2O_2 (13, 14). Unfortunately these enzymes cannot be expressed in *E. coli*, our expression host of choice due to its amenability to genetic manipulation, high transformation efficiency and engineered periplasmic/surface display oxidase platform (**chapter 3**). To overcome these problems, **chapter 4** describes the engineering of an oxidase to exhibit peroxidase activity as well as oxidase activity. Through engineering, AldO was equipped with an extra functionality by fusing it to a microperoxidase. Expression in the periplasm of *E. coli* and subsequent purification resulted in the isolation of a synthetic bi-functional enzyme that was both fully flavinylated and heminylated: an oxiperoxidase. Characterization revealed that both the oxidase and peroxidase components were active. Due to the complementarity of these two activities the construct functioned as a biosensor, enabling detection of xylitol. In a related effort, we describe a novel peroxidase belonging to the dye-decolorizing (DyP-type) superfamily in **van Bloois, Winter et al. Appl Microbiol Biotechnol (2010)**. The results presented in this chapter are significant as for the first time oxidase activity is coupled directly to peroxidase activity. In this way, with the peroxidase moiety can be employed as an oxidase sensing unit. This could enable the development of a whole-cell ultra-high throughput screening assay for novel oxidase activities. Expression of oxidases in the *E. coli* periplasm means that substrate accessibility is not a problem, and equipping

them with peroxidase activity signifies the ability to detect the oxidase activity in a generic fashion.

8.8 A useful diversion: engineering oxidase thermostability

Mutations in the active sites of enzymes can sometimes have an advantageous effect on activity, while reducing the overall (thermo)stability of the protein (15). This often results in such variants being missed in high throughput screens. To overcome this one can first engineer a protein for enhanced (thermo)stability, before screening it against improved activity. Alternatively, one can search for a more thermostable homologue by genome mining and use this as an alternative platform for enzyme engineering. This is what we have done in [chapter 5](#), where we describe the identification and characterization of a thermostable alditol oxidase, HotAldO, from *Acidothermus cellulolyticus* 11B. Characterization revealed the protein to be a covalent flavoprotein of 47 kDa with a remarkably similar reactivity and substrate specificity to that of our model flavoprotein oxidase AldO from *Streptomyces coelicolor* A3(2) with which it shares 48% protein sequence identity. Thermostability measurements revealed that the novel oxidase is a highly thermostable enzyme with a melting temperature of 84°C and an activity half-life at 75°C of 112 min, prompting the name HotAldO. In order to understand the molecular basis for the relatively high thermostability of HotAldO we attempted to improve the thermostability of *S. coelicolor* AldO by replacing residues with high B-factors with the corresponding residues from *A. cellulolyticus* HotAldO. None of these mutations resulted in a more thermostable oxidase, a fact that was corroborated by *in silico* analysis. The results in this chapter are significant for two reasons; firstly we show that genome mining can be a valuable tool to relatively easily identify homologues that are more thermostable and hence more suitable as scaffolds for enzyme engineering. Secondly, we show that engineering a mesophilic protein to become more thermostable can be a complex undertaking.

8.9 Oxidase redesign and ultra-high throughput screening

In [chapter 6](#) we use the groundwork laid out in the previous chapters to design and screen a library of oxidase variants with completely new active site architectures. As no method existed to screen this large library of oxidase first shell mutants, we had to develop one. [Chapter 6](#) first details the pioneering of a generic ultra-high throughput screening assay for oxidase activity. Based on the hydrogen peroxide specific deprotection of a boronated fluorophore, our screening assay has the advantage that it can be applied generically to any oxidase activity. Furthermore, the fluorescent signal

is trapped intracellularly, enabling ultra-high throughput (10^7 cells hour⁻¹) screening with FACS (Fluorescent Activated Cell Sorter) technology. Using the model flavoprotein eugenol oxidase (EUGO), we show that our screening assay can be used under mock conditions to sort *E. coli* cells expressing active eugenol oxidase from cells expressing inactive oxidase. Following this success, we designed and obtained a first shell library of eugenol oxidase comprising 10^7 unique variants. Unfortunately, our attempts to isolate active variants using our novel screening assay from this large library of mutants have so far been unsuccessful. The results are significant as for the first time a screening assay is pioneered specifically for the ultra-high throughput FACS based screening in bacteria of large oxidase libraries. While not yet fully operational, we believe that the methodology described here shows enormous potential.

8.10 EUGO: an ideal oxidase for educational purposes

In [chapter 7](#) we design a practical course suitable for undergraduate university students. It highlights the biotechnological potential of oxidases by using EUGO to synthesize the common flavouring agent vanillin (vanilla aroma). We describe a multi-day laboratory experiment exposing students to some of the cornerstones of biochemistry: protein purification and enzyme kinetics. Bacterial expression is utilized to produce the enzyme eugenol oxidase (EUGO) which is purified from cell extracts using inexpensive gravity-flow ion-exchange chromatography. Vanillin, characterized by its typical aroma, is produced by EUGO through the enzymatic oxidation of vanillyl alcohol. Due to its highly visual and olfactory nature we believe that this is an ideal experiment to expose undergraduate students to the basics of biochemistry, namely enzyme production and purification and elementary enzyme kinetics. The practical described in [chapter 7](#) is one of the first laboratory practicals described to date suitable for undergraduate students where a flavoprotein oxidase is characterized and used in a mock biotechnological process (synthesis of vanillin).

8.11 Oxidase engineering: future prospects

The engineering of oxygen reactivity, an activity that typifies all oxidases, has proved to be a complex undertaking. Mapping the O₂ entry pathways revealed that oxygen can take multiple routes through the protein matrix and that blocking all these pathways can be difficult. It appears that oxidases by nature have been optimized to exhibit good oxygen reactivities. Possibilities exist to engineer oxidases into dehydrogenases; for some applications (e.g. diagnostic, biocatalysis) it may be useful that an oxidase can use an alternative electron acceptor instead of oxygen. This has in fact been done

in reverse where a single mutation (the 'gatekeeper' residue) turned the enzyme l-galactono- γ -lactone dehydrogenase (GALDH) into a catalytically competent oxidase (16). From a fundamental viewpoint it would be very interesting to use the approach described in **chapter 2** to follow the pathway hydrogen peroxide takes after its formation in the active site. This could lead to valuable insights, useful when designing oxidase-peroxidase chimeras like in **chapter 4** (substrate channelling) or when optimizing oxidases for biocatalysis (inactivation by H₂O₂).

HotAldO described in **chapter 5** is a very thermostable alditol oxidase. At the moment heterologous expression of HotAldO in *E. coli* is quite low. There are many indications, however, that this can be alleviated with further gene optimization (17). In light of the robust bacterial over-expression of its close homologue AldO, it seems unlikely that other issues like toxicity of the protein or the availability of FAD cause the low expression of HotAldO. Due to its thermostability, HotAldO has significant biotechnological potential (18). It is also useful as a thermostable template for enzyme engineering; we expect it to be more tolerant to mutations that are deleterious to the stability of its mesophilic counterpart AldO.

Expression in the periplasm or on cell surface of *E. coli* is a very powerful tool when screening libraries of enzyme variants. Accessibility for target substrates, product dissipation or accessibility for (large, fluorescent) reporter molecules is then no longer an issue. While the expression levels of periplasmically expressed AldO were moderate (**chapter 3**), there is evidence that suggests that the total surface charge of the protein plays a role when optimizing periplasmic transport via the twin arginine translocation (Tat) pathway. Future oxidase engineering projects would benefit from optimizing the periplasmic expression levels, as obtaining high expression levels in the periplasm would be useful when attempting to screen for variants with poor activities. Fusing an oxidase to Ice Nucleation Protein (INP) was shown to be an effective way of getting high yields of AldO expressed on the cell surface of *E. coli*. There are, however, indications that prominent endogenous surface molecules like lipopolysaccharides (LPS) inhibit the activity of surface displayed AldO. This could be solved by the introduction of peptide linkers between INP and AldO.

Positive aspects notwithstanding, there is one problem with surface display, namely the all important linking of phenotype to genotype. In the case of screening for novel oxidase activities based on H₂O₂ production with a hydrogen peroxide sensitive dye, the fluorescent signal needs to remain linked to the cell. The PG1 based screening assay described in **chapter 6** is an intracellular screening assay, but should also be compatible with recently developed emulsion technology for FACS screening (19). In such an approach the PG1 screening assay could be applied in conjunction with our periplasmic expression or surface display oxidase scaffolds. An alternative that would

enable the utilization of our oxidase-microperoxidase fusions developed in **chapter 4** involves the use of tyramide signal amplification technology. Here, tyramide derivatives react with peroxidases and hydrogen peroxide (produced by oxidases in this case) to form radicals that covalently bind in a random fashion to the tyrosine side chains of membrane proteins. The tyramide signalling molecules can be functionalized with a variety of fluorescent probes or affinity tags to enable antibody labelling or detection with FACS technology. The obvious advantage is that the activated tyramide moiety is bound covalently to the cell, enabling phenotype-genotype linking and full compatibility with surface display. This technology has been used to screen lipase, HRP and oxidase libraries (20-23). We believe that this technology has a lot of perspective when applied to oxidase engineering. It could combine the surface display or periplasmic expression described in **chapter 3** and co-expression of microperoxidase (fusions) described in **chapter 4**, to enable the development of a very powerful, ultra-high throughput, activity based screening method suitable for virtually all oxidases (Figure 8.3).

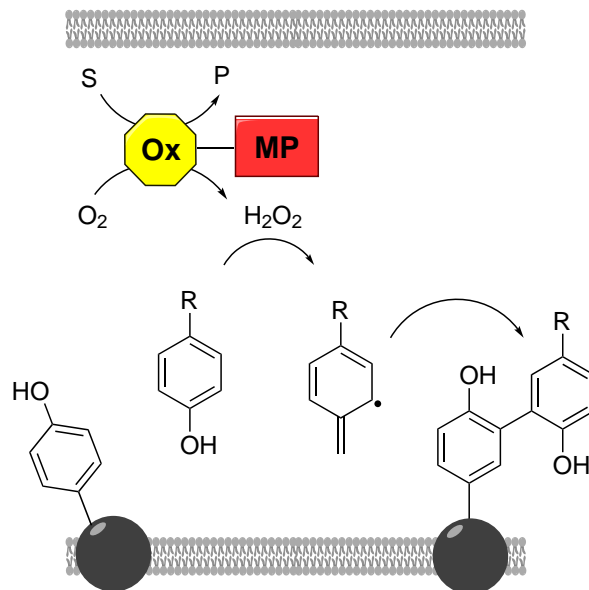


Figure 8.3 Screening for new oxidase activities with oxiperoxidases. Fusions between oxidases and microperoxidases (oxiperoxidases) and tyramide derivatives may be used to develop an ultra-high throughput screening assay for novel oxidase activities in the *E. coli* periplasm. Ox, oxidase; MP, microperoxidase; S, target substrate for oxidase; P, oxidase product; R, fluorescent group.

In **chapter 6** we describe a novel screening methodology, suitable for the ultra-high throughput FACS based screening of oxidase libraries for those variants with altered substrate specificities. The screening method we pioneer in this chapter, based on a H₂O₂ selective fluorescent dye, has enormous potential, despite the fact that our initial efforts to screen a large first shell library of eugenol oxidase variants were not successful. In the future it could benefit from trials with an alternate oxidase system, a different, bigger, cellular expression system (bigger cells are easier to detect with current FACS technology) and from using emulsion technology, where the individual cells are contained in oil droplets (water/oil/water emulsion) and which would make the screening technology compatible with surface display and reduce competition from intracellular hydrogen peroxide scavengers.

After reading **chapter 6** one must wonder: 'oxidase engineering, where do we go from here?' As discussed in **chapter 1**, enzyme engineers can follow many different paths when engineering a protein and these paths are generally inspired by one of two approaches; rational or random engineering. The tendency in current enzyme engineering literature is to go for a more rational approach, if only to scientifically validate what one is doing. Many enzyme engineering success stories are, however, essentially based on random approaches (*see 24-26 for a selection that is by no means complete*). Often a more rational based approach to enzyme engineering is sought after, simply because the bottleneck is the screening method available and the resulting amount of variants that can efficiently be screened. Thus, one must reduce the size of the library to a number that can be screened. It is my opinion, however, that big advances will always come from the screening of very large, and hence complete, libraries. While major achievements have been booked by screening, multiple small, semi-rational libraries (27), it is obvious that we are a long way off from designing every desired enzyme activity *de novo*. It is therefore my opinion that if the possibility of obtaining a robust ultra-high throughput screening assay exists, then one should always choose this path, and extensively screen very large libraries, like the *first shell library* we describe in **chapter 6**. Ultimately more can be learned from such an approach; if you can extensively screen multiple first shell libraries for changed substrate specificities then valuable knowledge will be gained as to which mutations are beneficial and which are deleterious or neutral. This knowledge can be applied to other enzyme systems for which no ultra-high throughput screening assay can ever be developed, enabling rationalized choices for library size reduction, and ultimately leading to the true *de novo* design of new substrate specificities, activities or other desired properties. When considering oxidase engineering as a specific example of enzyme engineering, my opinion is particularly applicable, due to the possibilities for creating generic ultra-high throughput activity based screening assays. The

production of hydrogen peroxide is generic to most oxidases, and we have shown that hydrogen peroxide can be used to screen for oxidase activity with FACS based technology, enabling the accurate screening and sorting of an enormous number of clones in several hours. Ultra-high throughput screening for oxidase activity also has the potential to screen for other enzyme activities, besides novel oxidase activities, in a coupled fashion. In theory it is possible to screen for any enzyme activity as long as a product is generated that will be accepted as an oxidase substrate. For example lipases or transaminases generate functional groups (hydroxyl and amino groups, respectively) that can be accepted as oxidase substrates. Thus, if an ultra-high throughput screening assay is not available for the enzyme and reaction of interest, coupling it to an (engineered) oxidase activity should enable ultra-high throughput screening of very large protein libraries. In conclusion, the work presented in this thesis allows us to conclude that the future for oxidase engineering is bright (yellow)!

8.12 References

1. **OECD** (2001) The application of biotechnology to industrial sustainability (OECD, Paris).
2. **OECD** (1998) Biotechnology for clean industrial products and processes: towards industrial sustainability (OECD, Paris).
3. **Schoemaker HE, Mink D & Wubbolts MG** (2003) Dispelling the myths - biocatalysis in industrial synthesis. *Science* **299**: 1694-1697.
4. **Sanders J & van der Hoeven D** (2008) Opportunities for a bio-based economy in The Netherlands. *Energies* **1**: 105-119.
5. **Morley KL & Kazlauskas RJ** (2005) Improving enzyme properties: when are closer mutations better? *Trends Biotechnol* **23**: 231-237.
6. **Yang G & Withers SG** (2009) Ultrahigh-throughput FACS-based screening for directed enzyme evolution. *Chembiochem* **10**: 2704-2715.
7. **Givan AL** (1992) Flow cytometry: first principles. (Wiley-Liss, New York).
8. **Shapiro HM** (2004) Practical flow cytometry. (Wiley-Liss, New York).
9. **Leferink NG, Heuts DP, Fraaije MW & van Berkel WJ** (2008) The growing VAO flavoprotein family. *Arch Biochem Biophys* **474**: 292-301.
10. **Heuts DP, van Hellemond EW, Janssen DB & Fraaije MW** (2007) Discovery, characterization, and kinetic analysis of an alditol oxidase from *Streptomyces coelicolor*. *J Biol Chem* **282**: 20283-20291.
11. **Forneris F, Heuts DP, Delvecchio M, Rovida S, Fraaije MW & Mattevi A** (2008) Structural analysis of the catalytic mechanism and stereoselectivity in *Streptomyces coelicolor* alditol oxidase. *Biochemistry* **47**: 978-985.
12. **Jin J, Mazon H, van den Heuvel RH, Janssen DB & Fraaije MW** (2007) Discovery of a eugenol oxidase from *Rhodococcus* sp. strain RHA1. *FEBS J* **274**: 2311-2321.
13. **Regalado C, García-Almendárez BE & Duarte-Vázquez MA** (2004) Biotechnological applications of peroxidases. *Phytochem Rev* **3**: 243-256.

14. **Veitch NC** (2004) Horseradish peroxidase: a modern view of a classic enzyme. *Phytochem* **65**: 249-259.
15. **Peisajovich SG & Tawfik DS** (2007) Protein engineers turned evolutionists. *Nat Methods* **4**: 991-994.
16. **Leferink NG, Fraaije MW, Joosten HJ, Schaap PJ, Mattevi A & van Berkel WJ.** (2009) Identification of a gatekeeper residue that prevents dehydrogenases from acting as oxidases. *J Biol Chem* **284**: 4392-4397.
17. **Welch M, Govindarajan S, Ness JE, Villalobos A, Gurney A, Minshull J & Gustafsson C** (2009) Design parameters to control synthetic gene expression in *Escherichia coli*. *Plos One* **4**: e7002.
18. **van Hellemond EW, Vermote L, Koolen W, Sonke T, Zandvoort E, Heuts DP, Janssen DB & Fraaije MW** (2009) Exploring the biocatalytic scope of alditol oxidase from *Streptomyces coelicolor*. *Adv Synth & Catal* **351**: 1523-1530.
19. **Aharoni A, Amitai G, Bernath K, Magdassi S & Tawfik D** (2005) High-throughput screening of enzyme libraries: thiolactonases evolved by fluorescence-activated sorting of single cells in emulsion compartments. *Chem Biol* **12**: 1281-1289.
20. **Becker S, Michalczyk A, Wilhelm S, Jaeger K & Kolmar H** (2007) Ultrahigh-throughput screening to identify *E coli* cells expressing functionally active enzymes on their surface. *Chembiochem* **8**: 943-949.
21. **Becker S, Höbenreich H, Vogel A, Knorr J, Wilhelm S, Rosenau F, Jaeger KE, Reetz MT & Kolmar H** (2008) Single-cell high-throughput screening to identify enantioselective hydrolytic enzymes. *Angew Chem Int Ed* **47**: 5085-5088.
22. **Antipov E, Cho AE, Wittrup KD & Klivanov AM** (2008) Highly L and D enantioselective variants of horseradish peroxidase discovered by an ultrahigh-throughput selection method. *Proc Natl Acad Sci U S A* **105**: 17694-17699.
23. **Prodanovic R, Ostafe R, Scacioc A & Schwaneberg U** (2011) Ultrahigh throughput screening system for directed glucose oxidase evolution in yeast cells. *Comb Chem High T Scr* **14**: 55-60.
24. **Reetz MT, D Carballeira J & Vogel A** (2006) Iterative saturation mutagenesis on the basis of B factors as a strategy for increasing protein thermostability. *Angew Chem Int Ed* **45**: 7745-7751.
25. **Moore JC & Arnold FH** (1996) Directed evolution of a para-nitrobenzyl esterase for aqueous-organic solvents. *Nat Biotechnol* **14**: 458-467.
26. **Carr R, Alexeeva M, Enright A, Eve TS, Dawson MJ & Turner NJ** (2003) Directed evolution of an amine oxidase possessing both broad substrate specificity and high enantioselectivity. *Angew Chem Int Ed* **42**: 4807-4810.
27. **van Leeuwen JGE, Wijma HJ, Floor RJ, van der Laan J & Janssen DB** (2011) Directed evolution strategies for enantiocomplementary haloalkane dehalogenases: from chemical waste to enantiopure building blocks. *Chembiochem* doi: 10.1002/cbic.201100579.

English summary
(suitable for the casually interested layman)



Life requires enzymes

Life can be considered as an enormously complex collection of constantly ongoing chemical reactions. Most of these chemical reactions would not occur unless there were enzymes. Enzymes are biological catalysts; molecular tools that life uses to perform the myriad of chemical reactions that are required for its existence. Enzymes are proteins, large biomolecules consisting of one or more polypeptide chains. These chains are built up by various combinations of the 20 naturally occurring amino acids, and can be more than 1000 amino acids long (Figure 1). Both the chemical nature of the amino acids and the three dimensional conformations of the polypeptide chains determine the specificity and catalytic prowess of enzymes. Enzymes catalyse (=speed up) nearly all the chemical reactions required by an organism for survival. Without enzymes many of these reactions simply would not occur.

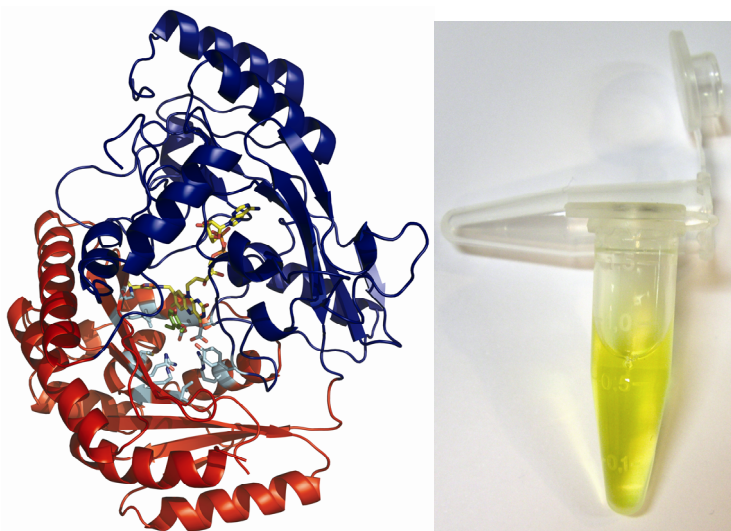


Figure 1 Enzymes are large, complex molecules built up from long chains of amino acids. At left is the structure of eugenol oxidase (EUGO). Flavoprotein oxidases are bright yellow enzymes; on the right a concentrated solution of EUGO is shown.

Enzymes are green

There is much interest in enzymes for their application in the chemical industry. Enzymes are seen as desirable biocatalysts, as they have the potential to replace many industrial processes with “greener” alternatives. This is because enzymes generally function under mild conditions without requiring excessive temperatures, pressures,

pHs (acidic or basic) or harmful solvents. A well-known example is the use of enzymes in washing detergent to enable a reduction in the washing temperature.

A major drawback to the widespread application of enzymes in industry, however, is that enzymes have evolved to fulfil a distinct physiological role in the particular organism in which they are found. This means that they work very well in their own ecological niche, but that they cannot directly be employed in an industrial setting. A solution to this problem is enzyme engineering.

Enzymes can be engineered

Enzyme engineering is a field of research where scientists manipulate enzymes in an attempt to change their properties, such as their stability, speed, selectivity and type of compounds they act on. The reason for performing such research may be to enable the industrial application of an enzyme. Generally, however, the goal is much more fundamental: by manipulating the various characteristics of enzymes we gain a better understanding of how they function.

This PhD thesis is entitled “*Novel approaches for the redesign of flavoprotein oxidases*” and is an example of enzyme engineering. Specifically, it deals with the redesign (engineering) of a specific class of enzymes: flavoprotein oxidases.

Flavoprotein oxidases are yellow enzymes

Flavoprotein oxidases are enzymes that catalyse the oxidation of a wide variety of chemical compounds using molecular oxygen. Oxidases are very precise in the way they carry out this reaction; the target compound is oxidized in the same way every time and hydrogen peroxide or water is the only by-product formed. Oxidases are a relatively rare type of enzyme, but because the oxidation chemistry they carry out is often difficult to perform via conventional chemical methods, they are the focus of some industrial interest. Flavoprotein oxidases are special because they are bright yellow in colour (Figure 1). This is due to the fact that they contain a flavin cofactor: FAD (from Latin: *flavus* = yellow). This cofactor (= helper molecule) is tightly bound in the centre of the protein, and enables it to perform oxidation reactions.

This thesis focusses on the engineering of two flavoprotein oxidases: eugenol oxidase (EUGO) and alditol oxidase (AldO). They originate from two different bacteria and have been discovered by former PhD students. They were chosen as model oxidases to engineer for a number of reasons. They are easy to produce in *E. coli*, crystal structures are available for both and both catalyse the oxidation of two different classes of (industrially relevant) compounds. The preferred reaction of AldO

is the oxidation of xylitol (the same as found in sugar-free chewing gum) to D-xylose. EUGO preferentially converts eugenol (essence of cloves) to coniferyl alcohol (Figure 2).

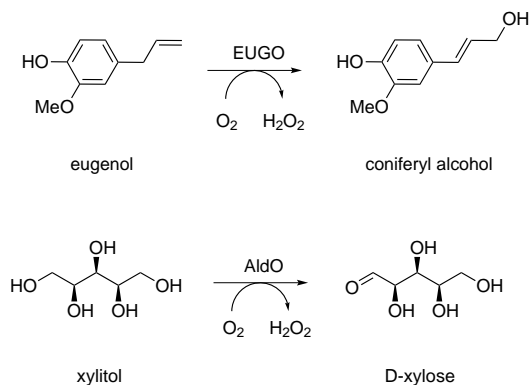


Figure 2 Preferred reaction catalysed by oxidases EUGO and AldO. EUGO reacts with eugenol (essence of cloves); AldO reacts with xylitol (in sugar free chewing gum).

A day in the life of an Enzyme Engineer

Having established that the subject of this thesis concerns enzyme engineering, specifically the engineering of yellow oxidases, the curious layman may wonder how this research is typically carried out: what does a day in the life of an enzyme engineer involve? To answer this question one can refer to **chapter 7** of this thesis, which details a practical experiment suitable for undergraduate/first year university students. This experiment involves the production, purification, characterization and utilization of the model oxidase EUGO described above. Many of the tasks described in **chapter 7** are simplified yet representative examples of the actual work I carried out in the last four years. Roughly speaking “a day in the life of an enzyme engineer” involves the following aspects:

Produce: enzyme needs to be produced or expressed. For this an expression host is used: an organism that can be genetically manipulated to produce the desired enzyme. Many different hosts are available, but in this thesis we only use *E. coli* bacteria.

Purify: Once produced by *E. coli*, the enzyme needs to be purified from the rest of the bacterial components. This can be done with a variety of chromatographic techniques. Basically, material is used that selectively binds our enzyme of interest, enabling us to purify enzyme from the rest of the unwanted cellular components.

Characterize: The fun part. Once we have the pure protein we want to know its characteristics. There are many things that can be measured but we are predominantly interested in an enzyme's kinetic parameters and substrate specificity. In other words: how fast is the enzyme? And what compounds does it convert?

Utilization: Once an enzyme has been purified and characterized, we sometimes test a mock-up of an envisaged application. In the practical course described in [chapter 7](#) this is the synthesis of the vanilla flavouring agent using the enzyme EUGO.


The above aspects are all combined in a practical course suitable for undergraduate students ([chapter 7](#)) with little or no practical experience on dealing with enzymes. It misses one essential portion of work carried out by enzyme engineers however, namely: mutagenesis & screening.

Mutagenesis & screening: A very important part of any enzyme engineering effort involves the creation of new enzyme variants (through mutagenesis) that display altered (improved) characteristics. New enzyme variants are created on DNA level; the gene encoding the enzyme is mutated, where after the expression host produces the altered enzyme. The advantage of such an approach is that large collections of altered genes can easily be produced, resulting in large collections of altered enzymes. Screening is the next step: here the mutated variants are all examined (screened) for the desired characteristics. Designing a suitable screening method is often the bottleneck in an enzyme engineering approach ([chapter 6](#)).

The goal of this thesis

Having established the subject matter of this PhD thesis, and its context and relevance, we can now state its principal goal. The aim of the research in this thesis was to engineer the oxidases AldO and/or EUGO so that they would convert different compounds (different to xylitol or eugenol, respectively). We aimed to do this by creating a vast collection of mutated genes ($\sim 10^8$ different genes) and then screening all these mutants. To effectively do this we aimed to develop a new screening assay (described in [chapter 6](#)) allowing us to examine the vast collection of oxidase variants ($\sim 10^8$ different EUGO or AldO variants).

The following section gives a chapter by chapter guide to this thesis, detailing the what, why and most important conclusions of chapters 2–6 in simplified language. Chapter 1 contains the introduction and goal of this thesis, and has already been described above, as has chapter 7 (a student practical). The final chapter (chapter 8) is a summary of the result obtained in this thesis.



A guide to this thesis

Chapter 2

Title: Multiple pathways guide oxygen diffusion into flavoenzyme active sites.

Translation of title: Funnel-like structures are used by oxidases to channel oxygen.

What: As mentioned above, oxidases are enzymes that use molecular oxygen (dioxygen; O_2) to perform the reactions they catalyse. This reaction takes place in the active site, a cavity roughly situated in the centre of the enzyme. In this chapter we study how oxygen travels from the water the oxidase is dissolved in, through the enzyme, until it reaches the active site cavity. We do this in two ways. As the movement of molecular oxygen through a protein is very difficult to measure directly we simulate this by using a computer simulation. Essentially, one oxidase molecule is placed in an imaginary box along with water molecules and with a lot of oxygen molecules. A simulation is run and the movement of the oxygen molecules through the oxidase is tracked. Following this we know how the oxygen is channelled through the protein. This computer simulation is then checked with experiments. By mutating some of the amino acid residues in the oxidase we attempt to block the paths molecular oxygen takes through the oxidase. We can detect this (partial) blocking of oxygen as a change in the rate of catalysis.

Why: Our goal was to engineer oxidases. Hence it was important to fully understand all aspects of an oxidase reaction. Oxygen reactivity of proteins is an important concept that is currently receiving a lot of interest. Concerning oxidases, a lot of work has been done on the overall reactivity, but the issue of oxygen channelling has never been studied in detail. For the first time we showed how such a small gas molecule travels through a protein to reach the active site. In the future this may also open doors to new kinds of biocatalysts. For example, our results have been used to identify an oxygen gatekeeper residue, which can completely block the accessibility of the active site for oxygen. Removing this residue can influence the oxygen reactivity dramatically, turning the enzyme (a dehydrogenase) into an oxidase.

Conclusion: The most important conclusion is that molecular oxygen uses multiple, funnel like structures to channel oxygen from the surface of the protein to the active site. In the oxidase we studied (AldO) this oxygen channelling is very efficient, and it was difficult to completely block the oxygen activity. From an engineering point of view this was important, as we wanted to engineer the reactivity of the protein, changing it so that it would act on other substrates. This study confirmed our belief that the oxygen reactivity is a firmly ensconced and robust part of the protein.

Chapter 3

Title: Export of functional *Streptomyces coelicolor* alditol oxidase to the periplasm or cell surface of *Escherichia coli* and its application in whole-cell biocatalysis.

Translation of title: Getting *E. coli* bacteria to transport the model oxidase, AldO, onto their cell surface.

What: In this chapter we describe a method for getting *E. coli* bacteria to produce the model oxidase, AldO, on their cell surface or in their periplasm. The periplasm of *E. coli* is the space found between the inner and outer membrane of these bacteria (Figure 3).

Why: Obtaining purified enzyme for industrial applications is often a laborious, costly and hence undesirable process. Using a whole cell biocatalyst—an enzyme contained in a living cell—is often preferred. Growing expression hosts like *E. coli* or yeast for example is a relatively straightforward process. If a whole cell biocatalyst is used, however, then one must be certain that the compounds to be converted can enter the cell. This is not always the case. An elegant solution is getting the expression host to transport the target protein from inside the cell to the periplasm or onto the cell surface, where accessibility is not an issue (Figure 3). This was also important for our envisaged engineering approach, as we wanted to test a large collection of different oxidase variants for new reactivities using whole cells instead of purified protein.

Conclusion: The oxidase AldO can successfully be produced on the cell surface and in the periplasm of *E. coli*, allowing it to be used as a whole cell biocatalyst. While this has been done many times for other enzyme types, the fact that AldO is a flavoprotein oxidase makes it a special case, as it means it has to be exported in a fully folded form, instead of being threaded through a small hole in the membrane as is the case for most other exported proteins.

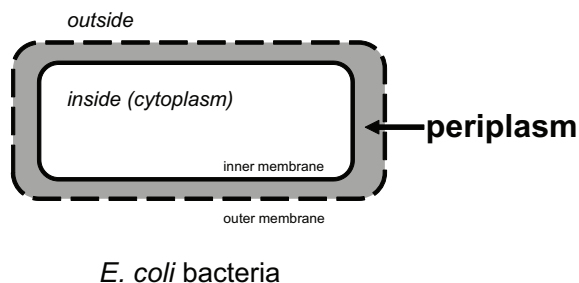


Figure 3 *E. coli* cells have an inner and an outer cell membrane. The space between the two (grey) is the periplasm.

Chapter 4

Title: Functionalizing oxidases with peroxidase activity creates oxiperoxidases, a new breed of hybrid enzymes capable of cascade chemistry.

Translation of title: Fusing portions of two different enzymes to create a hybrid enzyme.

What: The detection of oxidase activity is difficult to measure directly. Thus, it is important when designing and testing new oxidase variants for novel activities that a reliable method is available for the detection of enzyme activity. In this chapter we design a new sensor capable of measuring oxidase activity. The by-product of all reactions catalysed by oxidases is hydrogen peroxide (H₂O₂). Peroxidases are a different class of enzymes that can react with H₂O₂ to form easily detected coloured compounds. Measuring oxidase activity with peroxidases is common, but relatively cumbersome and not compatible with whole cell systems. In this chapter we describe a solution to this problem by fusing a peroxidase to an oxidase, creating a hybrid enzyme that can be produced by *E. coli*.

Why: The aim of my PhD work was to rapidly test a very large collection of oxidase variants, using a whole cell approach. To enable the detection of oxidase activity in whole cells a suitable detection method had to be developed. A possible solution was fusing another type of enzyme to the oxidases and expressing both in *E. coli*. This other enzyme, a peroxidase, enables detection of oxidase activity.

Conclusion: We successfully created a bi-functional enzyme by fusing an oxidase to a peroxidase. We could produce this enzyme in *E. coli*, and it was also functional in whole cells. In the future, this approach may be used to rapidly test a large collection of oxidase variants for new activities.

Chapter 5

Title: Hot or not? Discovery and Characterization of a thermostable alditol oxidase from *Acidothermus cellulolyticus* 11B.

Translation of title: Finding an oxidase that is stable at high temperatures.

What: We describe the search for an oxidase that can tolerate high temperatures. This is done by examining the genomes of thermophilic organisms (=heat loving; live at high temperatures) for genes that are very similar to the AldO gene. In a bacterium that inhabits the hot springs of Yellowstone National Park, USA (*Acidothermus cellulolyticus* 11B) we found a gene encoding a protein very similar to AldO: HotAldO. We then produce and study this protein.

Why: For eventual industrial applications it is often necessary that an enzyme can tolerate high temperatures (=thermostable). From an enzyme engineering viewpoint this thermostability is also desirable. Mutating an enzyme can create variants that display a different, desired reactivity, while at the same time reducing the stability of the enzyme. If a more thermostable enzyme is used to begin with then one has a better chance of finding a variant with both improved reactivity and acceptable stability.

Conclusion: We discovered and were able to produce and purify an oxidase that is closely related to our model oxidase AldO. This new oxidase is highly similar to AldO, except that it is much more thermostable: it is stable for long periods at high temperatures. We hence named this enzyme HotAldO.

Chapter 6

Title: Redesign of oxidases by active site randomization.

Translation of title: Trying to create new oxidases by rigorous mutation of the active site.

What: We try to create new oxidase activities by taking one of our model oxidases, EUGO, and rigorously mutating the portion of the enzyme that is responsible for recognition and binding of the normal substrate, eugenol (essence of cloves). As we create more than 10 million different EUGO variants we also develop a method to quickly test all these variants for altered activity. This is done with a dye that becomes fluorescent in the presence of hydrogen peroxide, the by-product of successful oxidase conversions. With a cell sorter, a device that can measure the fluorescence of individual cells extremely rapidly ($10000 \text{ cells s}^{-1}$) we can then identify those cells producing active oxidase variants.

Why: By drastically mutating the area of the enzyme responsible for recognition and binding we hope that the enzyme will be able to recognize, bind and convert completely new compounds, some of which are also interesting for eventual industrial applications. The method we develop to rapidly examine the millions of mutants also has the potential to be applied to other oxidases.

Conclusion: We were unsuccessful in finding new activities amongst the millions of oxidase variants. This was predominantly due to the fact that our method using a hydrogen peroxide sensitive dye and a cell sorter still has to be optimized for the screening of such a huge library.


Final conclusions of this thesis

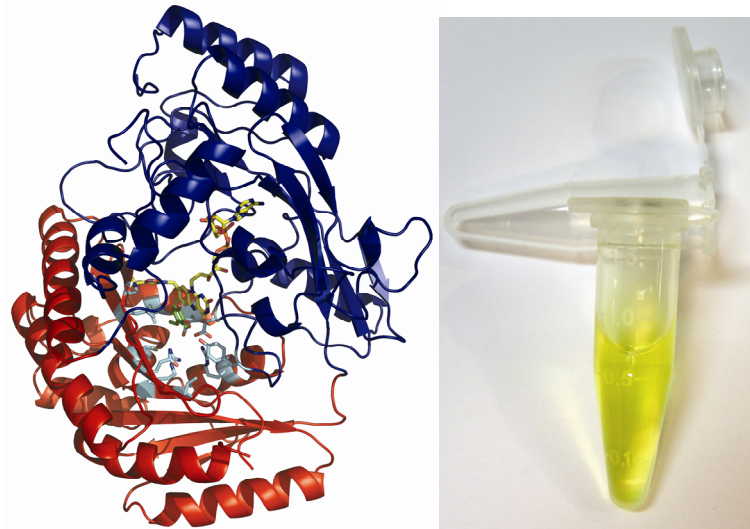
The work presented in this thesis is diverse, describing a variety of different approaches that can be followed when engineering oxidases. The principal goal of the research, namely the development of a fully operational ultra-high throughput screening assay for oxidases, and the corresponding discovery and characterization of new oxidase variants was not completely attained. However, as the other chapters will attest, valuable results were obtained. These include the insight gained into the channelling of oxygen in an oxidase; the development of an oxidase secretion platform; the production of an oxiperoxidase enzyme hybrid and the discovery of a thermostable oxidase. Taken together, this thesis highlights the potential of flavoprotein oxidases for enzyme redesign and engineering.

Nederlandse samenvatting
(geschikt voor de geïnteresseerde leek)



Het leven vereist enzymen

Het leven kan worden beschouwd als een enorm complexe verzameling van chemische reacties die continue aan de gang zijn. De meeste van deze chemische reacties zouden niet plaatsvinden wanneer er geen enzymen waren. Enzymen zijn biologische katalysatoren; moleculaire tools die het leven gebruikt om talloze chemische reacties uit te voeren, die essentieel zijn voor het bestaan hiervan. Enzymen zijn eiwitten, grote biomoleculen bestaande uit één of meer polypeptide ketens. Deze ketens zijn opgebouwd uit verschillende combinaties van de 20 natuurlijk voorkomende aminozuren, en kunnen meer dan 1000 aminozuren lang worden (Figuur 1). Zowel de chemische aard van de aminozuren, als de driedimensionale vorm van de polypeptiden ketens, bepalen de specificiteit en de katalytische kracht van enzymen. Enzymen katalyseren (= een reactie versnellen) bijna alle chemische reacties die een organisme nodig heeft om te overleven.



Figuur 1 Enzymen zijn grote, complexe moleculen, bestaande uit lange ketens van aminozuren. Links is de structuur van eugenol oxidase (EUGO) weergegeven. Flavoproteïne oxidases zijn fel gele enzymen. Rechts is een geconcentreerde oplossing van EUGO weergegeven.

Enzymen zijn groen

Er is veel interesse voor enzymen en hun toepassing in de chemische industrie. Enzymen worden gezien als wenselijke biokatalysatoren, omdat ze als "groenere" alternatieven de potentie hebben een groot aantal industriële processen te vervangen. Dit komt omdat enzymen doorgaans onder mildere omstandigheden functioneren

zonder de noodzaak van extreme temperaturen, druk, pH (zuur of basisch) of schadelijke oplosmiddelen. Een bekend voorbeeld is het gebruik van enzymen in wasmiddelen waardoor de wastemperatuur omlaag kan.

Doordat een enzym binnen een organisme zo geëvolueerd is om één fysiologische rol te vervullen, is het lastig om enzymen rechtstreeks te gebruiken in de industrie. Om enzymen waardevol te maken voor de industrie is “enzym engineering” nodig. Dit maakt het o.a. mogelijk dat een enzym dat voorheen maar één reactie uit kon voeren, nu meerdere reacties kan katalyseren.

Knutselen met enzymen

“Enzym engineering” is een tak van sport waar wetenschappers enzymen manipuleren in een poging om hun eigenschappen—zoals hun stabiliteit, reactiesnelheid, selectiviteit en het type van verbindingen waarop ze actief zijn—te veranderen. Het doel kan zijn om de industriële toepassing van een enzym mogelijk te maken. Veel vaker, echter, is het doel veel fundamenteeler: door het manipuleren en de resulterende effecten op de verschillende kenmerken van enzymen te bestuderen, krijgen we een beter begrip van hoe ze functioneren.

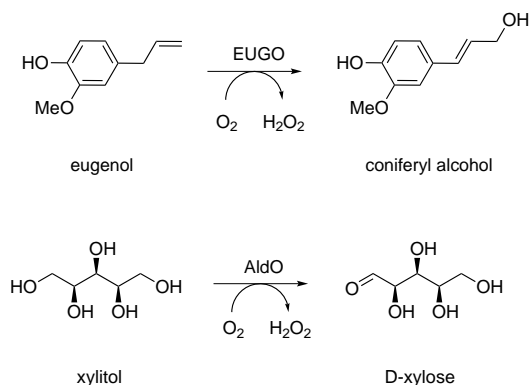
Dit proefschrift is getiteld “*Nieuwe benaderingen voor het herontwerp van flavoproteïne oxidases*” en is een voorbeeld van enzym engineering. Specifiek gaat dit proefschrift over het herontwerpen van een specifieke klasse van enzymen: de flavoproteïne oxidases.

Flavoproteïne oxidases zijn gele enzymen

Flavoproteïne oxidases zijn enzymen die de oxidatie van een breed scala aan chemische verbindingen katalyseren met behulp van moleculaire zuurstof. Oxidases zijn zeer nauwkeurig in de manier waarop ze deze reactie uitvoeren; de uitgaansstof wordt elke keer op dezelfde manier geoxideerd en waterstofperoxide is het enige bijproduct dat gevormd wordt. Oxidases zijn een relatief zeldzaam soort enzym, maar omdat de oxidatie chemie die zij verrichten vaak moeilijk uit te voeren is via conventionele chemische methoden is er behoorlijk wat industriële interesse. Flavoproteïne oxidases zijn bijzonder omdat ze fel geel van kleur zijn (Figuur 1). Dit komt omdat ze een flavine cofactor bevatten: FAD (Latijn: *flavus* = geel). Deze cofactor (= hulp molecuul) wordt stevig gebonden door het eiwit, en maakt het mogelijk dat flavoproteïne oxidases oxidatie reacties kunnen uitvoeren.

In dit proefschrift richten we ons op het herontwerpen van twee flavoproteïne oxidases: eugenol oxidase (EUGO) en alditol oxidase (AldO). Ze zijn afkomstig uit twee verschillende bacteriën en zijn ontdekt in voorgaand promotieonderzoek. Zij werden

geselecteerd als model oxidases om te herontwerpen voor een aantal redenen. Ze zijn eenvoudig te produceren in *E. coli*, kristalstructuren zijn voor allebei beschikbaar en beide katalyseren de oxidatie van twee verschillende klassen van (industriële relevante) verbindingen. De geprefereerde reactie van AldO is de oxidatie van xylitol (dezelfde stof die men vindt in suikervrije kauwgom) naar D-xylose. EUGO zet bij voorkeur eugenol (kruidnagel geur) om naar coniferyl alcohol (Figuur 2).



Figuur 2 Reactie gekatalyseerd door oxidases EUGO en AldO. EUGO reageert met eugenol (kruidnagel geur), AldO reageert met xylitol (ingrediënt in o.a. suiker vrij kauwgom).

Een dag uit het leven van een Enzym engineer

Na te hebben vastgesteld dat het onderwerp van dit proefschrift “enzym engineering” en dan vooral het herontwerpen van gele oxidases betreft, vraagt de nieuwsgierige leek zich misschien af hoe dit onderzoek doorgaans wordt uitgevoerd: wat houdt een dag in het leven van een enzym engineer nou eigenlijk in? Om deze vraag te beantwoorden kan verwezen worden naar [hoofdstuk 7](#) van dit proefschrift, waar een praktisch experiment is beschreven dat geschikt is voor eerstejaars scheikunde/biologie studenten. Dit experiment beschrijft de productie, zuivering, karakterisatie en gebruik van het model oxidase EUGO. Veel van de taken zoals beschreven in dit hoofdstuk geven een zeer vereenvoudigd doch representatief voorbeeld van het eigenlijke werk dat ik verricht heb in de afgelopen vier jaar. Ruwweg bevat "een dag uit het leven van een enzym engineer" dus de volgende aspecten:

Produceren: een enzym moet geproduceerd worden (= expressie). Voor deze expressie wordt een gastheer gebruikt: een organisme dat genetisch gemanipuleerd kan worden om het gewenste enzym te produceren. Er zijn verschillende gastheren beschikbaar, maar in dit proefschrift hebben we alleen gebruik gemaakt van *E. coli* bacteriën.

Zuiveren: Eenmaal geproduceerd door *E. coli*, moet het enzym gezuiverd worden van de rest van de bacteriële componenten. Dit wordt gedaan d.m.v. chromatografische technieken. We gebruiken materiaal dat selectief ons enzym bindt, waardoor we het kunnen zuiveren van de overige cellulaire componenten.

Karakteriseren: het leuke gedeelte. Als we eenmaal zuiver eiwit hebben willen we het karakteriseren. Er zijn vele dingen die we kunnen bepalen, maar we zijn vooral geïnteresseerd in de kinetische parameters en het substraatbereik. Met andere woorden: hoe snel is het enzym? En welke verbindingen kan het omzetten?

Gebruik: Als een enzym eenmaal gezuiverd en gekarakteriseerd is, testen we soms een proef opstelling van een beoogde toepassing. In het practicum in hoofdstuk 7 is dit de synthese van vanille geurstof met behulp van het enzym EUGO.

De bovengenoemde aspecten zijn allemaal gecombineerd in een practicum dat geschikt is voor studenten (**hoofdstuk 7**) zonder veel praktische ervaring met enzymen. Een essentieel deel van de werkzaamheden van een enzym engineer ontbreekt echter in dit practicum, namelijk: mutagenese en screening.

Mutagenese & Screening: Een zeer belangrijk onderdeel van elk enzym herontwerp project betreft de creatie van nieuwe enzym varianten (door middel van mutagenese) met veranderde (verbeterde) kenmerken. Nieuwe enzym varianten worden gemaakt op DNA niveau, door het gen te muteren dat voor het enzym codeert, waarna de expressie gastheer het aangepaste enzym produceert. Het voordeel van deze aanpak is dat grote verzamelingen van gemuteerde genen eenvoudig gemaakt kunnen worden, wat resulteert in grote verzamelingen van aangepaste enzymen. Screening is dan de volgende stap: hier worden de gemuteerde varianten onderzocht (gescreend) op gewenste eigenschappen. Het ontwerpen van een geschikte screeningsmethode is vaak de uitdaging bij enzym engineering projecten (**hoofdstuk 6**).

Het doel van dit proefschrift

Na het onderwerp, de context en relevantie van dit proefschrift vastgesteld te hebben, kunnen we nu het doel omschrijven. Het doel van het onderzoek in dit proefschrift was om de oxidases AldO en/of EUGO te herontwerpen, zodat ze andere stoffen zouden omzetten (anders dan xylitol of eugenol). Ons doel was om dit te doen door een uitgebreide collectie van gemuteerde genen ($\sim 10^8$ verschillende genen) te creëren en deze vervolgens allemaal te controleren op andere activiteit. Hiervoor richtte wij ons op het ontwikkelen van een nieuwe screeningsmethode (**hoofdstuk 6**) zodat we de uitgebreide collectie van oxidase varianten ($\sim 10^8$ verschillende EUGO of AldO varianten) effectief konden onderzoeken op nieuwe activiteit.

Hieronder volgt een gids voor dit proefschrift, waarin de wat, waarom en de belangrijkste conclusies van hoofdstuk 2 t/m 6 in vereenvoudigde taal zijn beschreven. Hoofdstuk 1 bevat de introductie en het doel van dit proefschrift, zoals hierboven beschreven. De bovenstaande paragraaf beschrijft ook de inhoud van hoofdstuk 7; een practicum voor studenten. In hoofdstuk 8 zijn de conclusies van dit proefschrift samengevat.

Een gids voor dit proefschrift

Hoofdstuk 2

Titel: Multiple pathways guide oxygen diffusion into flavoenzyme active sites.

Vertaling van de titel: Trechterachtige tunnels worden gebruikt door oxidases om zuurstof te kanaliseren.

Wat: Zoals hierboven vermeld, zijn oxidases enzymen die moleculaire zuurstof (O_2) gebruiken om oxidatie reacties te katalyseren. Deze reacties vinden plaats in het actieve centrum, een holte dat ruwweg in het centrum van het enzym ligt. In dit hoofdstuk bestuderen we hoe zuurstof vanuit het water waarin de oxidase is opgelost, door het enzym heen beweegt tot aan het actieve centrum. We doen dit op twee manieren. Omdat de beweging van zuurstof binnen een eiwit zeer moeilijk is om rechtstreeks te meten, simuleren we deze beweging met computers. Dit houdt in dat één oxidase molecuul in een denkbeeldige doos wordt geplaatst samen met veel water en zuurstof moleculen. Een simulatie wordt uitgevoerd en de beweging van de zuurstof moleculen door de oxidase bijgehouden. Na deze simulatie denken we te weten hoe zuurstof door het eiwit beweegt. De voorspelling van deze computersimulatie wordt vervolgens gecontroleerd met experimenten. We proberen

de route die zuurstof neemt door het oxidase te blokkeren door een aantal aminozuren te muteren. We kunnen het (gedeeltelijk) blokkeren van zuurstof detecteren als een wijziging van de reactiesnelheid.

Waarom: Ons doel van dit proefschrift was het herontwerp van oxidases. Daarom was het belangrijk om volledig inzicht te krijgen in alle aspecten van een oxidase reactie. Zuurstofreactiviteit van eiwitten is een belangrijk concept dat op dit moment veel in de belangstelling staat. Wat oxidases betreft, is de algemene reactiviteit goed bestudeerd, maar hoe zuurstof gekanaliseerd wordt was niet eerder onderzocht. Voor het eerst laten we zien hoe een dergelijk klein gasmolecuul door een eiwit beweegt naar het actieve centrum. In de toekomst kan deze kennis leiden naar nieuwe vormen van biokatalysatoren. Onze resultaten zijn bijvoorbeeld gebruikt bij het identificeren van een 'zuurstof poortwachter residu', dat de toegankelijkheid van het actieve centrum voor zuurstof volledig kan blokkeren. Het verwijderen van dit residu kan drastische invloed hebben op de zuurstof reactiviteit van een enzym (dehydrogenase) en kan het in een oxidase veranderen.

Conclusie: De belangrijkste conclusie is dat zuurstof gebruik maakt van meerdere trechterachtige structuren om zuurstof te kanaliseren van het oppervlak van het eiwit naar het actieve centrum. In AldO is deze zuurstof kanalisering zeer efficiënt. Het was dan ook moeilijk om de zuurstof activiteit volledig te blokkeren. Vanuit een "enzym engineering" oogpunt was dit belangrijke informatie, want we wilden de reactiviteit van het eiwit herontwerpen: het dusdanig aanpassen zodat het andere verbindingen zou oxideren. Deze studie bevestigde onze overtuiging dat de zuurstofreactiviteit van oxidases een robuust onderdeel is van dit type eiwitten, en niet eenvoudig te verwijderen.

Hoofdstuk 3

Titel: Export of functional *Streptomyces coelicolor* alditol oxidase to the periplasm or cell surface of *Escherichia coli* and its application in whole-cell biocatalysis.

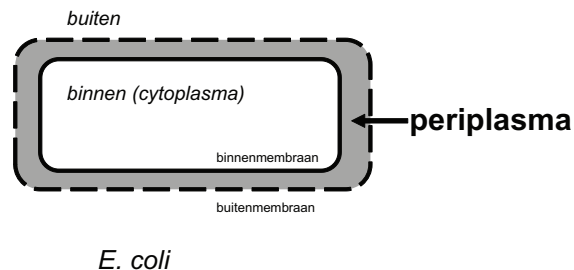
Vertaling van de titel: Transport van het model oxidase, AldO, naar de celoppervlakte van *E. coli* bacteriën.

Wat: In dit hoofdstuk beschrijven we een methode om het model oxidase, AldO, te produceren op het celoppervlak of in het periplasma van *E. coli* bacteriën. Het periplasma van *E. coli* is de vrij toegankelijke ruimte die zich bevindt tussen de dubbele celwand die deze bacteriën hebben (Figuur 3).

Waarom: Het verkrijgen van gezuiverd enzym voor industriële toepassingen is vaak een moeizaam, duur en dus ongewenst proces. Een hele-cel biokatalysator (een enzym

in een levende cel) heeft dus vaak de voorkeur. Het kweken van expressie gastheren, zoals *E. coli* of gist, is een relatief eenvoudig proces. Als een hele-cel biokatalysator wordt gebruikt, echter, dan moet men er wel zeker van zijn dat de verbindingen die worden omgezet de cel in en uit kunnen. Dit is niet altijd het geval. Een elegante oplossing is ervoor zorgen dat de gastheer voor expressie het eiwit transporteert vanuit de binnenkant van de cel naar het periplasma of het celoppervlak. Substraat bereikbaarheid is dan geen probleem. Dit was ook belangrijk voor onze beoogde screeningsaanpak, omdat we een grote verzameling van verschillende oxidase varianten wilden testen voor nieuwe reactiviteiten met behulp van hele cellen in plaats van gezuiverd eiwit.

Conclusie: De oxidase AldO kan geproduceerd worden op het celoppervlak en in het periplasma van *E. coli*, waardoor het gebruikt kan worden als een hele-cel biokatalysator. Hoewel dit al eerder gedaan is voor andere eiwitten, is AldO als flavoproteïne oxidase een speciaal geval, omdat de aanwezigheid van de FAD cofactor betekent dat het geëxporteerd wordt in een volledig gevouwen vorm. Dit is in plaats van rijgen door een klein gat in het membraan zoals het geval is voor de meeste andere geëxporteerde eiwitten.



Figuur 3 *E. coli* bacterien hebben een binnenmembraan en een buitenmembraan. De ruimte tussen deze twee (grijs) is het periplasma.

Hoofdstuk 4

Titel: Functionalizing oxidases with peroxidase activity creates oxiperoxidases, a new breed of hybrid enzyme capable of cascade chemistry.

Vertaling van de titel: Twee verschillende enzymen fuseren om een hybride enzym te maken.

Wat: Oxidase activiteit is moeilijk om direct te meten. Zo is het belangrijk bij het ontwerpen en testen van nieuwe oxidase varianten dat er een betrouwbare methode beschikbaar is om enzymactiviteit te detecteren. In dit hoofdstuk ontwerpen we een nieuwe sensor die oxidase activiteit kan meten. Het bijproduct van alle reacties

gekatalyseerd door oxidases is waterstofperoxide (H_2O_2). Peroxidases zijn een andere klasse van enzymen die met H_2O_2 reageren en eenvoudig te meten gekleurde verbindingen vormen. De oxidase activiteit kwantificeren m.b.v. peroxidases komt vaak voor, maar is relatief omslachtig en niet compatibel met hele cellen. In dit hoofdstuk beschrijven we een oplossing voor dit probleem door een peroxidase aan een oxidase te fuseren. Hiermee creëren we een hybride enzym dat geproduceerd kan worden door *E. coli*.

Waarom: Het doel van mijn promotieonderzoek was om een zeer grote collectie van oxidase varianten te testen voor nieuwe activiteit, met behulp van een hele-cel aanpak. Om oxidase activiteit in hele cellen te kunnen detecteren moest een geschikte detectie-methode worden ontwikkeld. Een mogelijke oplossing was oxidases te fuseren aan een ander enzym type en dit hybride enzym vervolgens produceren in *E. coli*. Dit andere enzym, een peroxidase, maakt detectie van oxidase-activiteit mogelijk.

Conclusie: Wij hebben met succes een bi-functioneel enzym gecreëerd door het fuseren van een oxidase en een peroxidase. We kunnen dit enzym produceren in *E. coli*, en het was ook functioneel in hele cellen. In de toekomst kan deze benadering wellicht worden gebruikt om een grote verzameling oxidase varianten te testen voor nieuwe activiteiten.

Hoofdstuk 5

Titel: Hot or not? Discovery and characterization of a thermostable alditol oxidase from *Acidothermus cellulolyticus* 11B.

Vertaling van de titel: Het vinden van een oxidase die stabiel is bij hoge temperaturen.

Wat: We beschrijven de zoektocht naar een oxidase die bestand is tegen hoge temperaturen. Dit wordt gedaan door in de genomen van organismen die thermofiel (= warmte minnend; leven bij hoge temperaturen) zijn te zoeken naar genen die heel erg lijken op het gen van het model oxidase AldO. Een bacterie die leeft in de heetwaterbronnen van Yellowstone National Park, Verenigde Staten (*Acidothermus cellulolyticus* 11B) bevat een gen dat codeert voor een eiwit dat sterk lijkt op AldO: HotAldO. We hebben dit eiwit geproduceerd en bestudeert.

Waarom: Voor eventuele industriële toepassingen is het vaak noodzakelijk dat een enzym hoge temperaturen (= thermostabiel) kan verdragen. Vanuit een "enzym engineering" oogpunt is deze thermostabiliteit ook wenselijk. Een enzym muteren kan resulteren in varianten die een andere, gewenste reactiviteit vertonen, maar kan het

tegelijkertijd minder stabiel maken. Indien een meer thermostabiel enzym wordt gebruikt om mee te beginnen, dan geeft dit een betere kans op het vinden van een variant met zowel verbeterde activiteit als voldoende stabiliteit.

Conclusie: We ontdekten een oxidase en waren in staat deze te produceren en te zuiveren. Deze nieuwe oxidase is zeer vergelijkbaar met AldO, maar is veel thermostabieler is: het blijft actief gedurende lange perioden bij hoge temperaturen. Vanwege deze eigenschap noemen we dit enzym HotAldO.

Hoofdstuk 6

Titel: Redesign of oxidases by active site randomization.

Vertaling van de titel: Proberen om nieuwe oxidase activiteit te creëren door grootschalige mutaties van het actieve centrum.

Wat: We probeerden nieuwe oxidase activiteiten te maken door bij één van onze model oxidasen, EUGO, het gedeelte van het enzym dat verantwoordelijk is voor herkenning en binding van het normale substraat, eugenol (kruidnagel geur), grootschalig te muteren. Omdat we meer dan 10 miljoen verschillende EUGO varianten creëerden, ontwikkelden we tegelijkertijd een screeningsmethode om snel deze varianten te kunnen testen voor aangepaste activiteit. Dit werd gedaan met een kleurstof die fluorescent wordt in de aanwezigheid van waterstofperoxide, het bijproduct van een succesvolle reactie door een oxidase. Met een “cel sorter”, een apparaat dat de fluorescentie van individuele cellen zeer snel kan meten (10.000 cellen per seconde) proberen wij de cellen die actief oxidase produceren te identificeren.

Waarom: Door het gebied van het enzym dat verantwoordelijk is voor de herkenning en binding van verbindingen drastisch te muteren, hopen we dat het enzym in staat zal zijn nieuwe verbindingen te herkennen, te binden en te oxideren. Sommige van deze nieuwe verbindingen zijn interessant voor eventuele industriële toepassingen. De screeningsmethode die wij ontwikkelen om snel miljoenen mutanten te onderzoeken heeft ook de potentie om toegepast te worden op andere oxidases.

Conclusie: We hebben geen nieuwe oxidase activiteit gevonden tussen de miljoenen oxidase varianten. Dit was voornamelijk te wijten aan het feit dat onze screeningsmethode met behulp van een waterstofperoxide gevoelige kleurstof en een “cel sorter” nog verder geoptimaliseerd moet worden.

Uiteindelijke conclusies van dit proefschrift

Het werk gepresenteerd in dit proefschrift is divers, het beschrijft een verscheidenheid aan verschillende benaderingen die gevolgd kunnen worden bij het herontwerpen van oxidases. Het belangrijkste doel van het onderzoek, namelijk de ontwikkeling van een screenings methode voor oxidasen, en de bijbehorende ontdekking en karakterisering van nieuwe oxidase varianten is niet volledig geslaagd. Echter, zoals beschreven in de overige hoofdstukken zijn er een hoop andere waardevolle resultaten behaald. Er is inzicht verkregen in de zuurstofkanalisering door oxidases; er is een platform ontwikkeld om oxidases aan de cel oppervlakte te krijgen; er is een hybride enzym ontwikkeld, de oxiperoxidase, en er is een thermostabiele oxidase ontdekt en beschreven. Concluderend benadrukt dit proefschrift het potentieel dat flavoproteïne oxidases hebben voor “enzym engineering”.

Curriculum Vitae & List of Publications



Curriculum Vitae

Remko Tsjibbe Winter werd geboren op 7 januari 1982 te Libreville, Gabon (West Afrika). Zijn jeugd bracht hij door in New Orleans (Verenigde Staten) en Adelaide (Australië). In januari 2000 behaalde hij het International Baccalaureate diploma (IB) aan Glenunga International High School te Adelaide, Zuid Australië als Dux of School (valedictorian). In september van datzelfde jaar begon hij met de opleiding Scheikunde aan de Rijksuniversiteit Groningen. Tijdens deze studie specialiseerde hij zich in de richting Moleculaire Biologie en Biotechnologie en heeft hij afstudeeronderzoeken verricht bij de onderzoeksgroepen Biotransformation & Biocatalysis (Prof. D.B. Janssen) en Pharmaceutical Biology (Prof. W.J. Quax). In januari 2007 behaalde hij het Doctoraal diploma Scheikunde. Aansluitend begon hij aan zijn promotieonderzoek in de Molecular Enzymology groep van Prof M.W. Fraaije. In een STW gefinancierd project werkte hij aan het herontwerpen van flavoproteïne oxidases. De resultaten van dit onderzoek staan beschreven in dit proefschrift. Sinds maart 2011 werkt hij als (post)doctorale onderzoeker in de groep van Prof. M.W. Fraaije aan een project in samenwerking met Lucite International.

List of Publications

Winter RT, van den Berg TE, Colpa DI, van Bloois E & Fraaije MW. Functionalizing oxidases with peroxidase activity creates oxiperoxidases, a new breed of hybrid enzyme capable of cascade chemistry. *ChemBiochem* (accepted).

Winter RT, Heuts DP, Rijpkema EM, van Bloois E, Wijma HJ & Fraaije MW. Hot or not? Discovery and characterization of a thermostable alditol oxidase from *Acidothermus cellulolyticus* 11B. *Appl Microbiol Biotechnol* (in press) DOI: 10.1007/s00253-011-3750-0.

Winter RT, van Beek HL & Fraaije MW. The nose knows: biotechnological production of vanillin. *J. Chem. Educ.* (in press) DOI: 10.1021/ed200271u.

van Bloois E, **Winter RT**, Kolmar H & Fraaije MW (2010). Decorating microbes: surface display of proteins on *Escherichia coli*. *Trends Biotechnol* 29: 79-86.

van Bloois E, Torres Pazmiño DE, **Winter RT** & Fraaije MW (2010). A robust and extracellular heme-containing peroxidase from *Thermobifida fusca* as prototype of a bacterial peroxidase superfamily. *Appl Microbiol Biotechnol* 86: 1419-1430.

Baron R, Riley C, Chenprakhon P, Thotsaporn K, **Winter RT**, Alfieri A, Forneris F, van Berkel WJ, Chaiyen P, Fraaije MW, Mattevi A & McCammon JA (2009). Multiple pathways guide oxygen diffusion into flavoenzyme active sites. *Proc Natl Acad Sci U S A*. 106: 10603-10608.

van Bloois E, **Winter RT**, Janssen DB & Fraaije MW (2009). Export of functional *Streptomyces coelicolor* alditol oxidase to the periplasm or cell surface of *Escherichia coli* and its application in whole-cell biocatalysis. *Appl Microbiol Biotechnol* 83: 679-687.

Boersma YL, Pijning T, Bosma MS, van der Sloot AM, Godinho LF, Dröge MJ, **Winter RT**, van Pouderooyen G, Dijkstra BW & Quax WJ (2008). Loop grafting of *Bacillus subtilis* lipase A: inversion of enantioselectivity. *Chem Biol* 15: 782-789.

Winter RT, Heuts DP, Popken P, van Bloois E & Fraaije MW (2008). Exploring the oxygen reactivity of alditol oxidase from *Streptomyces coelicolor*. In: **Flavins and Flavoproteins** (Frago S, ed.) 237-242.

Heuts DP, **Winter RT**, Damsma GE, Janssen DB & Fraaije MW (2008). The role of double covalent flavin binding in chito-oligosaccharide oxidase from *Fusarium graminearum*. *Biochem J* 413: 175-183.

Ferreira MIM, **Winter RT** & Janssen DB (2007). Screening of soil bacteria for degradation of fluoroorganics. In: Bacterial degradation of fluorinated compounds (**Dissertation, Ferreira MIM**, University of Groningen) 43-65.

Dankwoord



Groningen, november 2011

Beste mensen,

Het is af...en dat werd wel eens tijd ook! Inmiddels zit ik al meer dan 10 jaar in Groningen: na een studie scheikunde ben ik toch maar gebleven om promotieonderzoek te doen. Als mijn 14 jaar durend verblijf in Adelaide ervoor heeft gezorgd dat vele mij als halve Australiër beschouwen (don't know if my Australian friends would agree with this, though!), dan vraag ik mij af wat 11 jaar Groningen mij maakt ;-). Het een mooie, leerzame en leuke tijd geweest; toch ben ik blij dat ik nu eindelijk op het punt ben aangekomen dat ik dit dankwoord kan schrijven!

Allereerst Marco. Ik ben van mening dat het goed doorlopen van een promotie traject staat of valt bij de kwaliteit van de begeleiding. En een betere begeleider dan jij kan een promovendus zich niet wensen. Ik wil je dan ook bedanken voor de heel erg prettige samenwerking deze afgelopen vier en een half jaar. Je bent een echte MBWA ("manager by wandering around"; bestaat echt, zoek maar op!) wat je als begeleider heel erg betrokken en bereikbaar maakt. Ik heb veel van je geleerd, en het enthousiasme dat jij overbrengt voor het onderzoek vind ik inspirerend en is iets dat ik hoop vast te houden in mijn toekomstige loopbaan. Ik kan alleen maar zeggen: ga zo door!

Dick, jij ook bedankt. Omdat ik de eerste AIO van Marco ben waar hij alleen als promotor optreed had jij niet zo veel te maken met mijn dagelijkse onderzoek. Toch heb ik je wetenschappelijk-kritische blik als groepsleider (en natuurlijk als leescommissielid) altijd gewaardeerd. Ik ben niet vergeten dat deze kritische blik, heel lang geleden tijdens mijn Bachelor onderzoek, ervoor gezorgd heeft dat ik alles eruit heb gehaald wat er toen in zat. Zonder deze duw was ik wellicht nooit zo ver gekomen!

Verder wil ik de andere twee leden van mijn leescommissie, Gerard Roelfes en Willem van Berkel bedanken voor de tijd en moeite die ze hebben genomen om mijn proefschrift door te nemen.

Edwin, als post-doc op het STW project hebben wij erg veel samengewerkt. Ik heb dan ook erg veel gehad aan jouw expertise en ervaring. Zonder deze samenwerking was dit boekje een stuk dunner geweest (en had het ook een stuk minder blotjes bevat). Heel erg bedankt!

Omdat een dankwoord in een proefschrift vooral is voor diegene die hebben bijgedragen aan het onderzoek wil ik ook heel ver terug gaan en mijn oud-begeleiders tijdens mijn verschillende afstudeerprojecten bedanken: Ykelien, Martijn en Niek. Jullie waren allen enthousiaste begeleiders waar ik veel van heb geleerd en mede door jullie invloed heb ik besloten om te gaan promoveren.


Verder ben ik veel dank verschuldigd aan al mijn bachelor en master studenten: Petra, Andrew, Tom, Dana, en Egon. Ik vond het leuk en erg leerzaam om jullie te begeleiden tijdens jullie verschillende projecten. En ik wil nogmaals benadrukken dat jullie zeker geen pipetteer slaafjes waren, maar allemaal een waardevolle bijdrage hebben geleverd aan dit proefschrift (en voor sommige zelfs aan een publicatie!). Veel succes met de rest van jullie studies/carrières! Alle andere bachelor en master studenten die aan oxidases hebben gewerkt maar die niet volledig onder mijn hoede stonden (Sonja, Geeske, Esmer, Stijn) jullie hebben ook (ondanks het af en toe inhoudelijk moeizaam lopen van jullie projecten) bijgedragen aan de resultaten in dit proefschrift, dus veel dank hiervoor!

Toen ik begon aan dit promotieonderzoek scheelde het enorm dat er al veel werk was gedaan aan de 'gele enzymen' door de eerste lichting FraAIOs: Danny, Jin, Erik en Niek. Dit maakte een hoop van mijn werk eenvoudiger, en zorgde dat ik een vliegende start kon maken. Verder waren jullie altijd zeer relaxte collega's.

Hugo & Fred, bedankt dat jullie mijn paranimfen wilden zijn. Hugo, als kantoorgenoot hoop ik dat ik een goed voorbeeld ben, vooral voor hoe je het niet moet doen als promovendus (laat het dus niet allemaal tot het laatst)! Fred, ik vind het mooi dat wij als Tuinhuysch-genoten straks (als alles goed gaat) allemaal de doctor titel dragen (Johan, jij bent natuurlijk al dokter!)

Ik ben al zo lang van stof, dus om iedereen te sparen ga ik niet alle (oud) collega's verder individueel bedanken. Maar ik wil wel benadrukken dat ik jullie allemaal erg dankbaar ben voor vier jaar hulp en een zeer prettige werksfeer! Special mention gaat natuurlijk naar de vaste koffiehoek bewoners.

Familie, vrienden, mates Down-Under, clubgenoten en mannen van de 12+: de meeste van jullie zijn over de jaren heen langzaam weg getrokken uit het hoge noorden. Toch heb ik jullie interesse in mijn 'amoebe' onderzoek altijd gewaardeerd, en ben ik blij dat ik jullie eindelijk kan opzadelen met een exemplaar van mijn proefschrift! Ik hoop



dat ik in de toekomst jullie wat vaker kan zien, waneer wij eenmaal ook het hoge noorden verlaten. Pappa en mamma, ik ben jullie erg dankbaar: jullie hebben mij goed op weg geholpen in het leven. Opa en oma, jullie hebben de afgelopen jaren heel erg met mij meegeleefd en dit heb ik altijd enorm gewaardeerd. Ik vind het erg leuk dat jullie mijn promotie bijwonen.

Noortje, natuurlijk bedank ik je voor het formatteren van mijn proefschrift. Maar ik wil je vooral bedanken voor je liefde, steun en geduld. Met jou is mijn leven leuk! De toekomst is nog onzeker, maar ik weet zeker dat hij met jou mooi en spannend gaat worden.

Seeya!

Remko "Mike" Winter

inside joke ██████████

